Investigating the cholesterol-independent (pleiotropic) effects of selected hypolipidaemic agents in functional and dysfunctional endothelial cells.

by
Corli Westcott

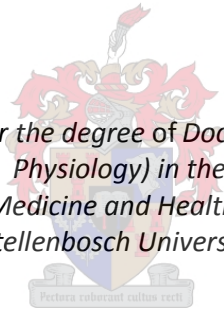

Dissertation presented for the degree of Doctor of Philosophy (Medical Physiology) in the
Faculty of Medicine and Health Sciences at
Stellenbosch University

Supervisor: Prof Hans Strijdom
Co-supervisor: Prof Barbara Huisamen

March, 2015

Declaration

By submitting this thesis electronically, I declare that the entirety of the work contained therein is my own, original work, that I am the sole author thereof (save to the extent explicitly otherwise stated), that reproduction and publication thereof by Stellenbosch University will not infringe any third party rights and that I have not previously in its entirety or in part submitted it for obtaining any qualification.

Corli Westcott

Date: 20 October 2014

Abstract

Vascular endothelium forms the first line of defence against harmful stimuli in the circulation. Endothelial dysfunction is a valuable predictor of cardiovascular disease and therapies aimed at improving endothelial function are therefore needed. The anti-dyslipidaemic agents, simvastatin and fenofibrate, are known for their beneficial effects on lipid parameters, however additional pleiotropic effects have been shown for both. These include improved endothelial function due to increased levels of nitric oxide (NO), as well as anti-oxidant and anti-inflammatory actions. NO is produced by the enzyme, nitric oxide synthase (NOS), which exists in the endothelial NOS (eNOS), inducible NOS (iNOS) and neuronal NOS (nNOS) isoforms. Most studies investigating the endothelial effects of simvastatin and fenofibrate are performed on macrovascular-derived endothelial cells, and there is a lack of data on endothelial cells (ECs) from the microcirculation, particularly the cardiac microvessels.

This dissertation aimed to investigate and elucidate mechanisms underlying the pleiotropic effects of simvastatin and fenofibrate on ECs and vascular tissue using *in vitro*, *ex vivo* and *in vivo* experimental models. *In vitro* investigations included flow cytometry-based intracellular measurements of NO, as well as different types of reactive oxygen species (ROS) and cell viability parameters. Signalling pathways involved with these changes were measured by western blot analyses of the expression and phosphorylation of critical proteins involved in vascular function.

Results on cardiac microvascular ECs (CMECs) demonstrated that fenofibrate (50 µM) exerted a potent, increasing effect on NO production after short periods (1 and 4 hour treatments), but after 24 hours the effects were less robust. Exhaustive investigations suggested that the NO-increasing effects of fenofibrate in baseline CMECs were NOS-independent, a novel finding as far as we are aware. Fenofibrate's ability to protect ECs against injury was demonstrated when CMECs incubated with the pro-inflammatory cytokine, TNF-α, were pre-treated with fenofibrate, resulting in increased NO and improved cell viability parameters. Simvastatin (1 µM) increased NO to a lesser extent in baseline CMECs, and resulted in increased apoptosis and necrosis.

Following the cell studies, their effects on vascular reactivity was measured by aortic ring isometric tension studies. The effects of acutely administered fenofibrate to pre-contracted

aortic rings were investigated, and results showed a modest, but significant NOS-dependent vasodilatory response. Next, an *in vivo* model of Wistar rats treated with simvastatin (0.5 mg/kg/day) and fenofibrate (100 mg/kg/day) for 6 weeks was established. Data showed that neither drug was able to improve aortic ring contraction and dilation above baseline values. Both drug treatments increased iNOS expression, which is usually associated with harmful actions. However, in our hands, increased iNOS expression was associated with a beneficial anti-contractile response in the simvastatin-treated animals. Fenofibrate treatment increased NO bioavailability in the blood of these animals.

In conclusion, fenofibrate showed endothelio-protective pleiotropic effects with regards to NO production after short treatment periods in CMECs. These effects were mediated via a NOS-independent mechanism, a novel finding. Fenofibrate pre-treatment was also protective against the harmful effects of TNF-α. Simvastatin did not show pronounced pleiotropic effects *in vitro* or *in vivo* on endothelial function.

Opsomming

Die vaskulêre endoteellaag is die eerste linie van verdediging teen skadelike stimuli in die bloedsirkulasie. Endoteeldisfunksie is 'n waardevolle voorspeller van kardiovaskulêre siektes en enige terapeutiese behandeling wat kan bydra tot verbeterde endoteelfunksie is belangrik. Simvastatien en fenofibraat word as anti-dislipidemiese middels voorgeskryf en hoewel hulle primêr gebruik word om cholesterolvlakke te verbeter, toon hulle ook pleiotropiese (cholesterol-onafhanklike) eienskappe. Dit sluit in bevordering van endoteelfunksie (via verhoogde stikstofoksied (NO) produksie), asook anti-oksidant en anti-inflammatoriese effekte. NO word vervaardig deur die ensiem, stikstofoksiedsintase (NOS) wat voorkom in drie isovorme: endoteel-afgeleide NOS (eNOS), induseerbare NOS (iNOS) en neuronale NOS (nNOS). Die meerderheid studies wat pleiotropiese effekte van simvastatien en fenofibraat ondersoek, gebruik endoteelselle van makrovaskulêre bloedvate, wat beteken daar is 'n tekort aan data aangaande endoteelselle vanaf mikrovaskulêre vate, veral kardiale mikrovaskulêre vate (CMECs).

Hierdie proefskrif het dit ten doel gehad om meganismes betrokke by die pleiotropiese effekte van simvastatien en fenofibraat te ondersoek deur van *in vitro, ex vivo* en *in vivo* modelle gebruik te maak. Die *in vitro* ondersoeke het gefokus op vloeisitometrie-gebaseerde metings van intrasellulêre NO, reaktiewe suurstof-radikale (ROS) en sellewensvatbaarheid. Seintransduksie paaie betrokke by hierdie veranderinge was bepaal deur proteienuitdrukking en -fosforilasie vlakke te meet van belangrike proteïene, met behulp van die Western-blot tegniek.

Resultate van die CMEC eksperimente het getoon dat fenofibraat (50 µM) 'n kragtige en verhogende effek op NO produksie uitgeoefen het na kort behandelingstye (1 en 4 ure), maar na 24 uur was hierdie effek minder uitgesproke. Uitvoerige ondersoeke het getoon dat fenofibraat se basislyn effekte op CMECs deur NOS-onafhanklike meganismes teweeggebring is, en sover ons kennis strek, is dit 'n nuwe bevinding. Fenofibraat se endoteel-beskermende effekte kon ook aangetoon word deur CMECs vir een uur te behandel voor byvoeging van die pro-inflammatories sitokien, tumor nekrose faktor alpha (TNF-α), wat gelei het tot verhoogde NO vlakke en verbeterde seloorlewing. Simvastatien (1 µM) het tot 'n mindere mate NO produksie verhoog in CMECs, tesame met pro-apoptotiese en -nekrotiese effekte.

Vervolgens was die effekte op vaskulêre reaktiwiteit geëvalueer d.m.v. isometriese spanningsondersoeke. Akute effekte van fenofibraat is gemeet deur byvoeging daarvan tot ‘n vooraf saamgetrekte aorta-ring, wat tot matige, maar beduidende NOS-afhanklike verslapping gelei het. Hierna is ‘n *in vivo* model opgestel deur Wistar rotte vir ses weke met 0.5 mg/kg/dag simvastatien of 100 mg/kg/dag fenofibraat te behandel. Resultate toon dat geen van die behandelings basislyn kontraksie of verslapping van aorta ringe kon verbeter nie. Beide behandelings het tot verhoogde iNOS uitdrukking gelei, wat gewoonlik met nadelige effekte geassosieer word, maar in ons studies was dit met voordelige, anti-kontraktiele effekte in aorta-ringe van simvastatien-behandelde rotte geassosieer. Fenofibraat behandeling het die NO-biobeskikbaarheid in die rotte se bloed verhoog.

Ten slotte, fenofibraat het met endoteel-beskermende, pleiotropiese effekte op endoteelselle gepaard gegaan, veral t.o.v. NO-produksie na akute middeltoediening in die CMECs. Die meganisme was ‘n NOS-onafkanklike proses, wat ‘n nuwe bevinding is. Fenofibraat pre-behandeling het teen die skadelike effekte van TNF-α beskerm. Geen uitgesproke pleiotropiese effekte is *in vitro* of *in vivo* gevind met simvastatien behandeling nie.

Dedication

Dedicated to:

My loving husband, **Jacques** and our wonderful daughter **Dané.** Thank you for all your unconditional love and support throughout the study! You made it all worth while!

My parents, **Jan** and **Edna Faber**. You have always supported my academic aspirations and I appreciate your love and motivation immensely!

Acknowledgements

I would like to sincerely acknowledge the following people for their contributions:

- My supervisor, Prof Hans Strijdom for his support, motivation and enthusiasm throughout the study. Thanks Prof for all your dedication, time and efforts! It was a privilege to be your student.
- My co-supervisor, Prof Barbara Huisamen for her valuable inputs and advice.
- The endothelial research group, especially Dr Amanda Genis for all her technical assistance when things were hectic in the cell culture lab and Eva Mthethwa for your encouragement.
- All my colleagues from Medical Physiology, especially my office mates Dr Ingrid Webster and Dr Suzèl Hattingh for their support and understanding. Dr Derick van Vuuren for his inputs and encouragement as well as help with blots!
- Dirk Loubser for setting up the aortic ring system as well for technical assistance.
- Honours students, Roxy Graham and Wiehan van Wyk for their help and contributions to experiments.
- Jacques Westcott, Jan Faber and Edna Faber for your assistance on the technical aspects of the dissertation, checking figure numbers etc.
- Dr Frikkie Kruger for his valuable insights and proof-reading of the dissertation.
- Janine Nortjé for her time and efforts to create the puzzle animations.
- Centre for Proteomic and Genomic Research, especially Jacqueline Meyer for their assistance with qPCR analysis.
- Funding agencies for providing the necessary finances: NRF Thuthuka and Harry Crossley foundation.

To all my family and friends, thank you for your interest and support! Especially my sisters, Louise and Janine, I love you to bits! I am truly blessed to have you all in my life!

And most importantly, thank you to my Heavenly father for giving me the strength, abilities and support to start and finish my PhD study.

"For He gives power to the weak, and to those who have no might He increases strength. Even the youth shall faint and be weary, and young men shall utterly fall. But those who wait on the Lord shall renew their strength. They shall mount up with wings like eagles. They shall run and not be weary, they shall walk and not faint" Isaiah 40:29-31; The Bible

List of tables

List of figures

Chapter 1:

Table of Abbreviations

AC	Absolute control
ADMA	Asymmetric dimethylarginine
AECs	Aortic endothelial cells
AGE	Advanced glycated end-product
AMPK	AMP activated protein kinase
AP-1	Activating protein-1
ATP	Adenosine 5'-triphosphate
AUC	Area under the curve
BAEC	Bovine aortic endothelial cells
Bcl-2	B-cell lymphoma 2
bFGF	Basic fibroblast growth factor
BH_4	(6R-)5,6,7,8-tetrahydro-L-biopterin
BPAEC	Bovine pulmonary artery endothelial cells
BSA	Bovine serum albumin
Ca^{2+}	Calcium
CAD	Coronary artery disease
CaM	Calmodulin
CaMKII	Ca^{2+}/Calmodulin-dependent protein kinase
CAR	Constitutive Androstane Receptor
Cav-1	Caveolin-1
cGKII	cGMP-dependent protein kinase II
cGMP	Cyclic guanosine monophosphate
CMECs	Capillary derived endothelial cells
CVD	Cardiovascular disease
DAF-2/DA	Diaminofluorescein diacetate
DEA/NO	Diethylamine NONOate
DHE	Dihydroethidium
DHR-123	Dihydrorhodamine-123
Dil-ac-LDL	dioctadecyl-3,3,3',3'-tetramethylindo-carbocyanine perchlorate
DMNQ	Dimethoxy-1,4-naphthoquinone
DMSO	Dimethyl sulfoxide
DNA	Deoxyribonucleic acid
EC	Endothelial cell
ECL	Enhanced chemiluminescence
ED	Endothelial dysfunction
EDRF	Endothelium-derived relaxing factor
EEC	Endocardial endothelial cells
EGM-2	Endothelial cell growth medium
eNOS	Endothelial nitric oxide synthase
ET-1	Endothelin-1
FAD	Flavin adenine dinucleotide
FBS	Foetal bovine serum
FIELD trial	The Fenofibrate Intervention and Event Lowering in Diabetes trial

FL1-H	Flow channel 1
FMN	Flavin mononucleotide
FPP	Farnesylpyrophosphate
FSC-H	Forward scatter
GAPDH	Glyceraldehyde 3-phosphate dehydrogenase
GGPP	Geranylgeranylpyrophosphate
GR	Glucocorticoid receptor
GSH	Glutathione
GSNO	S-nitrogluthathione
GTP	Guanine triphosphate
H_2O	Distilled water
H_2O_2	Hydrogen peroxide
HAEC	Human aortic endothelial cells
HDL	High density lipoprotein
HDL-C	High density lipoprotein cholesterol
hEGF	Human epidermal growth factor
HGMECs	Human glomerular microvascular endothelial cells
HMG-CoA	Hydroxy–3–methylglutarylcoenzyme A
HMG-CoA-R	3-Hydroxy-3-methylglutaryl coenzyme A reductase
HSP90	Heat shock protein 90
HUVECs	Human umbilical vein endothelial cells
ICAM	Intercellular adhesion molecule
IDL	Intermediate density lipoprotein
IHD	Ischaemic heart disease
IL-1β	Interleukin-1β
iNOS	Inducible nitric oxide synthase
KHB	Krebs Henseleit buffer
LDL	Low density lipoprotein
LDL-C	Low density lipoprotein cholesterol
L-NMMA	N^G-Monomethyl-L-arginine monoacetate
LPS	Lipopolysaccharide
MAP kinase	Mitogen activated protein kinases
MLCP	Myosin light-chain phosphatase
mPTP	Mitochondrial permeability transition pore
mRNA	Messenger ribonucleic acid
mtNOS	Mitochondrial nitric oxide synthase
NADPH	Nicotinamide-adenine-dinucleotide phosphate
NADPH Oxidase	Nox
NAP 110	Inducible NOS associated protein
NCD	Non-communicable diseases
NCS	Non-silencing control
NEMO	NF-κB essential modulator
NF-κB	Nuclear factor kappa B
NMDAR	N-methyl-D-aspartate receptor
nNOS	Neuronal nitric oxide synthase

NO	Nitric oxide
NO^-_2	Nitrites
NO^-_3	Nitrates
O_2	Oxygen
O^{2-}	Superoxide anion
$ONOO^-$	Peroxynitrite
ox-LDL	Oxidized-low density lipoprotein
P/T	Phosphorylated/total
PAI-1	Plasminogen activator inhibitor 1
PDZ	Post-synaptic density protein, discs-large, ZO-1
PFK-M	Phosphofructokinase
PI	Propidium iodide
PKA	Protein kinase A
PKB	Protein kinase B
PKC	Protein kinase C
PKG	Protein kinase G
PP1	Protein phosphatase 1
PP2A	Protein phosphatase 2 A
PP2B	Protein phosphatase 2 B
PPAR	Peroxisome proliferator-activated receptor
PPAR-α	Peroxisome proliferator-activated receptor alpha
PVDF	Polyvinylidene difluoride
PXR	Pregnane X Receptor
PYK2	Proline-rich tyrosine kinase 2
qPCR	Quantitative real-time polymerase chain reaction
ROCK	Rho/Rho Kinase
ROS	Reactive oxygen specie
rpm	Revolutions per minute
RXR	Retinoid X receptor
RyRs	Ryanodine receptors
SDS	sodium dodecylsulfate
Ser	Serine
sGC	Soluble guanylyl cyclase
SHR	Spontaneously hypertensive rat
SMC	Smooth muscle cell
SOD	Superoxide dismutase
SR	Sarcoplasmic reticulum
SSC-H	Side scatter
TGF-β	Transforming growth factor β
Thr	Threonine
TNF-α	Tumor necrosis factor alpha
t-PA	Tissue plasminogen activator
Tyr	Tyrosine
UC	Untreated control
USA	United States of America

VCAM	Vascular adhesion molecule
VEGF	Vascular endothelial growth factor
VLDL	Very low density lipoprotein
VSMC	Vascular smooth muscle cells
WHO	World Health Organisation

Table of Contents

Chapter 1

Literature Overview

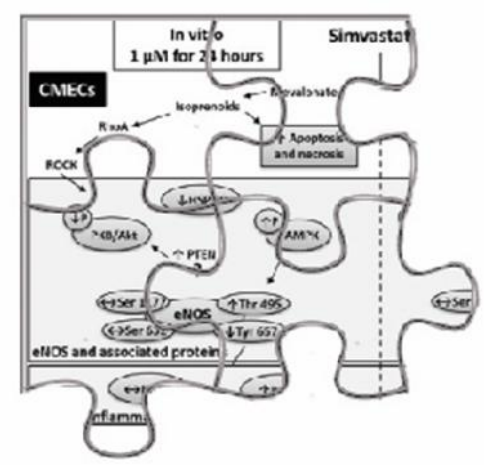

Chapter 1: Literature overview

1.1 Cardiovascular disease

1.1.1 Introduction

According to recent reports from the World Health Organisation (WHO), non-communicable diseases are the leading cause of mortality globally, while almost 80% of such deaths occur in low- and middle income countries (Mendis, 2011). Recent projections published in the SA Heart Journal (Mpe, 2010) indicated that cardiovascular-related deaths in the age group 35-64 years will increase by 41% in South Africa between the year 2000 and 2030. It is also stated that SA is already losing more young and economically active people (in the age group mentioned above) to cardiovascular disease (CVD) compared to the United States of America (USA) and Portugal. These statistics clearly indicate that CVD is not only a major problem globally, but one that cannot be ignored in South Africa.

According to Pearson *et al*., (1993) and Yusuf *et al*., (2001), most populations have experienced a shift from nutritional deficiencies and infectious diseases to degenerative diseases such as CVD, cancer and diabetes. This has been termed the "epidemiologic transition". Epidemiological transition consists of different stages, and at any given time populations in a particular country, or even in a particular region of a country, can be experiencing a specific stage of epidemiological transition. The different stages of epidemiological transition are shown in figure 1.1. Developing countries, such as those in Sub-Saharan Africa and rural areas of South America and South Asia, are initially burdened with infectious diseases (including rheumatic heart disease) and malnourishment. During the next stage, as infectious disease control and nutritional status improves, the countries or regions become burdened with hypertensive heart diseases, as has been observed in China and other Asian countries. During stage three, populations adopt the so-called "Western lifestyle", including factors such as consumption of high-fat diets, smoking and sedentary lifestyles. Non-communicable diseases (NCD) predominate during this stage, with

atherosclerotic CVD being the main cause of mortality (Yusuf *et al*., 2001). According to the Mendis (2011) 39% of global deaths could be attributed to CVD (figure 1.2). This increase in cardiovascular related diseases can again contribute to the burden of infectious and nutritional as well as perinatal diseases. This is called a "double burden". These diseases can be delayed in the fourth stage by interventions to treat and prevent ischaemic heart disease and stroke. Countries of Western Europe, North America, Australia and New Zealand are said to be in the fourth stage of epidemiological transition. The authors further propose a fifth stage of this transition, namely social upheaval or war. These events break down current social and health structures which will again lead to the flare-up of diseases seen in stages one and two (Russia) (figure 1.1) (Yusuf *et al*., 2001).

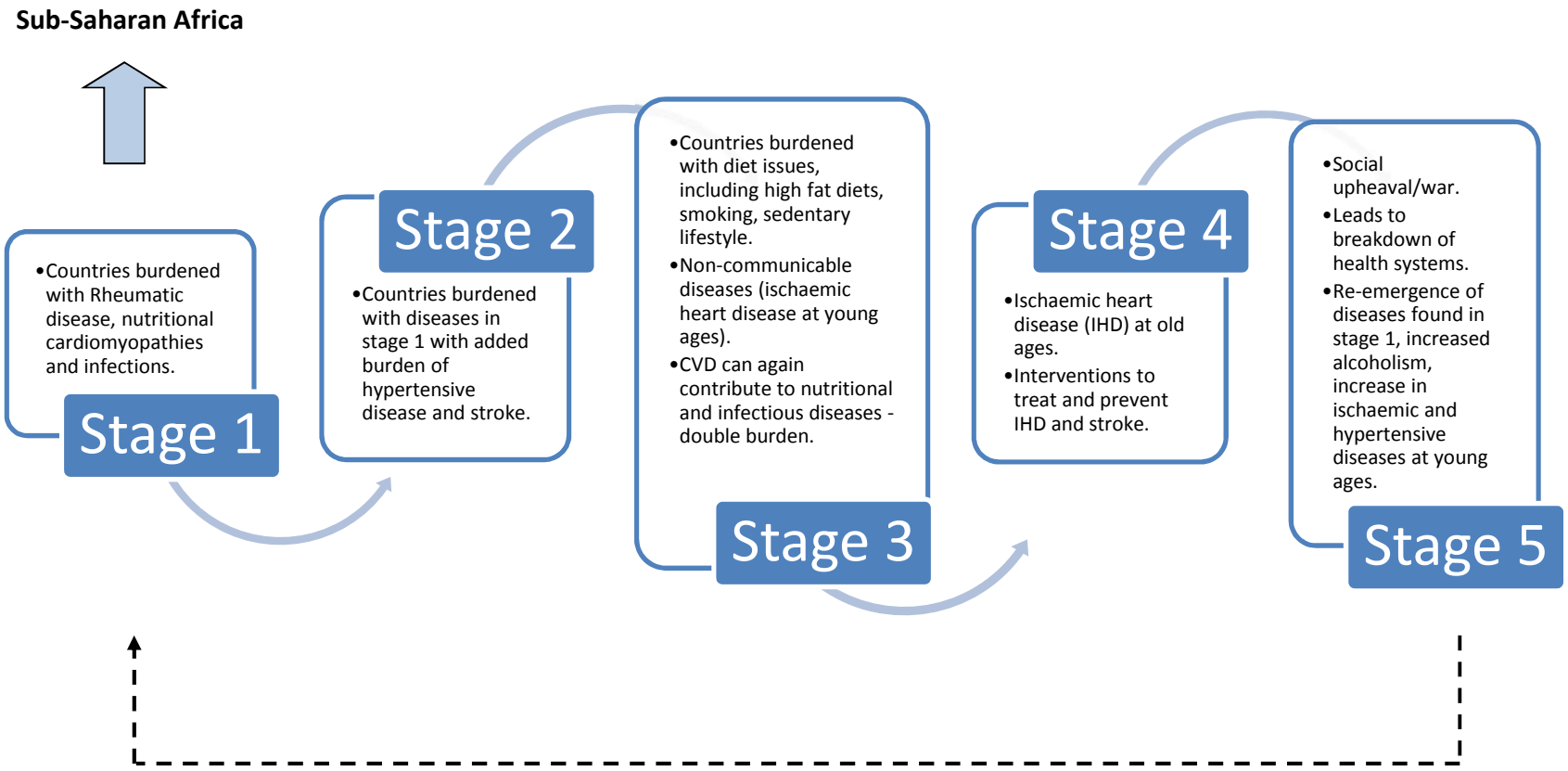

Figure 1.1: An illustration of the five stages of Epidemiological Transition adapted from Yusuf et al., 2001. It serves as an illustration of how populations experience a shift from nutritional deficiencies and infectious diseases to degenerative diseases such as cardiovascular disease, cancer and diabetes.

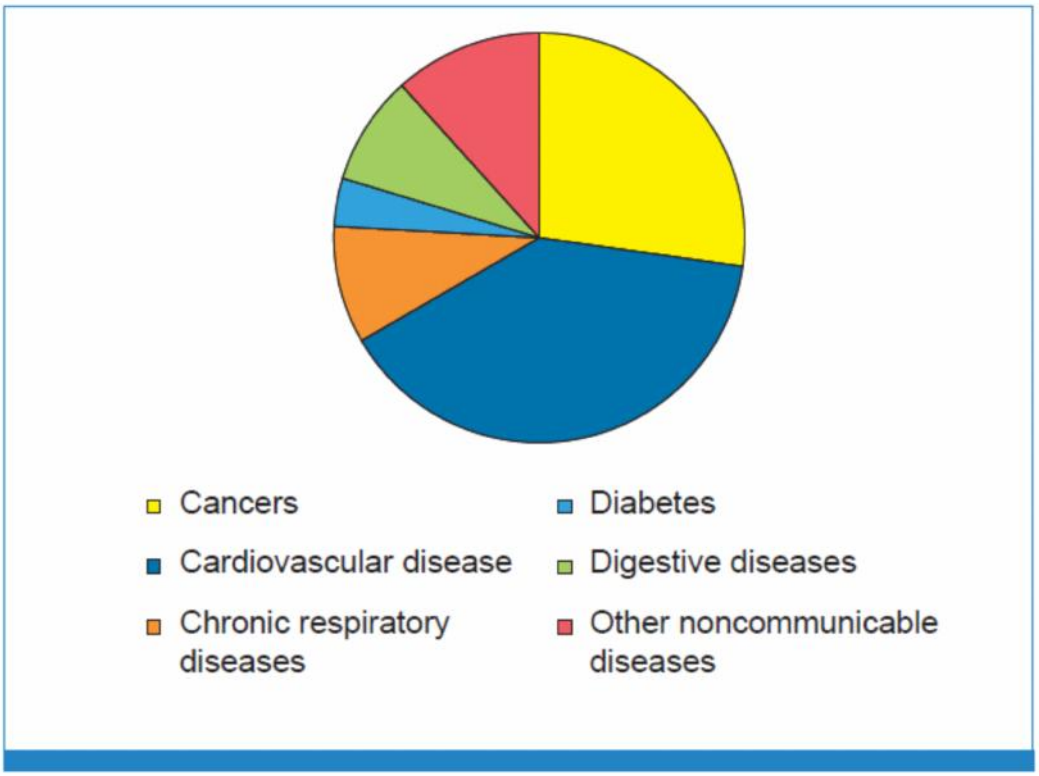

Figure 1.2: Pie chart indicating the proportion of global NCD deaths under the age of 70, 2008 (Mendis, 2011).

1.1.2 Risk factors contributing to CVD

Lin *et al*., 2013, described CVD as the result of chronic diseases that occur due to cumulative effects over a long period of time. The WHO reported that the four common and preventable risk factors leading to NCD such as CVD include: tobacco use, physical inactivity, unhealthy diet and alcohol abuse. These behavioural risk factors result in metabolic/physiological risk factors, namely raised blood pressure, overweight/obesity, hyperglycaemia and dyslipidaemia (Mendis, 2011). For the purpose of the current study, the focus will be on dyslipidaemia and anti-dyslipidaemic therapies.

1.1.2.1 Dyslipidaemia

Dyslipidaemia is a condition in which a patient has elevated plasma concentrations of total cholesterol, low density lipoprotein cholesterol (LDL-C), and triglycerides, together with subnormal concentrations of high density lipoprotein cholesterol (HDL-C) (Rached *et al*., 2014). Hence multiple lipid parameters are deregulated. Several clinical and epidemiological studies confirmed the relationship between high levels of serum cholesterol and CVD (Wilson *et al*., 1980; Downs *et al*. 1998; Bays *et al.,* 2001; Raza *et al.,* 2004). Such studies gave rise to treatment strategies focussed on decreasing total cholesterol and LDL-C levels. The different treatment strategies will be discussed in detail under section 1.6. Since the current study will be focussing on the pleiotropic effects of cholesterol drugs and not on their anti-dyslipidaemic effects, only a short discussion will follow on lipids, their classification and functions.

1.1.3 Lipids

1.1.3.1 Classification and function

Lipids can be classified as neutral fat or triglycerides, phospholipids and cholesterol. Fatty acids (long chain hydrocarbon organic acids) form the basic lipid moiety of triglycerides and phospholipids. Even though cholesterol does not contain fatty acids *per se*, the nature of its sterol nucleus (synthesised from portions of fatty acids) provides it with the physical and chemical properties of lipid substances. The main function of triglycerides in the body is to provide energy for metabolic processes. In addition, cholesterol, phospholipids and triglycerides form essential components of membranes in the cell (Guyton & Hall, 2000).

Lipoproteins

Lipoproteins are small particles circulating in the plasma and contain triglycerides, phospholipids, cholesterol and protein. They are classified according to their densities:

1) Very low density lipoprotein (VLDL) – contains a high concentration of triglycerides and only moderate concentrations of phospholipids and cholesterol.
2) Intermediate density lipoprotein (IDL) – VLDLs from which some of the triglycerides have been removed, leaving a higher concentration of cholesterol and phospholipids.
3) Low density lipoprotein (LDL) – they are again derived from IDLs from which almost all of the triglycerides have been removed. This yields a high concentration of cholesterol and moderately high levels of phospholipids.
4) High density lipoprotein (HDL) – these lipoproteins contain a high concentration of protein and only low concentrations of cholesterol and phospholipids.

All lipoproteins are synthesised in the liver. The liver is also the centre for synthesis of triglycerides, cholesterol and phospholipids (Guyton & Hall, 2000).

1.1.4 Ischaemic Heart Disease (IHD)

Cardiovascular diseases include diseases of the heart and blood vessels. The WHO reported that 46% of global CVD deaths in males and 38% in females could be contributed to IHD (Mendis *et al*., 2011). The myocardium does not extract oxygen and nutrients from the blood in the atria and ventricles, but it depends on blood supply from coronary arteries (figure 1.3). In coronary artery disease (CAD), changes to these arteries can lead to insufficient blood supply to the myocardium, resulting in ischaemia of the tissue supplied by the particular arteries (Widmaier *et al*., 2004). Atherosclerosis is the underlying cause most often associated with coronary artery disease, carotid artery disease and peripheral arterial disease (Falk, 2006). Atherosclerosis refers to the thickening and hardening of arteries, more specifically the intimal and medial layers which results in a loss of elasticity of the vasculature (Lahoz & Mostaza 2007). Fatty deposits, cholesterol and fibrous tissue form a plaque on the inner surfaces of these arteries which causes a narrowing of the artery and irregular surface area in the lumen (Mendis *et al*., 2011). Disruptions of these plaques can be either through fissures, ulcerations or ruptures which will lead to a thrombus on the area (Stary, 1995; Lahoz & Mostaza 2007), culminating in clinical complications such as myocardial infarction and stroke (Glass & Witztum 2001).

1.1.4.1 Process of atherosclerosis and plaque formation

Incremental decreases in the diameter of the lumen of coronary arteries occur as follows: Initially, minute depositions of cholesterol, mostly LDL-C, will occur on the intima and underlying smooth muscle cells. These deposits will grow larger and combine with others, which together with other surrounding fibrous and smooth muscle tissue, form large plaques, decreasing the lumen and increasing resistance to flow or even complete vessel occlusion (Guyton & Hall, 2000; Widmaier *et al*., 2004). Increased levels of plasma cholesterol, particularly LDL-C is highly associated with increased risk for atherosclerotic diseases (Rozman & Monostory 2010). The endothelium can express adhesion and chemotactic molecules and becomes more permeable to macro-molecules such as LDL particles in the arterial wall. These trapped LDL particles can be oxidised by vascular cells and will exert their pro-atherogenic effect on these cells. Resistant vascular cells will produce factors leading to monocyte recruitment and differentiation into macrophages. Completely oxidised LDL particles can be internalised by macrophages to form foam cells which is considered the hallmark of atherosclerotic lesions (Maiolino *et al*., 2013).

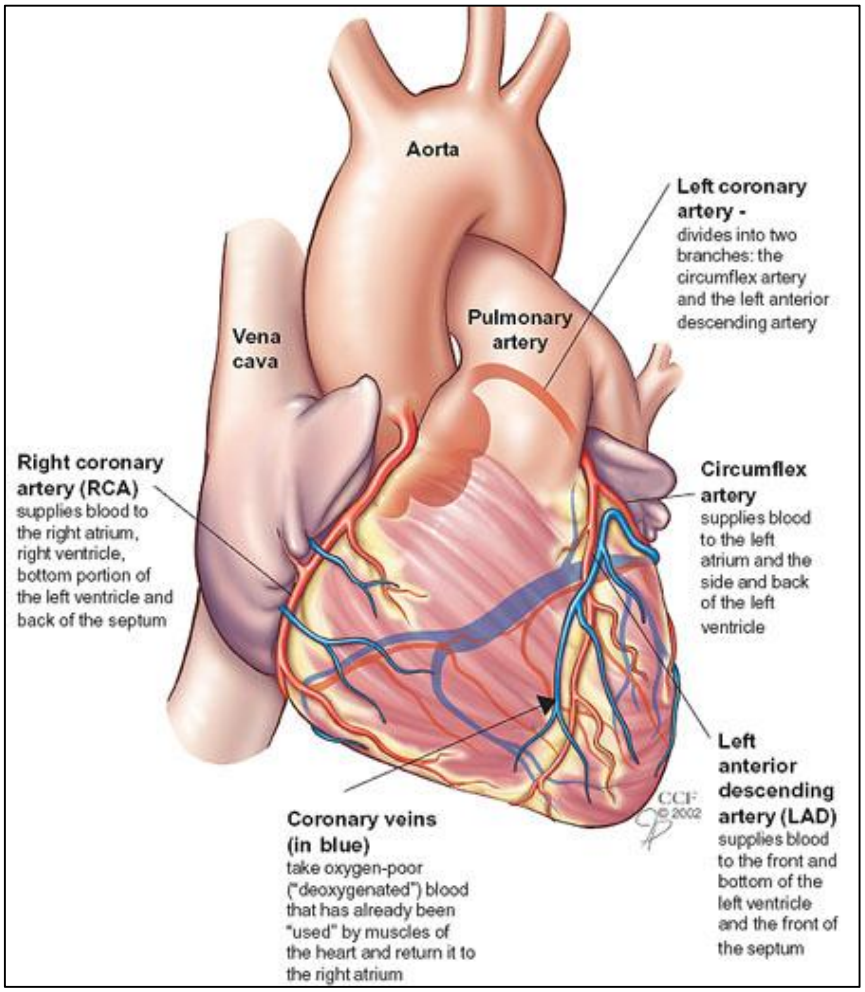

Figure 1.3: A graphic illustration of the coronary vascular network in the myocardium (http://my.clevelandclinic.org/heart/heart-blood-vessels/coronary-arteries.aspx)

1.1.4.2 The role of endothelial cells (ECs) in atherosclerosis – Endothelial activation/dysfunction

It has become evident over the last few decades that the initiation and progression of atherosclerosis is dependent on dynamic and profound changes in vascular biology (Ross 1999; Deanfield *et al*., 2007). Endothelial cells (ECs) are responsible for vascular health and their strategic positioning between blood and tissue renders them susceptible to changes in blood composition, hemodynamic forces and other circulating stressors. In response to these changes, they can release a variety of paracrine factors acting on the vessel wall and lumen to maintain vascular homeostasis (Brevetti *et al*., 2008), but during a state of endothelial activation or dysfunction, as during pre-atherosclerosis and atherosclerosis (Davignon & Ganz 2004; Deanfield *et al*., 2007), the "resting" ECs will switch to a phenotype involved with host defence (Deanfield *et al*., 2007). This involves expression of chemokines (e.g. monocyte chemoattractant protein-1), cytokines (e.g. tumor necrosis factor α) and adhesion molecules (e.g. vascular cell adhesion molecule-1) (Haas & Mooradian 2010; Mochizuki *et al*., 2010; Kiechl *et al*., 2012). The interaction between endothelium and leukocytes is a key event in the process of atherogenesis.

Based on research by Butcher (1991) and Springer (1994), Heemskerk *et al.* (2014) proposed a 5-stage process through which leukocytes transmigrate into the endothelium (figure 1.4). The process is initiated at stage 1 when E-selectin and P-selectin are expressed on the endothelial surface leading to the capture of leukocytes. During stages 2 and 3 activated integrins in leukocytes will firmly attach to intercellular adhesion molecule (ICAM) and vascular adhesion molecule (VCAM) and leukocytes starts crawling onto the endothelium. The leukocytes "dock" on the endothelium via actin rich "cups" (step 4). Step 5 of the process consists of leukocytes migrating through the endothelium via one of two mechanisms, either paracellularly, i.e. through the endothelial cell-cell junctions or transcellulary. The author also emphasises the importance of Rho-GTPase signalling during this process of transmigration and cytoskeletal remodelling (Heemskerk *et al*., 2014) (figure 1.4).

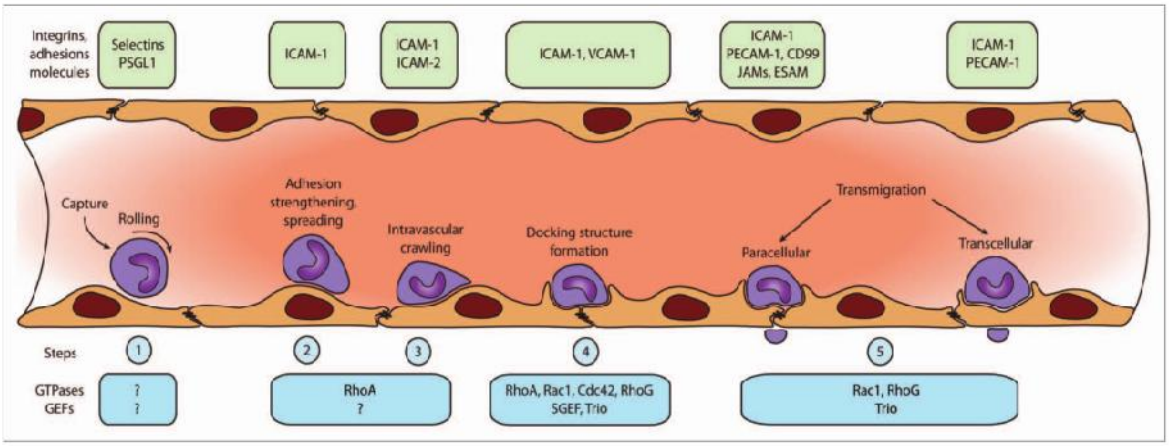

Figure 1.4: The multistage process of leukocyte transendothelial migration, divided into five stages. Stage 1: Rolling and tethering phase; Stage 2: Shows the initial adhesion of leukocytes to the endothelium; Stage 3: The firm adhesion and crawling part. Stage 4: Cup-like structures are formed, resulting in the next step. Stage 5: Actual transmigration, either para- or transcellular (modified from Heemskerk et al., 2014)

Endothelial dysfunction (ED) is characterised by a decrease in the bioavailability of nitric oxide (NO) leading to impaired endothelium-dependent vasodilation of blood vessels (Bonetti, 2003). ED is widely regarded as an early and reversible precursor and therefore predictor of atherosclerosis (Grover-Páez & Zavalza-Gómez, 2009; Mudau *et al*., 2012). Considering all of these findings, the endothelium is clearly an important target organ for the prevention and treatment of atherosclerotic disease.

1.2 The Vasculature

Blood ejected by the left ventricle, exits the heart via the aorta. The aorta divides into many arteries that become smaller arterioles before finally forming capillaries (Opie, 2004). The walls of large vessels, such as arteries, consist of three layers, namely the intima, media and adventitia with an endothelial layer separating the vessel wall and blood. The internal elastic lamina is made up of numerous bundles of elastic fibres that delimit the intima from the media. In contrast to the vascular wall of arteries, capillary walls only consist of connective tissue and endothelial cells, with no vascular smooth muscle cells; therefore capillaries are unable to induce their own contraction or dilation (Aird 2007; La Sala *et al*., 2012) (figure 1.5).

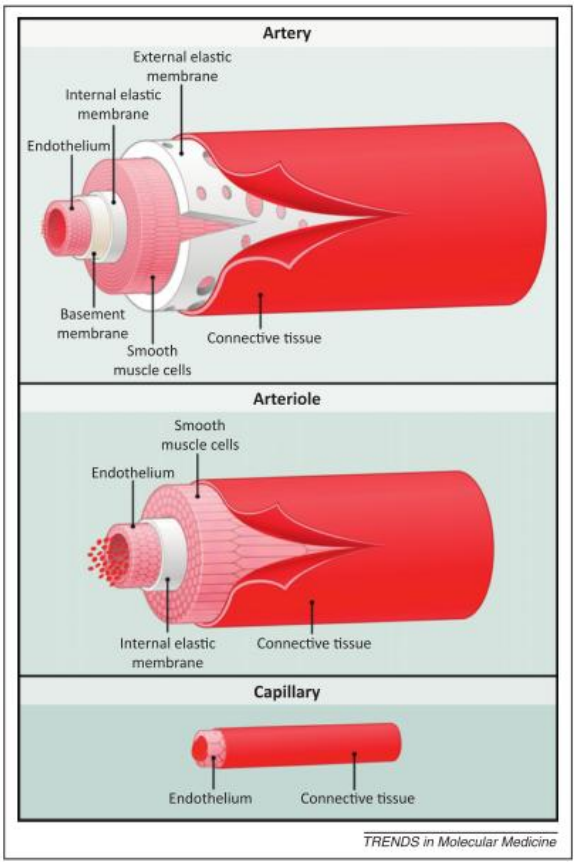

Figure 1.5: The anatomical structure of arteries, arterioles and capillaries (La Sala et al*., 2012)*

1.2.1 Endothelium - Structure and function

The vascular endothelium consists of a single layer of cells that line the entire vascular system (Mas 2009). It consists of nearly ten trillion (10^{13}) cells in adults and can weigh up to 1 kg (Galley & Webster 2004) with a surface area of 350 m^2 (Pries *et al.,* 2000). ECs are flat cells with a large nucleus that often protrudes into the vascular lumen. They are normally present as spindle-shaped cells, but can adopt more rounded shapes when present in the capillaries and venules (Mas 2009). The phenotypic variations between ECs can cause them to respond differently to similar stimuli (Galley & Webster 2004). ECs have caveolae in abundance. Caveolae are membrane invaginations and play a role in signal transduction and vesicular trafficking. ECs also have a prominent Golgi apparatus which has significant secretory activity and a large number of mitochondria (Mas 2009). Even though ECs have sufficient mitochondria, they receive most of their energy/adenosine 5'-triphosphate (ATP) from anaerobic glycolysis (Davidson & Duchen 2007). Vascular ECs are covered with a endothelial glycocalyx – extracellular glycoproteins and proteoglycans anchored to the ECs (Pries *et al.,* 2000; Tarbell & Pahakis 2006). The endothelium is a semi-permeable barrier and regulates the transport of small and large molecules across the membrane (Michiels 2003). ECs are linked to each other by means of junctions, structures formed by transmembrane adhesion molecules linked to cytoskeletal proteins. Three types of junctions have been described in the endothelium namely: tight junctions, adherence junctions and gap junctions (Schnittler 1998).

The endothelium is a dynamic organ and has metabolic and synthetic functions (Galley & Webster 2004; Mas 2009). One of the most important functions is the regulation of vaso-motor tone in the vasculature. Furchgott and Zawadzki (1980) showed that relaxation of vascular smooth muscle is dependent on the integrity of the endothelium. They ascribed this phenomenon to an endothelium-derived relaxing factor (EDRF), later identified as nitric oxide (NO).

1.2.1.1 Capillary derived endothelial cells (CMECs)

"EC heterogeneity" is a term that was coined when it was discovered that ECs across the vascular tree present with distinct phenotypes, differentially regulated in space and time (Aird 2007).

Two types of endothelial cells are present in the heart, namely the endothelial cells that line the capillaries (cardiac microvascular endothelial cells, CMECs) and endocardial endothelial cells (EECs). They are classified according to their effects on and proximity to cardiomyocytes. The cardiomyocytes are outnumbered by cardiac endothelial cells, and it is proposed that for every 3 cardiac ECs there is one cardiomyocyte. The anatomy of the heart allows for close proximity between cardiomyocytes and CMECs in particular, since the capillary network is situated around cardiomyocytes (figure 1.6) (Strijdom & Lochner 2009). Strijdom *et al.* (2006) showed that CMECs increased NO levels 26 fold higher than isolated cardiomyocytes. This was associated with a 22 fold higher expression in endothelial nitric oxide synthase (eNOS). These results clearly underlie the distinct differences in EC functioning. From a pathophysiological perspective, it is important to note that the myocardial capillaries (lined by CMECs), are regarded as a primary target (and therefore the site of end-organ damage) of cardiovascular risk factors such as hypertension and diabetes mellitus, rendering the CMECs particularly important in the development of ischaemic heart disease.

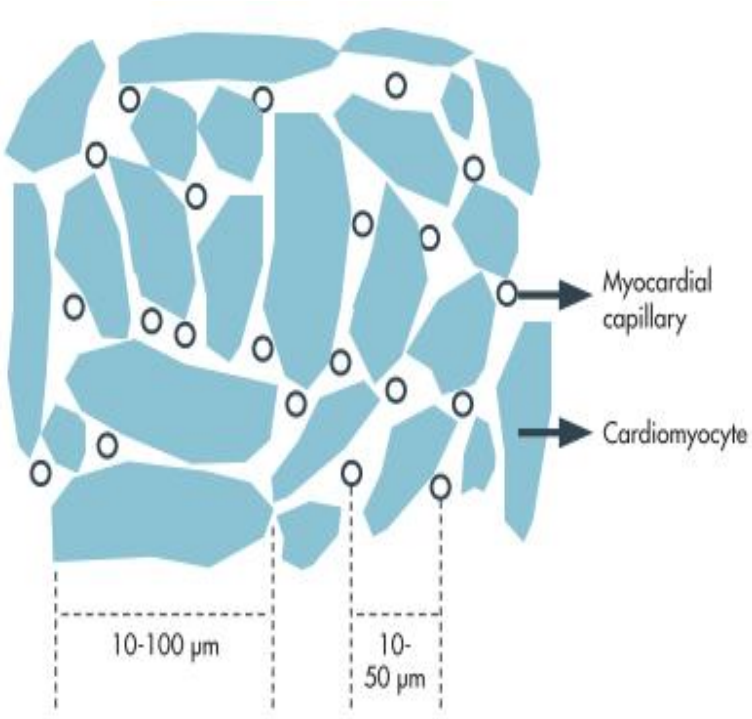

Figure 1.6: The CMEC-cardiomyocyte arrangement in the myocardium. Cardiomyocytes (approximately 10 – 100 µm in size) are surrounded by myocardial capillaries (average intercapillary distance of approximately 10 – 50 µm). Each cardiomyocyte is associated with at least 3-4 capillaries (Strijdom & Lochner 2009).

1.3 Nitric Oxide (NO)

The following sections will provide information on the properties of NO, its functional role and regulation.

1.3.1 NO properties

Various vasodilating substances are secreted by ECs. These include NO, prostacyclin, hydrogen sulphide, carbon monoxide, arachidonic acid metabolites, endothelium derived hyperpolarising factor (EDHF) and reactive oxygen species (ROS). All of these factors can hyperpolarise underlying vascular smooth muscle cell membranes and result in vasodilation (Félétou & Vanhoutte 2009). Induction of endothelial NO-release has been identified as the main mechanism by which some anti-dyslipidaemic drugs elicit their vasodilating and pleiotropic responses. In view of this, the current study focussed on NO-related mechanisms.

The story of NO started almost 25 years ago, when Robert Furchgott (Furchgott and Zawadzki 1980) discovered that isolated aortas relaxed in an endothelium-dependent manner after administration of acetylcholine. The endothelium-dependent factor that was released upon stimulation by acetylcholine was later identified as NO (Furchgott 1988). NO is a diatomic radical with a dichotomous nature. It can exert distinctly different actions under seemingly similar pathological conditions (Thomas *et al.,* 2010). It is a gas which makes it highly diffusible and enables it to move quickly between target and adjacent cells (Lei *et al.,* 2013) and has a half-life of 3-5 seconds (Rodeberg *et al.,* 1995).

In mammals NO can be synthesized by the enzyme nitric oxide synthase (NOS), which exists in three different isoforms, namely neuronal NOS (nNOS/NOS I), inducible NOS (iNOS/NOS II) and endothelial NOS (eNOS/NOS III) (Förstermann & Sessa 2011). NOS utilizes L-arginine as substrate and along with the co-substrates, molecular oxygen and reduced nicotinamide-adenine-dinucleotide phosphate (NADPH), it produces NO and L-citrulline as end- products (figure 1.7).

Furthermore, flavin adenine dinucleotide (FAD), flavin mononucleotide (FMN) and (6R-)5,6,7,8-tetrahydro-L-biopterin (BH_4) have been identified as co-factors for all three NOS isoforms (Strijdom *et al.,* 2009a; Michel & Vanhoutte 2010; Förstermann & Sessa 2011).

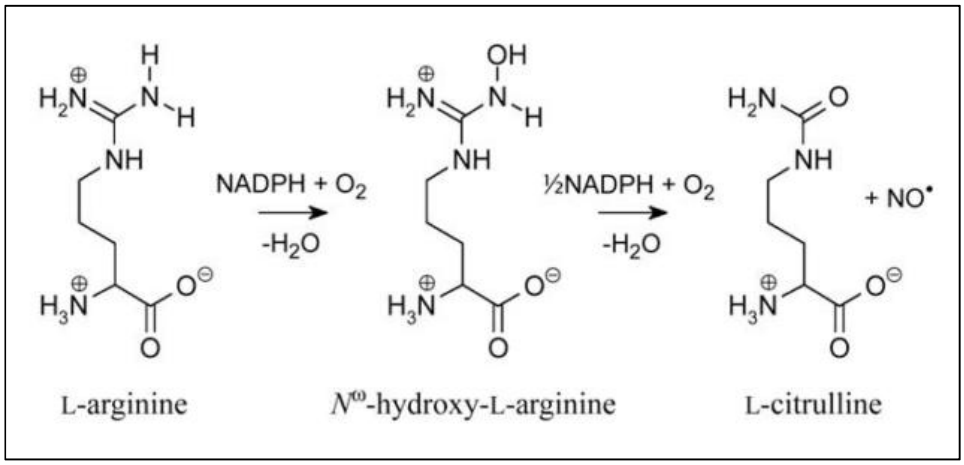

Figure 1.7: Illustration of the NOS-dependent NO synthesis process. A simple illustration of the process of electron transfer during NO synthesis (modified from Daff 2010).

Two molecules of oxygen are required for the synthesis of one NO molecule (Lepore 2000). The synthesis process will be discussed in more detail under section 1.3.4.

NO is oxidised and broken down into the stable end-products, called nitrites (NO_2^-) and nitrates (NO_3^-). Approximately 70% of all circulating inorganic nitrites is generated via the NOS/NO pathway (Kleinbongard *et al.,* 2003). Nitrites can serve as substrate for NO since they can be converted back to NO through a non-enzymatic reduction of deoxyhaemoglobin, which acts as nitrite reductase in the circulation (Cosby *et al.,* 2003). This provides an alternative pathway for NO synthesis and is especially relevant under conditions of hypoxia or ischaemia when there is a shortage of oxygen, which is a co-substrate for NO synthesis through the NOS pathway (Lepore 2000).

1.3.2 Functional role of NO

A variety of stimuli can elicit the release of NO. These stimuli include physical forces such as shear stress, circulating hormones (catecholamines, vasopressin, aldosterone), plasma constituents (thrombin, sphingosine-1-phosphate), platelet products (serotonin, adenosine diphosphate [ADP]), and autacoids (histamine, bradykinin, prostaglandin) (Lüscher and Vanhoutte, 1990; Vanhoutte *et al.,* 2009; Michel & Vanhoutte 2010). Once synthesised, NO can exert a variety of effects impacting on vascular homeostasis (figure 1.8).

A

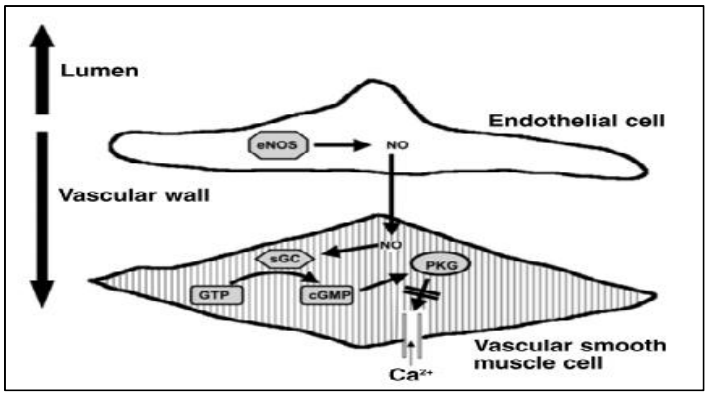

B

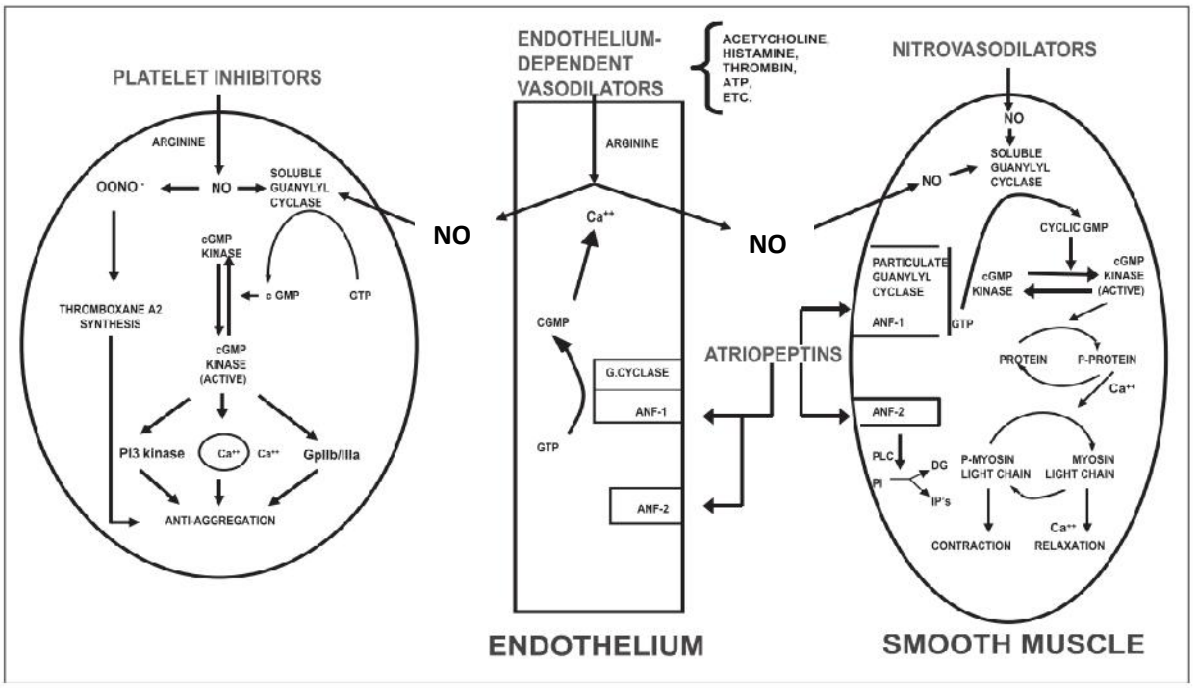

Figure 1.8: A) NO produced by NOS diffuses from the endothelial cells into underlying vascular smooth muscle cells (VSMC), activates the sGC-cGMP-PKG pathway and leads to closure of L-type Ca^{2+} channels, ultimately resulting in vasodilation. B) Effects of nitrovasodilators, endothelial-dependent vasodilators and atriopeptins on cyclin guanosine monophosphate (cGMP) and vascular relaxation. GTP indicates guanosine-5-triphosphate; ANF, atrial natriuretic factor; $ONOO^-$, peroxynitrite; NO, nitric oxide; sGC, soluble guanylyl cyclase; PI3, phosphoinositide 3; Gp, glycoprotein; PKG, protein kinase G; PLC, phospholipase, PI, phosphatidylinositol; DG, diacylglycerol; IP, inositol 3 or 4 phosphate (modified from Strijdom et al., 2009a and Bian & Murad 2008).

According to Dudzinski *et al.,* (2006), the interaction of NO with the metal centres of other molecules represents the classic mechanistic action of NO. The most well-known haemoprotein target of NO is guanylate cyclase, through which NO exerts its potent vasodilatory effects. It has been well described that once NO is released from the endothelial cells, it can lead to stimulation of soluble guanylyl cyclase (sGC) in underlying vascular smooth muscle cells which will catalyse the conversion of guanine triphosphate (GTP) to the second messenger cyclic guanosine monophosphate (cGMP). Increased levels in cGMP lead to the activation of protein kinase G (PKG), ultimately resulting in vasodilation via inhibition of the L-type calcium channels (figure 1.8 A) (Strijdom, *et al.,* 2009a) or via activation of the myosin light-chain phosphatase (MLCP) (figure 1.8 B) (Bian & Murad 2008).

NO is an important signalling molecule involved with mediating vascular endothelial growth factor (VEGF)-induced increases in endothelial cell proliferation and permeability. Furthermore, NO possesses anti-atherogenic properties by decreasing platelet aggregation, platelet and leukocyte adhesion, vascular smooth muscle cell proliferation as well as apoptosis (Radomski *et al*., 1987; Garg & Hassid 1989; Dimmeler *et al*., 2000; Venema 2002; Shaw *et al.*, 2011). NO protects the vascular wall by inhibiting the actions of powerful platelet-derived vasoconstrictive factors such as serotonin and thromboxane A_2. Whenever there is a disruption in the endothelial barrier, platelets can approach vascular smooth muscle cells, release vasoconstrictors and initiate the vascular phase of haemostasis (Michel & Vanhoutte 2010) (figure 1.9).

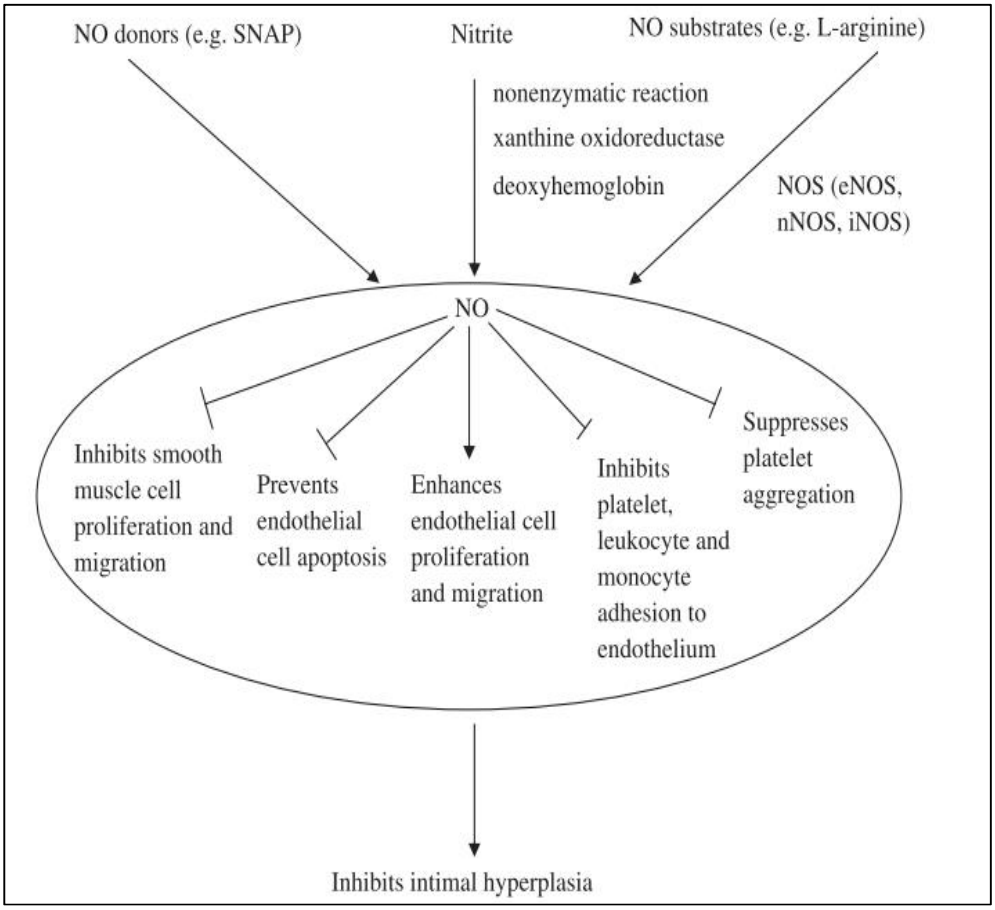

Figure 1.9: Vasculoprotective effects of NO. NO can be converted from NO donors; or released from nitrite by nonenzymatic reaction, or deoxyhaemoglobin, or xanthine oxidoreductase; or generated from substrate L-arginine via catalysis by NOS. NO inhibits smooth muscle cell (SMC) proliferation and migration; prevents endothelial cell apoptosis while enhancing endothelial cell proliferation and migration; NO also inhibits platelet, leukocyte and monocyte adhesion to endothelium and suppresses platelet aggregation. All of these effects account for inhibition of intimal hyperplasia (from Lei et al., 2013).

1.3.3 The effects of NO on the heart

NO exerts positive inotropic effects on the heart, enhancing basal cardiac function (Massion *et al.*, 2003; Rastaldo *et al.,* 2007). When intracoronary NOS is inhibited by inhibitors such as N^G-Monomethyl-L-arginine monoacetate (L-NMMA), left ventricular pressure is decreased (Cotton *et al.,* 2001). Basal heart rate is regulated by NO, this is evident by low concentrations of NO donors increasing heart rate, while high concentrations lead to a negative chronotropic effect (Cotton *et al*., 2001). Low concentrations of NO also result in an increased β-adrenergic response, while high NO concentrations will attenuate this response. Increased NO bioavailability further enhances the Frank-Starling mechanism leading to increased aortic output (Angelone *et al*., 2012).

Studies on the hearts of eNOS knock out mice showed larger infarct sizes following an ischaemia/reperfusion insult (Jones *et al*., 1999; Kanno *et al.,* 2000). Also, eNOS transgenic mice with overexpressed eNOS showed smaller infarct sizes (Ohashi *et al.*, 1998; Van Haperen *et al.*, 2002). These findings clearly demonstrate the cardioprotective role of NO in the heart. Of interest to the current study, anti-dyslipidaemic drugs such as statins and fibrates have previously been shown to exert pleiotropic effects on the eNOS-NO pathway (unrelated to their effects on lipid parameters) by increasing NO levels in the heart via activation of eNOS (Harris *et al.,* 2004; Murakami *et al*., 2006; Li *et al*., 2012). NO plays an important role in mitochondria where it binds to the oxygen binding centre of cytochrome C oxidase and can lead to cytochrome C oxidase inhibition. Binding of NO to cytochrome C is a reversible process. However, under conditions of oxidative stress, NO can combine with superoxide to form peroxynitrite, which binds irreversibly to cytochrome C oxidase (Srinivasan & Avadhani 2012). This results in decreased mitochondrial respiration and depolarization of the inner mitochondrial membrane. In the pathological context, NO-dependent regulation of mitochondrial respiration can contribute to cardiac hypertrophy and heart failure (Shiva *et al*., 2001).

1.3.4 Enzymatic sources of NO: eNOS, nNOS and iNOS

1.3.4.1 NOS isoforms

All three isoforms, eNOS, nNOS and iNOS are expressed in mammalian tissue (Förstermann & Sessa 2011). eNOS and nNOS are constitutively expressed, while iNOS expression can be induced upon stimulation by pro-inflammatory cytokines (Ziolo & Bers 2003; Strijdom *et al*., 2009a).

Even though the NOS isoforms share 50-60% sequence identity they have unique regulatory and catalytic activity (Michel & Vanhoutte 2010). Similar binding sites for NADPH, FAD, FMN and CaM have been identified in all three NOS isoforms (Bredt *et al.,* 1991; Lamas *et al.,* 1992; Lyons *et al.,* 1992). NOS enzymes consist of an oxygenase domain containing an N-terminal and reductase domain containing a C-terminal. The oxygenase and reductase domains are connected via a calcium-calmodulin binding domain. The haem and BH_4 binding sites are found on the oxygenase domain, while NADH, FAD and FMN binding sites reside in the reductase domain (figure 1.10). The reductase domain of NOS is structurally similar to the dual-flavin enzyme NADPH-cytochrome P-450 reductase (Gorren & Mayer 2007; Daff 2010). Both NOS and cytochrome P-450 function via the transfer of electrons from the NADPH prosthetic group in the reductase domain to haem (another redox component) in the oxygenase domain (Siddhanta *et al.,* 1998; Panda *et al.,* 2001). Following this, the haem iron binds to and activates oxygen to catalyse the oxidation of L-arginine to NO (Stuehr 1997). Dimerization of the NOS enzyme is required for full enzymatic activity (Stuehr 1997), however in the absence of substrates and co-factors NOS can "uncouple" and instead of producing NO it will produce the reactive oxygen specie, superoxide (Pou *et al.,* 1992; Govers & Rabelink 2001). eNOS uncoupling is a phenomenon associated with endothelial dysfunction and thus also with disease conditions such as atherosclerosis (Heitzer *et al*., 2001; Grover-Páez & Zavalza-Gómez 2009) (figure 1.10).

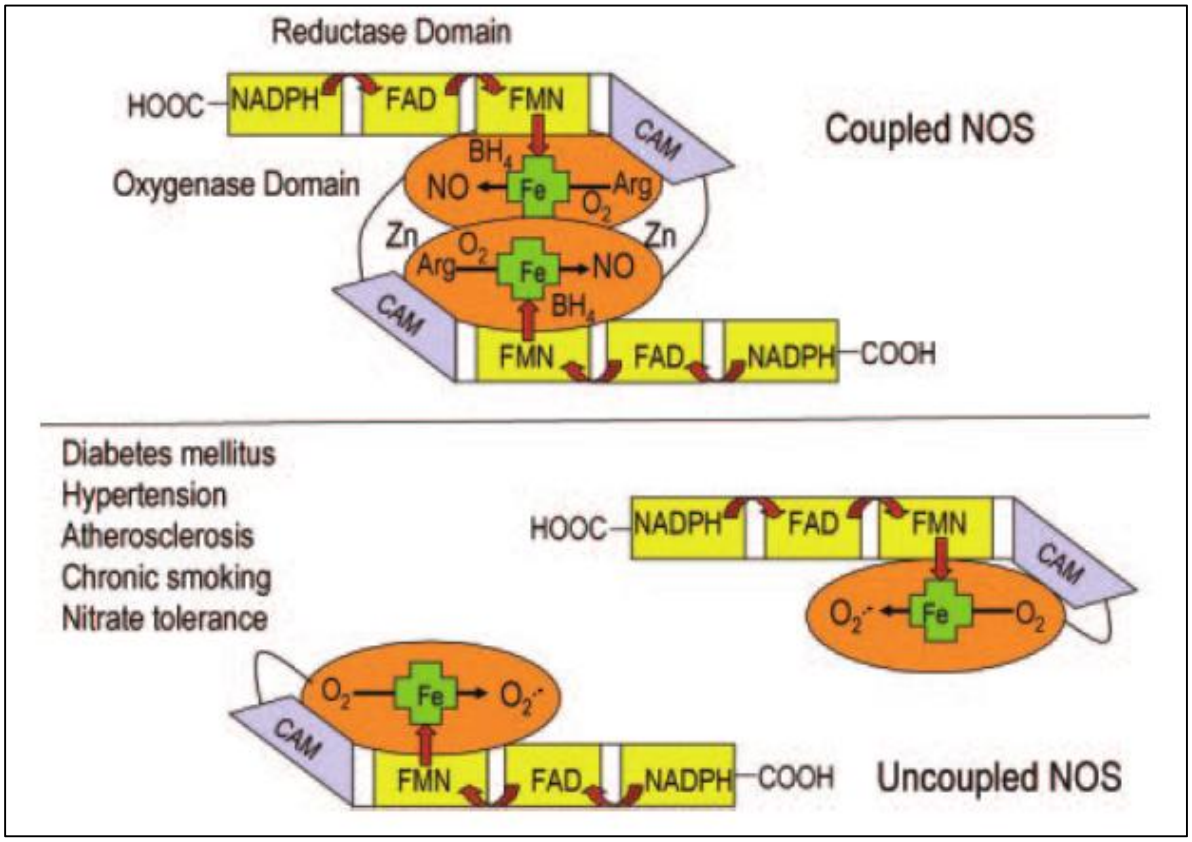

Figure 1.10: Scheme depicting electron flow in coupled vs uncoupled eNOS. Electron flow is initiated at NADPH and transferred to the flavins (FAD and FMN) of the reductase domain, which deliver the electrons to the iron of the haem (oxygenase domain). BH_4 is suggested to be an essential electron and proton donor to versatile intermediates in the reaction cycle of L-arginine/O_2 to L-citrullin/NO. Calmodulin (CaM) controls electron flow in eNOS. Zinc ions (Zn) bound to NOS are required for dimer formation and stability. Monomeric eNOS or BH_4/L-arginine-deficient eNOS is uncoupled and produces O_2^- (Münzel et al., 2005).

nNOS contains an extra 250-amino acid N-terminal leader sequence (PDZ domain) not found in eNOS or iNOS (figure 1.11). This domain is not required for dimerization, binding of co-factors or NO synthesis. It is only involved with binding proteins targeting nNOS to certain locations in the cell (Brenman *et al.,* 1996; Stuehr 1997). Binding of co-factors (haem and BH_4) is important for promoting dimerization (Marletta 1993), especially for iNOS (Michel & Vanhoutte 2010). Monomeric NOS does not bind BH_4 or substrate (Marletta 1993). The dimer interface is found between two N-terminal haem binding oxygenase domains and it is stabilised by a Zn^{2+} ion ligated to two cysteine thiols from each sub-unit (Raman *et al.,* 1998).

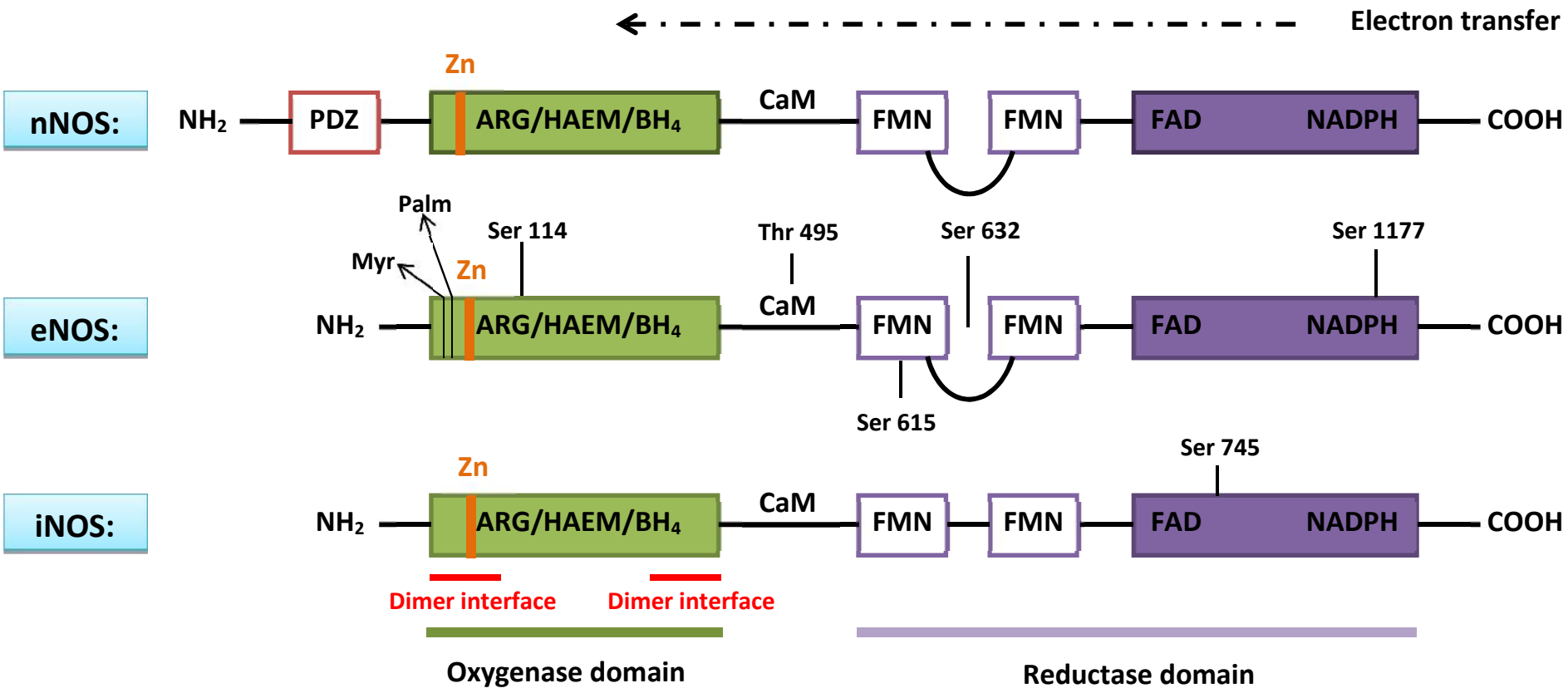

Figure 1.11: Structural composition of the three NOS enzymes involved with NO synthesis: nNOS, eNOS and iNOS. All three isoforms consist of a reductase domain containing FAD and NADPH binding sites and a FMN-FMN inhibitory loop, as well as an oxygenase domain with binding sites for arginine, haem and BH_4. nNOS has an additional PDZ-domain at the N-terminal end. Dimer formation is necessary for activation of NOS. PDZ: post-synaptic density protein, discs-large, ZO-1, Zn: zinc, CaM: calmodulin, FMN: flavin mononucleotide, FAD: flavin adenine dinucleotide, BH_4: (6R-)5,6,7,8-tetrahydro-L-biopterin, Arg: arginine (Adapted from Alderton et al., *2001 and Mount* et al., *2007).*

1.3.4.2 eNOS regulation

Considering that the current study focused on the post-translational regulation of eNOS by anti-dyslipidaemic agents, the following section will discuss this aspect of eNOS regulation in detail. Minimal attention will be given to transcriptional regulation.

1.3.4.2.1 Regulation of eNOS gene expression

In broad terms, factors influencing eNOS gene expression can be divided into physical and humoral factors as well as complex pathophysiological conditions (figure 1.12) (Braam & Verhaar 2007). Shear stress is an important modulator of the eNOS transcriptome in endothelial cells and can induce eNOS transcription (Nishida *et al.,* 1992; Malek *et al.,* 1999; Woodman *et al.,* 1999). This process is dependent on Ras, Raf and ERK 1/2 (Davis *et al*., 2001) and is mediated via nuclear factor kappa B (NF-κB) coupling to the shear stress response element *GAGACC*. NO can lead to inhibition of eNOS transcription and this is due to the inhibitory action of NO on NF-κB activity (Davis *et al.,* 2004; Grumbach *et al.,* 2005). eNOS gene expression can be down-regulated by calcium influx inhibitors and this effect seems to be enhanced by PI3-kinase (Malek *et al.,* 1999). Other humoral factors inducing eNOS gene expression include growth factors such as VEGF (Bouloumié *et al.,* 1999), basic fibroblast growth factor (bFGF), epidermal growth factor (EGF) and transforming growth factor-β (TGF-β) (Govers & Rabelink 2001). Inflammatory factors (Anderson *et al.,* 2004) and various peptide hormones (Zhang *et al.,* 2008; Sud & Black 2009) have also been shown to regulate eNOS transcription (Braam & Verhaar 2007).

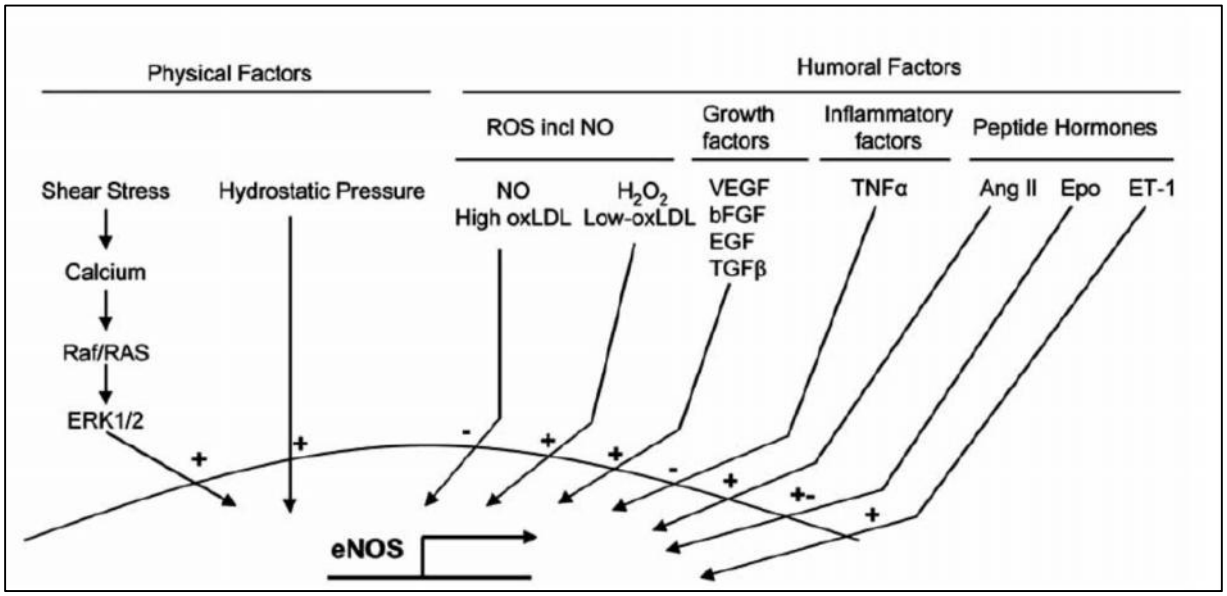

Figure 1.12: Physical and humoral factors influencing eNOS gene expression. Myr: myristoylation site, Palm: palmitoylation site, Zn: location of zinc-ligating cysteines. (From Braam & Verhaar 2007).

1.3.4.2.2 Post-translational regulation

For years eNOS was considered as solely regulated by the binding of Ca^{2+} to CaM (Bredt & Snyder 1990; Andrew & Mayer 1999; Mount *et al.,* 2007) but over the last decade or so it has become evident that the regulation of eNOS is much more complex and involves post-translational multi-site phosphorylation (Fulton *et al.,* 2001; Mount *et al.,* 2007) as well as essential co-factors and protein-protein interactions (Govers & Rabelink 2001; Fleming & Busse 2003). Post-translational modifications of eNOS underlie the dynamic regulation of its enzymatic activity (Michel & Vanhoutte 2010).

It is important to note that each regulatory mechanism does not take place in isolation but is usually interconnected with other mechanisms (Boo *et al.,* 2006). These post-translational mechanisms will subsequently be discussed.

1) Acylation and subcellular localisation

In resting cells, eNOS is targeted to the membrane, more specifically caveolae. These are membrane microdomains with caveolin as scaffolding protein (Dudzinski & Michel 2007). Caveolae are membrane lipid rafts that contain cholesterol and form flask-like invaginations of the plasma membrane (Head *et al.,* 2014). Due to their nature and location, caveolae sequester diverse receptors and signalling proteins from signalling cascades, including G-protein coupled receptors, G proteins, growth factor receptors and calcium regulatory proteins that transfer signals to downstream activators (Shaul *et al.,* 1996). eNOS can be post-translationally modified by myristoylation of Gly2 (Pollock *et al.,* 1992; Sessa *et al.*, 1992; Sase & Michel 1997) and palmitoylation of Cys 15 and Cys 26 (Robinson & Michel 1995). Myristoylation and palmitoylation anchor eNOS to the lipid bi-layer of caveolae by adding three acyl anchors (Fukata *et al.,* 2004). Depalmitoylation of eNOS, in response to prolonged agonist stimulation, will result in eNOS translocating to the cytoplasm (Michel *et al.*, 1997).

2) Intracellular calcium, calmodulin and caveolin

eNOS and nNOS contain an inhibitory loop (40-50 amino acids) within the FMN domain. This inhibitory loop destabilises calmodulin binding at low intracellular calcium levels (Fleming & Busse 1999). If calmodulin is not tightly bound to eNOS, electrons cannot be transferred from the reductase domain to the oxygenase domain, thus making catalytic activity impossible. Additionally, eNOS is inhibited by its protein-protein interaction with caveolin (Dudzinski *et al.,* 2006). Caveolins are 20kDa membrane proteins. Caveolin-1 and caveolin-2 are ubiquitously expressed and abundant in endothelial cells, whilst caveolin-3 is expressed in skeletal muscle and cardiomyocytes (Fridolfsson *et al.,* 2014). Caveolin-1 bound to eNOS serves as a gate-keeper for eNOS activation. Thus, increased intracellular Ca^{2+} fluxes lead to calmodulin binding, which leads

to the disruption of the caveolin-1 and eNOS interaction resulting in eNOS activation (Dudzinski *et al.,* 2006). According to Dudzinski *et al.* (2006), increased levels of intracellular calcium serve as the most rapid induction of eNOS activity. However, eNOS can be rapidly and strongly activated in the absence of calcium. cGMP-dependent protein kinase II (cGKII) and the catalytic subunit of cAMP-dependent protein kinase have been shown *in vitro* to phosphorylate eNOS on both Serine and Threonine residues in the absence of calcium (Butt *et al.,* 2000).

3) S-Nitrosylation

S-nitrosylation is another dynamic receptor-mediated post-translational modification which contributes to the regulation of eNOS when it is membrane localised (Dudzinski *et al.,* 2006). In resting endothelial cells, eNOS is inhibited as a result of S-nitrosylation at the cysteine residues, Cys 94 and Cys 99. Cys 94 and Cys 99 form part of the zinc tetrathiolate cluster. In response to eNOS agonist stimulation, eNOS will be rapidly denitrosylated at a rate similar to increased catalytic activity (Ravi *et al.,* 2004; Erwin *et al.,* 2005).

4) Phosphorylation of eNOS

Phosphorylation and dephosphorylation of the enzyme complement other mechanisms of regulation (Dudzinski & Michel 2007) and is an important post-translational modification on which we focussed in the present study. eNOS can be phosphorylated on serine (Ser), threonine (Thr) and tyrosine (Tyr) residues. Five serine/threonine phosphorylation sites have been identified. Phosphorylation of Ser 1177 and Ser 632 are associated with enhanced eNOS activity. Thr 495 phosphorylation is associated with eNOS inhibition and the actions of Ser 114 and Ser 615 remain controversial. Tyr 83 has been identified as a mediator of eNOS activity but little is known about the exact contribution. Tyr 657 has been shown to be involved with attenuation of eNOS activity. These phosphorylation sites will be discussed in detail in the next section (all of these sites are numbered according to their human sequence). Figure 1.13 summarises the factors involved with eNOS regulation. The following phosphorylation sites will be discussed:

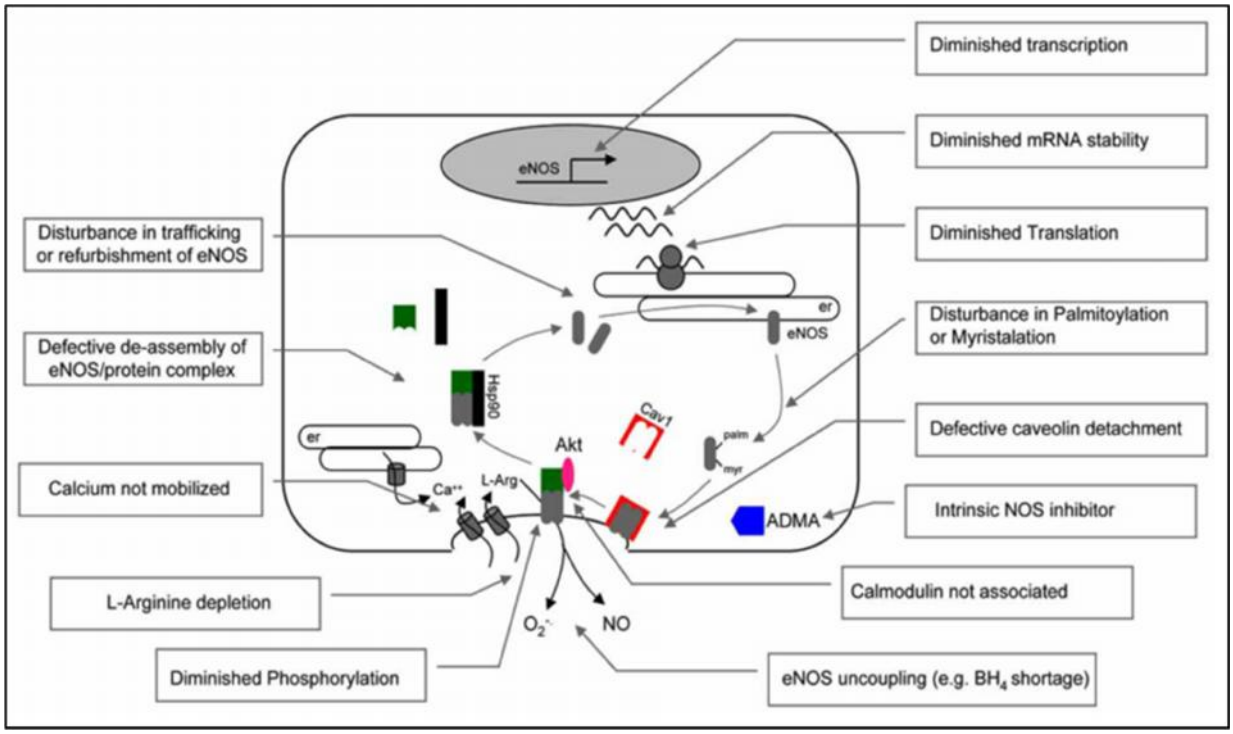

Figure 1.13: Principle disturbances in eNOS function to produce nitric oxide (Braam & Verhaar 2007).

a) eNOS Ser 1177

Phosphorylation of Ser 1177 is associated with enhanced activity of the enzyme (Schulz *et al.,* 2009). This phosphorylation site is situated in the reductase domain, close to the C-terminal (Mount *et al.,* 2007). Phosphorylation of this site was first described by Chen *et al.,* 1999 who showed Ser 1177 to be phosphorylated by AMPK during myocardial ischaemia. They showed recombinant and rat heart purified eNOS to be phosphorylated in the presence of AMPK. They also showed Ser 1177 to be the most prominent phosphorylation site. During ischaemia, eNOS phosphorylation at Ser 1177 was increased 3-fold, but not Thr 495 (Chen *et al.,* 1999). AMPK directly phosphorylates eNOS Ser 1177 by promoting its association with HSP90. The role of HSP90 will be discussed later in this section. Physiological stimuli known to induce AMPK-mediated activation of eNOS

include vascular endothelial growth factor, high-density lipoprotein, adiponectin, shear stress, hydrogen peroxide, ghrelin, thrombin and oestrogen (Schulz *et al.*, 2009)

Besides AMPK, several other upstream kinases have been identified as regulators of Ser 1177 phosphorylation. These include protein kinase B (PKB)/Akt (Dimmeler *et al.,* 1999; Michell *et al*., 1999; Strijdom *et al*., 2009b), protein kinase A (PKA) (Boo *et al.*, 2002), protein kinase C (PKC) (Michell *et al.,* 2001; Wang *et al.,* 2010b) and Ca^{2+}/Calmodulin-dependent protein kinase (CaMKII) (Chen *et al.,* 1999).

Heat shock protein 90 (HSP90) has been shown to play an important role in recruiting PKB/Akt to phosphorylate eNOS at Ser 1177. It has been identified as a chaperone protein for interaction with eNOS (Taipale *et al.,* 2010). Inhibiting HSP90 leads to deactivation of PKB/Akt (via degrading of PDK-1) and thus results in reduced phosphorylation of eNOS Ser 1177. HSP90 is important for initial phosphorylation of eNOS Ser 1177, but also the maintenance of this state. HSP90 can be seen as a scaffold for PKB/Akt to phosphorylate eNOS (Wei & Xia 2005).

Other types of stimuli activating Ser 1177 include mechanical (shear stress) (Michel *et al.,* 1997; Fisslthaler *et al.,* 2000), humoral factors such as bradykinin (Harris *et al.,* 2001; Lowry *et al.,* 2013), insulin (Zecchin *et al.,* 2007; Huisamen *et al.,* 2011), sphingosine 1-phosphate (Igarashi *et al.,* 2001; Rikitake *et al.,* 2002) as well as pharmacological activators such as statins (Harris *et al.,* 2004; Li *et al.,* 2012) and fibrates (Murakami *et al.,* 2006; Tomizawa *et al.,* 2011). Since many of these factors fall outside the scope of this study, for more detail see a review by Mount *et al*., (2007).

b) eNOS Ser 632

Phosphorylation of eNOS Ser 632 has been shown to increase the activity of the enzyme (Bauer *et al.,* 2003; Schulz *et al.,* 2009) and therefore NO synthesis. Bauer *et al.* (2003) stated that eNOS Ser 1177 is the major site for phosphorylation in response to agonist stimulation, while Ser 632 is responsible for basal levels of NO. It is known that many stimuli that activate and phosphorylate Ser 1177 also phosphorylate Ser 632; however, the rate of Ser 632 phosphorylation is much slower and Ca^{2+} -independent, and serves to maintain NO generation after the initial burst of NO via Ser 1177 phosphorylation (Schulz *et al.*, 2009).

Ser 632 is situated in the CaM autoinhibitory sequence of eNOS, which is contained in the FMN domain (Michell *et al.,* 2002; Bauer *et al.,* 2003). As stated above, several stimuli that activate eNOS Ser 1177 have also been shown to activate Ser 632, namely ATP, bradykinin, VEGF, shear stress and statins (Boo *et al.,* 2002; Michell *et al.,* 2002; Bauer *et al.,* 2003; Harris *et al.,* 2004). The primary kinase involved with Ser 632 phosphorylation and activation, has been identified as PKA (Boo *et al.,* 2002; Boo *et al.,* 2003; Harris *et al.,* 2004) whereas PKB/Akt is unable to phosphorylate this site (Michell *et al.,* 2002).

c) eNOS Thr 495

This site is situated in the CaM-binding sequence between the reductase and oxygenase domains (Chen *et al*., 1999). eNOS Thr 495 is a negative regulatory site and phosphorylation is associated with inhibition of enzyme catalytic activity (Fleming *et al*. 2001; Fleming & Busse 2003). According to Fleming & Busse (2003), eNOS Thr 495 is constitutively phosphorylated in all endothelial cells and substantially more CaM will bind to eNOS when it is dephosphorylated. Fleming *et al*. (2001) showed that before eNOS can be activated in response to Ca^{2+}-elevating agents such as bradykinin, rapid changes take place in Ser 1177 and Thr 495 and that the association of CaM with eNOS is dependent

on dephosphorylation of Thr 495. The interference of Thr 495 with CaM binding explains its inhibitory effect on eNOS (Fleming *et al.,* 2001).

The major kinase involved with Thr 495 phosphorylation is protein kinase C (Mount *et al.* 2007). Chiasson *et al*. (2011) identified the specific PKC isoform as $PKC\beta_{II}$. Increased levels of Thr 495 phosphorylation were also associated with endothelial dysfunction. Chen *et al.* (1999) found that in the absence of Ca^{2+}/CaM, AMPK is able to phosphorylate eNOS Thr 495 resulting in inhibition of the enzyme.

d) eNOS Ser 615

The exact role and contribution of eNOS Ser 615 to enzyme activity remain unclear. The available data on Ser 615 phosphorylation are mixed. Boo *et al.* (2002) showed that Ser 615 was phosphorylated under shear stress as well as in response to VEGF and cAMP stimulation. This was due to a PKA dependent, but PI3 kinase independent mechanism. The slow manner in which Ser 615 was phosphorylated suggests a possible role in chronic regulation of eNOS. Ser 615 as activator of eNOS has been suggested by different authors (Michell *et al.* 2002; Bauer *et al*. 2003; Harris *et al*. 2004) since it was also activated by eNOS agonists such as bradykinin, VEGF, ATP and statins, but even within these studies, the findings remained contradictory. Bauer *et al*. (2003) found increased activity with a S615D mutant while the serine to alanine mutant (S615A) which mimicked dephosphorylation, resulted in increased levels of basal and agonist induced NO release. Michell *et al.* (2002) found that a serine to aspartate mutation (S615D) mimicking phosphorylation at Ser 615, increased Ca^{2+}/calmodulin sensitivity without changing enzyme activity.

e) eNOS Ser 114

This is the only phosphorylation site situated in the oxygenase domain and the function of Ser 114 is also controversial (Mount *et al.,* 2007). It has been proposed that

dephosphorylation of this site results in activation of eNOS (Kou *et al.,* 2002). In contrast, another study found that shear stress and HDL resulted in phosphorylation of Ser 114 and it was proposed to be an activating stimulus (Gallis *et al*., 1999; Drew *et al*., 2004). Complicating the matter further, Boo *et al*. (2002) found no change in phosphorylation of Ser 114 with shear stress and VEGF as stimuli. The role of eNOS Ser 114 therefore remains inconclusive.

f) Tyrosine phosphorylation

Little is known about the effect of eNOS tyrosine phosphorylation on eNOS activity. Tyrosine kinase and phosphatase inhibitors can modulate eNOS derived NO (Fleming & Busse 1996; Fleming *et al.,* 1998; Fisslthaler *et al.,* 2000; Fleming & Busse 2003; Loot *et al.,* 2009). It has also been reported that tyrosine phosphatase inhibitors can activate eNOS independently of Ca^{2+} (Fleming *et al*., 1998).

Fulton *et al*. (2005) showed phosphorylation at eNOS Tyr 83 by the kinase c-Src and this was associated with increased enzyme activity. eNOS forms homodimers with a large dimer interface in the crystal structure and as already mentioned, dimerization is essential for activity (Govers & Rabelink 2001; Mount *et al.,* 2007; Förstermann & Sessa 2011). Tyr 83 is located on a β-strand of the crystal structure in close proximity of the dimer interface. Since Tyr 83 phosphorylation does not directly modulate eNOS activity it is possible to speculate that Tyr 83 acts as a docking station for Src-homology proteins (Fulton *et al*., 2005).

Phosphorylation of Tyr 657 has been linked to shear stress (Fisslthaler *et al*., 2008) as well as angiotensin II and low concentrations of hydrogen peroxide via proline-rich tyrosine kinase 2 (PYK2) (Loot *et al.,* 2009). Phosphorylation of the enzyme at this site attenuates NO production (Fisslthaler *et al*., 2008; Loot *et al*., 2009). Fisslthaler *et al*. (2000) and Fleming & Busse (2003) attributed the lack of information on this residue to the fact that researchers have been struggling to show tyrosine phosphorylation of eNOS in any cells

other than primary cell cultures or low passages of endothelial cells (Garcia-Cardena *et al*., 1996; Fleming *et al*., 1998).

1.3.4.3 nNOS regulation

nNOS is responsible for the NO production in neuronal tissues and is located in the synaptic spines (Zhou & Zhu 2009). It is expressed in skeletal muscle, cardiac muscle, smooth muscle cells (Schwarz *et al*., 1999; Xu *et al*., 1999; Rothe *et al*., 2005) and the pancreas (Arciszewski 2007). Schwarz *et al*. (1999) only found nNOS immunoreactivity in smooth muscle cells of rat aorta but not in the endothelium layer. Bers & Ziolo (2014) showed that nNOS is localized in the sarcoplasmic reticulum (SR) and co-immunoprecipitated with ryanodine receptors (RyRs).

1.3.4.3.1 Gene expression

nNOS has been shown to be upregulated under various conditions, including cutaneous wound repair (Boissel *et al*., 2004) and cardiac ischaemic preconditioning (Wang *et al*., 2004).

1.3.4.3.2 Post-translational regulation

The following post-translational mechanisms are involved with nNOS regulation:

1) **Dimerization**

As is the case with eNOS, dimerization is also required for activation and functioning of nNOS. It also requires the binding of substrate L-arginine and co-factors for activation, with electrons flowing from the reductase domain to the oxygenase domain (Zhou & Zhu 2009). nNOS activity can be inhibited by the protein inhibitor called PIN, an associated protein inhibitor of nNOS. Binding of PIN destabilizes nNOS dimerization (Fan *et al*., 1998).

2) Phosphorylation

nNOS phosphorylation is an important post-translational modification required for enhanced enzyme activity. Phosphorylation of nNOS at Ser 847 reduces nNOS activity by inhibition of Ca^{2+}/CaM binding. This is mediated via protein kinase CaMKII phosphorylation of nNOS (El-Mlili *et al*. 2008). Conversely, activity of nNOS can be increased by decreased levels of Ser 847 phosphorylation mediated via protein phosphatase 1 (PP1) (Rameau *et al*., 2004). Phosphorylation of nNOS Ser 1412 will result in increased levels of catalytic activity (Adak *et al*., 2001). It has also been shown that nNOS can be phosphorylated on tyrosine residues, resulting in increased levels of NO and protection against hypoxia in brain tissue (Mishra *et al*., 2009).

3) Cellular localization and protein-protein interactions

In neurons, nNOS occurs in a soluble and particulate protein form and subcellular localization varies greatly among cell types (Förstermann *et al*., 1998; Ziolo & Bers 2003).

As mentioned previously, nNOS is structurally different from eNOS and iNOS. It contains a PDZ (post-synaptic density protein, discs-large, ZO-1) domain in the N-terminal. This domain participates in dimer formation and activation since it can interact with various other proteins in specific regions of the cell (Cui *et al*., 2007; Chen *et al*., 2008 Zhou & Zhu 2009). The PDZ-domain is able to anchor nNOS to membrane or cytosolic proteins via direct PDZ-PDZ interactions, which can modify NO signalling. One example is the binding of the nNOS-PDZ domain to post-synaptic density protein-95 (PSD95), a synaptic scaffolding protein and integral component of the post-synaptic density, which links nNOS to N-methyl-D-aspartate receptor (NMDAR). This results in efficient activation of nNOS by NMDAR. Other protein targets for the PDZ domain have been identified, such as phosphofructokinase (PFK-M) and a nNOS adapter protein, CAPON (Zhou & Zhu 2009) however, since it falls outside the scope of this study, it will not be discussed in detail.

It has been suggested that CaM acts as an allosteric activator for nNOS (Zhou & Zhu 2009). As is the case with eNOS, increased levels of intracellular Ca^{2+} will result in CaM binding to nNOS and electron transfer from the reductase domain to the oxygenase domain (Roman & Masters 2006). In an immortalized neuroepithelioma cell line (A673), nNOS was shown to be inactive at basal levels of intracellular Ca^{2+} , whereas increased intracellular Ca^{2+} levels will cause CaM to bind to, and activate nNOS (Dreyer *et al*., 2004).

As is the case with eNOS, nNOS has also been reported to form complexes with HSP90 and caveolin. nNOS-HSP90 complex formation will increase NO production (Bender *et al.,* 1999) and this is a result of HSP90 enhancing binding between nNOS and CaM resulting in nNOS activation (Song *et al*., 2001).

Caveolin-3 (the skeletal muscle isoform of caveolin) can act as a gatekeeper for nNOS activation as it prevents CaM binding, thus inhibiting nNOS (Stamler & Meissner 2001).

1.3.4.4 iNOS regulation

While eNOS and nNOS are associated with the maintenance of basal levels of NO in a Ca^{2+}/CaM dependent fashion, iNOS has traditionally been associated with high output NO-release in response to pathological stimuli such as pro-inflammatory cytokines (Buchwalow *et al*., 2001) and in many cases associated with cytotoxic peroxynitrite formation (Strijdom *et al.,* 2009b; McNeill & Channon 2012).

1.3.4.4.1 Gene and protein expression

NO produced by iNOS is mostly regulated on a transcriptional level. Various signalling pathways have been identified in the activation of iNOS transcription. These include PKC, tyrosine kinase, janus kinases, raf-1 protein kinase and mitogen activated protein kinases (MAP kinase) (Aktan 2004). Regulation of iNOS is distinctly different from eNOS and nNOS regulation. iNOS is not normally expressed in cells, but expression can be induced by pro-inflammatory cytokines such lipopolysaccharide (LPS) (Nikolaeva *et al.,* 2012), interleukin-1β (IL-1β) (Lowry *et al.,* 2013) and

tumor necrosis factor alpha (TNF-α) (Yoshioka *et al*., 2012). Expression of iNOS is regulated by transcription factors such as nuclear factor kappa B (NF-κB) and activating protein-1 (AP-1) (Xia *et al*., 2001).

iNOS was initially identified in macrophages (Xie *et al*., 1992), where it plays an important role in the immune system due to its antimicrobial and anti-tumour function (Bogdan *et al*., 2000; Bogdan 2001; Blanchette *et al*., 2003) but its expression has since been shown in a variety of tissues including renal mesangial cells (Pheilschifter & Vosbeck 1991), cardiac myocytes (Strijdom *et al*., 2009b), endothelial cells (Singh et al., 1996), smooth muscle cells (Junquero et al., 1992), fibroblasts (Shindo *et al.,* 1994) and keratinocytes (Arany *et al.,* 1996), provided the appropriate agent is used for induction (Förstermann & Sessa 2011).

Interestingly, iNOS expression can also be related to peroxisome proliferator-activated receptors (PPARs). PPARs can antagonize the effects of transcriptional factors involved with iNOS expression (Chinetti *et al*., 1998)

1.3.4.4.2 Post-translational regulation

iNOS-derived NO is also regulated post-translationally, however, the mechanisms are not clear (Aktan 2004). The following mechanisms have been identified:

1) **Synthesis and Degradation**

The issue of the balance between synthesis and degradation is also valid for iNOS as post-translationally, it is regulated by either protein synthesis or degradation (Aktan 2004). A reduction in protein synthesis of iNOS results in a reduction of enzyme activity. On the other hand, transforming growth factor β (TGF-β) is known to down-regulate iNOS via increased degradation (Matsuno *et al.,* 2001). The effect of TGF-β on degradation is indirectly mediated by the proteasome pathway (Musial & Eissa, 2001).

2) Dimerization

iNOS can also be regulated via structural stability, i.e. factors that influence the ability to form a dimer. Kalirin (playing a neuroprotective role during inflammation), (Ratovitski *et al*., 1999a), macrophage product and inducible NOS associated protein (NAP 110) can prevent dimerization of iNOS and therefore exert an inhibitory effect on the enzyme (Ratovitski *et al.* 1999ba). Dimerization of iNOS is initiated by haem insertion. This leads to a conformational change in protein structure and allows incorporation of haem into the oxygenase domain (Panda *et al.,* 2002). Binding sites for L-arginine and BH4 are then exposed (Ghosh *et al.,* 1996) and iNOS forms a tight dimer (Panda *et al.,* 2002). BH4 is very important for iNOS dimerization (Stuehr 1999).

3) Substrate and co-factor availability

Of the three NOS isoforms, iNOS-protein has the shortest sequence. It is able to bind CaM at all physiological Ca^{2+} concentrations and is not dependent on Ca^{2+} regulation (Cho *et al*., 1992; Daff 2010). It is however, dependent on availability of substrate, L-arginine as well as co-factors haem, BH_4 and NADPH. A shortage of any of these factors can regulate iNOS activity on a post-translational level (Taylor *et al*., 1998; Mori & Gotoh 2000).

4) Phosphorylation

Little is known about the phosphorylation of iNOS. It has been shown by Pan *et al*. (1996) that iNOS can be phosphorylated on tyrosine residues by tyrosine kinases and phosphorylation was associated with increased activity of iNOS, even though no increase in total expression was found. Zhang *et al.* (2007) showed that iNOS can be phosphorylated at the Serine 745 site, which was associated with a "super output" of NO. This phenomenon was mediated via a B_1-kinin receptor dependent activation as well as the kinase ERK1/2. However, measuring iNOS phosphorylation is complicated and commercial antibodies are not available yet.

1.3.4.5 The controversial mitochondrial NOS (mtNOS)

Reports on the existence of another isoform of NOS, namely mitochondrial NOS (mtNOS) started appearing in the late 1990's (Bates *et al*., 1995; Bates *et al.,* 1996; Ghafourifar & Richter 1997). Bates *et al*. (1995) was able to present immunocytochemical evidence for the existence of a NOS isoform in the mitochondria of brain and liver tissue, located to the inner mitochondrial membrane, but could not conclude anything about its activity. A year later mtNOS was also discovered in heart, kidney and skeletal muscle tissue and the possible role of mtNOS in oxidative phosphorylation was alluded to (Bates *et al*., 1996). Ghafourifar & Richter (1997) were able to demonstrate in rat liver, functional and NO-generating mtNOS by using L-arginine as substrate; they also revealed that the enzyme was Ca^{2+} dependent and localized on the inner mitochondrial membrane, therefore acting in a similar manner as existing NOS enzymes. In 1998, however, Tatoyan & Giulivi purified mtNOS from liver-derived mitochondrial membranes and indicated that it was similar in structure and function to constitutive NOS (eNOS and nNOS), but that it did not cross-react with any known NOS antibodies. Furthermore, the mtNOS displayed the same tight binding of CaM and immunoreactivity as iNOS. They also showed mtNOS to be catalytically active and able to produce NO. This highlighted the possible role of NO production in the mitochondria as regulator of ATP production. Since then there have been several reports claiming that mtNOS was in actual fact eNOS or nNOS or even iNOS, but there are still studies claiming that mtNOS is in fact a distinct NOS isoform [reviewed in (Lacza *et al*. 2006)]. From the literature it seems that the existence of a distinct mtNOS isoform is inconclusive and could merely be a technical peculiarity (Lacza *et al*. 2006).

1.3.5 Non-enzymatic sources

The long held belief that nitrite is merely an inert metabolite of NO has been proven wrong. Nitrates and nitrites have been used in the food preservation industry for 5000 years! In the early 19th century it was discovered that nitrates are reduced to nitrites by bacteria which led to the rationale to only use nitrites. Nitrites have been shown to delay the development of botulinum toxin, develop cured meat flavour, retard the development of rancidity during storage

and to be responsible for the red colour of cured meat due to the reaction of nitrite and oxyhaemoglobin to form S-nitroxohaemoglobin (Bryan 2006).

In the body, NO can be inactivated to nitrates and nitrites via the reaction with haemoglobin (Doyle & Hoekstra 1981; Rassaf *et al.*, 2002). The concentrations of nitrites vary depending on the tissue and compartment it is stored in, as well as NOS activity (Rodriguez *et al*., 2003; Bryan *et al*., 2004). It has been shown that approximately 70-90 % of all plasma nitrites is derived from eNOS (Kleinbongard *et al*., 2003).

Plasma nitrite can remain stable for hours, however in whole blood it is rapidly oxidised to nitrate or NO. In blood, haemoglobin serves as a nitrite reductase and will convert nitrites to NO. This process is maximally effective at 50% oxygenation. The flavoprotein enzyme, xanthine oxidase, has also been implicated in nitrite reductase activities. It can reduce molecular oxygen to superoxide at low tensions of O_2 and low pH values. Oxygen is also considered as an important competitive inhibitor of nitrite reductase by xanthine oxidase (Bryan 2006).

Nitrite reduction to NO has been implicated in the protective effects against ischaemia/reperfusion injury (Lepore 2000; Kitakaze *et al*., 2001). During ischaemia there is a lack of blood flow and therefore sufficient oxygen cannot reach the ischaemic tissue. Duranski *et al.* (2005) ascribed the protective effects due to haemoglobin acting as a nitrite reductase and thus able to convert nitrite to NO. However, Webb *et al.* (2004) in studies performed on perfused isolated hearts, failed to demonstrate the conversion of nitrites to NO. It has to be considered, however, that isolated heart perfusion experiments are conducted in the absence of blood, which suggests that the myocardial tissue may express nitrite reductases such as xanthine oxidase. The traditional NOS/NO pathway requires oxygen as co-substrate for NO synthesis, and under conditions of oxygen deficiency it is unlikely to be a major contributor to NO synthesis. Ischaemia is also associated with a low tissue pH. These factors create optimal conditions for the reduction of nitrite to NO, a reaction that only requires one electron protonation step (Bryan 2006).

Considering the inter-relationship between nitrite-derived NO and NOS-derived NO in the body, Bryan (2006) suggested that NO homeostasis is maintained with a “NOS and nitrite concert”. Each mechanism has its role under certain physiological conditions.

1.3.6 NOS uncoupling – NO versus Superoxide

As mentioned previously, the process of NO synthesis involves substrate binding, namely L-arginine, molecular oxygen and NADPH, as well as the co-factors BH_4, FAD and FMN. Furthermore binding of CaM and haem to the enzyme is essential for NO synthesis. NOS uncoupling (i.e. uncoupling of NADPH oxidation and NO synthesis) is a process which results in the generation of superoxide instead of NO by NOS (Pou *et al.,* 1992; Govers & Rabelink 2001).

In the case of eNOS, superoxide generation occurs via the haem group of its oxygenase domain (Stroes *et al*., 1998) in the absence of sufficient substrate, L-arginine and/or co-factors (Wever *et al*., 1997; Vásquez-Vivar *et al*., 1998; Channon 2004). NO synthesis will be replaced by superoxide. If the concentration of BH_4 is low, for instance, due to the inhibition of its synthesis in endothelial cells via an inhibitor of the rate limiting enzyme in BH_4 synthesis, GTP cyclohydrolase I, or eNOS dysfunction, eNOS will uncouple and generate superoxide (Ishii *et al.,* 1997; Meininger *et al.,* 2000). BH_4 supplementation in conditions such as hypercholesterolaemia (Fukuda *et al.,* 2002), hypertension (Cosentino *et al.,* 1998), diabetes (Heitzer *et al.,* 2000) and coronary artery disease (Setoguchi *et al.,* 2001) has been shown to increase the bio-availability of NO. Not only is the absolute availability of BH_4 important in the regulation of eNOS activity and uncoupling, but also the ratio of fully reduced BH_4 to partially oxidised 7,8-dihydrobioterin (BH_2) (Vasquez-Vivar *et al.,* 2002).

Similar findings have been reported on the ability of nNOS to produce superoxide from its haem domain (Pou *et al.,* 1999; Vasquez-Vivar *et al.,* 1999). In the case of iNOS, uncoupling results in superoxide generation via the reductase domain (Xia *et al.,* 1998). McNeill & Channon (2012) stated that the role of BH_4 in the control of endothelial cell nNOS and iNOS is commonly overlooked, since emphasis is normally placed on eNOS. iNOS expression is normally regarded as detrimental, especially due to its role in septic shock, but it is also involved in host defence against pathological invaders (MacMicking *et al.,* 1995). iNOS induction in inflammatory cells is associated with increased levels of *GCH1,* the gene that encodes GTP cyclohydrolase (rate limiting enzyme in BH_4 synthesis) (Crabtree *et al.,* 2009), thereby increasing BH_4 synthesis necessary for

normal iNOS functioning (Hattori *et al.,* 1996). Besides the co-induction of iNOS and BH_4 synthesis, iNOS has also been shown to decrease BH_4 levels in diseased states such as atherosclerosis (Zhang *et al*., 2007). In atherosclerotic plaques, iNOS-derived NO has been shown to increase peroxynitrite formation and lipid peroxidation (Zhang *et al*., 2007), leading to increased ROS in the vasculature (Ponnuswamy *et al*., 2009). The regulation of iNOS-dependent NO and ROS production by available BH_4, plays and important role in vascular diseases. These effects may be opposing those of BH_4 and eNOS (McNeill & Channon 2012) (figure 1.14).

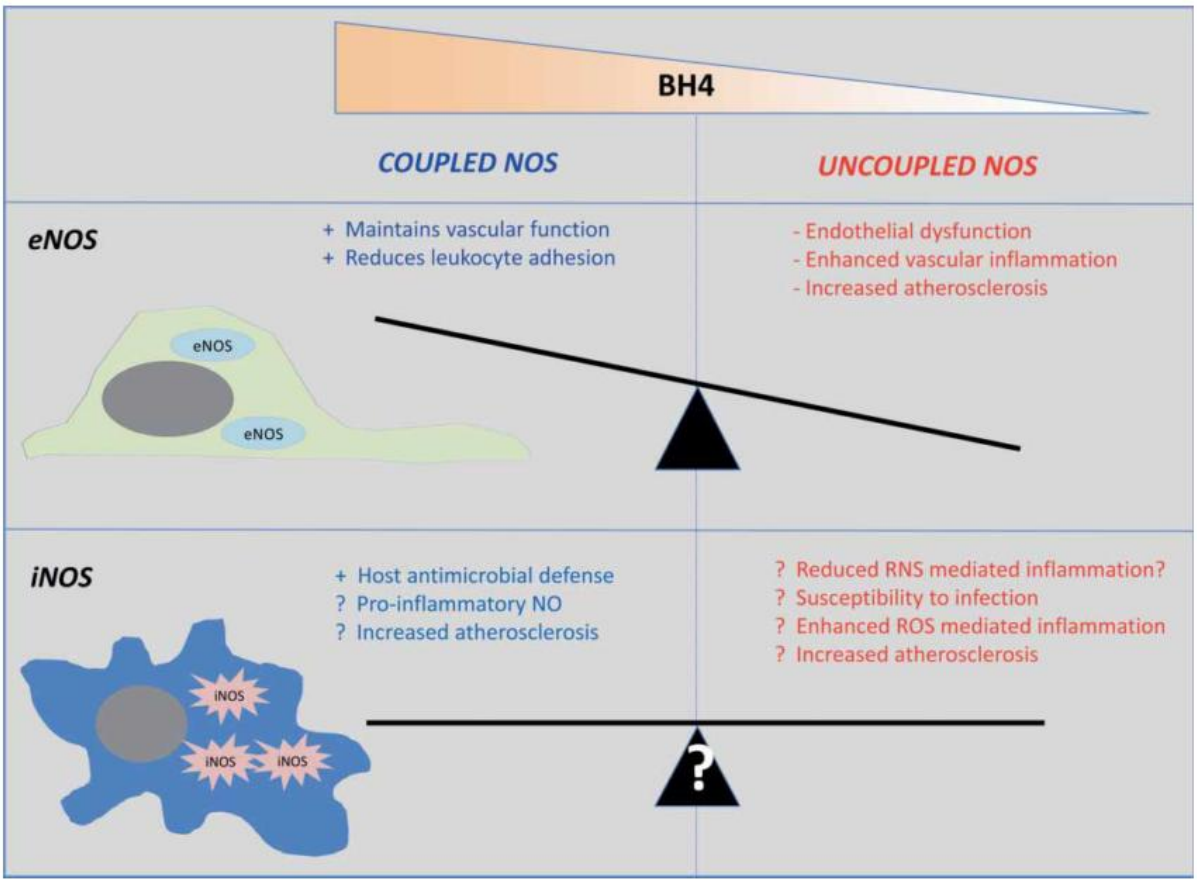

Figure 1.14: Whilst coupled and uncoupled endothelial cell eNOS has well defined roles and associations with vascular inflammation and disease, similar roles have not yet been assigned for iNOS (adapted from McNeill & Channon 2012).

1.4 Oxidative and nitrosative stress

According to a review by Mudau *et al*. (2012) the common underlying cause for endothelial dysfunction associated with cardiovascular risk factors, is oxidative stress, and includes NO, superoxide anion (O^{2-}), hydrogen peroxide (H_2O_2) and peroxynitrite ($ONOO^-$) (Griendling & FitzGerald 2003). Reactive oxygen species (ROS) are formed when radicals escape from the mitochondria. Additionally ROS can be formed accidentally as is the case with monoxygenases and dehydrogenases such as cytochrome P450 enzymes, xanthine oxidase and NOS (uncoupled). Superoxide (O_2^-) is formed by a one electron reduction from oxygen via a variety of oxidases (Griendling & FitzGerald 2003). Superoxide anions can inactivate/scavenge NO by binding to it resulting in the formation of the cytotoxic radical, peroxynitrite (Gryglewski *et al*., 1986):

$O_2^{\cdot -} + NO^{\cdot} \rightarrow ONOO^-$

When excessive amounts of NO are produced, as is often the case with iNOS (Buchwalow *et al.*, 2001), NO can become detrimental due to the formation of powerful peroxynitrite.

Another source of cellular ROS is the Nox family of NADPH oxidases. NADPH oxidase does not generate ROS via accidental mechanisms, but seems to exist for the purpose of producing superoxide anions (Braam & Verhaar 2007; Brandes *et al.,* 2010). The members of the Nox (**N**ADPH **OX**idase) family are named according to the large catalytic subunit which interacts with downstream signalling molecules such as GTPases, cytosolic phoxproteins and cytoskeletal proteins (Bedard & Krause 2007). Seven Nox-type NADPH oxidases have been identified in mammalian cells: Nox 1 to Nox 5; Duox 1 and Duox 2. Nox 1, Nox 2, Nox 4 and Nox 5 are significantly expressed in the cardiovascular system. Each Nox is unique with regards to the type of ROS generated, its mode of activation, expression and interaction with other proteins (Bedard & Krause 2007). In theory, due to a similar modular structure of the oxidoreductase, with binding sites for NADPH and FAD, all Nox isoforms should primarily release superoxide (Lambeth *et al.,* 2000). However, only Nox 1 (Suh *et al.,* 1999), Nox 2 and Nox 5 (Serrander *et al.,* 2007b) primarily release superoxide. Nox 4 is mainly responsible for the generation of hydrogen peroxide

(Serrander *et al.,* 2007a). An important NADPH oxidase subunit, P22phox, is a transmembrane scaffold protein and is required for Nox 1-4 activition (Ambasta et al., 2004). P22phox forms complexes with Nox 1, 2 and 4 and mutation of histidine 115 on Nox leads to disruption of these complexes (Ambasta *et al.,* 2004). Besides p22phox, other cytosolic subunits of NADPH oxidase include p47phox, p67phox and p40phox. Interaction has previously been shown between p22phox and Nox 2 (Ambasta *et al.,* 2004). This association provides stability to Nox 2. Phosphorylation of p47phox results in a conformational change and interaction with p22phox (Groemping & Rittinger 2005). Activation of Nox 2 requires cytosolic factors to translocate to the Nox 2/p22phox complex and p47phox facilitates this translocation. This brings the "activator subunit" p67phox into contact with Nox 2 (Han *et al.,* 1998). P40phox also joins the complex at this stage. Finally Rac (GTPase) interacts with Nox 2, directly followed by interaction with p67phox (Diebold & Bokoch 2001). The fully assembled complex is now ready to generate superoxide via electron transfer from NADPH to molecular oxygen (Bedard & Krause 2007). As demonstrated in figure 1.15, activation of the different Nox isoforms is slightly different, but the association of Nox with p22phox is an integral part of complex formation (with the exception of Nox 5).

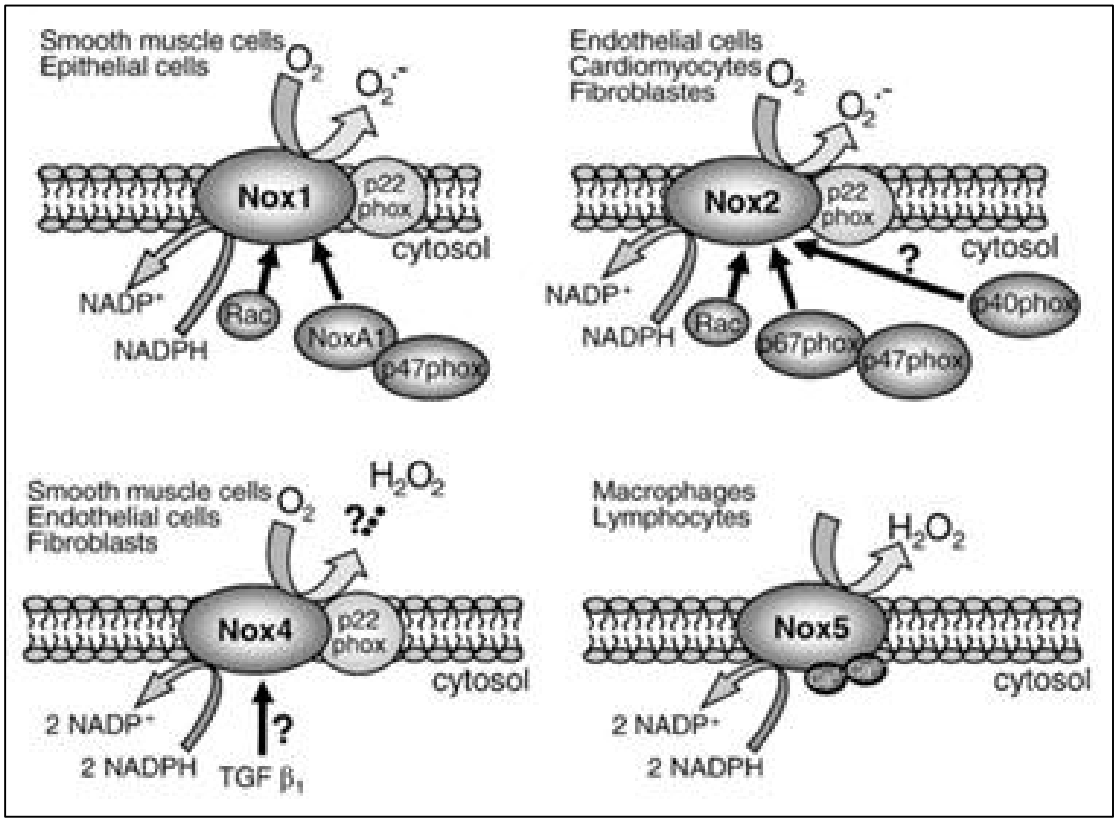

Figure 1.15: Activation model of Nox proteins. With the exception of Nox 4, the Nox homologues are basally inactive. Interactions with cytosolic proteins or increases in the calcium concentration are required to activate Nox 1, Nox 2 and Nox 5. Transforming growth factor β_1 appears to increase Nox 4 activity; the mechanism underlying this effect, however is unknown (from Brandes et al., 2010).

Peroxynitrite is a strong oxidant and can react with electron rich groups such as iron-sulfur centers (Castro *et al.,* 1994), sulfhydryls (Radi *et al.,* 1991) and zinc-thiolates (Crow *et al.,* 1995) as well as the sulfhydryl in tyrosine phosphatases (Takakura *et al*., 1999). At a pH of 8 and lower, Peroxynitrite will become protonated and form the unstable intermediate peroxynitrous acid which yields highly reactive oxidant species (Ferdinandy & Schulz 2003).

The production of peroxynitrite occurs at a low rate with minimal oxidative damage during a normal physiological state. This is due to endogenous antioxidant defence systems (Radi *et al.,* 2002). However during increased production of NO or superoxide, peroxynitrite formation will increase significantly, i.e. a 10-fold increase in superoxide and NO results in a 100-fold increase in peroxynitrite, as is the case during pathological conditions. Due to substantial oxidation by peroxynitrite, cellular constituents will be broken down leading to dysfunction of critical cellular processes and cell death by apoptosis and necrosis (Virág *et al.,* 2003) (figure 1.16).

According to Ferdinandy & Schulz (2003), mitochondrial Mn-superoxide dismutase (SOD), cytosolic Cu-Zn SOD, extracellular Cu-Zn SOD, glutathione (GSH), uric acid and catalase are important endogenous antioxidant enzymes responsible for controlling ROS production.

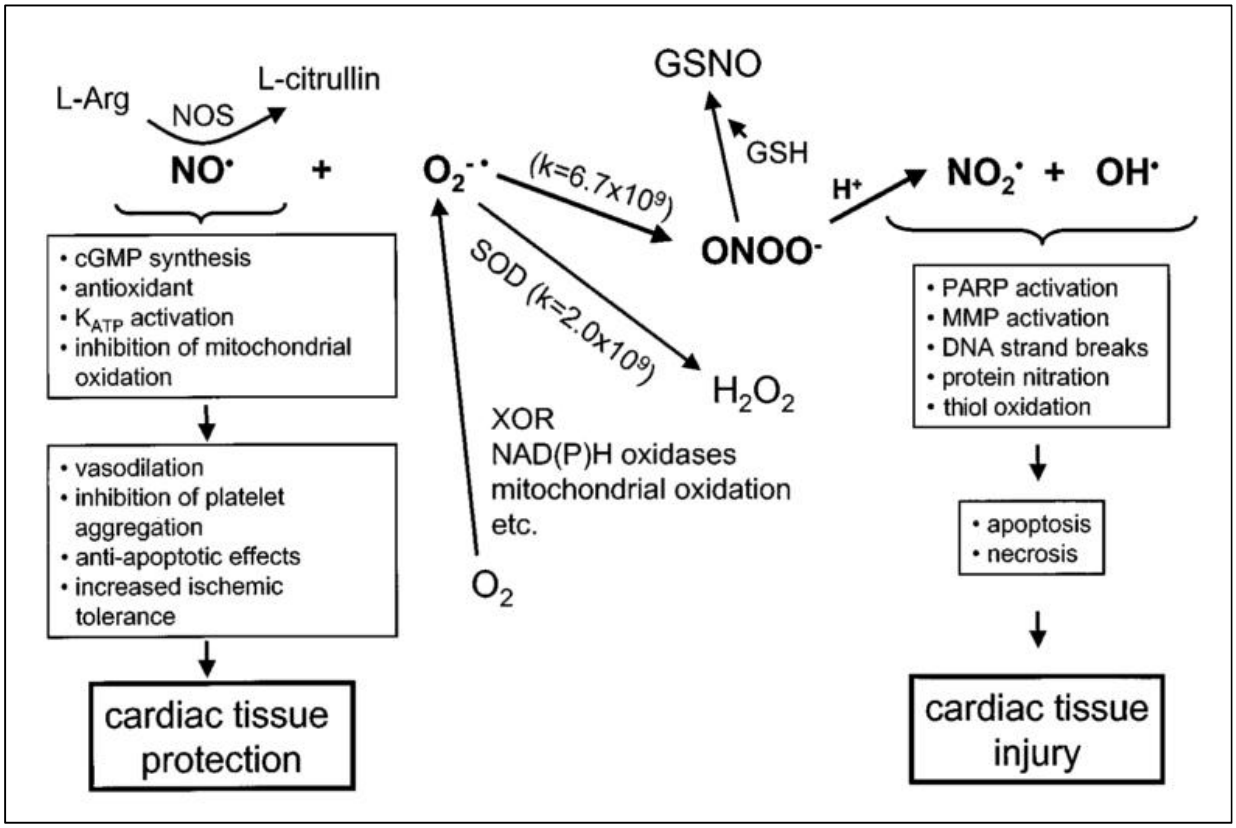

Figure 1.16: Cellular mechanisms of nitric oxide (NO), superoxide (O_2^-) and peroxynitrite ($ONOO^-$) actions. NO is an important cardioprotective molecule via its vasodilatory, antioxidant, antiplatelet, and antineutrophil actions and it is essential for normal heart functions. However, NO can become detrimental when it combines with superoxide to form peroxynitrite, which rapidly decomposes to highly reactive oxidant species leading to tissue injury. There is a critical balance between cellular concentrations of NO, superoxide and superoxide dismutase (SOD). Under physiological conditions, NO production is favoured, but under pathological conditions such as ischaemia and reperfusion, peroxynitrite formation is favoured. Peroxynitrite is detoxified when it combines with reduced glutathione (GSH) or other thiols to form S-nitrogluthathione (GSNO) or nitrothiols (NO donor molecules). MMP – matrix metalloproteinase; NOS – NO synthase; PARP – poly-ADP ribosepolymerase; XOR – xanthine oxidoreductase (from Ferdinandy & Schulz 2003).

1.5 Inflammation

Inflammation is characterised by local recruitment and activation of leukocytes. This process is an important component of the innate immune response to pathogens and damaged cells (Pober 2002). Inflammation can be triggered by different types of stimuli (Sullivan *et al*., 2000). One such stimulus is microbial infection (Nieminen *et al*., 1993). Bacteria or virally infected cells are destroyed by inflammatory cells. Another stimulus for inflammation, is tissue trauma as seen in organs stressed by ischaemia/reperfusion (Kin *et al*., 2006) or haemorrhagic shock (Shah & Billiar 1998). As long as the inflammatory response is short-lived and localised to the site of invasion or trauma it is not detrimental (Sullivan *et al.,* 2000). Chronic stimulation of inflammatory processes in the cardiovascular system has been associated with the development of atherosclerotic plaques (Jang *et al.,* 1993) and other vascular diseases (Folkman & Shing 1992).

According to Libby (2006), inflammation occurs during atherosclerosis from the initial stages through to the end when thrombotic complications occur. Once the ECs express adhesion molecules such as VCAM-1, an attachment surface is provided for T lymphocytes and monocytes (leukocytes present during the initial stages of atherogenesis). Once inflammatory cells have infiltrated the area of injury or infection they release cytokines, proteases, and ROS which trigger vasoconstriction or vasodilation (Groth *et al.*, 2014), thrombus formation (Carter 2005; Libby 2006), angiogenesis and tissue remodelling (Wilensky *et al*., 1995).

Nuclear factor kappa B (NF-κB) has emerged as a key regulator of inflammation and is activated in many chronic inflammatory diseases and cancers (Wolfrum *et al*., 2007; Gyrd-Hansen & Meier 2010; Ben-Neriah & Karin 2011; Cao *et al.*, 2013). The NF-κB family of nuclear transcription factors consists of NF-κB1 (p50 and its precursor p105), NF-κB2 (p52 and its precursor p100), RelA (also called p65), c-Rel, and RelB. All the members of the NF-κB family are characterised by an N-terminal Rel homology domain (RHF) responsible for homo- and heterodimerization and sequence specific DNA binding (Vallabhapurapu & Karin 2009). P52 and p50 do not rely on interactions and associations with other factors in order to regulate transcription, however RelA,

c-Rel and RelB contain a C-terminal transcription activation domain (TAD) (Hayden & Ghosh 2008).

NF-κB normally resides in the cytosol and needs to translocate to the nucleus to perform its transcription role in the activation of DNA synthesis of target genes. The group of proteins involved with retaining NF-κB in the cytosol is known as the IκB family of proteins. They include IκBα, IκBβ, IκBε and the precursor proteins p100 and p105. Another IκB protein, IκBγ, has been identified in mice, but its relevance remains unknown. Two inducible forms of IκB proteins have also been identified, namely BCL-3 and IκBζ. Upon stimulation by pro-inflammatory cytokines such as tumor necrosis factor alpha (TNF-α) and interleukin-1β (IL-1β), the kinase complex IKKα and IKKβ (catalytic subunits) is activated, as well as the regulatory subunit NEMO (NF-κB essential modulator). IKK proteins phosphorylate IκB, leading to its ubiquitination and dissociation from the NF-κB complex. Dissociation of IκB provides the stimulus for NF-κB dimers to translocate to the nucleus. IκB in turn will undergo proteasomal degradation (Hoffmann *et al*. 2006; Hayden & Ghosh 2008; Vallabhapurapu & Karin 2009) (figure 1.17).

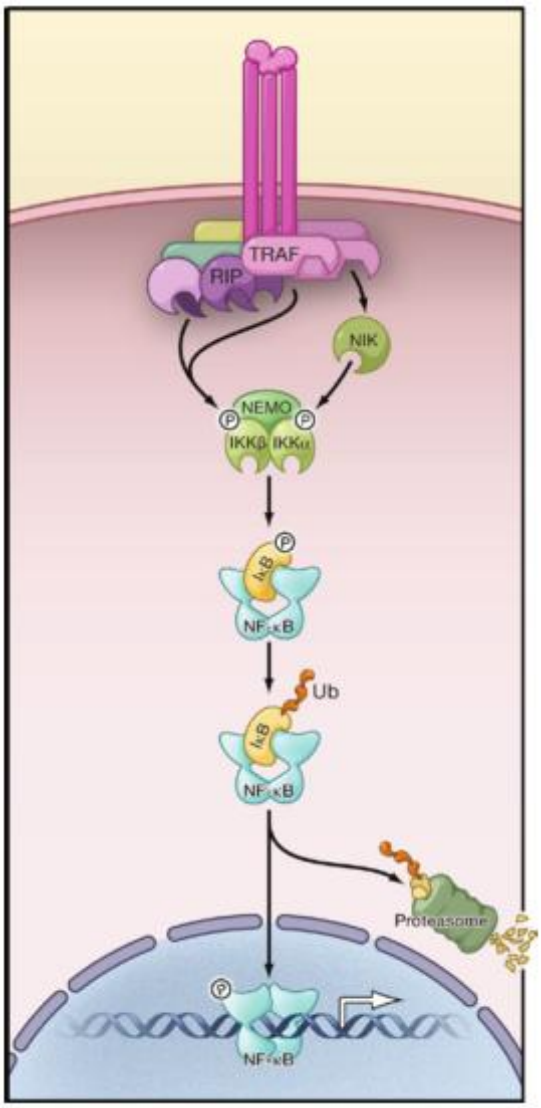

Figure 1.17: NF-κB signalling pathways. Following receptor ligation and recruitment of receptor proximal adaptor proteins, signalling to IKK proceeds through TRAF/RIP complexes. The IKK complexes phosphorylate IκB leading to proteasomal degradation and ultimately NF-κB translocates to the nucleus to induce transcription of target genes (adapted from Hayden & Ghosh 2008).

1.6 Anti-dyslipidaemic / Hypolipidaemic therapies

1.6.1 General background

An array of anti-dyslipidaemic drugs is available on the market today, each targeting different physiological endpoints. These therapies have been shown to decrease the incidence of cardiovascular events and atherosclerosis (Rikitake & Liao 2005; Ii & Losordo 2007). Therapies aimed at lowering cholesterol, are essential in preventing plaque progression in vascular linings (Rozman & Monostory 2010) as well as reducing pro-inflammatory markers in these patients (Ascer *et al.,* 2004; Blanco-Colio *et al.*, 2007). 3-Hydroxy-3-methylglutaryl coenzyme A reductase (HMG-CoA-R) inhibitors, otherwise known as statins, provided a breakthrough in the search for drugs that lower circulation levels of LDL-cholesterol (LDL-C) (Gotto & Farmer 2006) and are currently the most widely prescribed class of cholesterol-lowering drugs. Statins serve as first line therapy for lowering LDL-C levels (Noto *et al*., 2014). The beneficial effects of statins are not only due to their cholesterol lowering effects, since they have also been shown to exert cholesterol-independent (or pleiotropic) effects such as the improvement of ED, increasing NO bio-availability and reduction of vascular inflammation (Rikitake & Liao 2005; Ii & Losordo 2007; Zhou & Liao 2010). However, besides all of these beneficial effects, side-effects have been documented, such as adverse muscular reactions as well as hepatic and renal complications (Kashani *et al.,* 2006; Kapur & Musunuru 2008). Cerivastatin was retracted from market in 2001 due to 31 deaths related to myotoxicity (Staffa *et al*., 2002).

Even though statins have showed a 25-40% cardiovascular risk reduction in clinical trials, a residual cardiovascular risk remains (LaRosa *et al*., 2005). Combination therapy has been implemented to address this problem. This also improves the lipid profile of very high-risk patients for whom the efficacy and tolerability of only statin therapy are not sufficient (Davidson 2005; Hou & Goldberg 2009; Rozman & Monostory 2010). The rationale is, if the highest tolerable statin dose does not succeed in decreasing LDL-C to target values, another drug, with a different mode of action, can be combined with the statin in order to be more effective. This can be done in order to either further decrease LDL-C values or to selectively increase HDL-C.

Simultaneous targeting of LDL-C and HDL-C would then account for additive effects on cardiovascular risk reduction (Hausenloy & Yellon 2008; Polonsky & Davidson 2008).

A variety of alternative therapies exist that have different modes of action, and show greater efficiency at targeting different parameters, such as LDL-C or HDL-C. These include fibrates, ezetimibe, niacin, bile acid sequestrants, thiazolidinediones or cholesterol enzyme inhibitors (Rozman & Monostory 2010).

1.6.2 Statins

The mechanism by which statins exert their effect, is via the inhibition of the *de novo* cholesterol biosynthesis process. The HMG-CoA-R inhibitors, i.e. statins, limit the rate limiting step in the cholesterol synthesis process, namely conversion of HMG-CoA to mevalonate by 3β-hydroxy3-methylglutharyl coenzyme A reductase (HMGCR) (figure 1.18). The reduction of downstream metabolites results in increased expression of the LDL-receptor on hepatocytes as well as increased uptake of LDL from the circulation (Endo 2004; Rozman & Monostory 2010). In terms of their structure, statins can be classified as follows: Type 1 inhibitors include simvastatin and pravastatin, and contain a decalin ring. Type 2 inhibitors include rosuvastatin, atorvastatin, cerivastatin and fluvastatin which contain a fluorophenyl group allowing them additional binding properties (Istvan *et al.,* 2000; Rozman & Monostory 2010). The differences in their pharmacokinetic properties are due to differences in structure. The very first statin, mevastatin, was extracted from *penicilliium citrinum.* Lovastatin, simvastatin and pravastatin are all derivatives of fungal products and are manufactured with an open lactone ring, which is transformed in the body to an open acid form. Pravastatin is administered in a biologically active open acid form. Fluvastatin is a purely synthetic statin with a different structure (Schulz 2005) (figure 1.19).

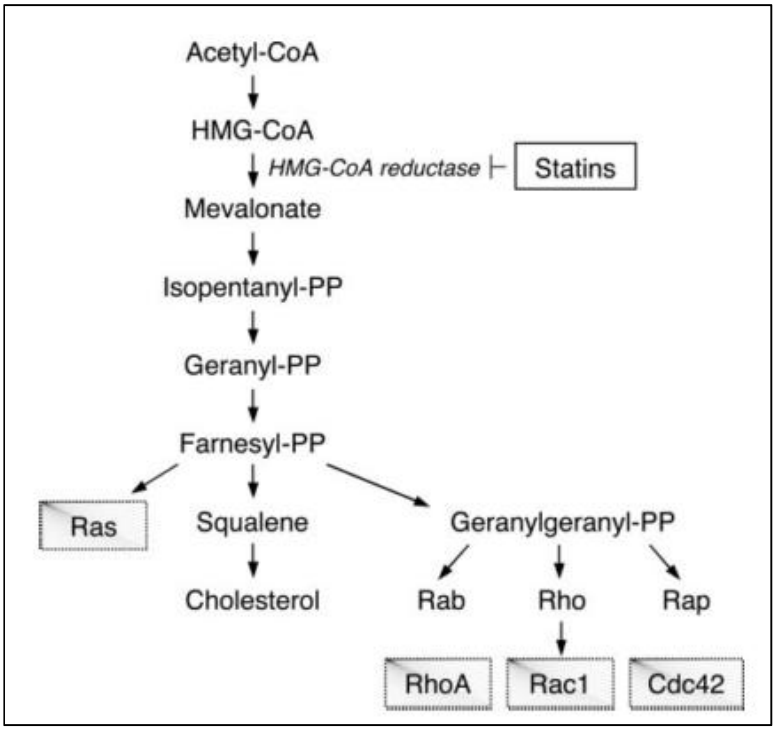

Figure 1.18: Cholesterol biosynthesis pathway. CoA: coenzyme A; PP: pyrophosphate (from (Rikitake & Liao 2005).

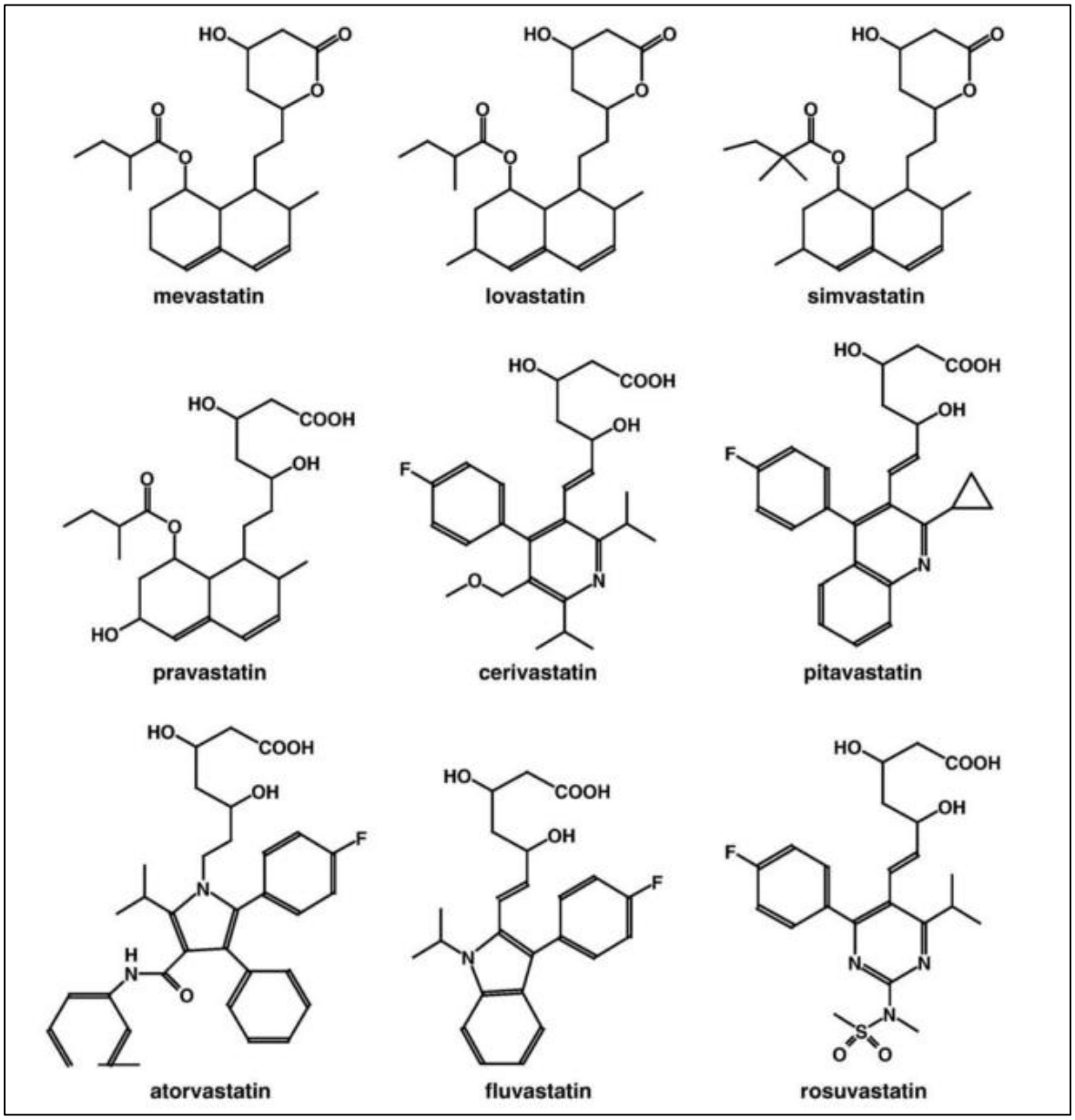

Figure 1.19: Chemical structures of different statins, inhibitors of 3ϐ-hydroxy3-methylglutharyl coenzyme A reductase (HMGCR) (Rozman & Monostory 2010).

1.6.2.1 Simvastatin: Effects on cholesterol

Several clinical trials have confirmed the efficacy of simvastatin to decrease LDL-C, total cholesterol and triglycerides as well as beneficial primary and secondary outcomes (Olsson *et al*., 2003; meta-analysis by Rogers *et al*., 2007; Armitage *et al.*, 2010). Some studies indicated that simvastatin is less effective than atorvastatin to reach target levels (Olsson *et al*., 2003; Rogers *et al*., 2007). The focus of the current study is however not on the cholesterol effects of simvastatin, but rather the pleiotropic effects.

1.6.2.2 Simvastatin: Pleiotropic effects

The pleiotropic effects observed with all statins are mainly a result of the inhibition of isoprenoid formation, farnesylpyrophosphate (FPP) and geranylgeranylpyrophosphate (GGPP) due to mevalonic acid inhibition. These isoprenoids are responsible for post-translational regulation of proteins such as the small GTPases Ras, Rac and Rho. Statins inhibit the activation of RhoA, which normally inhibits PKB/Akt, resulting in the inhibition of one of its major downstream targets, eNOS. eNOS is involved with keeping the mitochondrial permeability transition pore (mPTP) closed, which ultimately results in cardioprotection. Statins can also directly activate PKB/Akt (Liao & Laufs 2005; Rikitake & Liao 2005). Rho/Rho Kinase (ROCK) is a protein serine/threonine kinase, and a downstream effector of the small GTPase Rho (Rikitake & Liao, 2005; Zhou & Liao, 2010). Statins lead to the inhibition of ROCK and it has been suggested that ROCK can regulate eNOS mRNA (Rikitake & Liao, 2005; Zhou & Liao, 2010). Inhibition of the Rho/ROCK pathway leads to the upregulation of eNOS, which contributes to cardioprotection (Rikitake & Liao, 2005; Zhou & Liao, 2010). This pathway represents the mechanism by which statins mostly exert their pleiotropic effects especially in the cardiovascular system. A novel mechanism relevant to the effect of statins on leukocyte trafficking and T-cell activation has been described by Weitz-Schmidt *et al*. (2001). They showed that statins bind to a novel allosteric site within the β2 integrin function associated antigen-1 (LFA-1). This mechanism was found to be independent of mevalonate inhibition.

The group of statins can further be divided into lipophilic or hydrophilic statins. Lipophilic statins such as simvastatin are likely to have a more potent pleiotropic effect due to the fact that they can enter endothelial cells via passive diffusion (Liao & Laufs 2005). Of further relevance to the pleiotropic effects of statins on vascular tissue, more specifically simvastatin, is the inhibitory effect on endothelin-1. Endothelin-1 (ET-1) is a powerful vasoconstrictor and growth factor involved with the regulation of vascular tone and vascular smooth muscle mitogenesis (Gomez Sandoval & Anand-Srivastava 2011; Kawanabe & Nauli 2011). Simvastatin has also been shown to significantly increase the vasodilatory response of spontaneously hypertensive rats due to increased formation of NO and prevented endothelial dysfunction in rabbits on a high cholesterol diet (Carneado *et al*., 2002). This was, however, not associated with increased activation of eNOS, but decreased expression of Cav-1 and increased total expression of eNOS (Arora *et al*., 2012). A summary of studies demonstrating vascular pleiotropic effects of simvastatin is shown in Table 1.1.

The pleiotropic effects of simvastatin stretch further than just site specific alterations in the vascular wall. In the myocardium, simvastatin was shown to be anti-hypertrophic (Zou *et al.,* 2013), provide protection against ischaemia/reperfusion injury (Iliodromitis *et al*., 2010), reduce inflammation (due to ischaemia) (Iliodromitis *et al.,* 2010), limit infarct size (Ye *et al.,* 2010) and inhibit angiotensin II induced oxidative stress (Takemoto *et al.,* 2001). Simvastatin has also been shown to protect against ischaemic stroke (Zhu *et al.,* 2014). The major pleiotropic effects, however, are seen in the vascular wall.

In general, statins seem to have biphasic effects. As expected, not only beneficial pleiotropic effects have been documented. Even though there are many studies indicating the anti-inflammatory effect of statins, statins have also been shown to lead to a super-induction of E-selectin, ICAM-1 and VCAM-1 in TNF-α stimulated vascular endothelial cells (Schmidt et al. 2002). Kaneta *et al.* (2003) conducted a study on rat pulmonary vein endothelial cells using lovastatin, simvastatin, atorvastatin, fluvastatin, cerivastatin and pravastatin, in which it was found that lipophilic (all except pravastatin) statins induced apoptosis and decreased cell viability due to DNA fragmentation, DNA laddering and activation of caspase-3.

Table 1.1: Pleiotropic effects of Simvastatin on the vascular wall.

Effect	Mechanism	Dose and model	In vitro
Post-conditioning mediated protection.	PKB/Akt activation.	BPAEC – 0.5–10 µM	Wu *et al*. 2010
Antioxidant	↑ Catalase ↑ SOD	Wistar rats (Streptozotocin induced) – 1 mg/kg/day i.p.	El-Azab *et al*. 2012
	↑ SOD ↑ glutathione peroxydase	Wistar Kyoto and SHR rats – 5 mg/kg/day	Carneado *et al.* 2002
Inhibits vasoconstrictor ET-1	Via inhibition of Rho/ROCK pathway. Speculate due to the inhibition of PKB/Akt and eNOS.	• Sprague-Dawley rat aortas – 0.1-10 µM (in organ bath). • SMC – 0.1-10 µM	Mraiche *et al.* 2005
Contributes to plaque stability	Inhibition of Rho and subsequent inhibition of COX-2 and MMP-9	HUVECs, HSVECs, BAECs – 0.1-10 µM	Massaro *et al.* 2010
Inflammation	↓ IFN-γ induced CD40 expression and signalling	ECs, SMCs, macrophages and fibroblasts – 80 nM-5 µM	Mulhaupt *et al*. 2003
	↑ synthesis of t-PA and ↓ PAI-1 via geranylgeranyl modified intermediates ↓ NFκB and AP-1	HPMCs and HT1080 fibrosarcoma cells – 5 µM	Haslinger *et al.* 2003
Re-endotheliazation	↑ VEGF release	Hamsters – 2 mg/kg/day	Matsuno *et al.* 2004
	↑ mobilization of EPCs from bone marrow	Sprague Dawley rats – 0.2/1 mg/kg/day	Walter 2002
Pro-angiogenesis	↑ PKB/Akt and eNOS activation	HUVECs – 1 µM	Kureishi *et al*. 2000
	↑ PKB/Akt activation/translocation	BAECs and HUVECs – 0.5 µM	Skaletz-Rorowski *et al*. 2003
Vasodilatory	↓ caveolin-1 ↔ eNOS activation	New Zealand white rabbit aortas – 5 mg/kg/day	Arora *et al*. 2012
	↑ NO	Wistar Kyoto and SHR rats – 5 mg/kg/day	Carneado *et al.* 2002

t-PA: tissue-type plasminogen activator (t-PA); PAI-1: plasminogen activator inhibitor-1; ET-1: endothelin-1; eNOS: endothelial nitric oxide synthase; ROS: reactive oxygen species; SMC: smooth muscle cell; BPAEC: bovine pulmonary arterial endothelial cells; HUVECs: human umbilical vein endothelial cells; HSVECs: human saphenous vein endothelial cells; BAECs: bovine aortic endothelial cells; COX-2: cyclooxygenase-2; MMP-9: metalloproteinase-9; SOD:

superoxide dismutase; i.p.: intra peritoneal; Cav-1: caveolin-1; HPMCs: human peritoneal mesothelial cells; AP-1: activator protein-1; SHR: spontaneously hypertensive rats; ECs: endothelial cells

1.6.3 Fibrates

Low levels of HDL-C are a strong, independent and inverse predictor of coronary heart disease (CHD). The Framingham Heart study investigated men and women between the age of 49-82 years with no CHD at initial recruitment, and found HDL-C to be the most potent lipid risk factor for CHD, more so than LDL-C, total cholesterol or triglycerides (Gordon *et al*., 1977; Castelli *et al*., 1986; Assmann *et al*., 1996; Sharrett *et al*., 2001). Gordon *et al.* (1977) also found a 2-3% reduction in cardiovascular risk factors for every 1 mg increase in HDL. Statins have been shown to be distinctly effective in decreasing LDL-C, but their effect on HDL-C is not that prominent (Natarajan *et al*., 2010). A meta-analysis showed that statins resulted in a 7.5% increase in HDL-C in patients suffering from CHD. This increase was independently associated with coronary atherosclerosis regression (Nicholls *et al*., 2007). Peroxisome proliferator-activated receptor alpha (PPAR-α) agonists decrease LDL-C by approximately 10% - 20%, triglycerides by 25% - 45% and increase HDL-C by 10%-15% (Saku *et al*., 1985; Birjmohun *et al*., 2005).

PPARs consist of a family of three nuclear receptor isoforms, namely α, γ and β/δ. They are key regulators of metabolism and inflammation. Increasingly, studies are indicating that PPAR activation is an important mechanism by which atherosclerosis can be reduced and cardiovascular function improved (Fuentes & Palomo 2014). Ligands of PPAR-α are regulators of lipid and lipoprotein metabolism and therefore play an important role in limiting plasma risk factors contributing to atherosclerosis. Fibrates are synthetic ligands of PPARs. They have been used clinically since the late 1960s and include clofibrate, bezafibrate, gemfibrozil, ciprofibrate and latest member of the family, fenofibrate (Farnier 2008), which will be discussed next.

1.6.3.1 Fenofibrate: Effects on cholesterol

Fenofibrate (2-[4[(4-chlorobenzoyl)phenoxy]-2- methyl-propanoic acid, 1-methylethyl ester) is a synthetic ligand of PPAR-α and is highly lipophillic. Once bound, PPAR-α forms a complex with the retinoid-receptor X and will translocate from the cytosol to the nucleus where it plays a role in transcription of genes involved with fatty acid metabolism (figure 1.20). Mechanisms that lead to triglyceride lowering include suppression of hepatic apo-CIII gene expression and stimulation of lipoprotein lipase (LPL) transcription, which promote increased cellular fatty acid uptake, oxidation as well as decreased production (Berger & Moller 2002; Steiner 2008; Alagona 2010).

A meta-analysis of randomized controlled trials by Birjmohun *et al.,* (2005) in which 15 trials with fenofibrate were included, showed that fenofibrate had the following effects on lipid parameters: reduction of total cholesterol levels by 13.3%, 40.1% reduction of triglyceride levels, 10.5% reduction of LDL-C levels, and 10.2% increase in HDL-C levels (although increases of up to 23% have been reported) (Kon Koh *et al.,* 2006). Adverse effects of fenofibrate treatment include increased creatinine and homocysteine levels (Farnier 2008). Even though fenofibrate reduced CVD events, it did not significantly improve primary outcomes in trials (Birjmohun *et al.,* 2005; Keech *et al*., 2005).

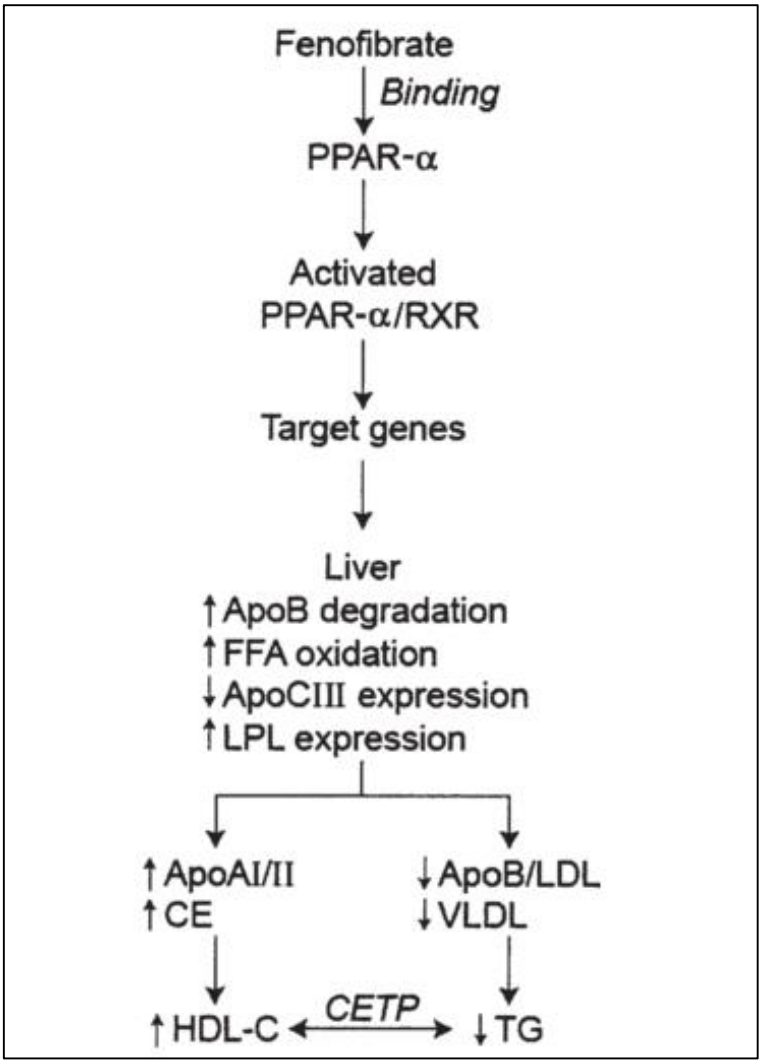

Figure 1.20: Binding of fenofibrate to peroxisome proliferator-activated receptor-α (PPAR-α) affects lipid metabolism and regulates the cholesterol dependent effects thereof. Apo: apolipoprotein; CE: cholesteryl ester; CETP: cholesteryl ester transfer protein; FFA: free fatty acids; HDL-C: high density lipoprotein cholesterol; LDL: low density lipoprotein; LPL: liprotein lipase; RXR: retinoid X receptor; TG: triglycerides; VLDL: very-low-density lipoprotein (adapted from Steiner 2008).

1.6.3.2 Fenofibrate: Pleiotropic effects

Besides the primary purpose of fenofibrate treatment to improve lipid parameters, a plethora of studies have appeared showcasing its numerous pleiotropic effects (Wiel *et al*., 2005; Lee *et al*., 2009; Balakumar *et al.,* 2011; Tomizawa *et al.,* 2011; Walker *et al.,* 2012). The pleiotropic effects mainly revolve around the improvement of endothelial function, antioxidant, anti-inflammatory and anti-thrombotic effects (Tsimihodimos *et al*., 2005).

Fenofibrate can protect the endothelium against nicotine induced endothelial dysfunction (Kaur *et al.,* 2010; Chakkarwar 2011) by increasing the bio-availability of NO as seen by increased nitrite/nitrate levels in blood and aortic tissue. Fenofibrate also improved endothelial function in obese Zucker rats (Zhao *et al.,* 2006). It protected vascular endothelial cells against apoptosis by up-regulating AMPK (Tomizawa *et al*., 2011) and also prevented hyperglycaemia-induced apoptosis (Zanetti *et al*., 2008). Fenofibrate has shown anti-inflammatory effects by down-regulation of NF-κB expression (Belfort *et al.*, 2010) although long term treatment resulted in increased pancreatic expression of NF-κB (Liu *et al*., 2011). Systemically, fenofibrate can decrease lymphocyte release of pro-inflammatory cytokines and inflammation (Krysiak *et al*., 2013). Fenofibrate also displays anti-oxidant effects via reducing plasma-oxidised LDL or increasing superoxide dismutase (Wang *et al*., 2010; Walker *et al.*, 2012). An anti-thrombotic and anti-platelet role has also been attributed to fenofibrate (Lee *et al.,* 2009). The main mechanism by which fenofibrate exerts its endothelio-protective effects is by activation of NOS. Fenofibrate has previously been shown to increase NO production via an increase in the phosphorylation and activation of eNOS at the Ser1177 residue (for details on the specific tissue and species, please refer to table 1.2) (Murakami *et al*. 2006; Katayama *et al*. 2009; Tomizawa *et al*. 2011; Becker *et al*. 2012). Furthermore, Del Campo *et al.* (2011) showed that fenofibrate can increase neuronal release of NO in mesenteric arteries from diabetic rats, by increased phosphorylation of nNOS. With regards to iNOS, one study found that fenofibrate increased pancreatic iNOS expression in monosodium glutamate-induced obese rats, which was associated with an increase in NF-κB activity (Liu *et al*. 2011). Another study on rat aortic tissue showed that fenofibrate induced endothelial dysfunction (observed as a diminished vasodilatory response) in a time-dependent fashion, but failed to show changes in iNOS expression (Blanco-Rivero *et al*. 2007). Controversy

remains with regards to the effects of fenofibrate on NOS mRNA, expression and posttranslational regulation (Table 1.2).

Even though many of the clinical trials of fenofibrate failed to show improved primary outcomes, an interesting finding was made in the The Fenofibrate Intervention and Event Lowering in Diabetes (FIELD) trial with regards to fenofibrate's effect on microvascular vessels. Fenofibrate treated patients with type 2 diabetes showed a reduction in the rate of laser treatment for retinopathy (by 30%), reduced progression of albuminuria and non-traumatic amputations (by 38%). The mechanisms by which these changes were achieved remain unknown, although the authors speculated that it could have been due to a protective effect on the endothelium of small blood vessels (Sacks 2008).

Table 1.2: Differences in results investigating eNOS related stimulation by fenofibrate.

Article	Model	Concentration and Duration	Method for NO	eNOS
Deplanque *et al*., 2003	Male apolipoprotein (Apo) E-deficient mice (hypercholesterolemic), C57BL/6 and SV129 wild-type mice and PPARalpha -deficient mice.	Fenofibrate intra peritoneally 50 mg/kg/day or 250 mg/kg/day for 14 days. 1 and 6 hours after the beginning of MCA occlusion.	Increased sensitivity to endothelial relaxation.	No change in eNOS expression. No change in iNOS expression
Goya *et al*., 2004	BAECs	1 – 100uM for 1-48h	Did not measure directly	↑ in eNOS activity assay rom 10uM – 100uM (peak at 50uM); no increase after 2, 5 min or 1 hour, only after 24-48 h. eNOS expression was dose-dependently increased (10-100uM) as well as eNOS mRNA levels (5-100uM) and mRNA stability by increasing eNOS mRNA half-life – unknown mechanism.
Murakami *et al*., 2006	HUVECs	20- 100uM for 2.5 min – 6 hours	DAF/2DA and spectrophotometry	↑ in p-eNOS after 2.5min to 10 min. No change in eNOS expression. ↑ p-AMPK. No effect on PKB/Akt phosphorylation (Thr308)
Alvarez De Sotomayor *et al*., 2007	Small mesenteric arteries – Wistar rats (12-14 weeks and 113-114 weeks old)	100mg/kg/day for 8 weeks	Did not measure NO bioavailability.	No change in expression.
Blanco-Rivero *et al*., 2007	Aortic rings – Wistar rats (4 months old)	100mg/kg/day for 1 week or 6 weeks. L-NAME (100uM)	DAF/2-DA in medium – measure with excitation and emission wave lengths.	No change in expression.

Katayama *et al*., 2009	C57BL/6J mice (male, 8 weeks old; weighing 20–25 g) HUVECs	100mg/kg/day for 28 days HUVECs – 10uM for 24h	↑Nitrate/nitrite levels in blood; Abolished when L-NAME was added.	No change in expression, ↑ in phosphorylation of eNOS in mouse aortic tissue – did not mention a specific eNOS site.
Balakumar *et al*., 2009	Aortic rings - Wistar rats 200-250g	32mg/kg/day for 7 weeks Diabetic group – 50 mg streptozotocin once off.	↑Nitrate/nitrite in blood serum and aortic segments. Fenofibrate did not increase nitrate/nitrite levels in non-diabetic rats, only in diabetic animals.	Did not investigate.
Kaur *et al*., 2010	Aortic rings - Wistar rats 200-250g	Nicotine 2mg/kg/day for 4 weeks Sodium arsenite 1,5mg/kg/day for 2 weeks Fenofibrate 30mg/kg/day for 4 weeks Atorvastatin 30mg/kg/day for 4 weeks L-NAME 25mg/kg/day for 4 weeks. Started with the day of nicotine administration Fenofibrate and statin started 3 days before administration of nicotine and arsenite.	↑Nitrate/nitrite in blood serum and aortic segments.	Suggest NOS to be involved with the endothelioprotective effects of fenofibrate and reduction in oxidative stress. Used the non-specific NOS inhibitor L-NAME and found the vasodilatory effect to be abolished.
Tomizawa *et al*., 2011	HGMECs, mouse SVEC4 and HepG2	100uM for 15, 30 and 60 min	Nitrite/Nitrate levels in medium with automated liquid chromatography system.	AMPK ↑ PKB ↑ Increase in eNOS activity assay after 30 min treatment with fenofibrate (effect

				abolished when silencing AMPK / inhibiting with compound C) . p-eNOS ↑ (peak after 30min).
Liu *et al*., 2011	Male Wistar rats – injected with MSG to create an obese model.	100mg/kg/day for 12 weeks.	↑Nitrate/nitrite in blood serum. Increased levels of NO associated with increased oxidative stress.	Found increased expression of iNOS and NFkB. Did not investigate eNOS.
Chakkarwar 2011	Aortic rings – Wistar rats 200-250g	Fenofibrate 32mg/kg/day for 4 weeks Nicotine 2mg/kg/day Fenofibrate treatment started 3 days before nicotine.	↑Nitrate/nitrite in blood serum and aortic segments.	↑ in mRNA eNOS expression.
Becker *et al*., 2012	Airway reactivity - Nine-week-old male C57BL/6 mice.	1.5, 3, or 15 mg/day for 1, 3 or 10 days. L-NAME administered i.p. 1 h before airway reactivity measurement at the dose of 0.75 mg.	Did not measure directly – found vasodilatory response.	↑ p-eNOS Ser 1177 in lung tissue.

NO: nitric oxide; eNOS: endothelial nitric oxide synthase; HUVECs: human umbilical vein endothelial cells; SVECs: saphenous vein endothelial cells; BAECs: bovine aortic endothelial cells; i.p.: intra peritoneal; MCA: middle cerebral artery occlusion; mRNA: messenger ribonucleic acid; DAF-2/DA: diaminofluorescein diacetate; L-NAME: L-NG-Nitroarginine Methyl Ester; ↑: increase.

1.7 Motivation and aims

1.7.1 Problem identification, rationale and motivation

The growing problem of cardiovascular disease and high incidence of ischaemic heart disease, also in developing countries such as South Africa, are having detrimental effects on a population regardless of variables such as age, race and gender. Atherosclerosis is the main underlying pathological cause of ischaemic heart disease, and the earliest predictor of atherosclerosis is endothelial dysfunction. Endothelial dysfunction is regarded by many as a reversible process; hence, investigating the underlying mechanisms of therapies aimed at slowing down or reversing endothelial dysfunction is extremely relevant.

Drugs targeting dyslipidaemia and hypercholesterolaemia are essential tools in the hands of clinicians in the quest to reduce cardiovascular risk; however, it has become increasingly evident that these drugs are multi-mechanistic. Among the important first-line anti-dyslipidaemic drugs are the statins. They have indeed been shown to improve lipid parameters (especially LDL-C), along with improved primary and secondary outcomes. Statins, particularly lipophilic statins such as simvastatin, exert many (lipid-independent) pleiotropic effects, including (and of interest for the current study), the improvement of endothelial function.

Among the newer generation anti-dyslipidaemic drugs are the fibrates, with fenofibrate as the most common fibrate prescribed by clinicians. Fenofibrate, like simvastatin, is a lipophilic compound and shows beneficial effects on lipid parameters, especially via increasing HDL-C levels; however, it is also known to exert pleiotropic effects. Since statins (especially high dose statins) are often associated with adverse effects such as muscle toxicity and ineffective in correcting multiple lipid parameters in dyslipidaemic patients, the prescription of combination therapy has become an increasingly popular trend.

Although statins have been used in clinical practice for many years and have been studied quite extensively with regards to their underlying mechanisms, less is known on fenofibrate. One of the main objectives of the current study is therefore to focus more on the endothelioprotective effects and underlying mechanisms of fenofibrate. This is particularly important since fenofibrate seems to have a distinct effect on microvascular vessels most

likely due to endothelium-dependent mechanisms. Capillary-derived endothelial cells are quite different from macrovascular endothelial cells ("endothelial heterogeneity"), and most studies investigating the endothelioprotective effects of fenofibrate are performed on endothelial cells harvested from large bloodvessels.

Therefore, the first part of the study is aimed at investigating the underlying lipid-independent, ***pleiotropic*** mechanisms exerted by simvastatin and fenofibrate in *in vitro* models of different types of cultured endothelial cells, with a special focus on microvascular endothelial cells. The study also aimed to compare the results obtained from the fenofibrate experiments with those obtained from simvastatin-treated microvascular endothelial cells, as well as to investigate the possible additive effects when combining the drugs. The second part of this study investigates the *in vivo* and *ex vivo* effects of the drugs on endothelial function. This study did not investigate the cholesterol related effects of simvastatin and fenofibrate.

1.7.2 Research aims

1) **Simvastatin: *In vitro* investigations**

To measure concentration and time responses for simvastatin with regards to NO and ROS production and investigate the effects thereof on cell viability of CMECs purchased commercially. As discussed in the introduction, increased bio-availability of NO and decreased levels of ROS are some of the basic pleiotropic effects associated with statin treatment and served as the ideal starting point for this study. We also aimed to investigate the underlying signalling mechanisms involved with NO and ROS production. Finally, the study also aimed to investigate whether pre-treatment with simvastatin was able to protect endothelial cells from a harmful insult (pro-inflammatory stimulation with TNF-α).

2) **Fenofibrate: *In vitro* investigations**

In this part of the study, we aimed to focus specifically on the *in vitro* lipid-independent pleiotropic effects of fenofibrate in cultured CMECs, especially in light of the interesting clinical findings of fenofibrate on microvasculature (FIELD trial). Firstly, we aimed to measure concentration and time responses for fenofibrate via baseline measurements of nitric oxide, ROS and cell viability. In order to assess possible endothelial heterogeneity, selected

experiments were repeated on cultured macrovascular endothelial cells (aortic endothelial cells; AECs). We also aimed to investigate the underlying signalling mechanisms involved with fenofibrate's pleiotropic effects, especially with regards to the involvement of NOS and associated proteins. As with simvastatin, we aimed to determine whether pre-treatment with fenofibrate was able to protect endothelial cells from a pro-inflammatory insult (TNF-α stimulation).

3) **Simvastatin and fenofibrate: *In vivo* and *ex vivo***

In this part of the study, we aimed to investigate the effects of *in vivo* treatment with simvastatin and fenofibrate on vascular responses by means of *ex vivo* aortic ring isometric tension studies. Simvastatin and fenofibrate were administered orally to Wistar rats for 6 weeks after which mechanisms involved with vasodilation or vasoconstriction induced by these therapies were investigated. The involvement of NOS was determined by selective NOS inhibitors and signalling pathways were investigated by Western blotting techniques.

4) Combine and compare*: In vitro, in vivo and ex vivo*

The final objective was to compare the results from all three models (*in vitro*, *ex vivo* and *in vivo*) and interpret the combined endothelio-pleiotropic effects of simvastatin and fenofibrate on the vascular tissue.

Chapter 2

Material and Methods: In vitro studies

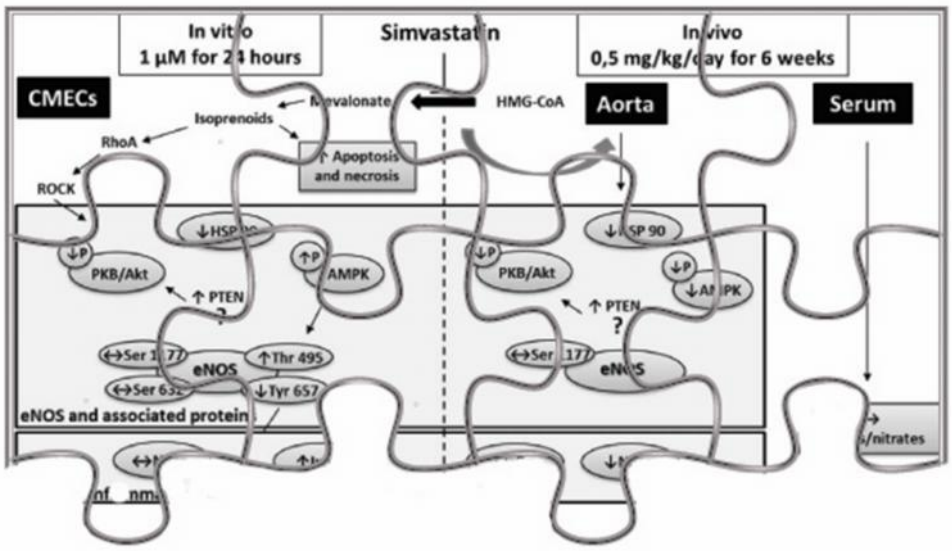

Chapter 2: Materials and Methods: *In vitro* studies

This chapter contains all of the methods employed for the *in vitro* cell culture experiments. For *in vitro* investigations a cell culture model of cardiac microvascular endothelial cells (CMECs) was used, with selected experiments repeated in aortic endothelial cells (AECs). The results of these studies will follow in Chapter 3.

2.1 Endothelial cell cultures

2.1.1 Materials

Endothelial cell growth medium (EGM-2) was purchased from Clonetics (Cambrex Bio Science, Walkersville, USA). Attachment factor and trypsin (500 BAEE units trypsin / 180 µg EDTA•4Na per ml in Dulbecco's PBS) were from Life Technologies (Carlsbad, California, USA). Foetal bovine serum (FBS) was obtained from Highveld Biological (Lyndhurst, RSA). 1,1'-dioctadecyl-3,3,3',3'-tetramethylindo-carbocyanine perchlorate (Dil-ac-LDL) was purchased from Biomedical Technologies (Stoughton, MA, USA). Dimethyl sulfoxide (DMSO) was purchased from Sigma-Aldrich (St Louis, Mo, USA).

2.1.2 Passaging of CMECs and AECs

Primary adult rat CMEC and AEC cultures were purchased from VEC Technologies (Rensselaer, New York, USA). Cells were received in culture in 75 cm^3 flasks and grown in EGM-2 growth medium in our laboratory until fully confluent in a standard tissue culture incubator (Forma Series II, Thermo Electron Corporation, Waltham, MA, USA) at 37 ^oC in a 40 – 60% humidified, 5% CO_2 atmosphere. Cultures were maintained in EGM-2 growth medium, supplemented with 10% FBS, and vascular endothelial growth factor - VEGF, human epidermal growth factor – hEGF, human fibroblastic growth factor hFGF, long chain human insulin-like growth factor - R3-IGF-1, ascorbic acid, hydrocortisone and antibiotics (gentamicin and amphotericin) in accordance with manufacturer's instructions. Cells received fresh growth medium every second day. Once cultures reached confluency, the cells were washed with PBS and incubated with pre-warmed (37^oC) trypsin until cells detached from the bottom of gelatin-containing

attachment factor-coated 35 mm petri dishes (after approximately 2-5 minutes). Detached cells were rapidly transferred into a 15 ml conical tube containing growth media and centrifuged for 3 minutes at 1000 revolutions per minute (rpm). The supernatant was aspirated and pellet resuspended in growth medium. Passaging to the next generation was performed at a 1:2 ratio. Cell aliquots were suspended in a freezing medium (90 % FBS, 5 % growth medium and 5 % DMSO) and stored in liquid nitrogen for future use. The passaging and storage procedures of the cells are shown in figure 2.1.

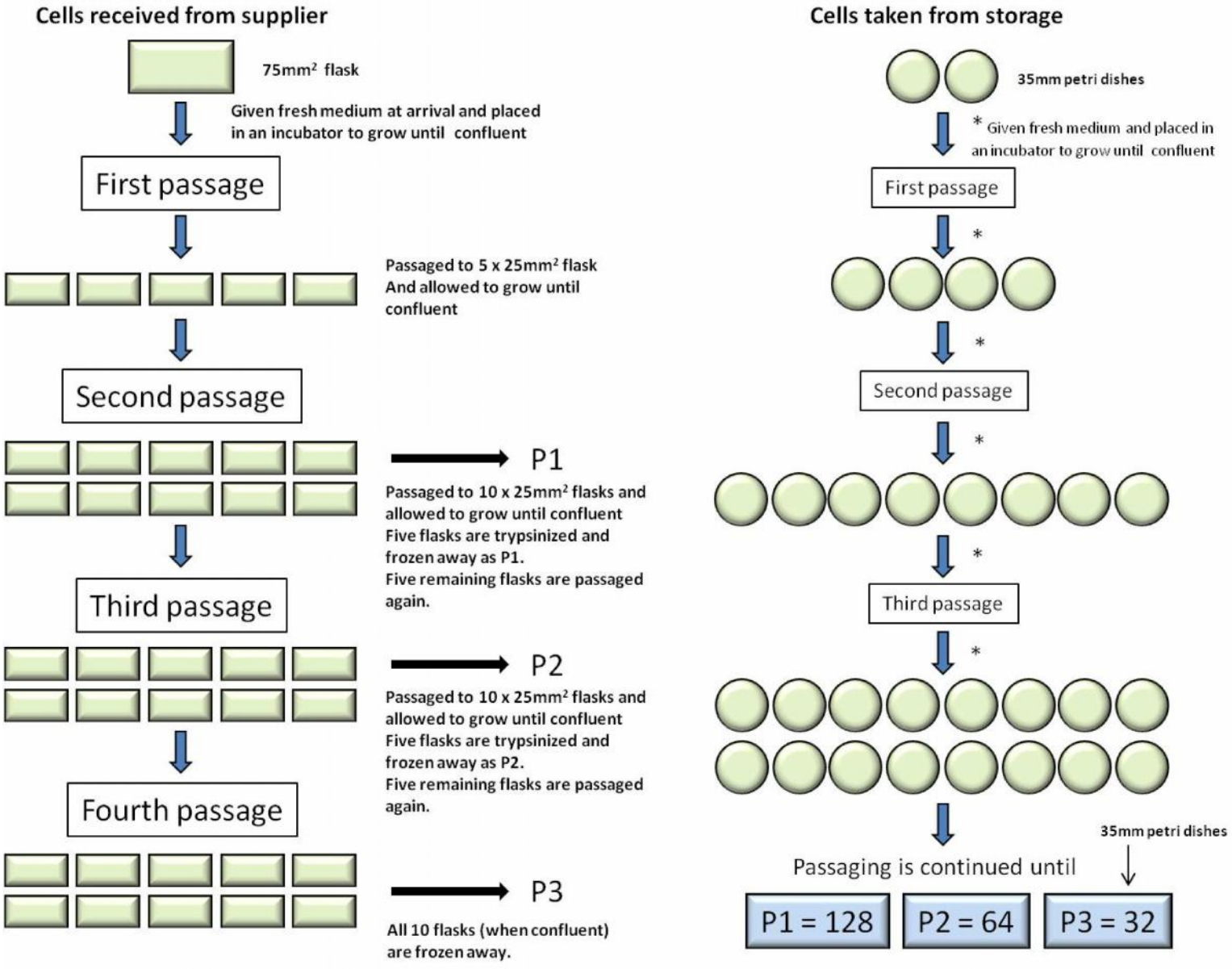

Figure 2.1: Passaging and cell aliquot storage procedures (from Genis, PhD thesis, University of Stellenbosch, April 2014)

Endothelial cell culture purity was regularly monitored by light microscopic validation of the typical monolayer, cobblestone appearance exhibited by cultured endothelial cells (Nishida *et al*., 1993; Piper *et al*., 1990) as well as confirmation by FACS analysis of >80% positive staining with the endothelial cell-specific marker, acetylated low density lipoprotein labeled with Dil-ac-LDL (figure 2.2) (Nishida *et al*., 1992; Piper *et al*., 1990).

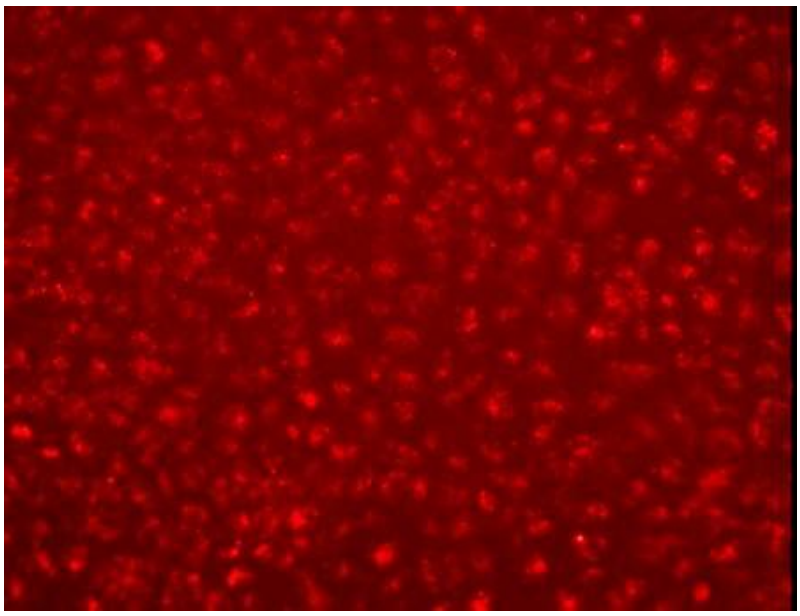

Figure 2.2: CMECs stained with Dil-ac-LDL to confirm endothelial cell purity. A representative microphotograph (20x magnification) of confluent CMECs showing the bright-red staining of endothelial cells that have taken up the fluorescently-labeled LDL (Olympus IX-81 inverted fluorescent microscope).

2.2 Simvastatin and Fenofibrate experimental protocols

A detailed description of the various treatment protocols will appear in the Results Chapter 3.

2.2.1 Simvastatin and Vehicle

50 mg of simvastatin (Merck, Damstadt, Germany) was dissolved in 1 ml ethanol. 813 µL of a 1N NaOH solution was added and pH adjusted to 7.2 by addition of small quantities of 1N HCl. The total volumes of all reagents added to dissolve as well as neutralize simvastatin were calculated and vehicle solutions prepared accordingly. Simvastatin and vehicle solutions were divided into aliquots and stored at -20^{o}C for 1 month. These steps ensure convertion of simvastatin to its active form.

2.2.2 Fenofibrate and Vehicle

Fenofibrate (Sigma, St Louis, Mo, USA) was dissolved in 0.2% DMSO. Equal volumes of DMSO were used for vehicle controls.

2.3 Flow cytometric analyses

Flow cytometric analyses formed a cornerstone of the *in vitro* experiments and were conducted on a Becton-Dickinson FACSCalibur flow cytometer (Franklin Lakes, NJ). Flow cytometric data were analysed by means of the WinMDI ® version 2.9 software package (Purdue University Cytometry Laboratories, West Lafayette, USA). For each experimental sample, a total of 5000 - 10 000 “events” (cells) were acquired and visualised on a so-called scatterplot (figure 2.3 A). The cell population of a given sample was subsequently gated (figure 2.3 A) in order to exclude any debris and non-cellular particles. From the gated populations, the mean fluorescent intensity emitted by the fluorescent probe was determined and depicted on histogram graphs (figure 2.3

B). Post-acquisition analysis allowed the user to perform overlays of the histograms, which enabled visualisation of shifts (if any) in the fluorescence intensity between control and treated samples (figure 2.4). All fluorescence data are expressed relative to control (control adjusted to 100%).

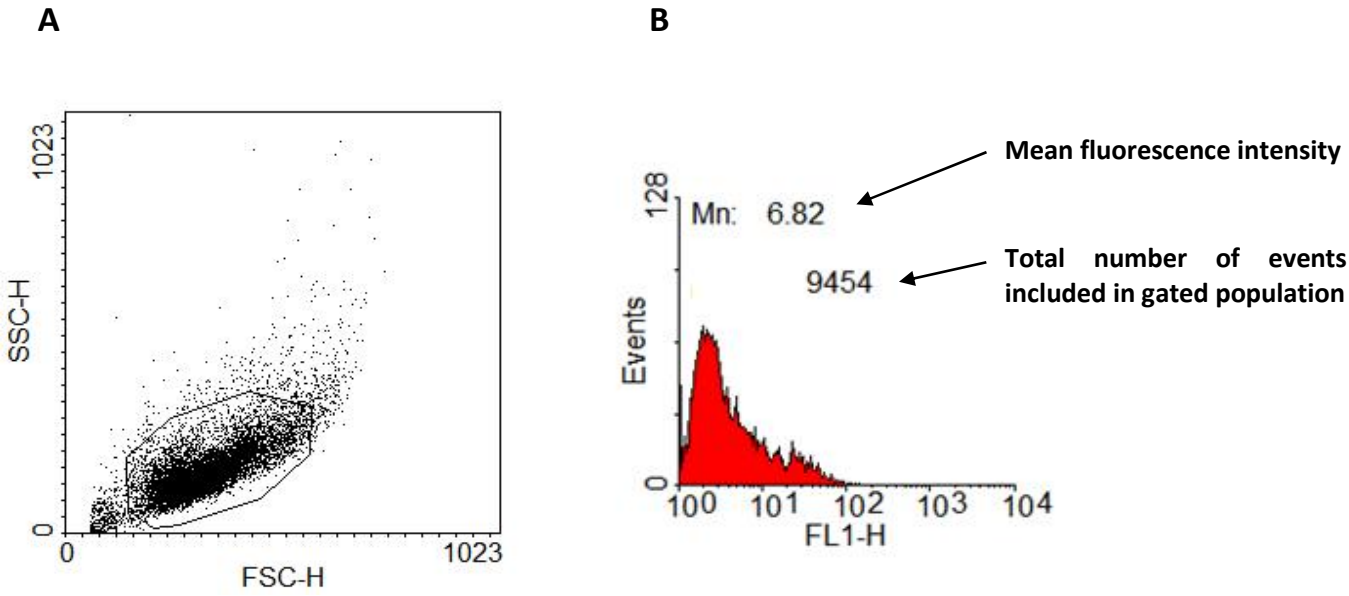

Figure 2.3: A) A representative scatterplot of a CMEC sample indicating the forward scatter (FSC-H; X axis), which measures cell size, and side scatter (SSC-H; Y axis) which measures cell granularity. The population of interest is gated and only events acquired within the gate will be taken into account in the histogram. B) A representative histogram plot showing the flow channel 1 (FL1-H; X axis) which measures fluorescence intensity and number of events (Events; Y axis). In this example, the mean fluorescence intensity is indicated by "Mn: 6.82", and a total number of 9454 gated events (cells) were analysed.

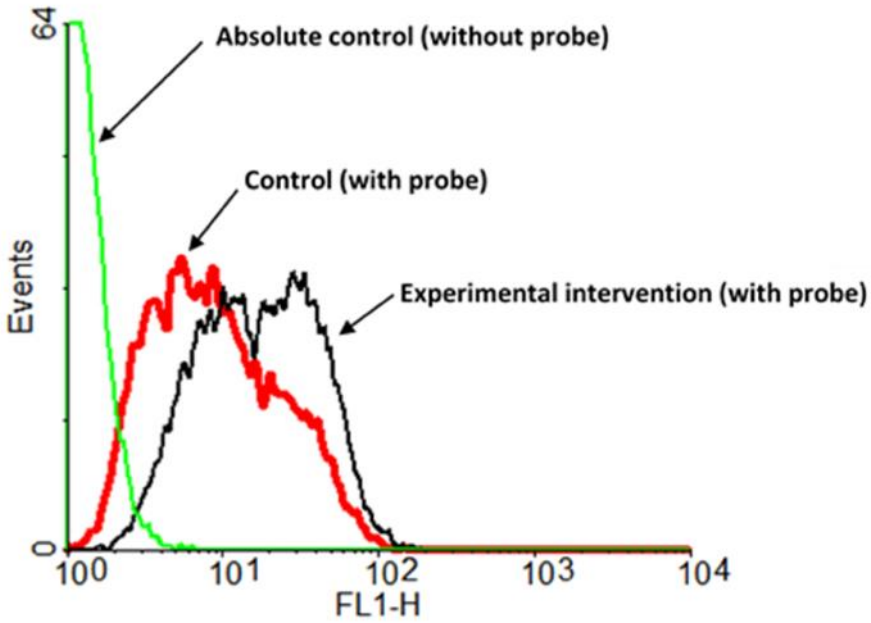

Figure 2.4: A representative histogram showing the overlay of three separate samples, namely: (i) Absolute control (sample without fluorescent probe representing baseline auto-fluorescence of the cells), (ii) Control (sample with fluorescent probe), and (iii) Experimental sample (with fluorescent probe). In the above example, the shift in mean fluorescence intensity between absolute control to control to experimental sample can be clearly observed.

2.3.1 Materials

4,5-Diaminofluorescein diacetate (DAF-2/DA) was from Calbiochem (San Diego, CA, USA) Dihydrorhodamine-123 (DHR-123), dimethoxy-1,4-naphthoquinone (DMNQ), and diethylamine NONOate (DEA/NO) were purchased from Sigma-Aldrich (St Louis, Mo, USA). Alexa Fluor 647 Annexin V, Propidium iodide (PI) solution, Annexin V binding buffer and cell staining buffer were purchased from Bio-Legend (Biochom-Biotech) (San Diego, CA, USA). Authentic peroxynitrite was from Millipore (Bedford, MA, USA). Dihydroethidium (DHE) and MitoSOX^{TM} Red were from Life Technologies (Carlsbad, California, USA). All other chemicals and buffer reagents were purchased from Merck (Damstadt, Germany).

2.3.2 Methods

All experiments were performed on cell cultures that were fully confluent. The reasoning behind this is that confluent cells develop cell cycle arrest at the G0 phase due to cell-to-cell contact. In this way, possible cell cycle variability is minimized since mitotic activity has ceased (Viñals & Pouysségur 1999).

2.3.2.1 NO measurements: DAF

Once confluent, cells were washed twice with sterile PBS and treated with fenofibrate and / or simvastatin. At completion of the drug treatment period, the drugs were washed out with PBS before administering 10 µM DAF-2/DA (in PBS) at 37 °C for 2 hours. DAF-2/DA is a NO-specific fluorescent probe which measures intracellular NO-production. Upon reacting with NO, DAF-2/DA is oxidized and emits a green fluorescent colour which can be analysed in flow channel 1 of the flow cytometer. This protocol has previously been established in the laboratory (Strijdom *et al*., 2004; Strijdom *et al*., 2006).

After 2 hours, the DAF-2/DA-PBS supernatant was aspirated, cells washed with PBS, trypsinized with pre-warmed trypsin and added to a conical tube containing cell staining buffer. Since flow cytometry is based on fluorescent colour emission, cell staining buffer is used instead of growth media. Cell staining buffer is colourless whereas growth media has a light pink colour. Cell

suspensions were centrifuged at 1000 rpm for 3 minutes after which the supernatant was aspirated. Pellets were resuspended in PBS in preparation for flow cytometric analysis.

All experimental groups included an absolute control (AC) sample without DAF-2/DA and represented the auto-fluorescence of cells as well as DAF-2/DA containing control samples.

Positive control: DEA/NO

DEA/NO, a NO donor, has previously been shown in the laboratory to be a consistent and reliable positive control for intracellular NO measured by DAF-2/DA (Genis, PhD thesis, University of Stellenbosch, April 2014). The protocol used for DEA/NO is outlined in figure 2.5. In short, petri dishes designated for DEA/NO were washed with sterile PBS and incubated with 10 µM DAF-2/DA for 1 hour, before adding 100 µM DEA/NO for an additional 2 hours (figure 2.6). After 3 hours the positive control samples were washed, trypsinized and prepared for flow cytometric analysis as previously described.

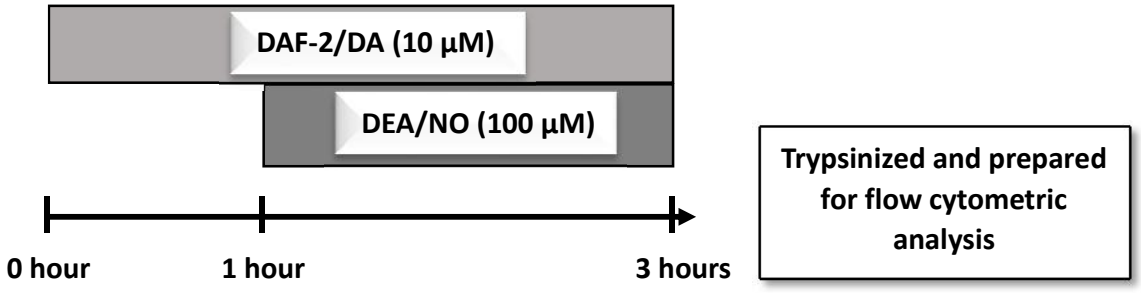

Figure 2.5: A schematic representation of the protocol used for the positive NO control, DEA/NO.

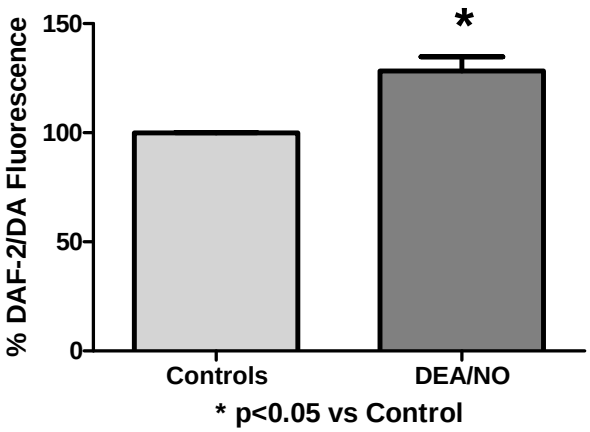

Figure 2.6: DEA/NO (100 µM; 2 hours) significantly increased mean DAF-2/DA fluorescence intensity and was included as a positive NO control in the study.

2.3.2.2 ROS measurements

Three types of ROS were measured by flow cytometry: superoxide anion by means of the DHE fluorescent probe (Nazarewicz *et al.,* 2013) or mitochondrial superoxide by means of MitoSOX™ Red (Hulsmans *et al*., 2012), and peroxynitrite and mitochondrial ROS by means of the DHR-123 fluorescent probe (Tiede *et al*., 2011) based on protocols previously established by Strijdom *et al*. (2006).

The superoxide-specific fluorescent probe, DHE, exhibits a blue-fluorescent colour when in the cytosol, however when it reacts with superoxide anions it becomes oxidized and translocates to the nucleus, where it intercalates with cellular DNA and emits a bright fluorescent red colour detected by flow channel 2 of the flow cytometer. MitoSOX™ is a fluorogenic dye targeted to the mitochondria and produces a red fluorescence when it becomes oxidized by superoxide. DHR-123 is an uncharged and non-fluorescent indicator of ROS that passively diffuse across the membrane, and is oxidized to form cationic rhodamine 123. Rhodamine-123 eventually localizes in the mitochondria and emits a green fluorescence detected by flow channel 3 of the flow cytometer. The protocol for DHE and DHR-123 are very similar to the one explained in section 2.2.1 for DAF-2/DA. At completion of the experimental intervention, (fenofibrate and /or simvastatin treatment) cells were washed with sterile PBS and DHE (5 µM) or DHR-123 (2 µM) added to cells in culture for 2 hours at 37 ^{o}C (Navarro-Antoli *et al*., 2001). MitoSOX™, however is only incubated for 10 min at 37^{o}C prior to trypsinization. The fluorescent probes were washed out and further prepared as described in section 2.3.2.1.

Positive controls: DMNQ and authentic peroxynitrite

The positive controls for DHE and DHR-123 were the ROS donor DMNQ (100 µM) and authentic peroxynitrite (100 µM) respectively. Petri dishes designated as positive controls were first incubated with DHE and DHR-123 respectively for 1 hour, prior to adding DMNQ and peroxynitrite for an additional 2 hours (figure 2.7 and 2.9). Subsequently, cells were washed and prepared for flow cytometric analysis (figure 2.8 and 2.10).

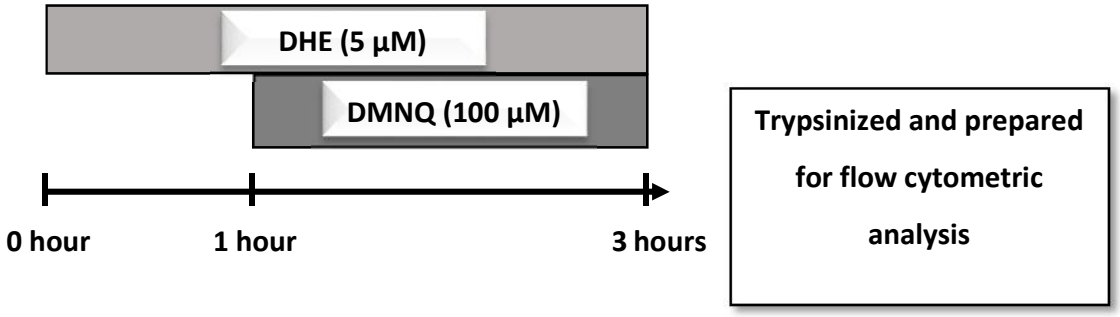

Figure 2.7: A schematic representation of the protocol used for the positive superoxide anion control, DMNQ.

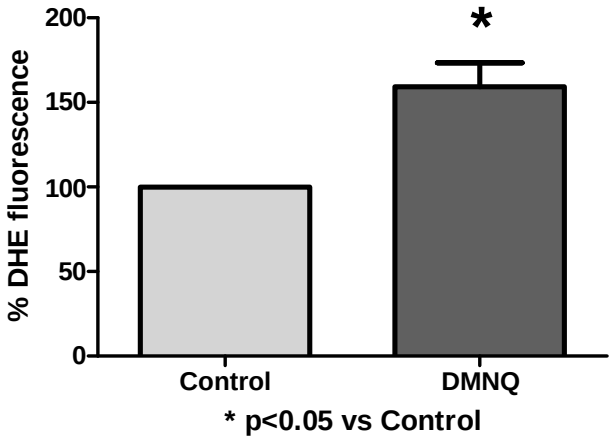

Figure 2.8: DMNQ (100 µM; 2 hours) significantly increased mean DHE fluorescence intensity and was included as positive control for DHE.

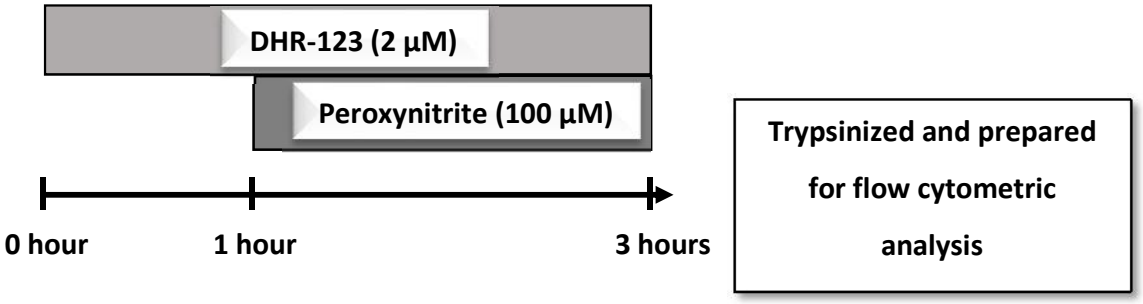

Figure 2.9: A schematic representation of the protocol used for the positive DHR-123 control, authentic peroxynitrite.

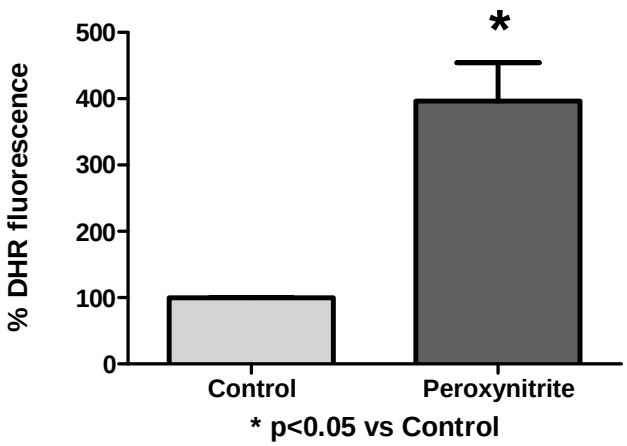

Figure 2.10: Peroxynitrite (100 µM; 2 hours) significantly increased mean DHR-123 fluorescence intensity and was included as positive control for DHR-123.

2.3.2.3 Cell viability measurements

Cell viability was assessed in all experimental groups by measuring apoptosis and necrosis. Cells were removed from culture by trypsinization followed by a washing procedure with cell staining buffer and binding buffer and centrifugation (700 rpm for 2 minutes). Cell suspensions were incubated in Alexa Fluor® 647 Annexin V conjugate (5 µM; marker of apoptosis) and propidium iodide (PI) (5 µM; marker of necrosis) for 15 minutes at 37 ^{o}C. During the process of apoptosis, phosphatidylserine will translocate from the inner membrane of a cell to the outer membrane. Annexin V will bind to phosphatidylserine on the outer membrane and thereby identify cells undergoing apoptosis. PI, on the other hand, will enter the nucleus of a cell when membrane integrity is lost due to necrosis (Wilkins *et al*., 2002).

Annexin V was measured in flow channel 4 and PI in flow channel 2 (figure 2.11 A – D). These two parameters were measured simultaneously and discrimination between the apoptotic and necrotic populations was achieved by creating quadrants of the gated populations (figure 2.12).

Positive control: H2O

As positive control for necrosis, AECs were treated with distilled water (H_2O) for 3 minutes. As a result of osmosis, H_2O will diffuse across a semi-permeable membrane from an area with low osmolarity (high H_2O concentration) to an area of high osmolarity (low H_2O concentration). Therefore the net result of treating the endothelial cells with distilled H_2O is the movement of H_2O molecules over the cell membrane and into the cell. Cells swell and eventually burst. Rupturing of the cell membrane due to necrosis allows the PI fluorescent probe to enter and stain the nucleus by intercalating with the DNA (figure 2.13).

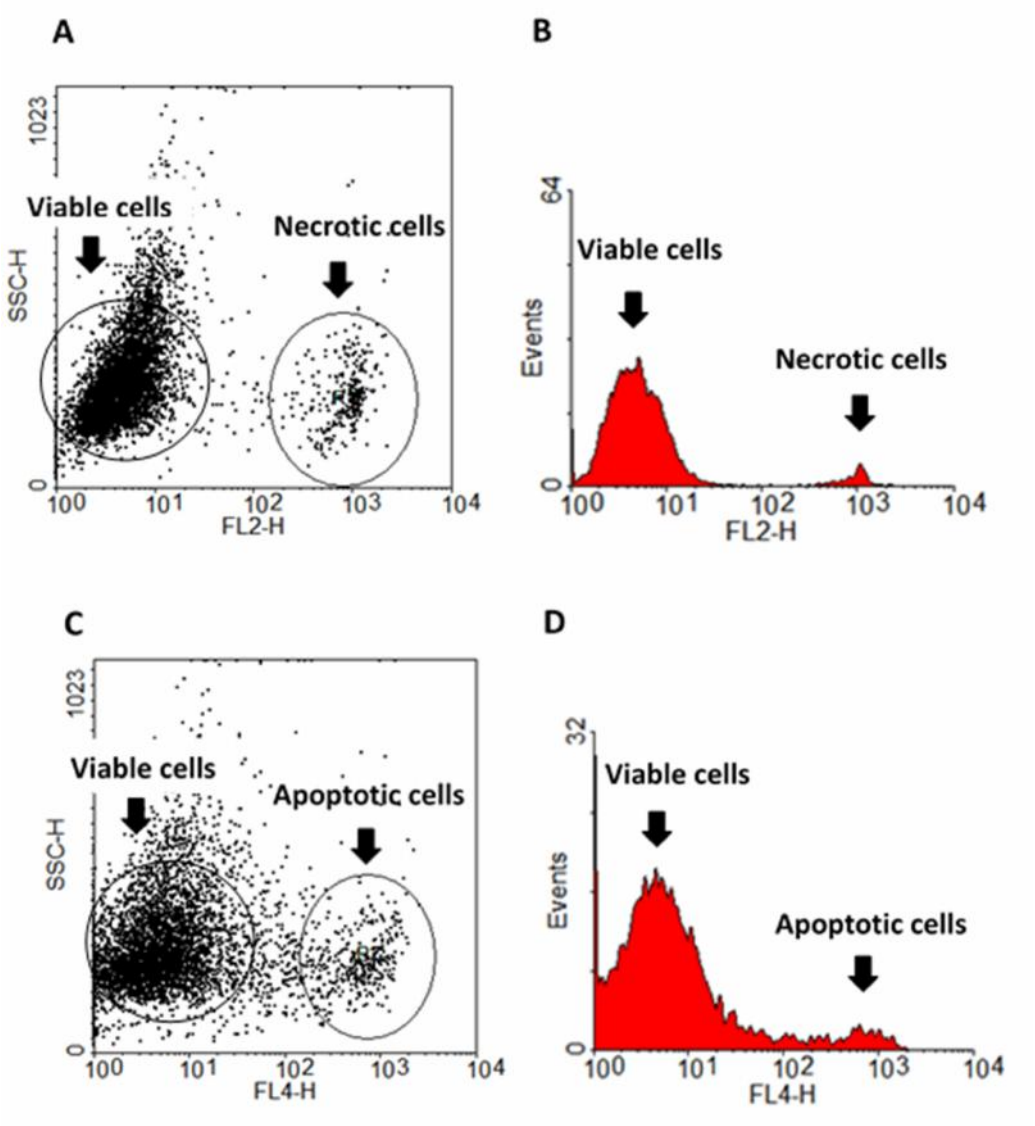

Figure 2.11: A) A representative scatterplot in which the sub-populations of viable and necrotic cells have been gated. PI fluorescence is measured on the x-axis (FL2-H). B) A representative histogram of the same sample in (A) which clearly shows the distinction between the viable sub-population and the necrotic sub-population respectively. C) A representative scatterplot in which the sub-populations of viable and apoptotic cells have been gated. Annexin V fluorescence is measured on the Y-axis (FL4-H). D) A representative histogram of the same sample in (C) which clearly shows the distinction between the viable sub-population and the apoptotic sub-population respectively.

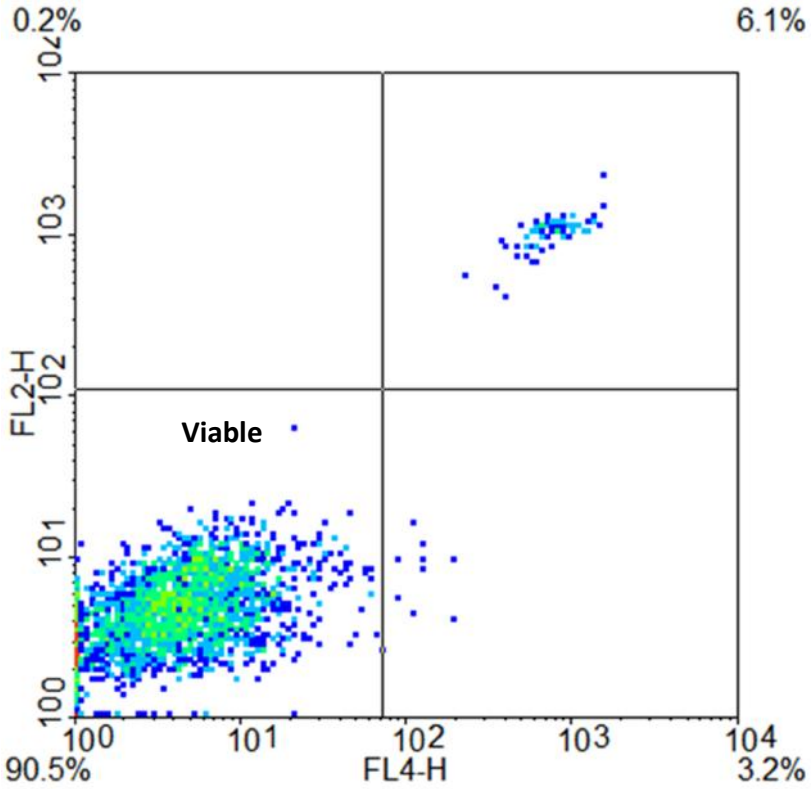

Figure 2.12: A density plot showing the simultaneous measurement of necrosis and apoptosis in the same sample (PI fluorescence measured in the FL2-H channel on the Y-axis and Annexin-V fluorescence measured in the FL4-H channel on the X-axis), showing the percentage of viable (Left lower quadrant), early apoptotic (Right lower quadrant) and necrosis (Right upper quadrant).

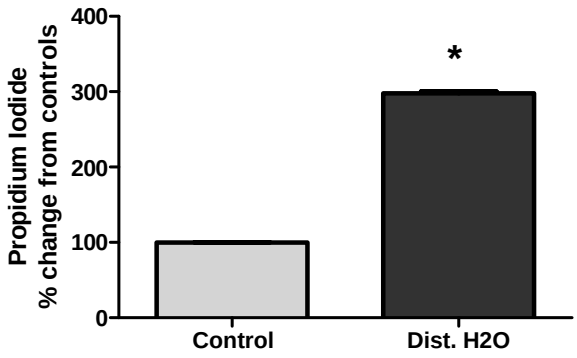

*Figure 2.13: Distilled H2O significantly increased propidium iodide staining in AECs. * p<0.05 vs Control.*

2.4 NO measurements with the Griess Reagent

As an alternative method for measuring NO synthesis the Griess reagent was utilised, which measures the break-down products of NO, namely nitrates and nitrites (Griess 1879). As discussed in chapter 1, nitrates can be converted to nitrites and nitrites can be converted back to NO under ischaemic/hypoxic conditions (Webb *et al.,* 2004; Duranski *et al*., 2005). This method is more than a hundred years old and is based on a colour reaction when nitrite reacts with the Griess reagent to form an azo dye, which can be measured spectrophotometrically or as a colorimetric reaction using a platereader (Giustarini *et al*., 2008).

2.4.1 Materials

The Griess Reagent kit was purchased from Sigma-Aldrich (St Louis, Mo, USA).

2.4.2 Methods

For the purpose of these experiments, CMECs and AECs were cultured in 24 well microplates. Once the cultured cells reached confluency, they were subjected to the various experimental conditions. At the end of the treatment periods, Griess reagent (Griess 1879) was added in a 1:1 volume:volume ratio to each well and incubated in the dark for 15 min at room temperature. The colorimetric reaction was measured at 540 nm on a FLUOstar Omega platereader from BMG Labtech (Ortenberg, Germany). A standard curve was included on each multiwell plate using a 200 µM stock solution of $NaNO_2$ and PBS. Serial dilutions (0.4-10 µM) were prepared as seen in figure 2.14. Colorimetric results from experimental samples were converted to µM nitrites using the corresponding standard curve on each multiwell plate (figure 2.16).

Positive control: DEA/NO DEA

The NO donor, DEA/NO, was included as positive control for increased nitrite concentration. DEA/NO was administered at a concentration of 10 µM for 3 hours after which Griess reagent was added to all sample-containing wells, incubated for 15 minutes (room temperature) and colorimetric reactions measured on the plate reader (figure 2.15 – 2.17).

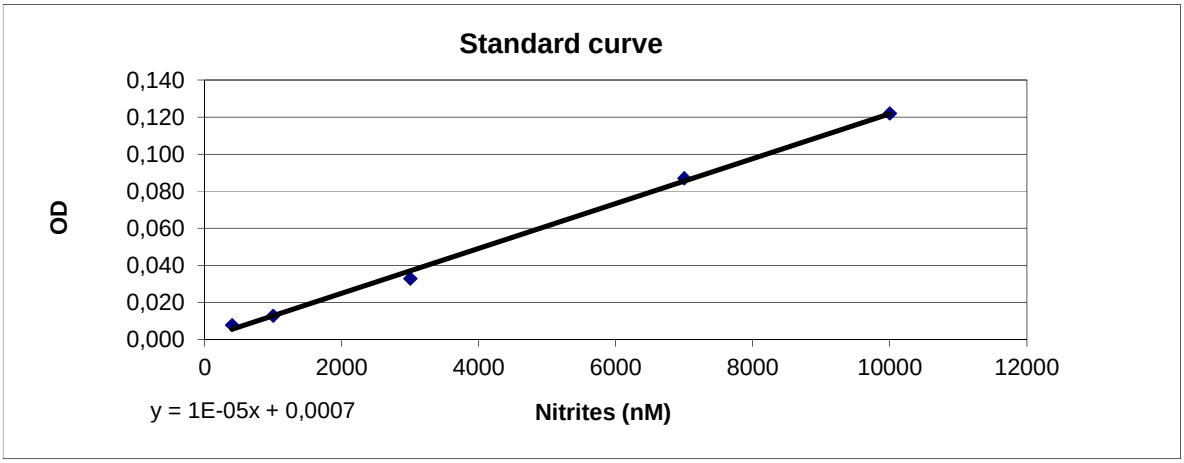

Figure 2.14: An example of the standard curve created for each experiment. Readings for the experimental samples were derived from the standard curve.

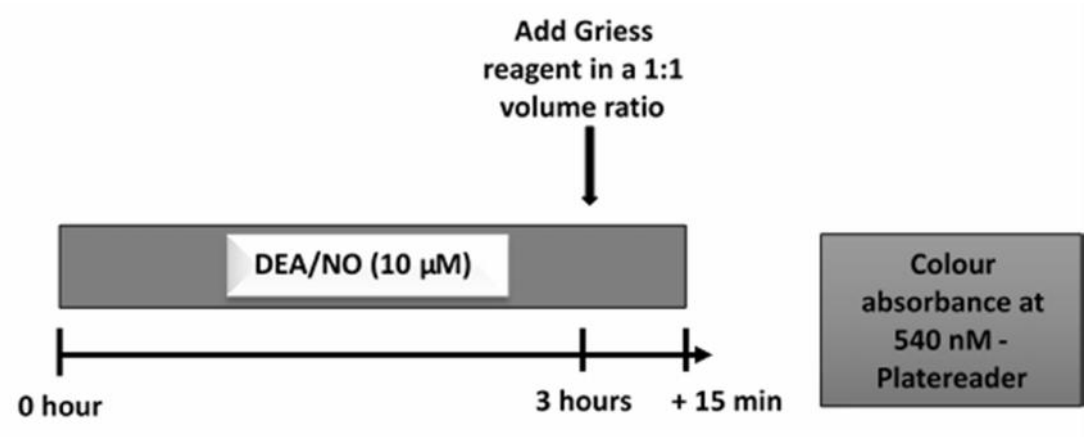

Figure 2.15: A schematic representation of the protocol used for the positive control DEA/NO in Griess reaction experiments.

Figure 2.16: A 24 well plate used for Griess reaction experiments. A gradual increase in colour intensity can be observed in row A and represents the increased $NaNO_2$ standard concentrations (0 µM; 0.4 µM; 2 µM; 4 µM; 7 µM and 10 µM). Row C represents the colour reaction observed after treating cells with 10 µM DEA/NO for 3 hours (NO positive control).

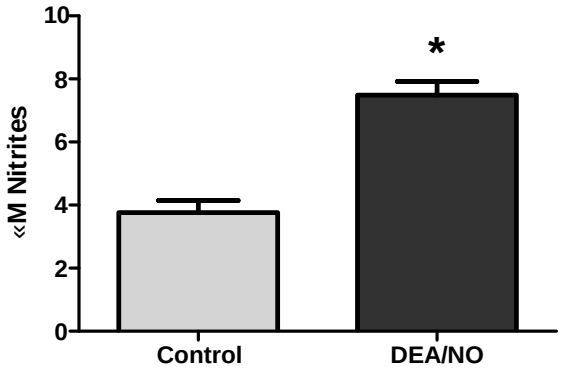

Figure 2.17: DEA/NO (10 µM for 3 hours) serves as a positive control for increased levels of nitrites observed with the Griess reaction.

2.5 Quantitative real-time polymerase chain reaction (qPCR)

2.5.1 Materials

High Capacity cDNA synthesis Kit (Lot # 1309189; Part # 4368814), TaqMan® gene expression assays and TaqMan® Universal Master Mix II (Lot # 1308032; Part # 4400040) were obtained from Life Technologies (Carlsbad, California, USA). RNeasy Mini Kit (Cat # 74104) and RNase-free DNase set (Cat # 79254) were from Qiagen (Hilden, Germany).

2.5.2 Methods

2.5.2.1 RNA extraction and cDNA synthesis

Control and experimental group CMECs were analysed for iNOS messenger ribonucleic acid (mRNA) accumulation by means of quantitative real-time PCR. Three biological replicates of each group were analysed. To account for technical variation, each replicate was assayed in triplicate. CMECs were lysed directly in the cell culture dish by adding Buffer RLT (Qiagen RNeasy Mini Kit component, Hilden, Germany) and the lysate removed using a cell scraper. The lysates were frozen on dry ice and transported to the Centre for Proteomic and Genomic Research (Cape Town, South Africa) for further analysis. RNA was extracted using the RNeasy Mini Kit (Qiagen, Hilden, Germany) in compliance with manufacturer's instructions. RNase-free DNase (Qiagen) was used for deoxyribonucleic acid (DNA) elimination. RNA was quantified using the NanoDrop ND-1000 (ThermoScientific, Waltham, MA, USA) and samples normalised to 500 ng/10 µL for cDNA synthesis. cDNA was synthesised using the High Capacity cDNA Synthesis kit (Life Technologies, Carlsbad, CA, USA) according to manufacturer's instructions. For each sample two cDNA synthesis reactions were performed. A master mix of reverse transcriptase buffer, dNTP mix, MultiScribe™ reverse transcriptase, random primers and nuclease free water was added to 10 µL of RNA for a total volume of 20 µL. Cycling was performed on the DNA Engine Tetrad 2 Peltier thermal cycler (BioRad, Hercules, CA, USA) and the reaction was kept at 25 ^{o}C for 10 min, after which the temperature was raised to 37 ^{o}C for 120 min and then 85 ^{o}C for 5 min.

2.5.2.2 Gene expression analysis

Quantitative real-time PCR was performed on the ABI 7900HT Fast Real Time PCR (Life Technologies, Carlsbad, CA, USA) using catalogued TaqMan® Gene Expression assays for each target gene combined with TaqMan® Universal Master Mix II. Each reaction consisted of 1 µL cDNA template (with a final concentration of 10 ng RNA), 0.5 µL of the Gene Expression assay, 5 µL of TaqMan® Universal Master Mix II and nuclease-free water sufficient to have a final volume of 10 µL. Thermal cycling consisted of one cycle of 10 min at 95 °C followed by 40 cycles of a denaturing step at 95 °C for 15 seconds and an annealing/extension step of 60 seconds at 60 °C. In order to exclude gDNA and template contamination, a water control and one replicate IL-1β treated sample was added as a no-reverse transcription control. SDS v2.3 software (Life Technologies) was used for raw data analysis and relative gene expression analysis was performed using qBase+ (BioGazelle, Zwijnaarde, Belgium) (Vandesompele *et al*., 2002). Outliers were identified as a replicate varying by >0.65 Cycle threshold (Ct) value. The amplification efficiencies of iNOS as well as three reference genes, HPRT, GAPDH and the gene encoding heat shock protein 90 (HSP90) were found to be within the range of 90%-110% (addendum). The stability of the three reference genes was assayed using GeNorm (in qBase+, BioGazelle) and found to be satisfactory (addendum). These reference genes were used to normalise gene expression data.

2.6 Signalling investigations – Western blot analyses

Signalling cascades and molecules were investigated by means of Western blot analyses. The following materials and methods were used for these investigations:

2.6.1 Materials

The following Western blot antibodies were obtained from Cell Signaling Technologies (Beverly, MA, USA): eNOS, phospho-eNOS (Ser 1177); protein kinase B (PKB)/Akt, phospho PKB/Akt (Ser

473); poly ADP ribose polymerase (PARP), AMP activated protein kinase (AMPK), phospho AMPK (Thr 172); cleaved caspase-3; IκBα, β-tubulin and glyceraldehyde 3-phosphate dehydrogenase (GAPDH). Antibodies for nitrotyrosine, p22PHOX, and iNOS were purchased from Santa Cruz Biotechnologies (Santa Cruz, CA, USA) and nNOS and phospho nNOS (Ser 1417) antibodies were purchased from Abcam (Biocom-Biotech). Antibodies for phospho-eNOS Ser 632 and phospho-eNOS Tyr 657 were purchased from ECM Biosciences. Enhanced chemiluminescence (ECL) detection reagent, ECL hyperfilm, and Horseradish peroxidase-linked anti-rabbit IgG were from AEC Amersham (Buckinghamshire, UK). Polyvinylidene difluoride (PVDF) membrane (Immobilon™-P), was from Millipore (Bedford, MA, USA). All other chemicals and buffer reagents were purchased from Merck (Darmstadt, Germany).

2.6.2 Methods

2.6.2.1 Cell lysates

The Western blotting procedure requires a high yield of protein. Initially, for a typical experiment, CMECs were grown in 35 mm petri dishes and cultured to the 7th passage (final number of petri dishes: 130) in order to accommodate a maximum of 4 experimental groups and a n-value of 3 or 4 per experimental group. These petri dishes were then pooled to have 9 to 10 petri dishes per lysate. Since it was quite a challenge to treat and trypsinize 130 petri dishes, it was decided to rather grow the cells in larger (100 mm) petri dishes and found one of them to yield a sufficient protein concentration for one lysate. These petri dishes were also easier to treat, especially short term treatments such as 5 and 10 minutes.

CMECs were removed from culture by trypsinisation and added to a conical tube containing growth media. Tubes were centrifuged for 3 minutes @ 1000 rpm, and pellets transferred to an eppendorff tube. CMECs were homogenized in a lysis buffer containing 20 mM Tris; 1mM EGTA; 150 mM NaCl; 1mM β-glycerophosphate; 1 mM sodium orthovanadate; 2.5 mM tetra-sodium diphosphate; 1 mM phenylmethylsulfonyl fluoride (PMSF); 0.1 % sodium dodecylsulfate (SDS); 10 µg/ml aprotinin; 10 µg/ml leupeptin; 50 nM NaF and 1 % triton-X100. Zirconium oxide beads (0.15 mm) were added to the pellet and lysis buffer followed by homogenization with a Bullet

Blender™ (Next Advance, Inc., NY, USA). 3 cycles of 1 min were performed on setting 5 of the Bullet Blender. In between cycles, samples were allowed to cool for 5 minutes. Samples were placed on ice for 30 minutes after which they were centrifuged for 15 minutes at 14 000 rpm at 4 ^{o}C. Protein content of the supernatant was determined using the Bradford assay (Bradford, 1976). Based on the Bradford assay findings, a sample was prepared containing 2X Laemmli buffer (4% SDS, 20% glycerol, 10 % 2-mercaptoethanol, 0.004 % bromophenol blue and 0.125 M Tris HCl) (Laemmli, 1970), lysis buffer and lysate , to ensure a final protein content of 20 - 50 µg/15 µl of sample.

2.6.2.2 SDS-polyacrylamide gel and membrane

These lysates were loaded on a SDS-polyacrylamide gel and transferred to a PDVF-membrane (Immobilon™-P, from Millipore). Table 2.1 indicates the percentage gel used for each antibody. Non-specific binding sites on membranes were blocked with 5 % fat-free milk in Tris-buffered saline, 0.1 % tween-20 (TBS-Tween) (Merck).

After blocking the non-specific sites, membranes were washed with TBS-Tween and incubated overnight at 4 ^{o}C with the specific primary antibody. The following morning, primary antibodies were washed off with TBS-Tween and membranes were incubated with a horseradish peroxidase-linked anti-rabbit IgG secondary antibody and subsequently protein bands were visualized with the ECL™ chemiluminescent system. Films were laser scanned and densitometrically analysed (UN-SCAN-IT, Silk Scientific, Orem, UT, USA). Equal loading was verified by blotting for the housekeeping proteins β-tubulin/GAPDH, and in some instances a ponceau stain was used. The specific primary and secondary antibody conditions of each antibody are shown in table 2.1.

Membranes were stripped of primary and secondary antibody with 0.2M NaOH and re-probed at a different molecular weight on the membrane than the initial antibody, therefore some proteins shared β-tubulin/ponceau loading controls. Since a soft strip with NaOH never removes the old signal completely this can to some extent avoid overlapping signals and false results.

2.7 Statistical Analysis

All flow cytometry data were calculated as mean ± standard error of the mean, with values expressed as % of control (control adjusted to 100%). For Western blot data, controls were adjusted to the value of 1. Total protein expression was calculated as a ratio of the loading control. Annexin V and propidium iodide data are expressed as % change in apoptotic or necrotic cells compared to control adjusted to 100%. Student's t-tests or one-way analysis of variance (with Bonferroni multiple comparison test) were used to determine statistical significance. Differences with a p-value < 0.05 were considered statistically significant. Data were analysed using GraphPad Prism 5 software (GraphPad Software, San Diego, CA, USA). Sample sizes are indicated below each graph in Chapter 3.

Table 2.1: Specifications for each antibody after optimization for Western blotting.

% SDS-polyacrylamide gel	Antibody	Primary Antibody conditions	Secondary antibody conditions
7.5%	**Total-eNOS 140 kDa**	1:1000 dilution in TBS-Tween	1:4000 dilution in 5% TBS-Tween milk
7.5%	**Phospho-eNOS Ser 1177 140 kDa**	1:1000 dilution in TBS-Tween	1:4000 dilution in 5% TBS-Tween milk
7.5%	**Phospho-eNOS Ser 632 (Mouse mAb) 140 kDa**	1:1000 dilution in TBS-Tween	1:4000 dilution in TBS-Tween (Anti-mouse)
7.5%	**Phospho-eNOS Thr 495 140 kDa**	1:1000 dilution in TBS-Tween	1:4000 dilution in TBS-Tween
7.5%	**Phospho-eNOS Tyr 657 140 kDa**	1:1000 dilution in TBS-Tween	1:4000 dilution in TBS-Tween
7.5%	**iNOS 131 kDa**	1:200 dilution in 2.5% TBS-Tween milk	1:4000 dilution in 5% TBS-Tween milk
7.5%	**Total-nNOS 160 kDa**	1:1000 dilution in TBS-Tween	1:4000 dilution in TBS-Tween
7.5%	**Phospho-nNOS 160 kDa**	1:416 dilution in TBS-Tween	1:4000 dilution in 2.5% TBS-Tween milk
10%	**Total-AMPK 63 kDa**	1:1000 dilution in TBS-Tween	1:4000 dilution in TBS-Tween
10%	**Phospho-AMPK 63 kDa**	1:500 dilution in TBS-Tween	1:4000 dilution in TBS-Tween

10%	**Total-PKB/Akt** **60 kDa**	1:1000 dilution in TBS-Tween	1:4000 dilution in 1% TBS-Tween milk
10%	**Phospho-PKB/Akt** **60 kDa**	1:500 dilution in TBS-Tween	1:4000 dilution in TBS-Tween
7.5% / 10%	**HSP90** **90 kDa**	1:1000 dilution in TBS-Tween	1:4000 dilution in 5% TBS-Tween milk
12%	**Cleaved Caspase-3** **17/19 kDa**	1:500 dilution in TBS-Tween	1:4000 dilution in 1% TBS-Tween milk
10%	**Cleaved PARP** **89 kDa**	1:500 dilution in TBS-Tween	1:4000 dilution in 2.5% TBS-Tween milk
7.5% / 10%	**Nitrotyrosine** **90 kDa**	1:5000 dilution in TBS-Tween	1:4000 dilution in TBS-Tween
12%	**P22phox** **22 kDa**	1:333 dilution in TBS-Tween	1:4000 dilution in 5% TBS-Tween milk
10%	**IκBα** **39 kDa**	1:1000 dilution in TBS-Tween	1:4000 dilution in TBS-Tween
7.5%/10%/12%	**β-tubulin** **55 kDa**	1:1000 dilution in TBS-Tween	1:4000 dilution in TBS-Tween
10%/12%	**GAPDH** **37 kDa**	1:1000 dilution in TBS-Tween	1:4000 dilution in TBS-Tween

Chapter 3

Results and discussions on the in vitro pleiotropic effects of Simvastatin and Fenofibrate

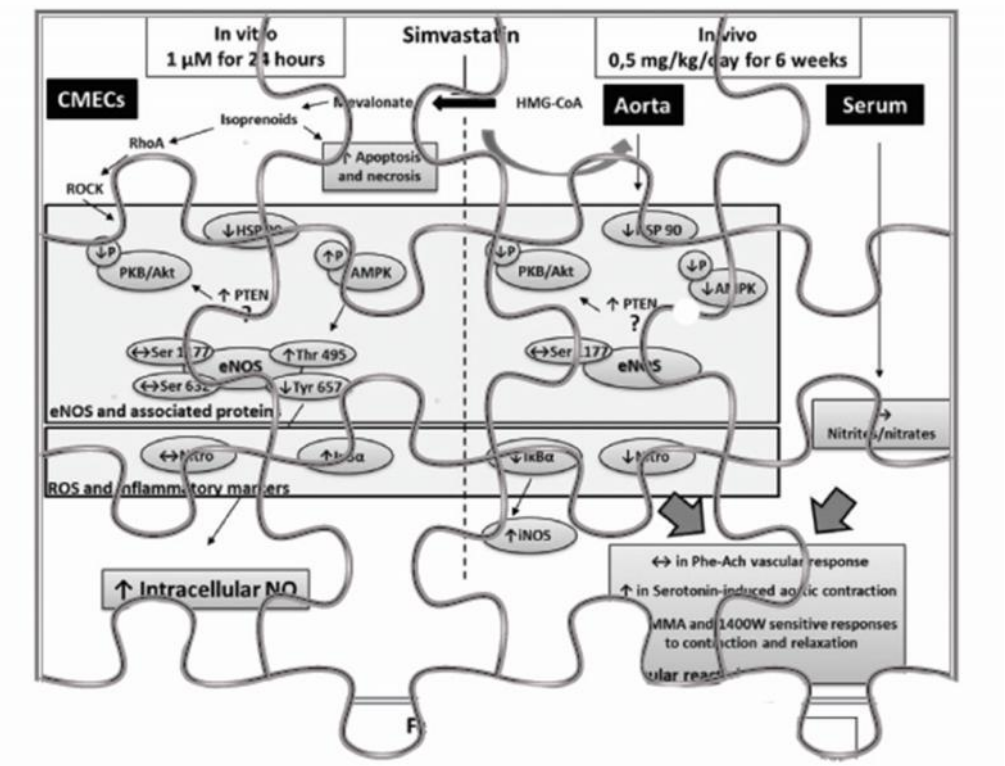

Chapter 3: Results and discussions on the *in vitro* pleiotropic effects of Simvastatin and Fenofibrate

3.1 Introduction

Most of the pleiotropic effects of simvastatin and fenofibrate revolve around their anti-oxidant anti-inflammatory, and anti-thrombotic properties, as well as an overall improvement in endothelial function (Davignon *et al.,* 2004; Tsimihodimos *et al*., 2005; Zhou & Liao 2010). *In vivo*, simvastatin is taken up by the liver where it inhibits the rate limiting step in *de novo* cholesterol synthesis and exerts the cholesterol-dependent effects explained in chapter 1 (Rikitake & Liao 2005). *In vivo,* fenofibrate acts as a synthetic ligand for the PPAR-α receptor, forms a heterodimer with retinoid-X receptor resulting in translocation of PPAR-α from the cytosol to nucleus where it transcribes genes involved with lipid metabolism (Berger & Moller 2002). Sure enough, improvement of lipid parameters in the blood has beneficial effects on the vascular endothelium, however there is evidence for direct pleiotropic effects of both simvastatin and fenofibrate on the endothelium, independent of *in vivo* cholesterol-dependent effects (Mulhaupt *et al*., 2003; Yang *et al*., 2005; Massaro *et al*., 2010).

The *in vitro* pleiotropic effects of simvastatin and fenofibrate have been investigated in many types of cell culture models, however with regards to endothelial cell models, it is evident that mainly large vessel-derived cultured endothelial cells were used (see table 1.1 and 1.2). Although fenofibrate was associated with improved microvascular function in a human study (Sacks 2008), few *in vitro* studies have investigated the effects of fenofibrate in cultured endothelial cells harvested from microvascular beds (Tomizawa *et al*., 2011). Furthermore, to the best of our knowledge, no studies have been performed on cardiac microvascular endothelial cells (CMECs).

NO production is one of the most important functions of the endothelium and increased bioavailability of NO is associated with cardioprotection (Jones *et al.*, 1999; Jones & Bolli 2006). Conversely, reduced bioavailability of NO is considered one of the major hallmarks of endothelial dysfunction (Bonetti 2003). NO is synthesised in the body by the enzyme, nitric oxide synthase

(NOS). NOS exists in three different isoforms, namely neuronal NOS (nNOS), inducible NOS (iNOS) and endothelial NOS (eNOS) and the concentration of NO synthesised is oftern isoform-dependent. An important NOS-independent source of NO is the conversion of nitrites and nitrates (breakdown products of NO) to NO, which can happen under hypoxic/ischaemic conditions (i.e. in the absence of co-substrate oxygen), thus contributing to protective mechanisms against ischaemic injury (Webb *et al.,* 2004; Duranski *et al.,* 2005).

Both simvastatin and fenofibrate have been shown to have a pronounced *in vitro* effects on activating endothelial eNOS, be it directly or indirectly (Sun *et al*., 2006; Arora *et al.,* 2012; Murakami *et al.*, 2006; Katayama *et al*., 2009; Tomizawa *et al.*, 2011). The main upstream activator for simvastatin-dependent eNOS activation is mostly identified as PKB/Akt although AMP-activated protein kinase (AMPK) has also been shown to be a role player. As for fenofibrate, AMPK is an important target resulting in activation and phosphorylation of eNOS (Ser 1177). AMPK is a nutrient-sensing serine/threonine kinase which becomes activated when the ratio of intracellular AMP:ATP is high. Phosphorylation at threonine (Thr) 172 is required for AMPK activation (Coughlan *et al*. 2014).

All of the *in vitro* studies performed with simvastatin and fenofibrate have focussed on the phosphorylation of eNOS at the Ser 1177 residue. Although it is considered as the most well described site of eNOS phosphorylation, the post-translational regulation of eNOS is a complex process and involves different types of positive and negative regulatory sites. To the best of our knowledge, no other studies have investigated the role of simvastatin and fenofibrate on multiple eNOS phosphorylation sites.

Contradictory results have been found for statins and fenofibrate with regards to their effects on cell viability. Statins have been shown to induce apoptosis (Blanco-Colio *et al.,* 2002*;* Demyanets *et al.,* 2006) or reduce apoptosis (Son *et al*., 2007). Similarly, fenofibrate treatment has resulted in decreased cell viability (Kubota *et al.,* 2005), and increased cell viability in HGMECs due to AMPK activation (Tomizawa *et al.,* 2011).

The inherent anti-oxidant properties of statins are not a new finding (Davignon *et al*., 2004b). It was first demonstrated by Girona *et al*., (1999) who showed that *in vitro* simvastatin treatment

(5-100 μM) delayed oxidation of low-density lipoprotein (LDL) molecules derived from non-dislipidaemic patients. They further showed that LDL and high density lipoproteins (HDL) molecules derived from simvastatin-treated patients had lower levels of aldehyde, a product of lipid peroxidation. Fenofibrate was also shown to exert anti-oxidant effects via reducing plasma-oxidised LDL or increasing superoxide dismutase activity (Wang, *et al*., 2010a; Walker *et al.*, 2012). Additionally, both drugs have been shown to be involved with an anti-inflammatory role in the vasculature (Yang *et al*., 2005; Ni *et al*., 2013).

The main mechanism by which the statins are thought to exert cholesterol and pleiotropic effects is due to inhibition of the rate-limiting step in cholesterol synthesis, namely the conversion of 3-Hydroxy-3-methylglutaryl coenzyme A (HMG-CoA) to mevalonate. Down-stream from mevalonate, isoprenoids such as farnesylpyrophosphate (FPP) and geranylgeranylpyrophosphate (GGPP) are formed. FFP and GGPP serve as lipid attachments for the post-translational modification of various proteins, including G proteins and small GTP binding proteins such as Ras, Rho, Rap and Rab GTPases. Thus if formation of the isoprenoid intermediates is inhibited, inhibition of small GTPase isoprenylation will follow (Ii & Losordo 2007; Rikitake & Liao 2005). RhoA is regarded as a molecular switch for many biological processes such as contraction, migration, adhesion, cell cycle progression and gene expression (Rikitake & Liao 2005). The main down-stream effector of RhoA is known as ROCK (Rho-kinase). Rho/ROCK has become a therapeutic target to prevent cardiovascular diseases. This is due to its involvement in rapid and dynamic reorganization of the actin cytoskeleton and effect on NO production. Activation of ROCK inhibits eNOS, thereby decreasing NO production (Nunes *et al.,* 2010). Similarly, one of the main mechanisms involved with fenofibrate-associated pleiotropic effects is the activation of the eNOS/NO pathway with all of the resulting down-stream signalling consequences.

3.2 Specific aims

Chapter 3 aimed to address aim 1 and 2 as set out in section 1.7.2 and included the following specific aims:

- First of all, we aimed to establish a concentration and time response curve for simvastatin and fenofibrate using NO, ROS and cell viability measurements as end-points. Since simvastatin is such a well researched therapy, special focus was given to fenofibrate investigations.
- To investigate, the underlying signalling mechanisms involved with changes in NO and ROS after simvastatin and fenofibrate treatment, especially with regards to NOS.
- To investigate the possible protective role of fenofibrate against injury induced by a pro-inflammatory cytokine such as TNF-α.

3.3 Simvastatin

3.3.1 Experimental protocol and methods: NO, ROS and cell viability

- Simvastatin concentrations: 100 nM, 1 µM and 3 µM.
- Time points: 1 hour and 24 hours.

Simvastatin (Merck, Darmstadt, Germany) was administered to CMECs in order to establish a concentration-time curve with NO, ROS and cell viability measurements as end-points. The rationale was to first explore the ability of 100nM, 1 µM and 3 µM simvastatin to increase NO levels at 1 or 24 hours, followed by confirmation that NO production is due to simvastatin-related effects by adding (RS)-Mevalonic acid lithium salt (Sigma-Aldrich, St Louis, Mo, USA) as co-treatment with simvastatin. Mevalonic acid, when co-administered with simvastatin, abolishes the effects of simvastatin. The pleiotropic effects of simvastatin are mainly derived from the inhibition of isoprenoid formation. These isoprenoids are down-stream of mevalonic acid in the cholesterol synthesis process. NO measurements were performed with the fluorescent probe 4,5-diaminofluorescein diacetate (DAF-2/DA), reactive oxygen species (ROS) by means of dihydrorhodamine-123 (DHR-123) fluorescence and cell viability using PI fluorescence and

Annexin V staining, as described in methods section 2.3.2.1 – 2.3.2.3. The experimental outline of each of these experiments is given in figure 3.1 (A-C).

Since the validation of the fluorescent probe selectivity by various positive controls (DEA/NO for DAF-2/DA, peroxynitrite for DHR-123 and DMNQ for DHE), were shown in Chapter 2 it will not be repeated in this chapter.

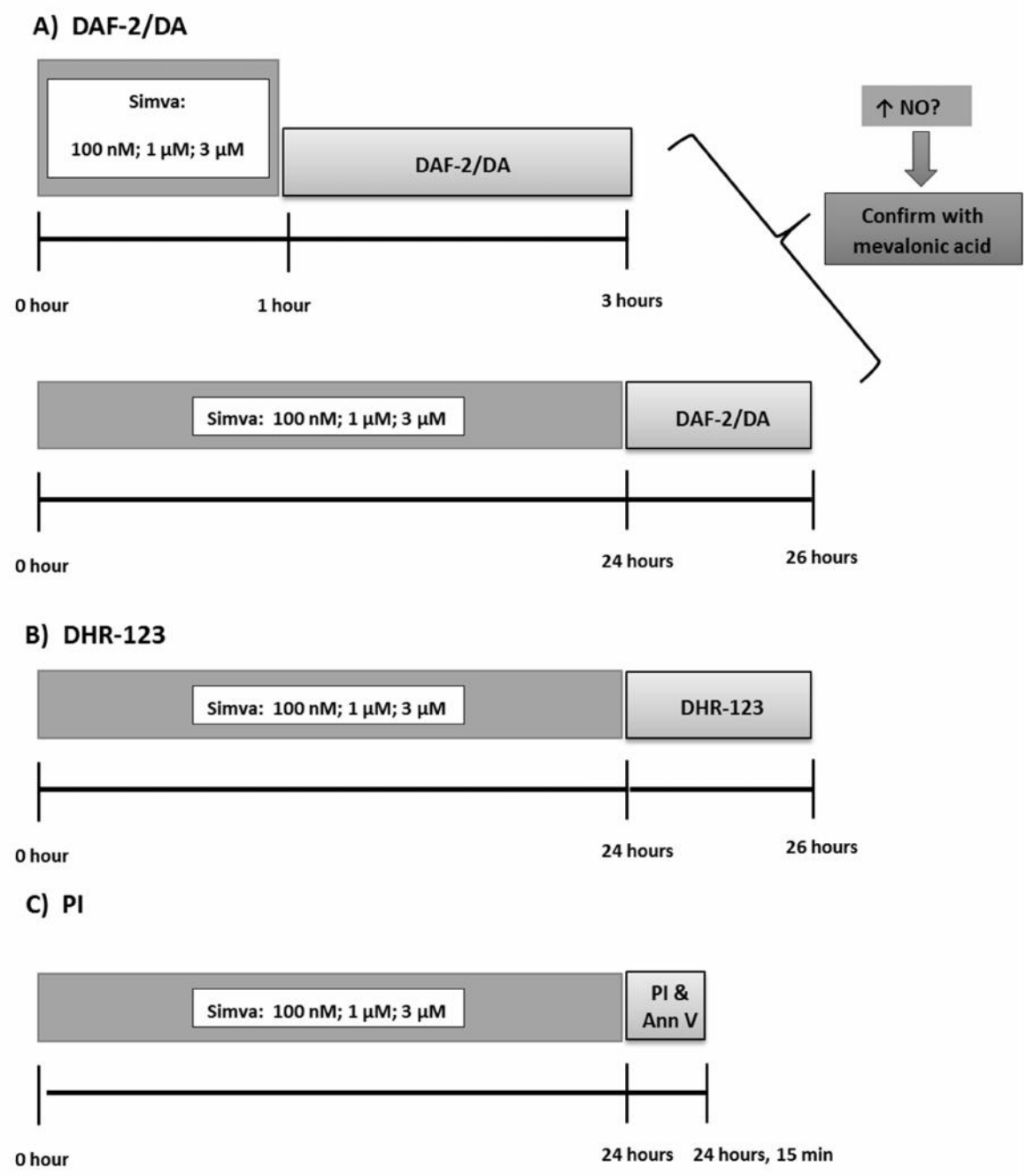

Figure 3.1: The experimental outline for NO, ROS and cell viability treatments with simvastatin. A) CMECs were treated with 100nM, 1 µM and 3 µM simvastatin for 1 and 24 hours, followed by a 2 hour incubation with DAF-2/DA, to investigate the effect on NO levels. If NO was elevated, mevalonic acid was added as co-treatment with simvastatin to confirm that increased NO levels are indeed due to simvastatin and inhibition of isoprenoid formation. B) CMECs were treated

with 100nM, 1 µM and 3 µM simvastatin for 24 hours, followed by a 2 hour incubation with DHR-123, to investigate the effect on ROS generation. C) Cell viability was measured using PI (necrosis) and Annexin V (apoptosis) staining after 24 hour incubation with simvastatin. Simva: simvastatin; NO: nitric oxide; DAF-2/DA: 4,5-Diaminofluorescein diacetate; DHR-123: Dihydrorhodamine-123; PI: propidium iodide; Ann V: Annexin V.

3.3.2 Results: The effect of simvastatin treatment on NO, ROS and cell viability.

3.3.2.1 NO measured with DAF-2/DA fluorescence

Initially, two treatment periods were included for NO investigations, namely 1 hour and 24 hours. 1 hour simvastatin treatment did not increase NO levels at any of the given concentrations. 100 nM simvastatin showed significantly lower DAF-2/DA fluorescence than its vehicle (Vehicle: 111.3% ± 3.6%; Simva: 94.4% ± 1.3%; $p<0.05$) (figure 3.2 A). However, 1 µM simvastatin did increase DAF-2/DA fluorescence significantly after 24 hour treatment (Vehicle: 95.9 ± 2.89%; 1 µM: 120.4% ± 6.9%; $p<0.05$) (figure 3.2 B). When mevalonic acid was administered in combination with 1 µM simvastatin treatment, DAF-2/DA fluorescence was reduced, however these values failed to reach significance (1 µM simvastatin: 120.4% ± 6.9%; 1 µM simvastatin + mevalonic acid: 93.7% ± 5.8%) (figure 3.2 C).

3.3.2.2 ROS measured with DHR-123 fluorescence

Considering the fact that 1 hour simvastatin treatment was not sufficient to elicit robust effects on NO production and changes were only observed after 24 hour simvastatin treatment, ROS and all other investigations were only performed on 24 hours incubations. Simvastatin 100 nM significantly increased DHR-123 fluorescence compared to its vehicle control (100 nM vehicle: 97.0% ± 7.1%; 100 nM simvastatin: 121.4% ± 6.9%; $p<0.05$ vs vehicle) (figure 3.3). No other changes were observed with regards to DHR-123 fluorescence (figure 3.3).

3.3.2.3 Cell viability measured by PI fluorescence and Annexin V staining

100 nM simvastatin had profound effects on cell viability, resulting in a significant increase in Annexin V fluorescence (Vehicle 100 nM: 83.5% ± 1.3%; Simvastatin 100 nM: 141.7% ± 2.3%; $p<0.05$) (figure 3.4 A) and PI fluorescence (Vehicle 100 nM: 102.6% ± 9.0%; Simvastatin 100 nM: 156.5% ± 6.9%; $p<0.05$) (figure 3.4 B). 1µM simvastatin similarly resulted in increased levels of Annexin V fluorescence (Vehicle 1µM: 62.1% ± 1.3%; Simvastatin 1µM: 110.5% ± 6.4%; $p<0.05$) (figure 3.4 A) and PI fluorescence (Vehicle 1 µM: 67.0% ± 4.4%; Simvastatin 1 µM: 124.3 ± 9.2%; $p<0.05$) (figure 3.4 B).

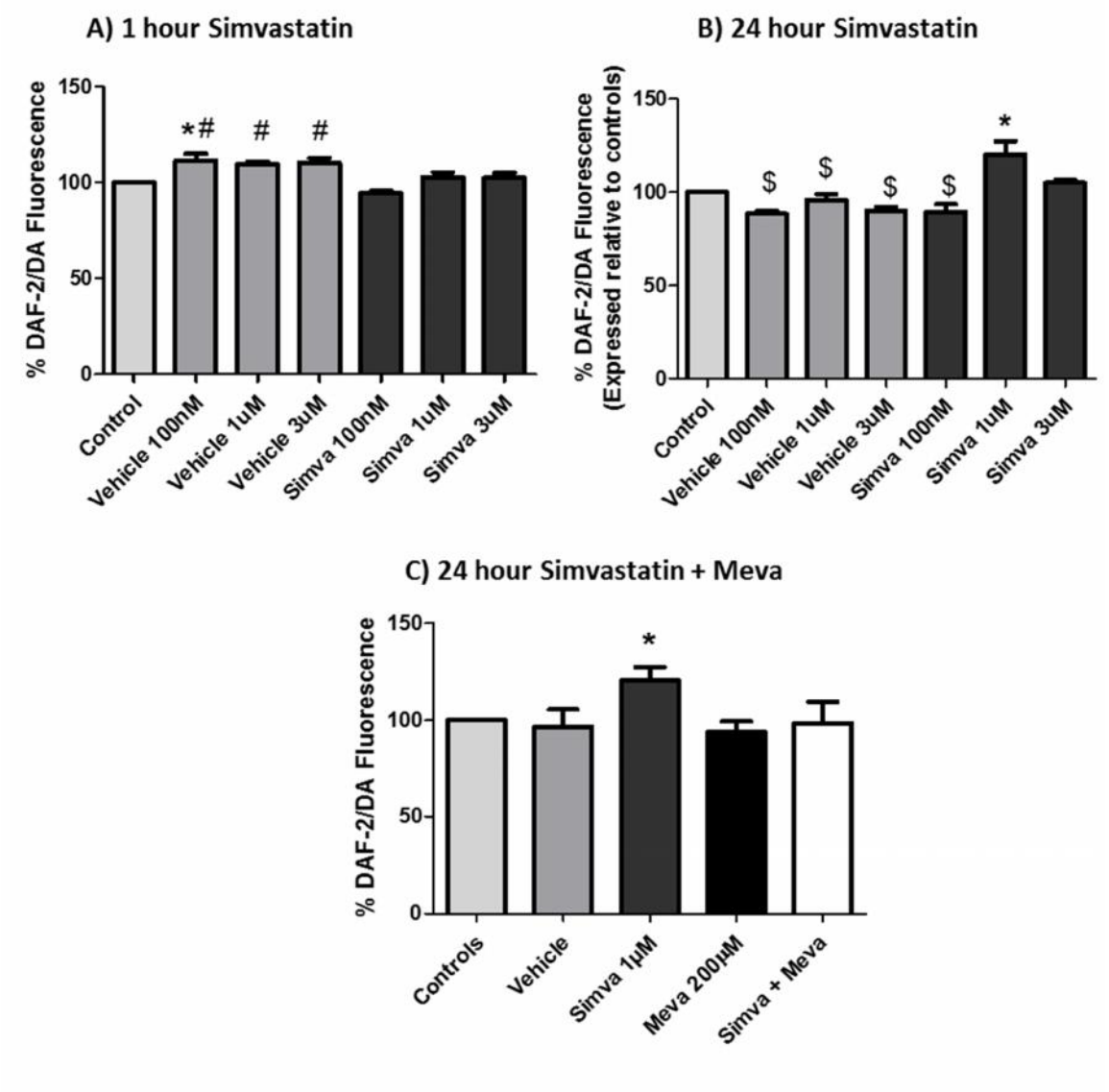

*Figure 3.2: The effect of simvastatin treatment on NO as seen by DAF-2/DA fluorescence (1 and 24 hours). A) 1 hour simvastatin treatment did not significantly alter NO levels. B) 1 μM simvastatin significantly increased NO levels after 24 hours. C) Administration of 200 μM mevalonic acid together with 1 μM simvastatin did not significantly alter NO levels. * p<0.05 vs Control; # p<0.05 vs Simvastatin 100 nM; $ p<0.05 vs Simvastatin 1 μM (n = 6 – 9). Simva: Simvastatin; Meva: Mevalonic acid.*

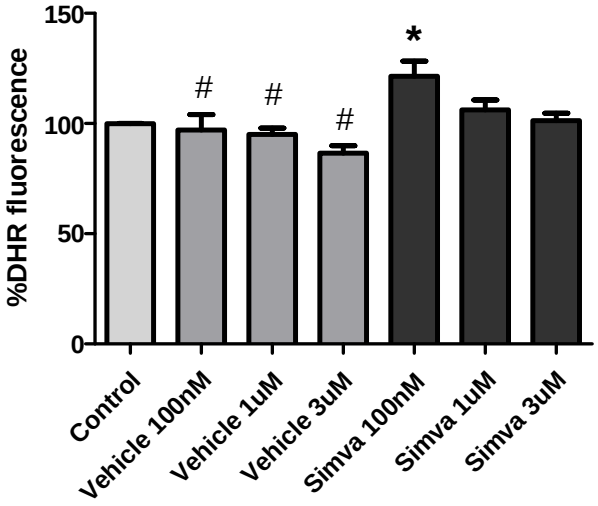

*Figure 3.3: The effect of 24 hour simvastatin treatment on ROS production. 100nM simvastatin increased DHR-123 fluorescence significantly (n = 6 – 8). *p<0.05 vs Control; # p<0.05 vs Simvastatin 100 nM. Simva: Simvastatin*

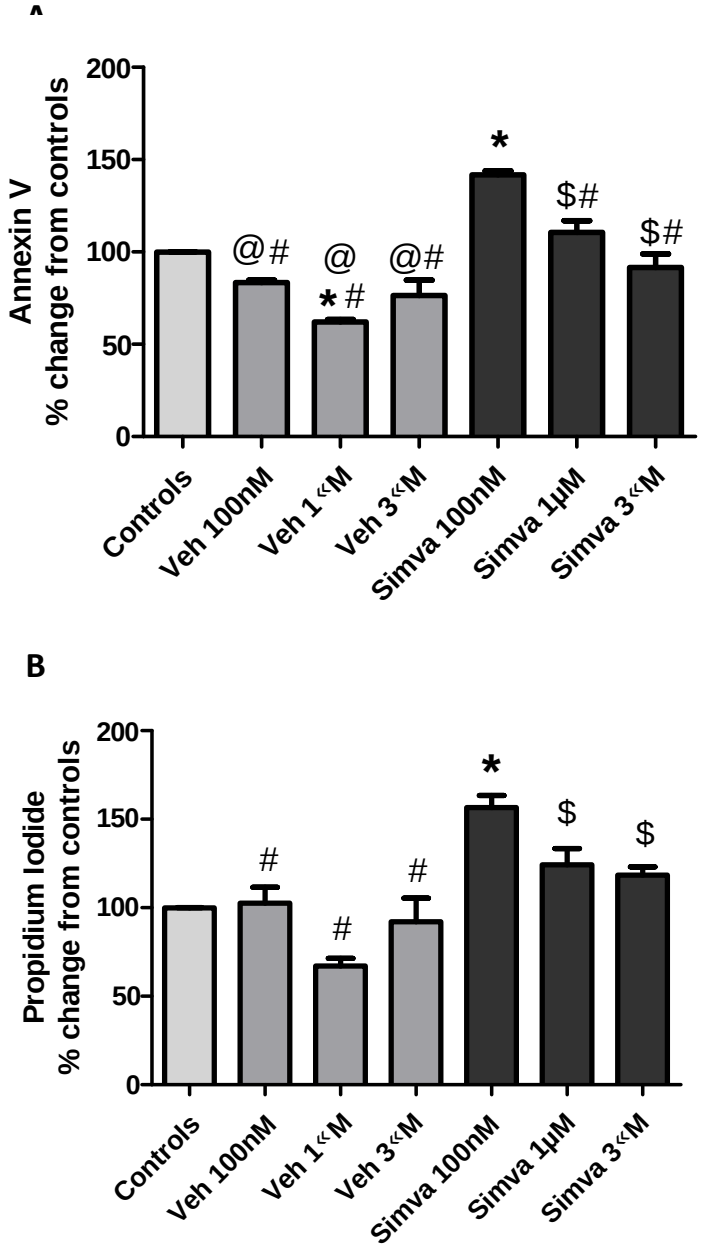

*Figure 3.4: The effect of 24 hour simvastatin treatment on cell viability. A) .% change in apoptosis indicated by Annexin V fluorescence (n = 4). B) % change in necrosis indicated by PI (propidium iodide) fluorescence (n = 4). *p<0.05 vs Control; # p<0.05 vs Simvastatin 100 nM; @ p<0.05 vs Simvastatin 1 µM; $ p<0.05 vs Vehicle 1 µM. Veh: vehicle; Simva: simvastatin.*

3.3.3 Experimental protocol and methods: Signalling investigations

Treating CMECs with simvastatin resulted in increased NO levels at a concentration of 1 µM. Western blot analyses were therefore performed on CMECs treated with 1 µM simvastatin and its vehicle control, for 24 hours (figure 3.5). Western blot analyses were performed as described in section 2.6 of Chapter 2. Experimental conditions for the antibodies used in the Western blot measurements are shown in table 2.1.

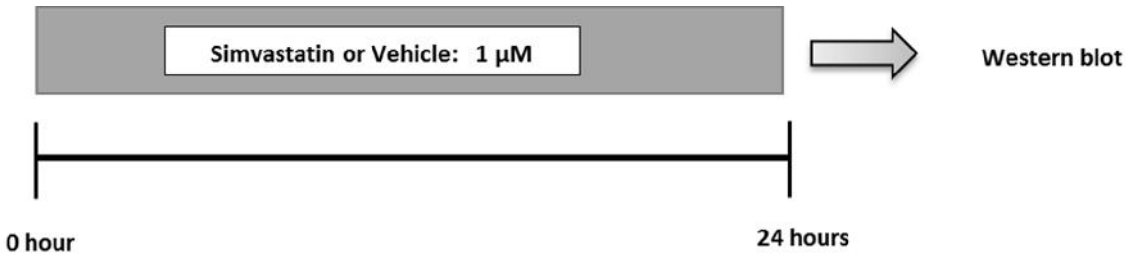

Figure 3.5: An illustration of the experimental protocol followed for simvastatin signalling investigations.

3.3.4 Results: Signalling investigations

It should be noted that all the total-protein expression blots were calculated and expressed as a ratio of the corresponding loading controls.

3.3.4.1 NOS

Even though a significant increase in NO (DAF-2/DA) was seen after 24 hour simvastatin (1 µM) treatment, the eNOS activation sites namely, Serine (Ser) 1177 and Ser 632 were not phosphorylated. No changes were found in total-eNOS (t-eNOS) (figure 3.6 B), phosphorylated eNOS (p-eNOS) Ser 1177 (figure 3.6 C) or p-eNOS Ser 632 (figure 3.6 E). Consequently the results showed no changes in the phosphorylated/total (P/T) ratio of eNOS Ser 1177 (figure 3.6 D) and Ser 632 (figure 3.6 F).

Simvastatin did however result in increased phosphorylation of the negative regulatory site, eNOS Threonine (Thr) 495 (Vehicle: 1; Simvastatin: 1.35 ± 0.06; $p<0.05$) (figure 3.7 C). Furthermore, decreased phosphorylation of eNOS Tyrosine (Tyr) 657 was found (Vehicle: 1; Simvastatin: 0.75 ± 0.02; $p<0.05$) (figure 3.7 E) which resulted in a decreased ratio in P/T eNOS Tyr 657 (Vehicle: 1; Simvastatin: 0.74 ± 0.05; $p<0.05$) (figure 3.7 F).

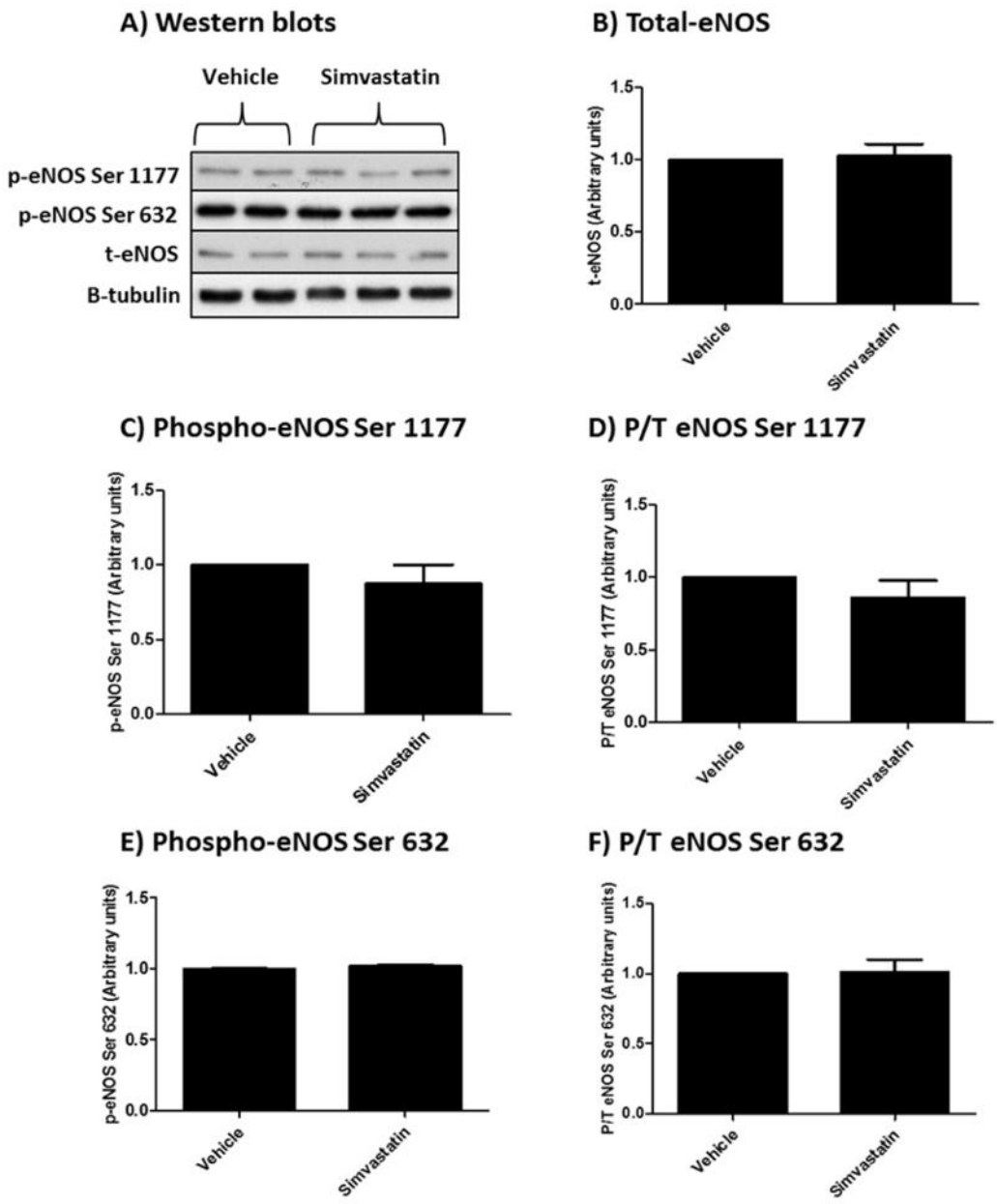

Figure 3.6: Bar charts indicating changes in eNOS expression and phosphorylation (Ser 1177 and 632) of CMECs treated with simvastatin (1 µM) and vehicle control for 24 hours. A) Western blots showing total-eNOS, phospho-eNOS Ser 1177 and Ser 632 as well as β-tubulin expression. B) Analysed results for total-eNOS. C) Analysed results for phospho-eNOS (Ser 1177). D) Phosphorylated over total (P/T) ratio of eNOS (Ser 1177). E) Analysed results for phospho-eNOS (Ser 632). F) Phosphorylated over total (P/T) ratio of eNOS (Ser 632) n=3.

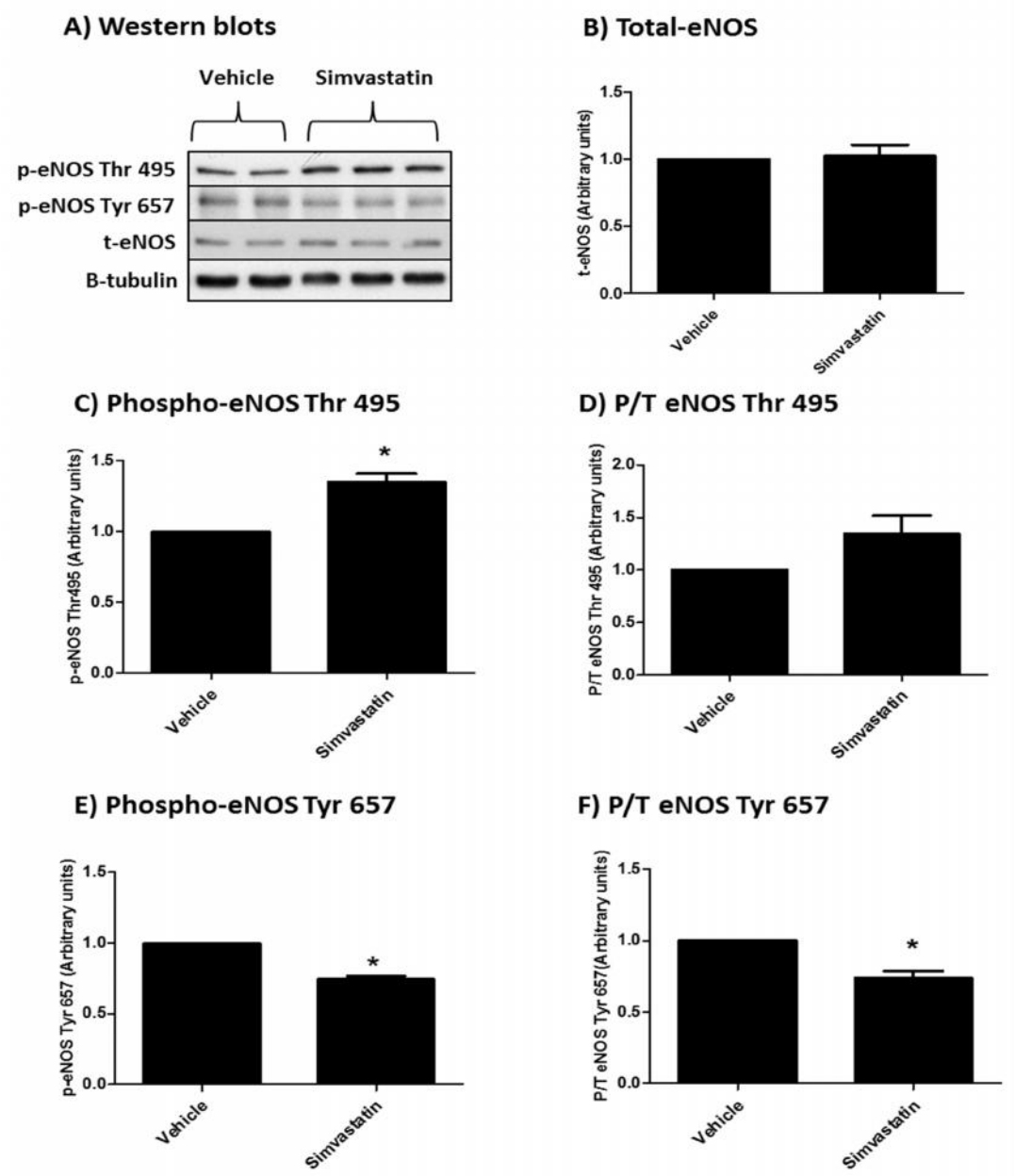

*Figure 3.7: Bar charts indicating changes in eNOS expression and phosphorylation (Thr 495 and Tyr 657) of CMECs treated with simvastatin (1 µM) and vehicle control for 24 hours. A) Western blots showing total-eNOS, phospho-eNOS Thr 495 and Tyr 657 as well as β-tubulin expression. B) Analysed results for total-eNOS. C) Analysed results for phospho-eNOS (Thr 495). D) Phosphorylated over total (P/T) ratio of eNOS (Thr 495). E) Analysed results for phospho-eNOS (Tyr 657). F) Phosphorylated over total (P/T) ratio of eNOS (Tyr 657). * p<0.05 vs Vehicle, n=3.*

3.3.4.2 Protein kinase B (PKB / Akt) and HSP 90

The upstream activator of eNOS, PKB/Akt, showed no changes in total protein expression (figure 3.8 B), however simvastatin treatment did result in decreased phosphorylation of Ser 473 (Vehicle: 1; Simvastatin: 0.75 ± 0.05; $p<0.05$) (figure 3.8 C). No changes in P/T PKB/Akt were seen (figure 3.8 D). The chaperone HSP 90, involved with recruitment of PKB/Akt to activate eNOS, showed significantly lower total protein expression (Vehicle: 1; Simvastatin: 0.92 ± 0.01; $p<0.05$) (figure 3.8 E).

3.3.4.3 AMPK

Another upstream activator of eNOS, AMPK showed significantly lower levels in expression (Vehicle: 1; Simvastatin: 0.83 ± 0.02; $p<0.05$) (figure 3.9 B), however simvastatin increased phosphorylation of AMPK (Thr 172) (Vehicle: 1; Simvastatin: 1.36 ± 0.04; $p<0.05$) (figure 3.9 C). Consequently the ratio of P/T AMPK was significantly increased compared to vehicle control (Vehicle: 1; Simvastatin: 1.65 ± 0.09; $p<0.05$) (figure 3.9 D).

3.3.4.4 Nitrotyrosine and IκBα

Nitrotyrosine is generated when peroxynitrite reacts with a tyrosine or tyrosine containing proteins and serves as a marker for nitrosative stress (Halliwell 1997). Simvastatin did not alter nitrotyrosine levels (figure 3.10 C). With regards to IκBα expression, simvastatin significantly increased total expression (Vehicle: 1; Simvastatin: 1.20 ± 0.02; $p<0.05$) (figure 3.10 D).

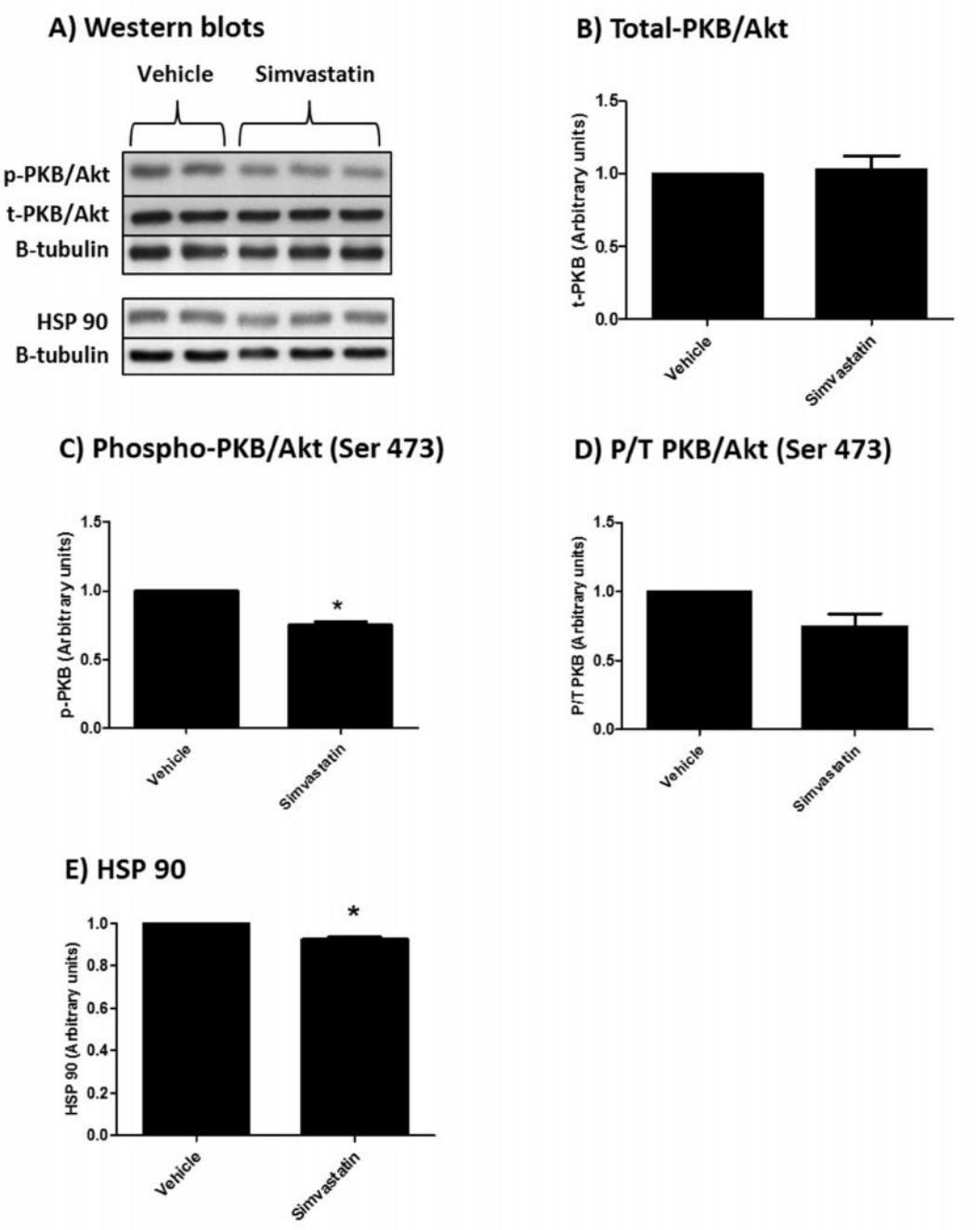

*Figure 3.8: Bar charts indicating changes in PKB/Akt and HSP 90 in CMECs treated with simvastatin (1 µM) and vehicle control for 24 hours. A) Western blots showing total-PKB/Akt, phospho-PKB/Akt (Ser 473) and heat shock protein 90 (HSP 90) as well as their respective ß-tubulin loading controls. B) Analysed results for total-PKB/Akt. C) Analysed results for phospho-PKB/Akt (Ser 473). D) Phosphorylated over total (P/T) ratio of PKB/Akt (Ser 473). E) Analysed results for total-HSP 90 expression. * p<0.05 vs Vehicle, n=3.*

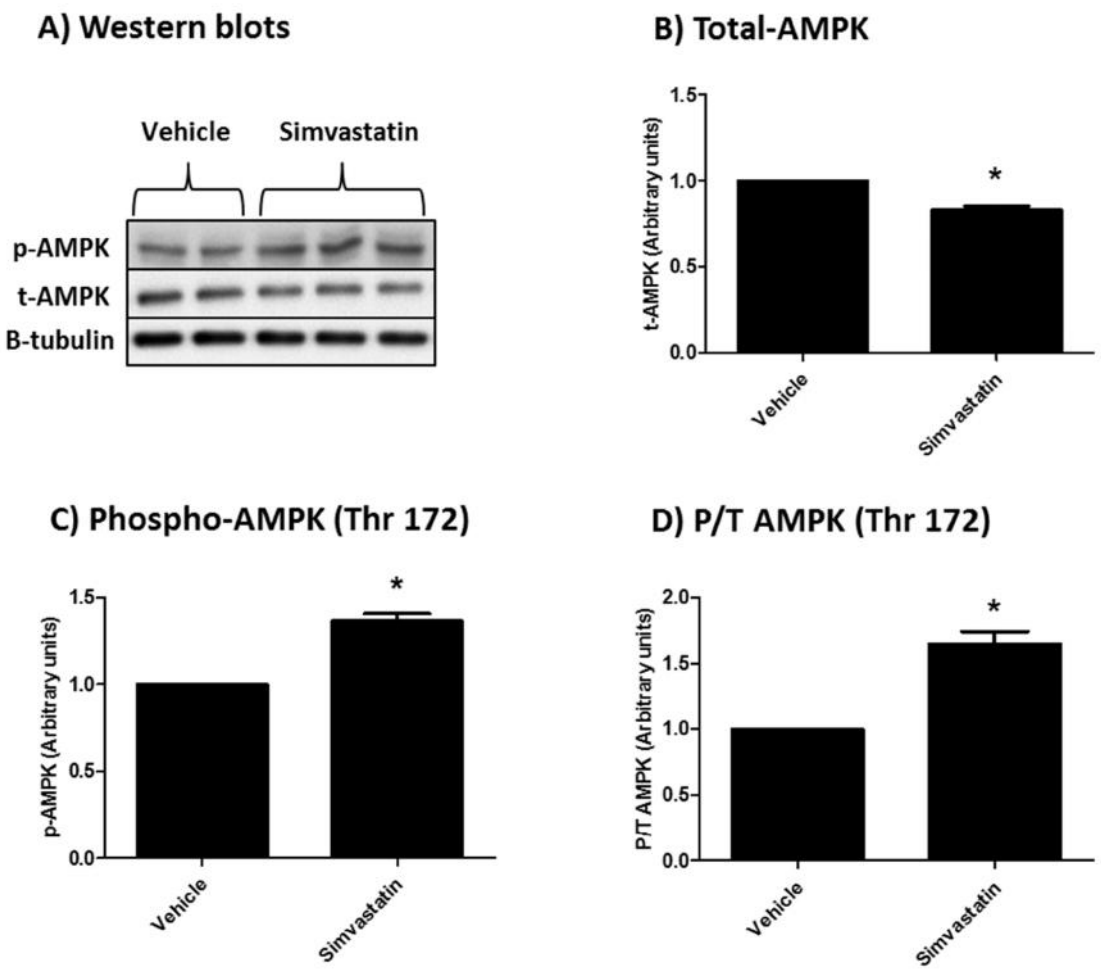

*Figure 3.9: Bar charts indicating changes in AMPK expression and phosphorylation (Thr 172) in CMECs treated with simvastatin (1 µM) and vehicle control for 24 hours. A) Western blots showing total-AMPK, phospho-AMPK (Thr 172) and β-tubulin expression. B) Analysed results for total-AMPK. C) Analysed results for phospho-AMPK (Thr 172). D) Phosphorylated over total (P/T) ratio of AMPK (Thr 172). * p<0.05 vs Vehicle, n=3.*

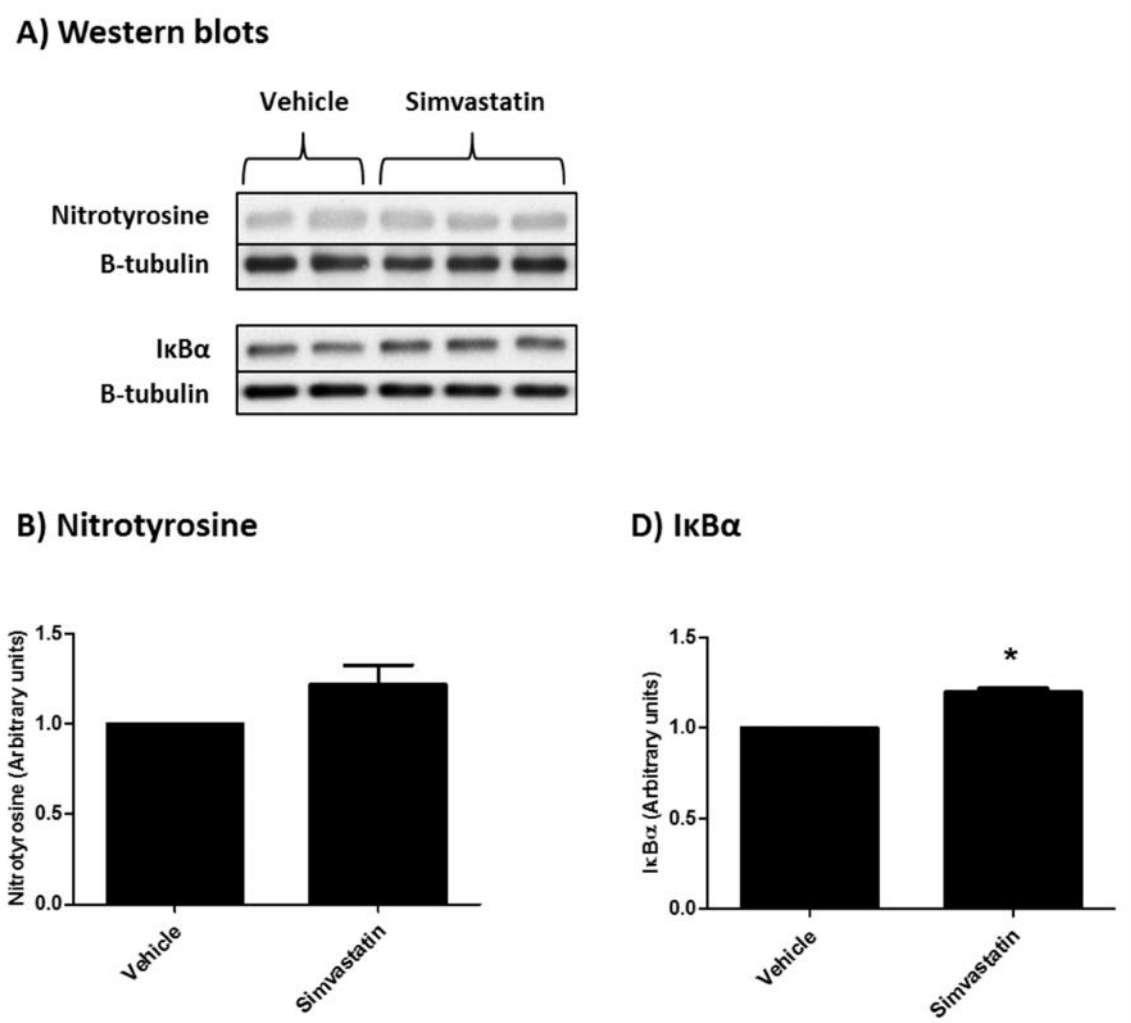

*Figure 3.10: Bar charts indicating changes in nitrotyrosine and IκBα of CMECs treated with simvastatin (1 µM) and vehicle control for 24 hours. A) Western blots showing nitrotyrosine and IκBα as well as their respective β-tubulin loading controls. B) Analysed results for nitrotyrosine. C) Analysed results for IκBα expression. * p<0.05 vs Vehicle, n=3.*

3.3.5 Discussion: Simvastatin

3.3.5.1 NOS/NO pathway

Intracellular NO measurements

CMECs were treated with 3 different concentrations of simvastatin, namely 100 nM, 1µM and 3 µM as well as vehicle controls, for either 1 or 24 hours. Increased levels of NO were only seen after 24 hour treatment with simvastatin at a concentration of 1 µM (figure 3.2 B). No changes were observed in 1 hour treated investigations (figure 3.2 A). It was therefore decided to conduct all further experiments at this concentration and time period. Barrett *et al*. (2006) investigated the concentration of simvastatin in plasma levels of patients treated with 80 mg/day and found the simvastatin levels to range between 0.10 – 16.00 ng/ml. Ahmed (PhD thesis, University of Kentucky, 2013) investigated simvastatin as anti-cancer drug and found a 7.5 mg/kg/day (25 fold higher than concentration used for dislipidaemia) resulted in a plasma concentration range of 0.08 – 2.2 µM. Even though the *in vitro* concentration of 1 µM simvastatin used in the study falls well within the range used in other *in vitro* endothelial based studies (Zhu *et al*., 2008; Chen *et al.*, 2010), it relates clinically to higher doses of simvastatin.

The main mechanism by which the statins exert cholesterol and pleiotropic effects is due to inhibition of the rate-limiting step in cholesterol synthesis, namely the conversion of HMG-CoA to mevalonate and consequently inhibition of isoprenoid formation. Therefore, in order to confirm that the NO-increasing effect was in fact due to simvastatin's inhibitory effect on isoprenoids and subsequent RhoA inhibition, mevalonic acid was added as co-treatment with simvastatin to CMECs in order to reverse the statin induced effect. Figure 3.2 C shows that addition of mevalonic acid to simvastatin reduced NO back to control levels, however no statistical significance was shown between simvastatin and simvastatin+mevalonic acid groups, it can therefore not be confirmed that simvastatin resulted in isoprenoid inhibition. Simvastatin is a pro-drug which is converted to its active open acid form, *in vivo* via the liver (Schulz 2005). However, in cell culture investigations, simvastatin manufactured for research purposes is

converted to its open acid form by different steps, pre-determined by the supplier. Some suppliers prescribe a two hour incubation at 50°C followed by a pH step to activate simvastatin. Simvastatin used for *in vitro* investigations of the current study were prepared according to manufacturer's instruction, however these did not include a two hour incubation at 50°C. It is possible that simvastatin was not properly converted to its active form prior to use on cells, which could explain the lack of proper mevalonate inhibition.

Phospho eNOS (Ser 1177 and Ser 637) and PKB/Akt

Considering the relatively small increase in NO levels found in the present study (≈ 20% increase with simvastatin 1 µM for 24 hours), we expected increased phosphorylation and activation of eNOS, as eNOS is usually associated with modest NO production. However, eNOS was not activated at either of the positive regulatory sites namely Ser 1177 (figure 3.6 C and D) or Ser 632 (figure 3.6 E and F). To the best of our knowledge no previous studies investigated eNOS phosphorylation at Ser 632 in the context of simvastatin treatment. Together with the lack of eNOS phosphorylation at Ser 1177, one of the most well described Ser 1177 activators, namely PKB/Akt, showed significantly reduced phosphorylation (Ser 473) after 24 hours (figure 3.8 C), which suggests that the PKB/Akt – eNOS (Ser 1177) pathway was unlikely to be involved. Furthermore, HSP 90 was found to be down regulated with simvastatin treatment (figure 3.8 E). HSP 90 acts a chaperone to PKB/Akt, maintaining its activity and promoting phosphorylation of eNOS via PKB/Akt (Sato *et al*., 2000). This finding is in contrast to other studies who showed increased PKB/Akt phosphorylation in human umbilical vein endothelial cells (HUVECs) (Kureishi *et al.,* 2000) and bovine aortic endothelial cells (BAECs) (Skaletz-Rorowski *et al*., 2003).

It has to be noted that phosphorylation of eNOS is a dynamic process and agonist induced stimulation by bradykinin has previously been shown to increase phosphorylation of Ser 1177 after only 30 seconds (Fleming *et al*., 2001). The same study showed that phosphorylation of Ser 1177 started decreasing after 5 min of bradykinin treatment. Similarly, phosphorylation of Thr 495 increased after 5 min of bradykinin treatment. These findings illustrate the complex, interactive and time-dependent relationship between the various eNOS phosphorylation sites. In the current study, there was no increase in NO production after 1 hour of simvastatin

treatment. Chen *et al*. (2010) showed that simvastatin increased NO in HUVECs at a similar concentration after 2 hour treatment, which was associated with increased eNOS expression and P/T eNOS ratio (no specific eNOS phosphorylation site was mentioned). These changes were associated with increased phosphorylation of PKB/Akt, however, the HUVECs in this study were pre-incubated with hydrogen peroxide for 30 min prior to simvastatin administration. The anti-oxidant and ROS systems in these cells were therefore stimulated and could explain the differences in results compared to ours.

Phospho eNOS (Thr 495) and AMPK

Although AMPK has previously been shown to induce eNOS phosphorylation and activation at Ser 1177, it can also phosphorylate Thr 495 *in vitro* (Chen *et al.,* 1999). Other studies have also found statins to increase AMPK phosphorylation which was associated with increased phosphorylation of eNOS Ser 1177. These include *in vivo* investigations in mouse aortic and myocardial tissue and *in vitro* in HUVECs, BAECs and human capillary derived endothelial cells (Sun *et al*., 2006) as well as in human iliac artery endothelial cells (Xenos *et al*., 2005). In the current study, simvastatin (1 µM for 24 hours), significantly increased AMPK phosphorylation (figure 3.9 C) and the P/T AMPK ratio (figure 3.9 D); however, this was not associated with increased phosphorylation of eNOS Ser 1177. At the same time, simvastatin significantly increased phosphorylation of the inhibitory eNOS site, Thr 495 (figure 3.7 C). It could therefore be speculated that under the *in vitro* conditions of the current study, AMPK phosphorylation resulted in eNOS Thr 495 phosphorylation (Chen *et al.,* 1999), rather than Ser 1177 phosphorylation.

Phospho eNOS (Tyr 657)

eNOS tyrosine phosphorylation is not a topic included in many studies and considerably less information is available. The current study included the measurement of eNOS Tyr 657 phosphorylation in order to expand and broaden our understanding of the complex interaction between eNOS phosphorylation sites and their contribution to simvastatin related changes in NO. Fleming & Busse (2003) and Fisslthaler *et al*. (2000) contributed the lack of information on this residue to the fact that investigators have been struggling to show tyrosine phosphorylation

of eNOS in any cells other than primary cell cultures or low passages of endothelial cells (Garcia-Cardena *et al*., 1996; Fleming *et al*., 1998). Despite a relative lack of data, phosphorylation of the enzyme at this site has been shown to decrease NO production (Loot *et al*., 2009; Fisslthaler *et al*., 2008). In the current study, baseline phosphorylation of eNOS Tyr 657 could be demonstrated, and simvastatin treatment resulted in a significant decrease in phosphorylation of eNOS Tyr 657 as well as an overall decrease in P/T eNOS Tyr 657 ratio (figure 3.7 E and F), thereby suggesting a potential mechanism for the modest increase in NO production.

Summary: role of various eNOS phosphorylation sites

In order to explain the source of increased NO production observed with simvastatin treatment at 1 µM for 24 hours, it could be speculated that simvastatin induced an increase in phospho-eNOS (Ser 1177) at an earlier stage than our measurements, resulting in sustained elevated levels of NO at the time of the experimental analyses. Another mechanism could possibly be due to decreased levels of Tyr 657 phosphorylation, which may result in a reduction in enzyme inhibition and thus explain the moderate increase in NO production observed. Pinzón-Daza *et al.* (2012) showed in human brain microvascular endothelial cells that simvastatin increased NO production, although only a slight increase in phospho-eNOS Ser 1177 was observed, which could not explain the full extent of the elevated NO levels. The authors ascribed the increase in NO to increased iNOS expression. iNOS expression was not measured in the simvastatin experiments of the current study. However, since only a modest increase in NO was observed, it is unlikely to be due to iNOS. iNOS is traditionally associated with large increases in NO, even up to a 1000 fold more than eNOS-derived NO production (Singh & Evans 1997). Our laboratory has never found nNOS to be a significant contributor to NO in the specific CMEC culture model, and it is therefore not likely to be the source.

3.3.5.2 ROS and cell viability

Simvastatin has previously been shown to exert anti-oxidant effects. Parihar *et al.* (2012) found that simvastatin decreased rat liver-derived mitochondrial ROS at a concentration of 1 µM. Heeba *et al*. (2007) showed that simvastatin (10 µM) significantly decreased peroxynitrite production in normal and dysfunctional HUVECs. In the current study simvastatin showed

unexpected effects on ROS production. 100 nM simvastatin significantly increased DHR-123 fluorescence compared to vehicle control, whereas 1 and 3 µM showed no changes in peroxynitrite/mitochondrial ROS (figure 3.3) or nitrotyrosine (figure 3.10 B). Together with the increase in ROS seen with 100 nM of simvastatin, an increase in apoptosis (figure 3.4 A) and necrosis (figure 3.4 B) was found. ROS has the ability to induce endothelial apoptosis and DNA damage (Wolin 2000) therefore the reduction in cell viability can be ascribed to increased ROS formation.

The effect of 1 µM simvastatin on ROS and cell viability is more complicated. No changes were found in DHR 123-sensitive ROS (peroxynitrite and mitochondrial ROS) (figure 3.3), however increased levels of apoptosis and necrosis (figure 3.4 A and B) occurred. In line with our findings, simvastatin has previously been shown to induce apoptosis in vascular smooth muscle cells and cardiomyocytes (Blanco-Colio *et al.,* 2002*;* Demyanets *et al.,* 2006). Interestingly, the very mechanism responsible for statin-induced pleiotropic effects is also thought to be responsible for pro-apoptotic actions. A reduction in the isoprenoid intermediates due to statin treatment, results in reduced prenylation of various proteins, which prevent these proteins from translocating from the cytoplasm and inserting into the cell membrane where they function as signal transducers (Katsiki *et al*., 2010). An example is the small GTPase protein, RhoA, which can downregulate expression of the anti-apoptotic protein B-cell lymphoma 2 (Bcl-2) via simvastatin-induced inhibition of its prenylation in vascular smooth muscle cells (Blanco-Colio *et al*., 2002). It can therefore be speculated that the latter could be a mechanism responsible for simvastatin induced apoptosis and necrosis found in the current study.

3.3.5.3 Inflammation: NF-κB signalling

Simvastatin treatment of CMECs resulted in a small but significant increase in IκBα expression (figure 3.10 C). Normally, a decrease in IκBα expression implies that IκBα phosphorylation was increased resulting in IκBα dissociating from NF-κB and consequently undergoing degradation by proteasomal pathways leading to reduced levels. Dissociation of IκBα from NF-κB allows NF-κB to become activated and translocate to the nucleus where it serves as a transcription factor of several pro-inflammatory proteins. In the current study, simvastatin treatment resulted in

increased IκBα expression, which implies that NF-κB was prevented from being activated (i.e. prevention of NF-κB-associated pro-inflammatory effects). Similar results were found by Ni *et al*., (2013) who induced plasminogen activator inhibitor-1 with high glucose concentrations in cardiac microvascular endothelial cells (CMECs), resulting in IκBα degradation. Simvastatin was able to completely block IκBα degradation.

3.3.6 Summary of the *in vitro* effects of simvastatin

In our hands, simvastatin treatment exerted modest pleiotropic effects in healthy CMECs, which included increased NO production and anti- NF-κB inflammatory signalling, accompanied by an increase in cell viability parameters. In view of the fact that the addition of mevalonic acid did not succeed in a significant reversal of simvastatin's effects on NO production, it is possible that the lack of robust pleiotropic effects could be ascribed to a failure of our protocol to effectively inhibit the conversion of 3-Hydroxy-3-methylglutaryl coenzyme A (HMG-CoA) to mevalonate. Furthermore, it has to be borne in mind that the *in vitro* effects of statins are dependent on the specific member of the statin family, the micro-environment surrounding the cells/tissue of interest, and concentration of the drug. Findings are summarized in figure 3.11.

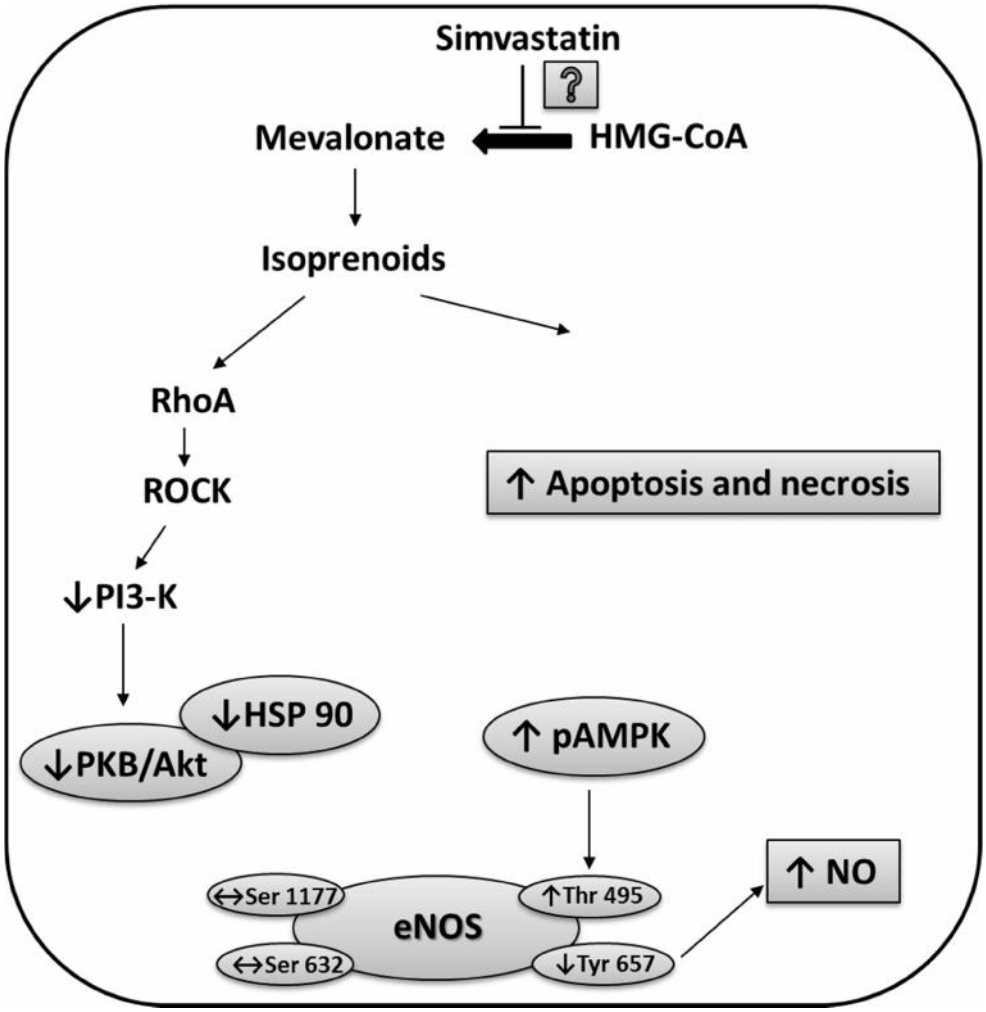

Figure 3.11: A cartoon depicting in vitro findings and proposed pathways of simvastatin (1 µM; 24 hours) related changes. Normally statins inhibit the conversion of HMG-CoA to mevalonate which results in inhibition of the Rho/ROCK pathway, increasing eNOS activity and NO production. The current study could only show partial inhibition of the conversion to mevalonate (as shown with the mevalonic acid co-treatment experiments), and therefore RhoA/ROCK inhibition may have been lost, or ineffective. The result of such a scenario would be isoprenoid formation and possible inhibition of Bcl-2 resulting in increased apoptosis and necrosis. Additionally, the inhibition of PKB/Akt and a loss of eNOS (Ser 1177) phosphorylation preventing large increases in NO. Despite the down-regulation of PKB/Akt and HSP 90, and a lack of eNOS activation via Ser 1177 phosphorylation a modest increase in NO was shown. AMPK can also increase NO via phosphorylation of eNOS (Ser 1177), and although increased AMPK phosphorylation was found,

eNOS Ser1177 remained unchanged. Increased phosphorylation of eNOS Thr 495 could be due to AMPK phosphorylation, however Thr 495 phosphorylation is associated with enzyme inhibition. Both eNOS Thr 495 and Tyr 657 are inhibitory sites of eNOS. Therefore, decreased eNOS (Tyr 657) phosphorylation could have resulted in the modest increase in NO. For this to be possible, the effect of reduced Tyr 657 phosphorylation had to be greater than increased phosphorylation of the other inhibitory site, eNOS Thr 495.

3.4 Fenofibrate

3.4.1 Experimental protocol and methods: NO, ROS and cell viability - Concentration and time response

Various investigations were performed to establish the optimal concentration of fenofibrate to use in *in vitro* experiments. CMECs were treated with 10 µM, 30 µM and 50 µM fenofibrate for 1, 4 and 24 hours. These concentration and time periods were derived from similar, previously published *in vitro* studies as summarised in table 1.2 (Chapter 1). Intracellular NO levels were assessed by the flow cytometric measurement of mean DAF-2/DA fluorescence intensity (figure 3.12 A). Two types of ROS were measured, namely superoxide with DHE-fluorescence and peroxynitrite/mitochondrial ROS with DHR-123 fluorescence (figure 3.12 B and C). Apoptosis and necrosis measurements were performed with Annexin V and PI fluorescence respectively (figure 3.12 D). All methods were performed as described under section 2.3.2.1 – 2.3.2.3.

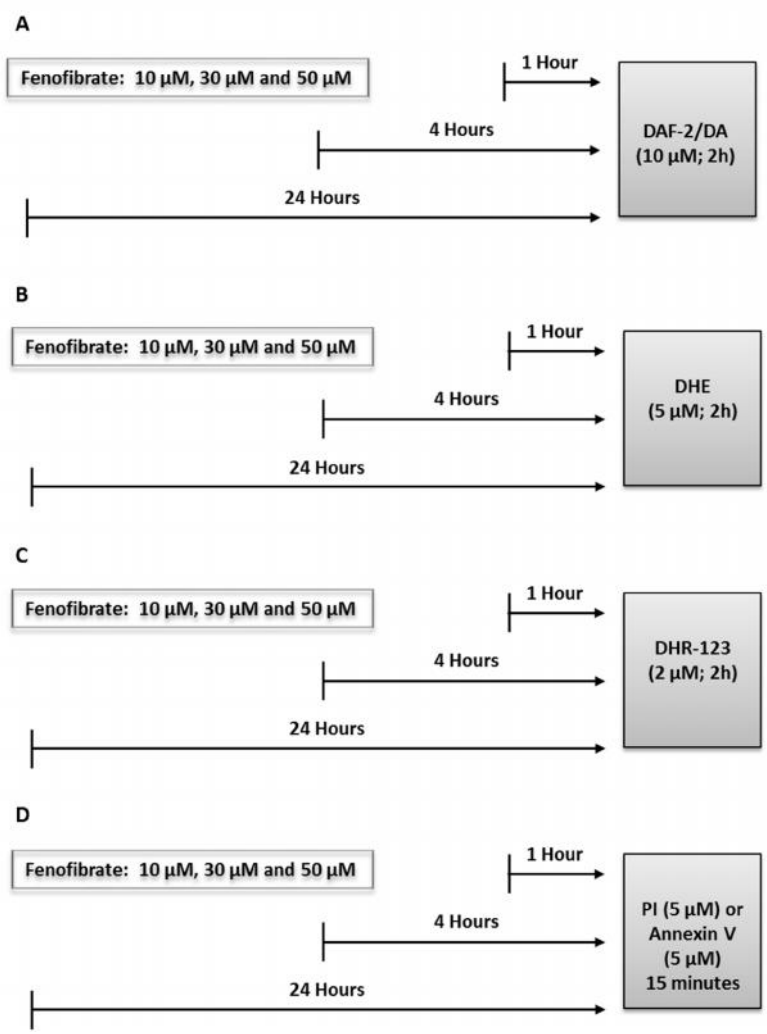

Figure 3.12: The experimental outline for NO, ROS and cell viability investigations with 10 µM, 30 µM and 50 µM fenofibrate. A) CMECs were treated with fenofibrate for 1, 4 and 24 hours, followed by a 2 hour incubation with DAF-2/DA, to investigate the effect on intracellular NO. B) CMECs were treated with fenofibrate for 1, 4 and 24 hours, followed by a 2 hour incubation with DHE, to investigate the effect on superoxide production. C) CMECs were treated with fenofibrate for 1, 4 and 24 hours, followed by a 2 hour incubation with DHR-123, to investigate the effect on ROS generation. D) Cell viability was measured using PI (necrosis) and Annexin V (apoptosis) staining after 1, 4 and 24 hour fenofibrate treatment. DAF-2/DA: 4,5-Diaminofluorescein diacetate; DHE: Dihydroethidium; DHR-123: Dihydrorhodamine-123 (DHR-123); PI: propidium iodide; Ann V: Annexin V.

3.4.2 Results: The effect of fenofibrate on NO, ROS and cell viability – Concentration and time response

3.4.2.1 NO measurements

The findings showed that fenofibrate increased DAF-2/DA fluorescence levels significantly with concentrations of 30 µM and 50 µM after 1 hour (Control: 100%; 30 µM: 164.1% ± 2.7%; 50 µM: 208.3% ± 19.6%, $p<0.05$) (figure 3.13 A) and 4 hour treatments (Control: 100%; 30 µM: 161.4% ± 7.9%; 50 µM: 222.4% ± 24.25%, $p<0.05$) (figure 3.13 B). 10 µM fenofibrate did not significantly alter DAF-2/DA fluorescence at any of the time points. After 24 hours the NO-increasing effects were less robust, and only 50 µM fenofibrate resulted in a significant elevation (Control: 100%; 24 hours [50 µM]: 135.3% ± 12.1%, $p<0.05$) (figure 3.13 C). No significant vehicle (DMSO) effects were observed at any of the concentrations or time points. Since 10 µM fenofibrate exerted no changes in NO production, this concentration was excluded from further investigations.

3.4.2.2 ROS measurements

Fenofibrate exerted variable effects on superoxide production as measured by DHE fluorescence. No changes were seen in DHE fluorescence after 1 or 4 hour treatment with 30 µM and 50 µM fenofibrate or the respective vehicle controls (figure 3.14 A and B). However, at 24 hours, 30 µM fenofibrate induced a statistically significant, albeit modest, increase in DHE fluorescence intensity (Control: 100%; 30 µM: 107.4% ± 2.6%; $p<0.05$ vs Control) (figure 3.14 C). As mentioned in the introduction, NO and superoxide can combine resulting in the formation of peroxynitrite (Ferdinandy & Schulz 2003). DHR-123 is a fluorescent probe that has previously been shown to be sensitive for both peroxynitrite and mitochondrial related ROS (Ischiropoulos *et al*. 1999; Navarro-Antolín *et al*. 2001; Chan & Miskimins 2012). In contrast to the DHE fluorescence findings, fenofibrate had robust effects on DHR-123 fluorescence at 1 and 4 hours. 30 µM and 50 µM fenofibrate significantly reduced DHR-123 fluorescence after 1 hour (Control: 100%; 30 µM: 71.1% ± 3.7%; 50 µM: 65.7% ± 3.6%; $p<0.05$ vs Control) (figure 3.15 A) and 4 hours (Control: 100%; 30 µM: 75.8% ± 5.4%; 50 µM: 63.5% ± 3.5%; $p<0.05$ vs Control) (figure 3.15 B). After 24 hours no changes were found in DHR-123 fluorescence (figure 3.15 C). Once again, no vehicle effects were observed for any of the concentrations, time periods or ROS probes.

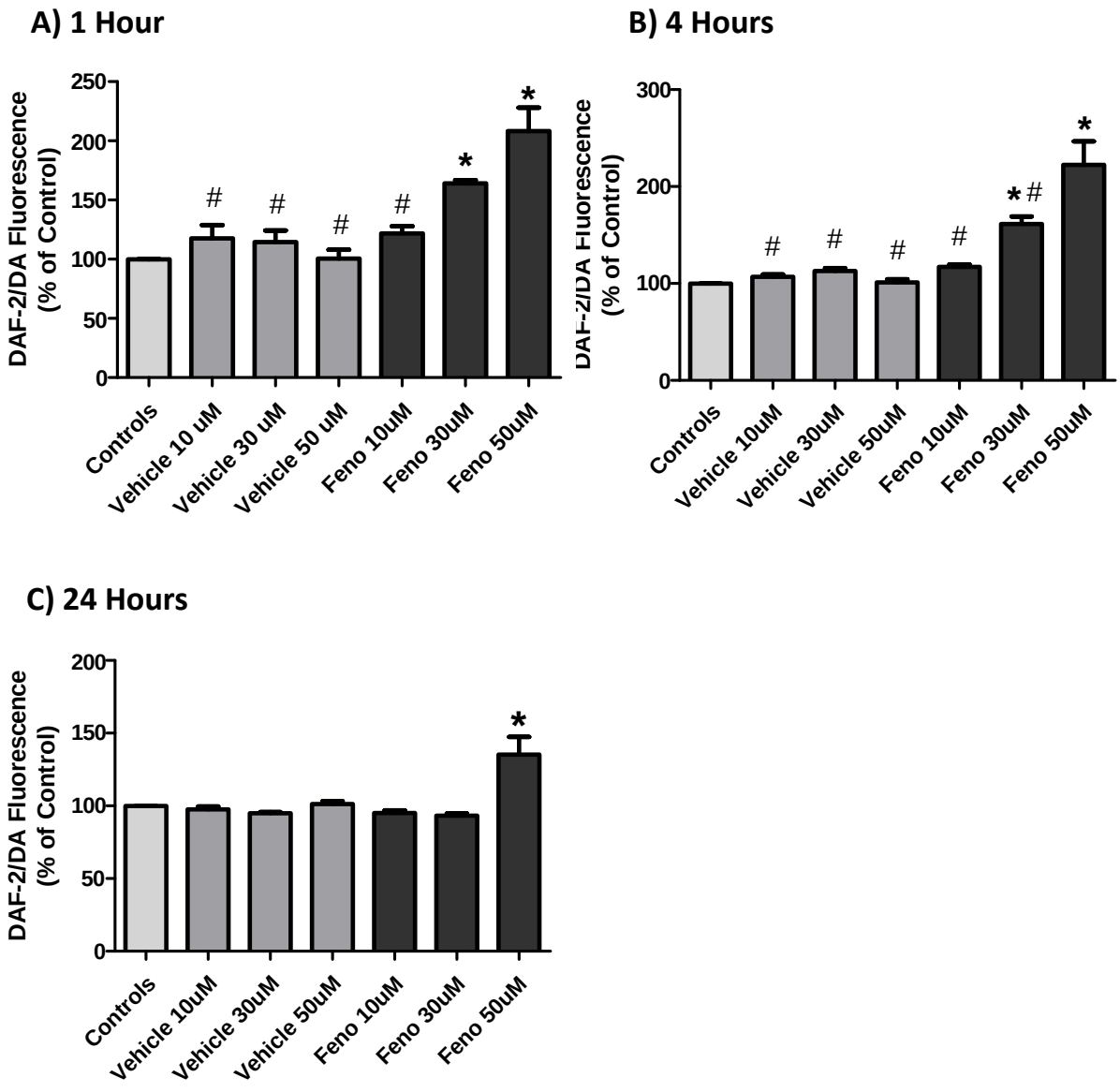

*Figure 3.13: Concentration and time response data of fenofibrate effects on NO generation. A) 1 Hour treatment with fenofibrate showed an increase in DAF-2/DA fluorescence with 30 µM and 50 µM (n = 5-9). B) 4 Hour treatment with fenofibrate also showed an increase in DAF-2/DA fluorescence with 30 µM and 50 µM (n = 5-11). C) After 24 hours only 50 µM fenofibrate significantly increased DAF-2/DA fluorescence (n = 6-15). *p<0.05 vs Control; # p<0.05 vs Fenofibrate 50 µM. Feno: fenofibrate.*

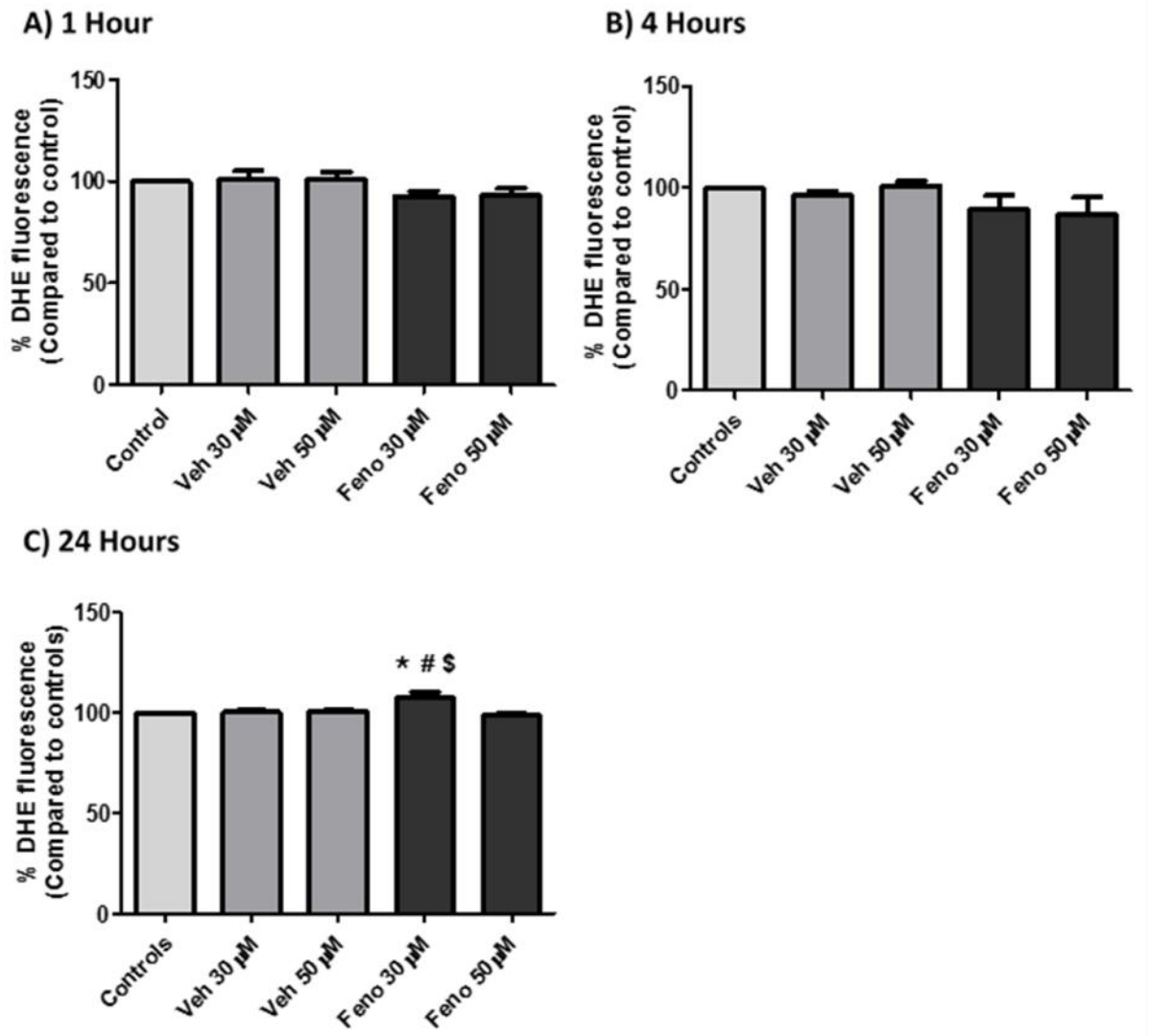

*Figure 3.14: Concentration and time response data of fenofibrate effects on superoxide generation. A) 1 Hour treatment with fenofibrate showed no changes in DHE fluorescence (n = 10 - 14). B) 4 Hour treatment with fenofibrate showed no changes in DHE fluorescence (n = 6 - 8). C) After 24 hours 30 µM fenofibrate significantly increased DHE fluorescence (n = 6 - 8). * p<0.05 vs Control, $ p<0.05 vs Vehicle 30 µM, # p<0.05 vs Fenofibrate 50 µM. Veh: Vehicle; Feno: fenofibrate.*

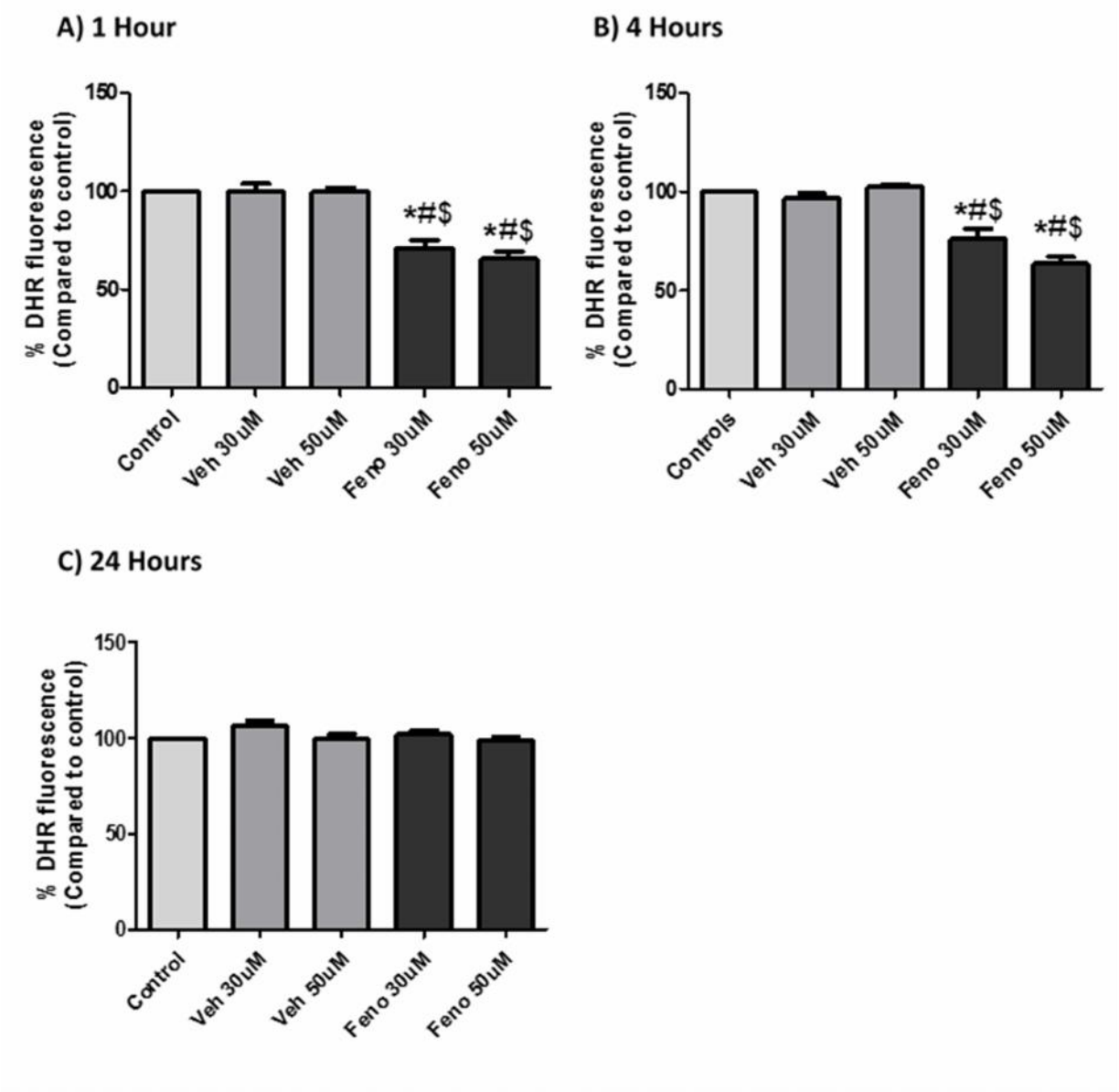

*Figure 3.15: Concentration and time response data of fenofibrate effects on mitochondrial ROS/peroxynitrite generation. A) 1 Hour treatment with fenofibrate showed reduced levels of DHR-123 fluorescence (n = 6 - 7). B) 4 Hour treatment with fenofibrate showed reduced levels of DHR-123 fluorescence (n = 4 - 8). C) After 24 hours no effect was seen on DHR-123 fluorescence (n = 6 - 8). * p<0.05 vs Control, $ p<0.05 vs Vehicle 30 µM, # p<0.05 vs Vehicle 50 µM. Veh: Vehicle; Feno: fenofibrate.*

3.4.2.3 Cell viability investigations

As can be clearly seen in Figure 3.16 (A and B), neither fenofibrate nor its vehicle controls altered cell viability parameters at 1 hour. The lack of effects on Annexin V persisted at 4 hours treatment; however, 4 hour treatment with 50 µM fenofibrate significantly decreased necrosis as measured by propidium iodide fluorescence (Control: 100%; 50 µM: 62.5% ± 10.6%, $p<0.05$ vs Control) (figure 3.17 B). However, no difference was seen between fenofibrate 50 µM and its vehicle control suggesting a possible vehicle effect. 24 hour treatment with 50 µM fenofibrate significantly reduced Annexin V fluorescence levels compared to controls as well as vehicle controls (Control: 100%; Vehicle 50 µM: 93.1% ± 4.9%; Fenofibrate 50 µM: 61.6% ± 2.4%*$^{\$}$; *$p<0.05$ vs control, $^{\$}p<0.05$ vs vehicle 50 µM) (figure 3.18 A). Even though 50 µM fenofibrate reduced Annexin V fluorescence after 24 hours, no changes were observed in the propidium iodide fluorescence measurements (figure 3.18 B).

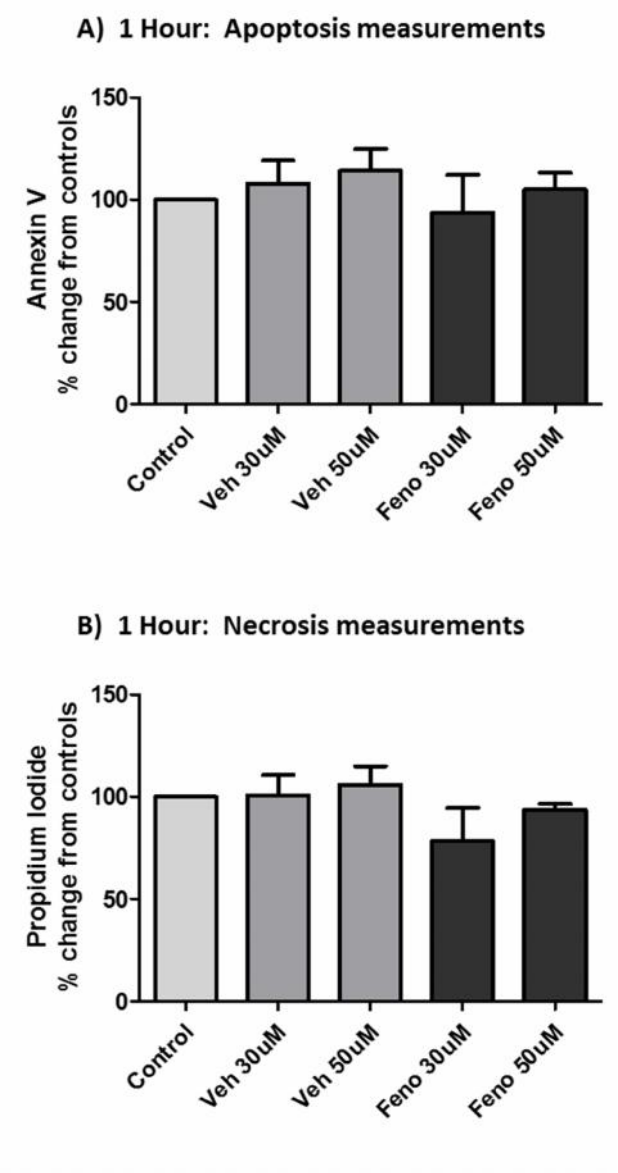

Figure 3.16: CMECs treated with fenofibrate for 1 hour to investigate cell viability changes. A) Neither vehicle controls nor fenofibrate treated samples changed Annexin V fluorescence after 1 hour (n = 5-10). B) Neither vehicle controls nor fenofibrate treated samples changed Propidium iodide fluorescence after 1 hour (n = 5-10). Veh: vehicle; Feno: fenofibrate.

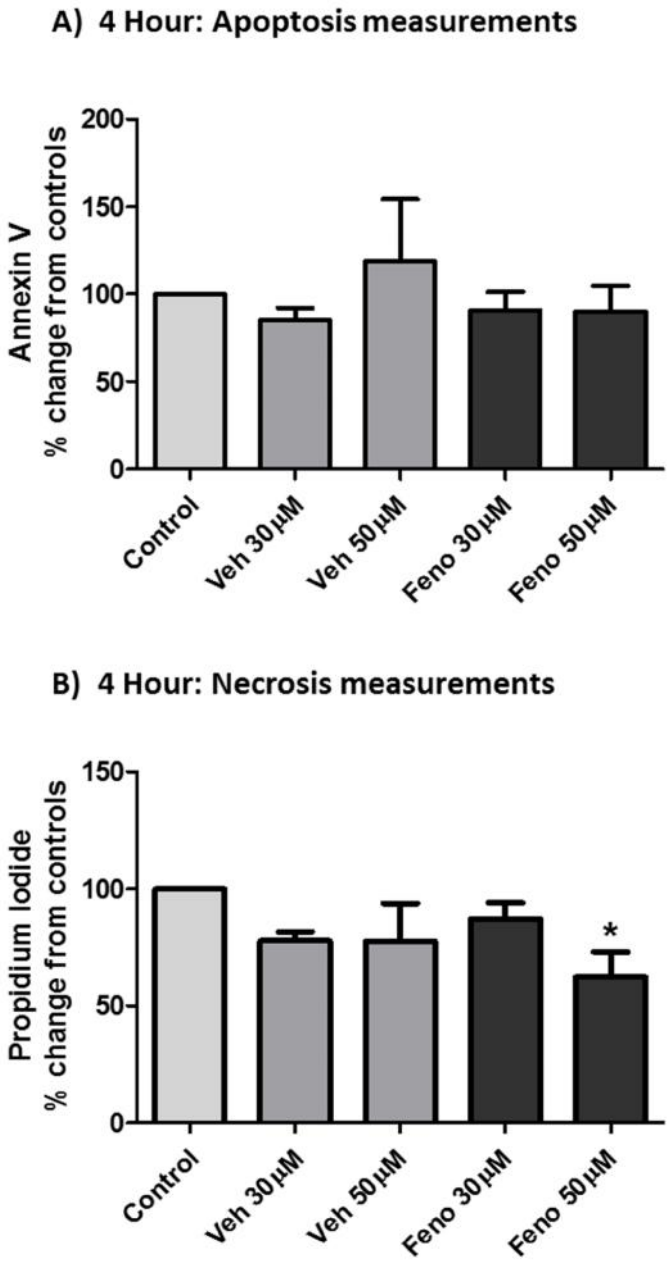

*Figure 3.17: CMECs treated with fenofibrate for 4 hours to investigate cell viability changes. A) Neither vehicle controls nor fenofibrate treated samples changed Annexin V fluorescence after 4 hours (n = 6 - 12). B) 50 µM fenofibrate significantly decreased propidium iodide fluorescence after 4 hours (n = 6 - 12). *p<0.05 vs Control; Veh: vehicle; Feno: fenofibrate.*

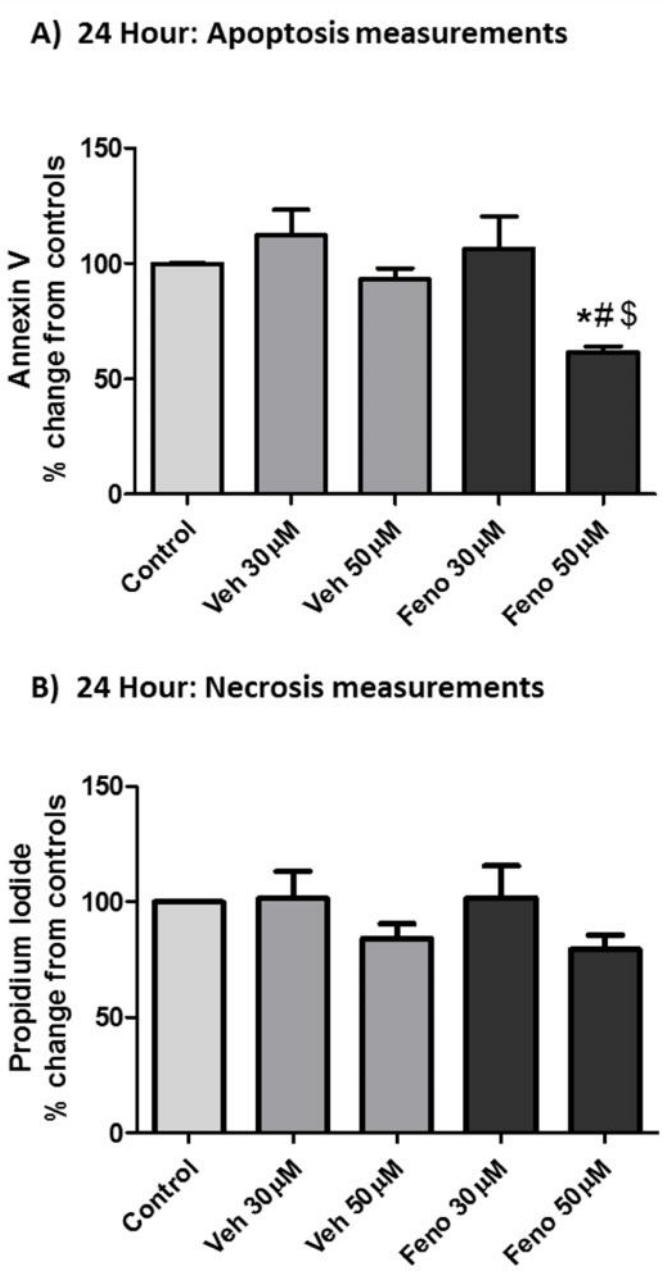

*Figure 3.18: CMECs treated with fenofibrate for 24 hours to investigate changes in cell viability. A) Annexin V fluorescence was significantly reduced after 24 hour treatment with 50 µM fenofibrate (n = 11 - 17). B) Neither vehicle controls nor fenofibrate treated samples changed Annexin V fluorescence after 24 hour (n = 11 - 17). *p<0.05 vs Control, #p<0.05 vs Vehicle 30 µM, $p<0.05 vs Fenofibrate 30 µM; Veh: vehicle; Feno: fenofibrate.*

3.4.3 Summary: Fenofibrate concentration and time response studies

Considering the combined results of concentration and time response studies, 50 µM fenofibrate was chosen as the concentration for all further investigations. The majority of further investigations were performed on 1 hour treatments, however selected experiments were performed with 24 hour treatments.

Due to the fact that simvastatin did not result in robust pleiotropic effects, such as seen with fenofibrate, at this stage it was decided to only continue *in vitro* investigations with fenofibrate. A further motivation for this decision, was the fact that there are significantly fewer publications in the literature available regarding *in vitro* fenofibrate studies compared to simvastatin.

3.4.4 Experimental protocol: NOS inhibition investigations

From concentration and time response studies it was evident that fenofibrate had a pronounced effect on NO synthesis, especially at the shorter treatment period of 1 hour. Previous studies have found that increased fenofibrate-induced NO synthesis was mainly due to the activation of eNOS. In the current study, the aim was to perform an in-depth exploration of the NOS-derived sources contributing to the observed increases in NO production, especially in view of the relatively large (>2.1 fold) increase in NO production at 1 and 4 hour treatment. The large increases in NO-production necessitated the employment of strategies to differentiate, among others, between the eNOS and iNOS isoforms, as iNOS is known to be responsible for the synthesis of large amounts of NO (Strijdom *et al.,* 2009a). It was therefore decided to employ two NOS inhibitors, each with different NOS isoform selectivity properties. The following two NOS inhibitors were used: (i) the non-selective inhibitor N^G-Monomethyl-L-arginine monoacetate (L-NMMA) (Calbiochem, San Diego, CA, USA) (Moore & Handy 1997), and (ii) 1400W dichloride (Sigma-Aldrich, St Louis, Mo, USA) known to be an iNOS-specific inhibitor (Garvey *et al*., 1997). L-NMMA competitively binds to the L-arginine binding site of NOS, thus preventing substrate (L-

arginine) binding leading to reduced NO synthesis (Boer *et al*., 2000). 1400W has previously been shown to be a 1000-fold more selective for iNOS than eNOS in rat tissue (Garvey *et al*. 1997). 1400W can act as competitive inhibitor of iNOS via binding of the amidine (in 1400W) to the guanidine binding site of L-arginine on the NOS enzyme (Garvey *et al*., 1997). Furthermore, Zhu *et al*., (2005) showed 1400W to be an irreversible inhibitor of iNOS. The same authors showed that 1400W prevented protonation of the haem peroxide intermediate and thus interfering with the oxygenation of L-arginine. Haem is converted to biliverdin and in the absence of haem the normal activation and dimerization of NOS cannot occur, thus resulting in irreversible inactivation of iNOS.

3.4.5 Validating the efficacy of L-NMMA and 1400W

As positive control for DAF-2/DA fluorescence we employed the use of the NO donor, DEA/NO (chapter 2, figure 2.5). However, NO donors do not stimulate NO release via NOS. They decompose spontaneously in solution and donate nitrate groups that release NO (Miller & Megson 2007). Therefore, in order to confirm the efficacy of NOS inhibitors, other suitable positive controls had to be employed. The humoral factor bradykinin has been shown to increase NO synthesis via activation and phosphorylation of eNOS (Harris *et al*., 2001) and served as a suitable positive control for NOS derived NO. CMECs were pre-treated with 100 µM L-NMMA for 10 minutes before administration of 10 µM Bradykinin for 30 minutes (figure 3.19). NO was measured by flow cytometric analysis of DAF-2/DA fluorescence, and results indicated that bradykinin resulted in a modest, but significant increase in NO levels, while pretreatment with L-NMMA abolished the increase. Noteworthy was the fact that L-NMMA also significantly decreased baseline levels of NO compared to untreated control (Control: 100%; L-NMMA: 86 ± 0.4 %*; BK: 109 ± 1.3 %*$^{\#}$; L-NMMA + BK: 97 ± 0.3 %$^{\#}$; * $p<0.05$ vs control; $^{\#}$ $p<0.05$ vs L-NMMA) (figure 3.20).

In order to control for the proposed iNOS-selectivity of the 1400W NOS inhibitor, a pro-inflammatory cytokine, interleukin-1β, was administered to stimulate iNOS. This strategy was based on the fact that several previous studies showed that iNOS is particularly responsive to cytokine treatment (Wu & Wilson 2009; Lowry *et al.* 2013). CMECs were pre-treated with 80 µM

1400W for 2 hours prior to administration of 5 ng/ml interleukin-1β for 24 hours (figure 3.21). Interleukin-1β showed potent NO-stimulating properties and increased NO levels significantly compared to controls. This increase was abolished by 1400W pre-treatment (Control: 100%; IL-1β: 165 ± 4.9 %*; 1400W + IL-1β: 65 ± 2.3 %$^{\#}$; * $p<0.05$ vs control; $^{\#}$ $p<0.05$ vs IL-1β) (figure 3.22).

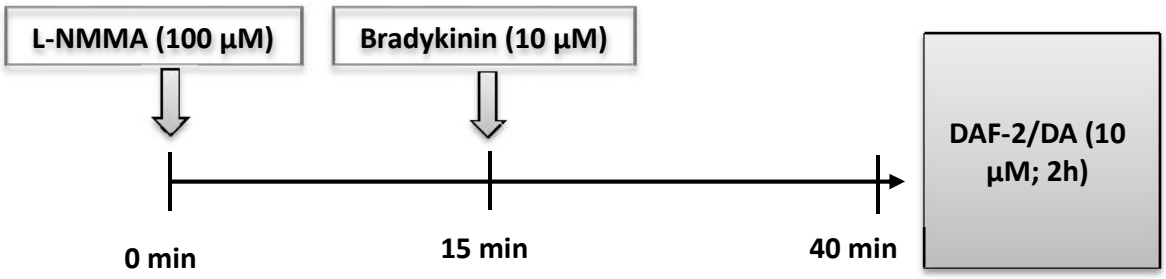

Figure 3.19: Protocol employed to confirm the efficacy of L-NMMA to inhibit NOS derived NO. CMECs were pre-treated with 100 µM L-NMMA for 15 minutes prior to addition of bradykinin (10 µM) for a further 30 minutes. NO was determined by DAF-2/DA fluorescence.

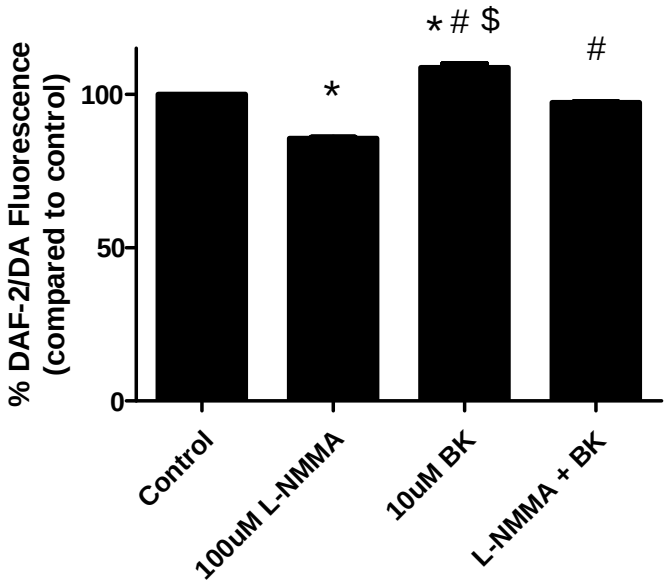

*Figure 3.20: Bar chart showing the effects of L-NMMA on bradykinin induced NO production. As confirmation to the efficacy of L-NMMA to inhibit eNOS derived NO, we found 10 µM bradykinin (BK) to significantly increase NO levels after 1 hour. This increase was effectively inhibited by L-NMMA, showing its effectiveness to inhibit eNOS derived NO. * $p<0.05$ vs control; # $p<0.05$ vs L-NMMA; $ $p<0.05$ vs L-NMMA + BK ($n = 3$). BK: bradykinin; L-NMMA: N^G-Monomethyl-L-arginine monoacetate.*

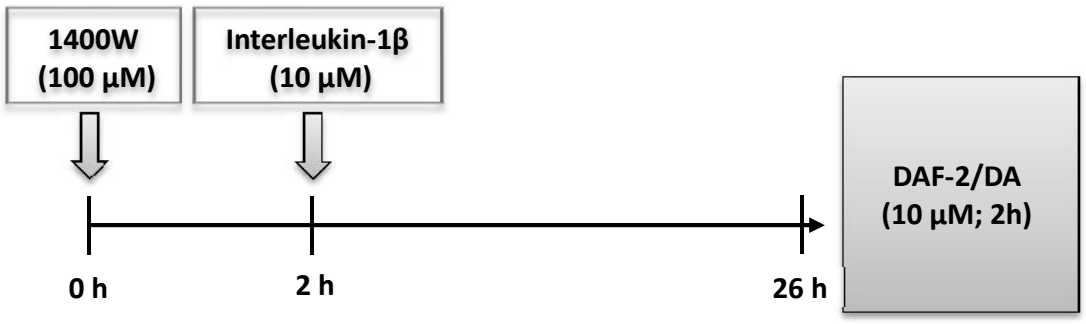

Figure 3.21: Protocol employed to confirm the efficacy of 1400W to inhibit iNOS derived NO CMECs were pre-treated with 80 µM 1400W for 2 hours prior to addition of interleukin-1ß for a further 24 hours. NO was determined by DAF-2/DA fluorescence.

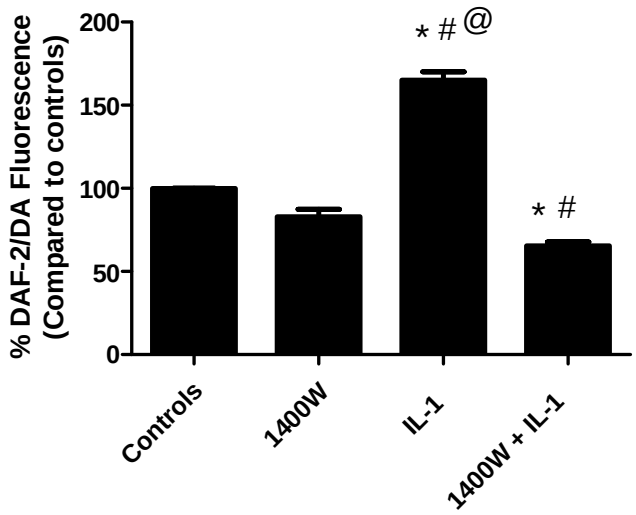

*Figure 3.22: Bar chart to show the efficacy of interleukin-1ß (5ng/ml) to induce iNOS derived NO. This increase was abolished by 1400W (80 µM) pre-treatment, thereby demonstrating its efficacy to inhibit iNOS derived NO (n = 3-4). * p<0.05 vs control; # p<0.05 vs 1400W; @ p<0.05 vs 1400W + IL-1ß. IL-1ß: Interleukin-1ß*

3.4.6 Experimental protocol and methods: L-NMMA and Fenofibrate

We have established that fenofibrate has a pronounced effect on NO production and that shorter treatment periods resulted in larger increases. In order to establish whether these effects were NOS derived, CMECs were pre-treated with L-NMMA according to the protocol described in the previous section (section 3.4.5). Fenofibrate (50 µM) was administered for either 1 or 24 hours and NO measured using DAF-2/DA fluorescence or the Griess method (figure 3.23).

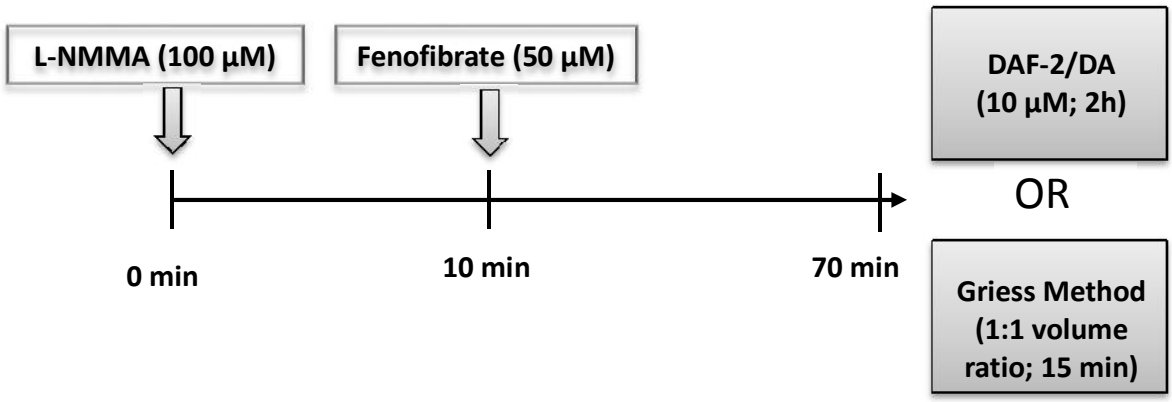

Figure 3.23: An illustration of the experimental protocol followed, using the non-selective NOS inhibitor L-NMMA and fenofibrate (50 µM) treatment for 1 hour.

3.4.7 Results: L-NMMA and Fenofibrate

Although L-NMMA decreased baseline NO by ≈25% compared to untreated control groups, this difference did not reach statistical significance. Unexpectedly, the increase in fenofibrate-derived NO levels was not altered by L-NMMA pretreatment (Fenofibrate: 164.2% ± 12.3%; L-NMMA + Fenofibrate: 175.2% ± 13.2; $p>0.05$) (figure 3.24 A). In order to validate the DAF-2/DA findings of the L-NMMA studies, the experiments were repeated with the Griess method, a different NO measurement assay. Furthermore, in order to establish whether the L-NMMA findings were CMEC-specific, we repeated the Griess investigations on aortic endothelial cells (AECs). Similar results were observed with the Griess method in both CMECs and AECs. Data are expressed as µM nitrites; **CMECs:** Control: 0.8 µM ± 0.2; L-NMMA: 0.9 µM ± 0.2; Fenofibrate: 1.8 µM ± 0.1$^{*\#}$; L-NMMA + Fenofibrate: 2 µM ± 0.2$^{*\#}$, * $p<0.05$ vs control; # $p<0.05$ vs L-NMMA), and **AECs:** Control: 2.7 µM ± 0.3; L-NMMA: 3.0 µM ± 0.3; Fenofibrate: 5.9 µM ± 0.6$^{*\#}$; L-NMMA + Fenofibrate: 6.1 µM ± 0.4$^{*\#}$, * $p<0.05$ vs control; # $p<0.05$ vs L-NMMA (figure 3.24 B and C).

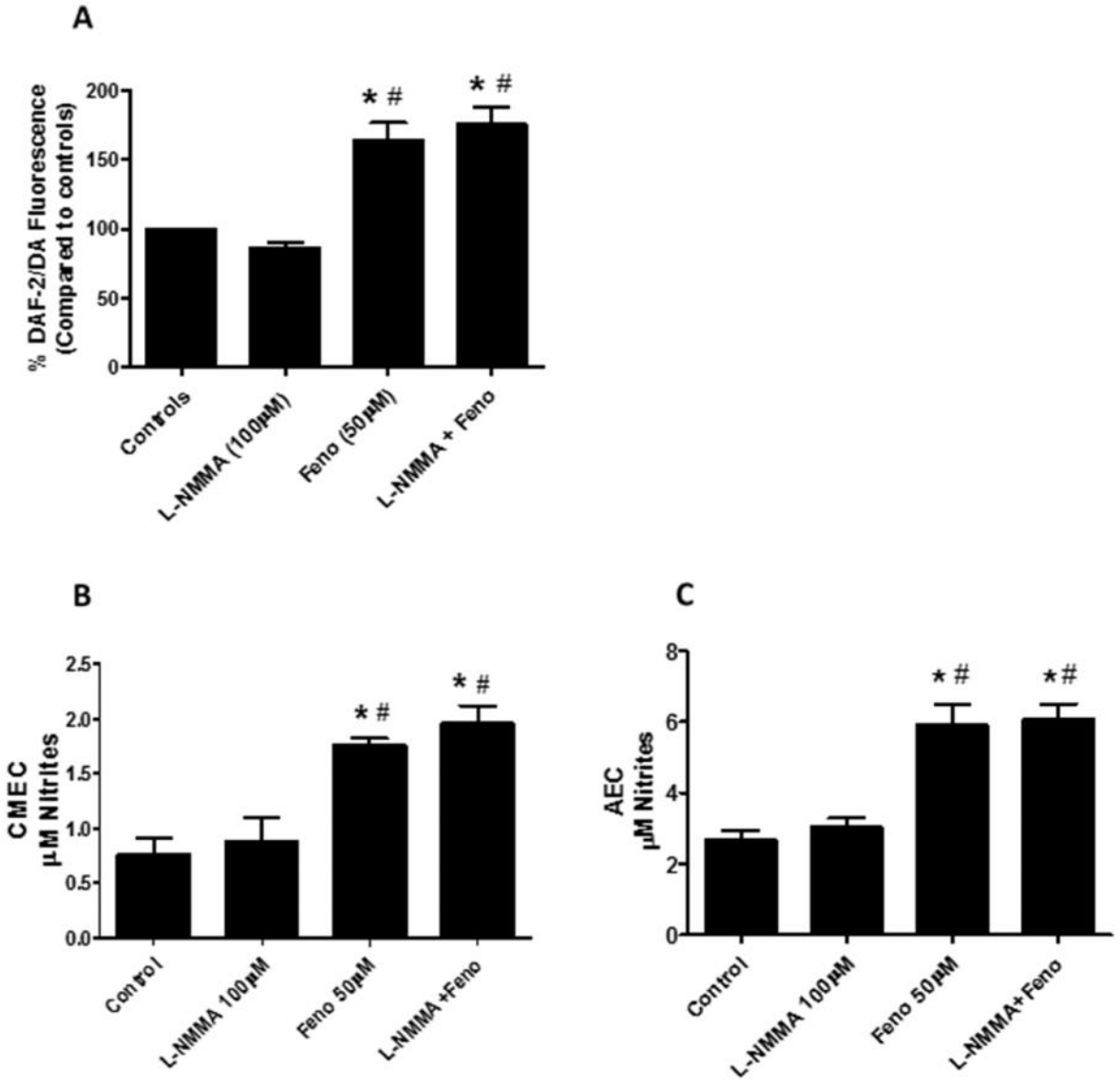

*Figure 3.24: Bar charts showing the effects of 15 minutes L-NMMA (100 µM) pretreatment on NO production. A) Flow cytometric analysis of DAF-2/DA in CMECs showing non-significant decrease in control CMECs pretreated with L-NMMA. Fenofibrate increased DAF-2/DA fluorescence; however, L-NMMA pretreatment failed to reduce the fenofibrate-induced increase (n = 13-15). B and C) Repeating these experiments in CMECs and AECs with the Griess method mirrored DAF-2/DA flow cytometry data (CMECs: n = 3-4; AECs: n = 4-8). * p<0.05 vs control; # p<0.05 vs L-NMMA. L-NMMA: NG-Monomethyl-L-arginine monoacetate; BK: Bradykinin; Feno: Fenofibrate; CMEC: Cardiac microvascular endothelial cells; AEC: Aortic endothelial cells.*

3.4.8 Experimental protocol: 1400W and Fenofibrate

Since inhibition with the non-selective NOS inhibitor, L-NMMA did not result in reduced levels of NO, we employed the iNOS-selective inhibitor, 1400W in the next set of experiments in order to establish whether the increased NO production was via iNOS induction. CMECs and AECs and were pre-treated with 1400W prior to 1 hour treatment with fenofibrate, as shown in figure 3.25. Description of the optimised protocol is described in section 3.4.5 was used. NO was measured by flow cytometric analysis of DAF-2/DA fluorescence and the Griess method.

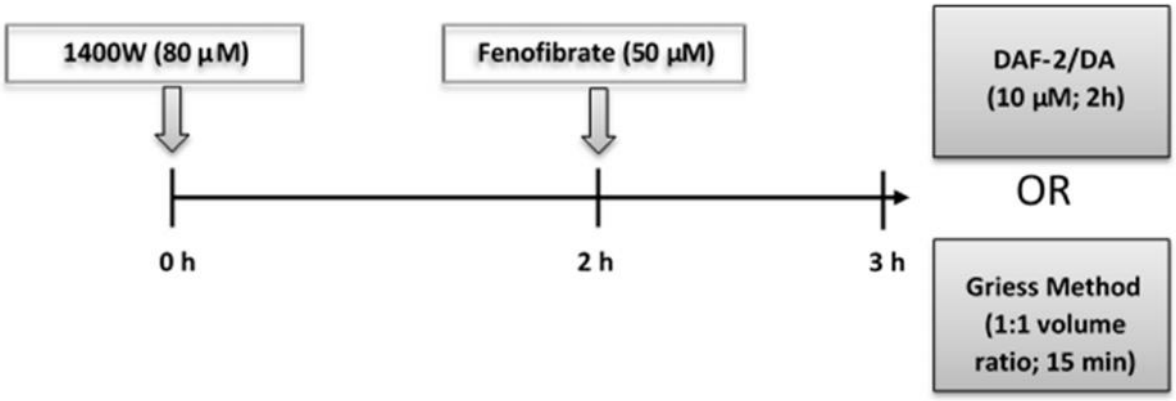

Figure 3.25: An illustration of the experimental protocol for the iNOS-selective inhibitor, 1400W and fenofibrate (50 µM) experiments (1 hour).

3.4.9 Results: 1400W and Fenofibrate

Similar to previous findings, fenofibrate (50 µM) increased DAF-2/DA fluorescence in CMECs as well as the concentration nitrites in CMECs and AECs after 1 hour treatment (figure 3.26 A-C). 1400W pretreatment failed to reduce fenofibrate-derived NO in any of the experiments. Figure 3.26 A shows the DAF/2-DA fluorescence data in CMECs: Control: 100%; Fenofibrate: 149.5% ± 6.5%*; 1400W+Fenofibrate: 134.4% ± 12.9%*; $p<0.05$ vs Control. Figure 3.26 B shows the concentration nitrites in CMECs: Control: 2.0 µM ± 0.2; Fenofibrate: 2.8 µM ± 0.1*; 1400W+Fenofibrate: 3.3 µM ± 0.2*; $p<0.05$ vs Control. Figure 3.26 C shows the concentration nitrites in AECs: Control: 1.9 µM ± 0.1; Fenofibrate: 3.1 µM ± 0.2*; 1400W+Fenofibrate: 4.3 µM ± 0.4*; $p<0.05$ vs Control.

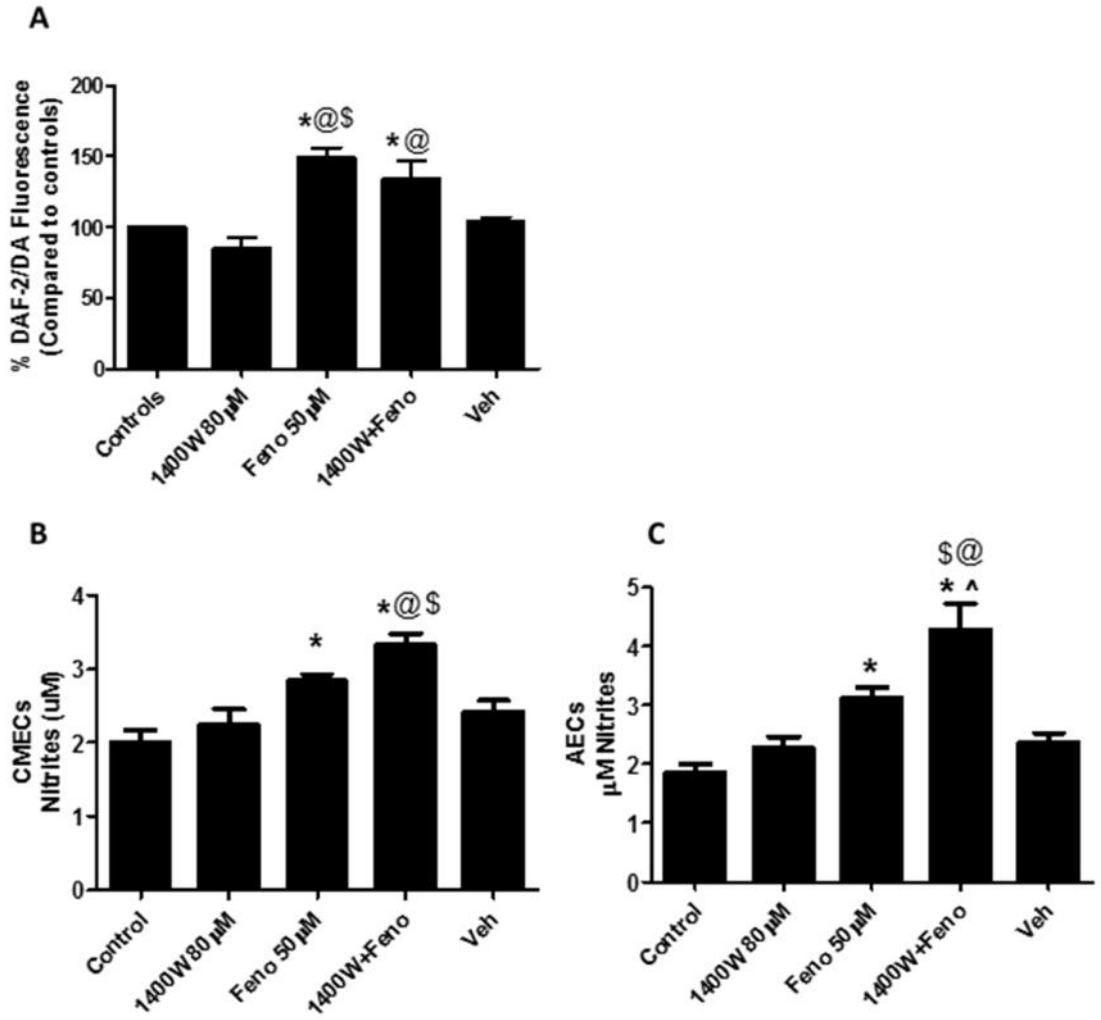

*Figure 3.26: Bar charts showing the effects of 2 hours 1400W (80 µM) pretreatment on NO production. A) Flow cytometric analysis of DAF-2/DA in CMECs showing fenofibrate (50 µM) significantly increased NO after 1 hour treatment, however, L-NMMA pretreatment failed to reduce the fenofibrate-induced increase (n = 8-12). B and C) Repeating these experiments in CMECs and AECs with the Griess method mirrored DAF-2/DA flow cytometry data (CMECs: n = 3-4; AECs: n = 4-8). * p<0.05 vs control; # p<0.05 vs L-NMMA. * p<0.05 vs control; $^{@}$ p<0.05 vs 1400W; $^{\$}$ p<0.05 vs vehicle (1400W+fenofibrate); ^ p<0.05 vs Fenofibrate. Feno: Fenofibrate; Vehicle: Vehicle for feno + 1400W combination.*

3.4.10 Experimental protocol: iNOS protein and gene expression investigations.

In view of the modest, albeit statistically non-significant reduction in DAF-2/DA fluorescence observed in fenofibrate-treated CMECs pretreated with 1400W (figure 3.26 A), we further explored the possible involvement of iNOS on protein and mRNA level. Buchwalow *et al*. (2001) has shown iNOS protein expression in endothelial cells and therefore we set out to determine whether iNOS expression could be detected in the CMECs used in the current study and if so, whether fenofibrate treatment affected iNOS expression. CMECs were treated with 50 µM fenofibrate for 1 hour after which cells were lysed and prepared for western blot analyses or quantitative Real-Time Polymerase Chain Reaction (qPCR) (figure 3.27) as described in section 2.5 of chapter 2. The pro-inflammatory cytokine interleukin-1β (5 ng/ml for 24 hours) was included in the series of experiments to serve as a positive control for iNOS protein and gene induction.

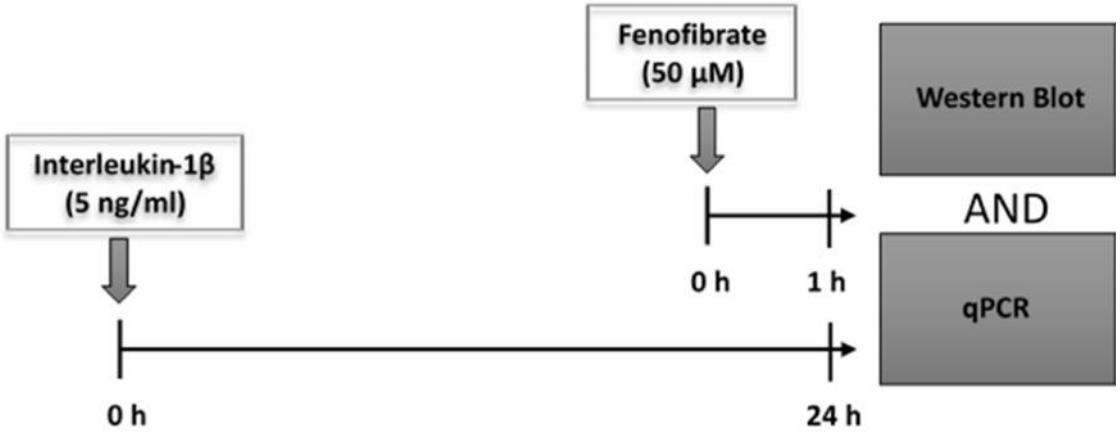

Figure 3.27: Experimental protocols for the iNOS protein and gene expression studies. Interleukin 1-ß (24 hour incubation) was included as positive control, and in separate experiments, CMECs were treated with 50 µM fenofibrate for 1 hour to investigate iNOS expression by western blots and quantitative Real-Time Polymerase Chain Reaction (qPCR).

3.4.11 Results: iNOS protein and gene expression investigations

Although interleukin-1β was successful in the significant induction of iNOS protein expression, the western blot results showed that 1 hour fenofibrate treatment failed to induce detectable expression of iNOS protein (figure 3.28 A). In order to confirm that the failure to detect iNOS protein expression by western blot measurements was also reflected on iNOS mRNA level, samples were subjected to quantitative real-time gene expression analyses. The results showed that there was no iNOS mRNA expression under control/baseline conditions. The positive control, interleukin-1β (5ng/ml), was successful in inducing iNOS mRNA expression, which was significantly attenuated by a margin of ~50% via the knockdown by two iNOS siRNA constructs. Similar to the iNOS protein expression data, there was no detectable iNOS gene expression after 1 hour fenofibrate treatment.

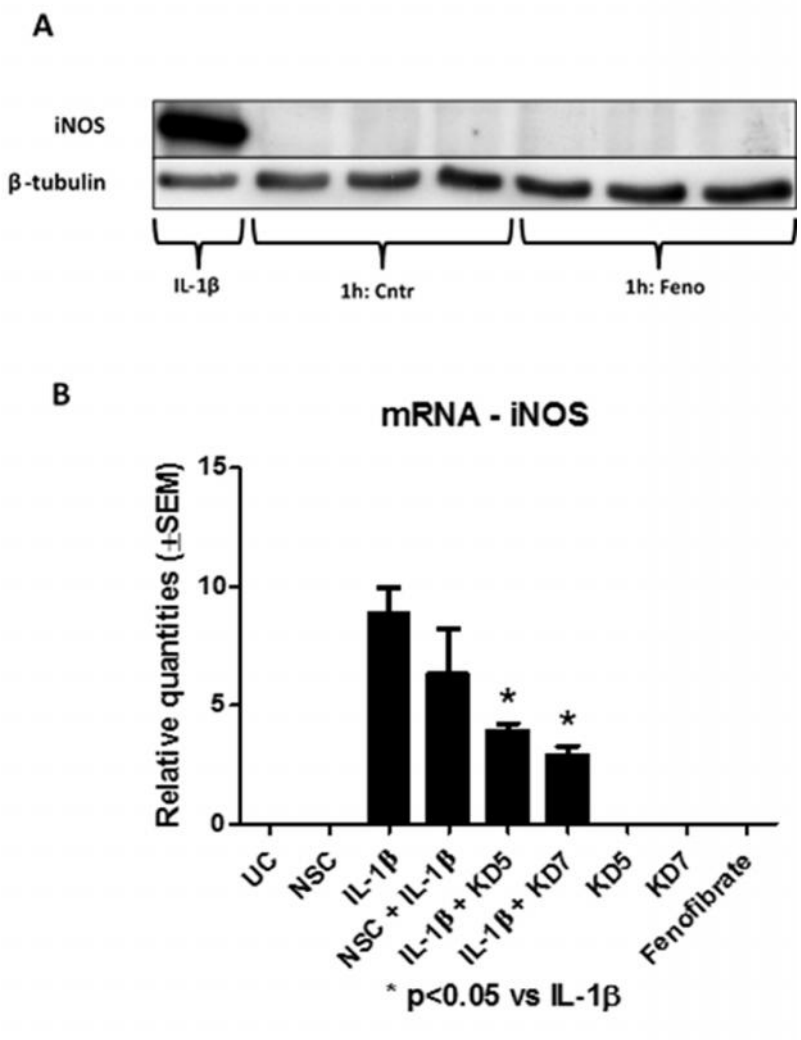

*Figure 3.28: CMECs treated with interleukin-1ß (5ng/ml for 24 hours) and fenofibrate (50 µM for 1 hour) to investigate iNOS protein and gene expression levels. A) Western blot indicating that although interleukin-1ß successfully induced iNOS protein expression in CMECs, iNOS expression was not detected under either control conditions or in response to fenofibrate treatment. B-tubulin shows equal loading of protein (n=3). B) Interleukin-1ß increased iNOS gene expression significantly, confirmed by knock down of iNOS mRNA at construct 5 and 7. No iNOS mRNA was detected in UC (untreated control), NSC (non-silencing control), KD5 (iNOS siRNA, construct 5), KD 7 (iNOS siRNA, construct 7) and fenofibrate treated samples (n=3 biological replicates, assayed in triplicate). * p<0.05 vs IL-1ß.*

3.4.12 Experimental protocols: Western blot analyses of signalling proteins

Thus far it has been established that fenofibrate exhibits pleiotropic, cholesterol-independent actions on endothelial cells, including increasing NO production after 1, 4 and 24 hour treatment, decreasing DHR-123 related ROS production as well as some anti-apoptotic and anti-necrotic properties. L-NMMA and 1400W however failed to significantly inhibit NO increases. Despite the fact that 1400W pretreatment resulted in a 15% reduction in NO production in fenofibrate-treated CMECs, iNOS protein and mRNA expression could not be detected. In order to investigate signalling pathways involved with these pleiotropic effects in more detail, western blot analyses were performed as described in section 2.6.

Western blot analyses were performed on CMECs treated with fenofibrate for 1 and 24 hours, as well as shorter durations namely, 5 min, 15 min and 30 minute according to figure 3.29. Initially CMECs were treated with 50 µM fenofibrate for 1 and 24 hours. After these initial experiments, shorter time periods were tested, namely, 5 min, 15 min and 30 min. Information on the proteins of interest as well as the antibodies are shown in table 2.1. For the purpose of verifying the correct position of proteins on the blots, 3 positive controls were included in the initial set of experiments: Interleukin-1β (5 ng/ml for 24 hours), AICAR (2 mM for 2 hours) and Okadiac acid (500 µM or 45 min).

Please note that all the total-protein expression blots were calculated and expressed as a ratio of the loading control.

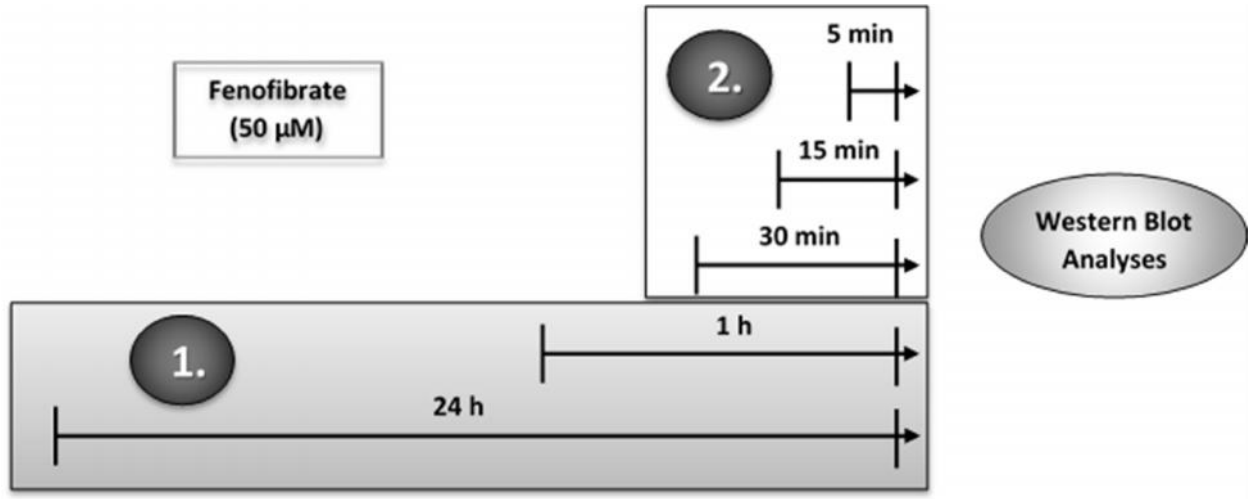

Figure 3.29: A graphic illustration of the experimental protocols followed for western blot investigations. The block marked with number 1 shows the 1 hour and 24 hour treatment protocols, whereas block 2 indicates protocols using shorter treatment periods (5, 15 and 30 minutes).

3.4.13 Results: 1 and 24 hour fenofibrate western blot analyses

3.4.13.1 NOS

Fenofibrate treatment had no effect on total eNOS expression after 1 and 24 hours (figure 3.30 B). Surprisingly, 1 hour fenofibrate significantly reduced phosphorylation of eNOS at Ser 1177 (1h Control: 1; 1h Fenofibrate: 0.56 ± 0.12, $p<0.05$) (figure 3.30 C) and a reduction in the P/T ratio of eNOS Ser 1177 was also found (1h Control: 1; 1h Fenofibrate: 0.64 ± 0.15, $p<0.05$) (figure 3.30 D). No differences were detected between the 24 hour fenofibrate treatment groups and their time-matched untreated controls with regards to phosphorylation of eNOS Ser 1177 (figure 3.30 C). Another interesting finding was the significant reduction in the phosphorylation of eNOS Ser 1177 observed in the untreated control samples at 24 hours compared to 1 hour incubation period (1h Control: 1; 24h Control: 0.17 ± 0.01, $p<0.05$) (figure 3.30 C). Okadaic acid (loaded in lane 3; figure 3.30 A), a phosphatase inhibitor, showed to be a functional positive control for all

phosphorylated proteins. AICAR (loaded in lane 2; figure 3.30 A) phosphorylates AMPK, an upstream activator of eNOS, and served as an alternative positive control for phosphorylated eNOS. The other positive regulatory site of eNOS, Ser 632, showed no change in phosphorylation (figure 3.31 C) and no changes were observed in the P/T ratio of Ser 632 (figure 3.31 D).

1 hour treatment with fenofibrate did not result in any changes in the phosphorylation of eNOS Thr 495 compared to 1 hour control, however 24 hour fenofibrate treatment significantly increased phosphorylation compared to 24 hour control group (24h Control: 0.63 ± 0.05; 24h Fenofibrate: 0.84 ± 0.03, $p<0.05$) (figure 3.32 C), but no changes were observed in the P/T eNOS Thr 495 ratio. Furthermore, phosphorylation of eNOS Thr 495 was significantly reduced in the 24 hour untreated control group, compared to 1 hour untreated controls (1h Control: 1; 24h Control: 0.63 ± 0.05, $p<0.05$) (figure 3.32 C) and this was the case for P/T eNOS Thr 495 ratio as well (1h Control: 1; 24h Control: 0.59 ± 0.05, $p<0.05$) (figure 3.32 D).

Phosphorylation of eNOS Tyr 657 was not altered by 1 hour fenofibrate treatment compared to the 1 hour untreated control group, or in the 24 hour fenofibrate treatment compared to 24 hour untreated control group (figure 3.33 C). However, the 24 hour untreated control group showed significantly lower levels of phosphorylation compared to 1 hour untreated control group (1h Control: 1; 24h Control: 0.36 ± 0.09, $p<0.05$) (figure 3.33 D). These changes translated into a similar decrease in the P/T ratio of Tyr 657 (1h Control: 1; 24h Control: 0.35 ± 0.09, $p<0.05$) (figure 3.33 D).

Total expression and phosphorylation levels of nNOS were too low to be detected and quantified and therefore no analyses were performed on experiments looking at this NOS isoform (figure 3.34).

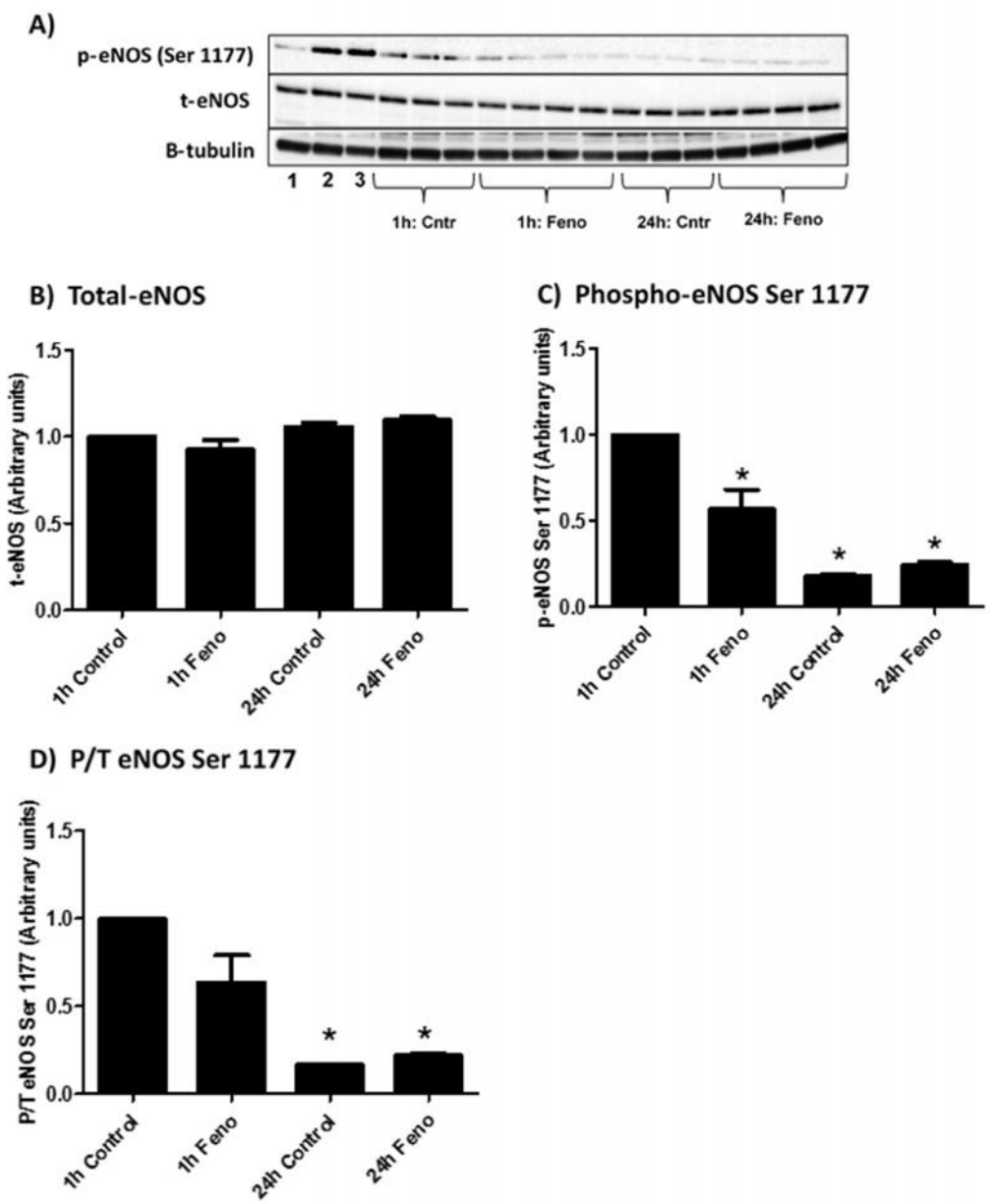

*Figure 3.30: Bar charts indicating changes in eNOS expression and phosphorylation (Ser 1177) of CMECs treated with fenofibrate (50 µM) for 1 and 24 hours. A) Representative western blots indicating total-eNOS, phospho-eNOS (Ser 1177) and ß-tubulin; Lane 1: Interleukin-1ß; Lane 2: AICAR; Lane 3: OA – Okadiac acid. B) Analysed results for total-eNOS. C) Analysed results for phospho-eNOS (Ser 1177). D) Phosphorylated over total (P/T) ratio of eNOS Ser 1177. * p<0.05 vs 1h Control; # p<0.05 vs 1h Feno. Cntr: Control; Feno: Fenofibrate. n=3-7*

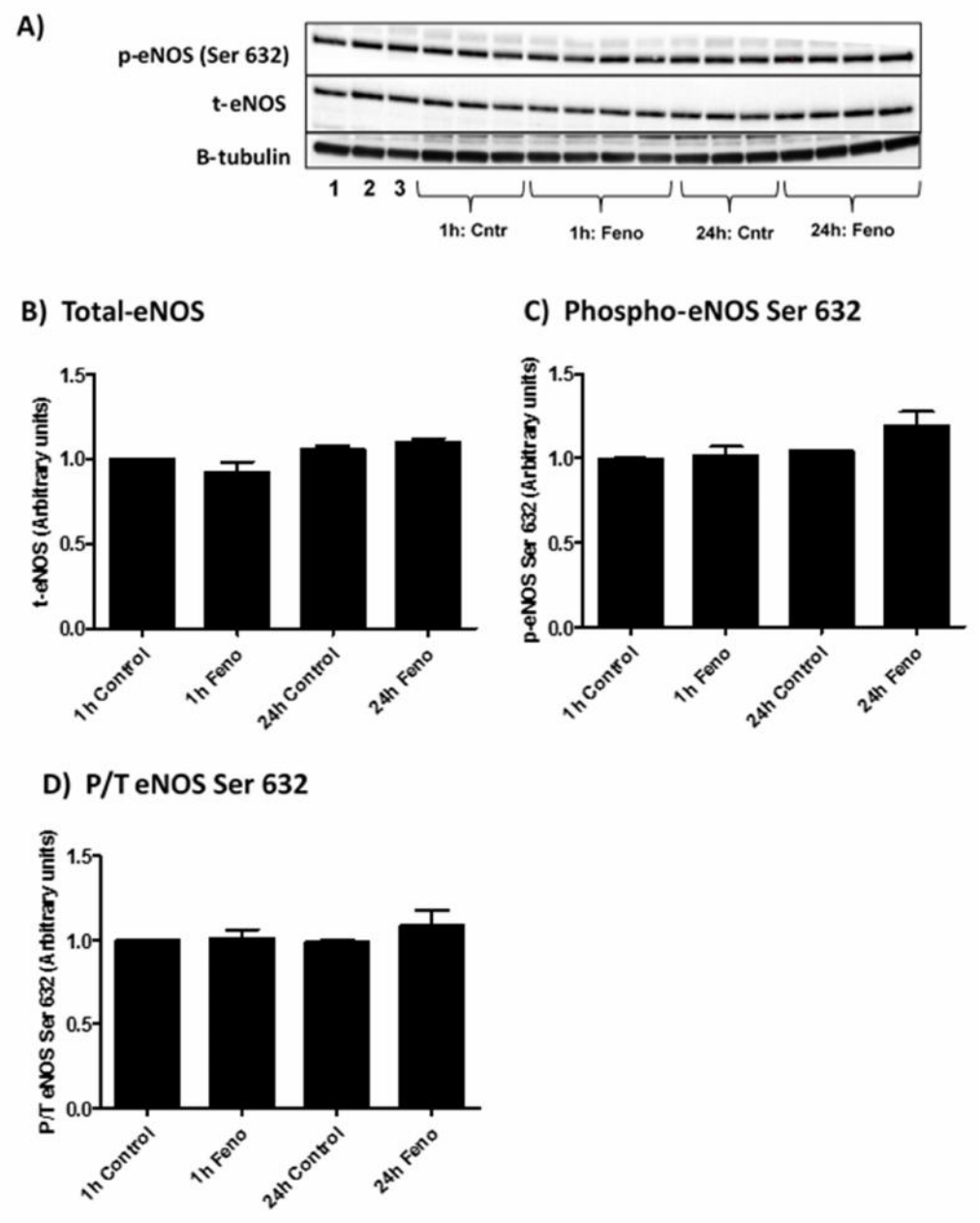

*Figure 3.31: Bar charts indicating changes in eNOS expression and phosphorylation (Ser 632) of CMECs treated with fenofibrate (50 µM) for 1 and 24 hours A) Representative western blots indicating total-eNOS, phospho-eNOS (Ser 632) and ß-tubulin; Lane 1: Interleukin-1ß; Lane 2: AICAR; Lane 3: OA – Okadiac acid. B) Analysed results for total-eNOS. C) Analysed results for phospho-eNOS (Ser 632). D) Phosphorylated over total (P/T) ratio of eNOS Ser 632. * p<0.05 vs 1h Control; # p<0.05 vs 1h Feno. ; Cntr: Control; Feno: Fenofibrate. n=3-7*

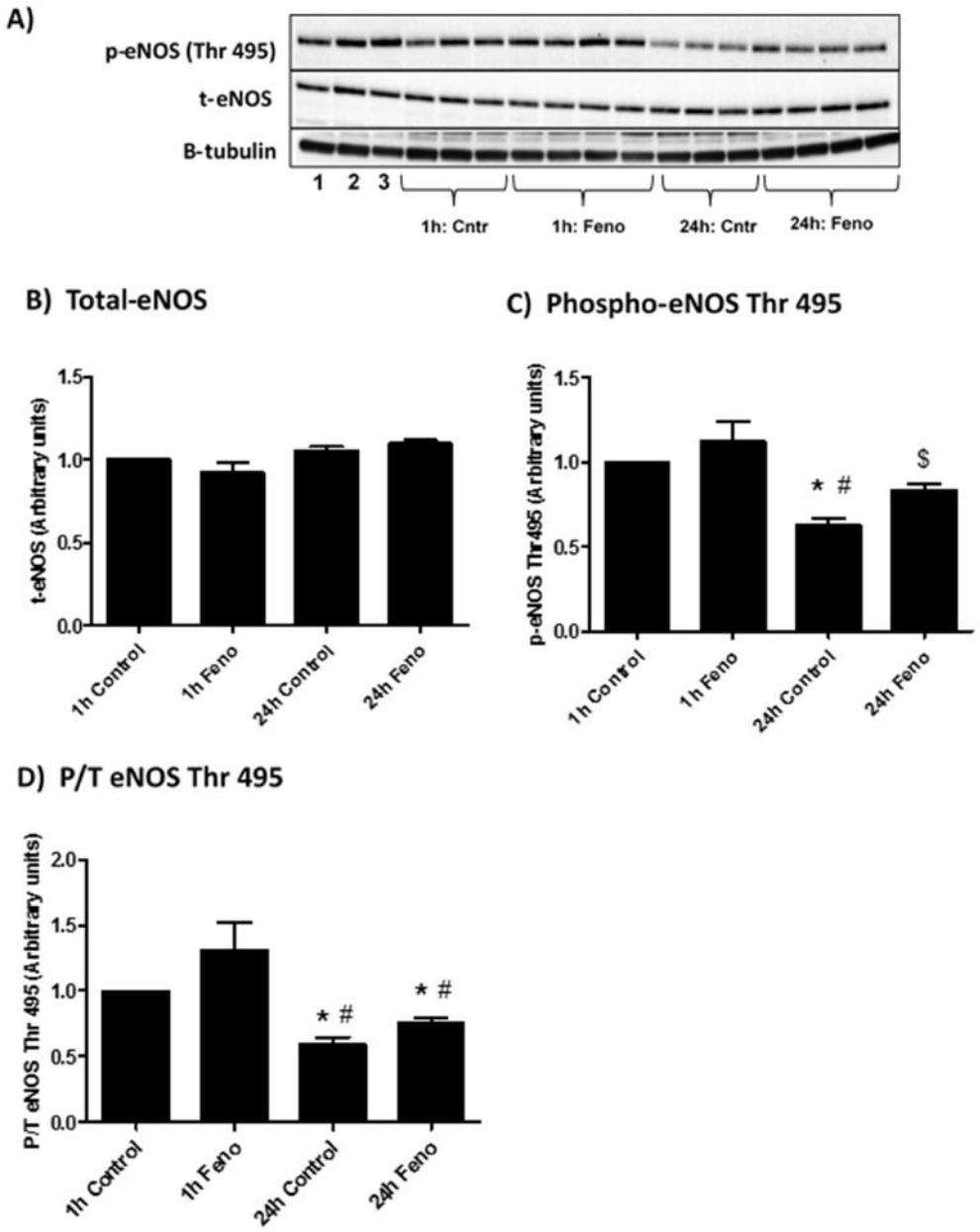

*Figure 3.32: Bar charts indicating changes in eNOS expression and phosphorylation (Thr 495) of CMECs treated with fenofibrate (50 µM) for 1 and 24 hours A) Representative western blots indicating total-eNOS, phospho-eNOS (Thr 495) and ß-tubulin; Lane 1: Interleukin-1ß; Lane 2: AICAR; Lane 3: OA – Okadiac acid. B) Analysed results for total-eNOS. C) Analysed results for phospho-eNOS (Thr 495). D) Phosphorylated over total (P/T) ratio of eNOS Thr 495. * p<0.05 vs 1h Control; # p<0.05 vs 1h Feno; $ p<0.05 vs 24h Control. Cntr: Control; Feno: Fenofibrate. n=3-7.*

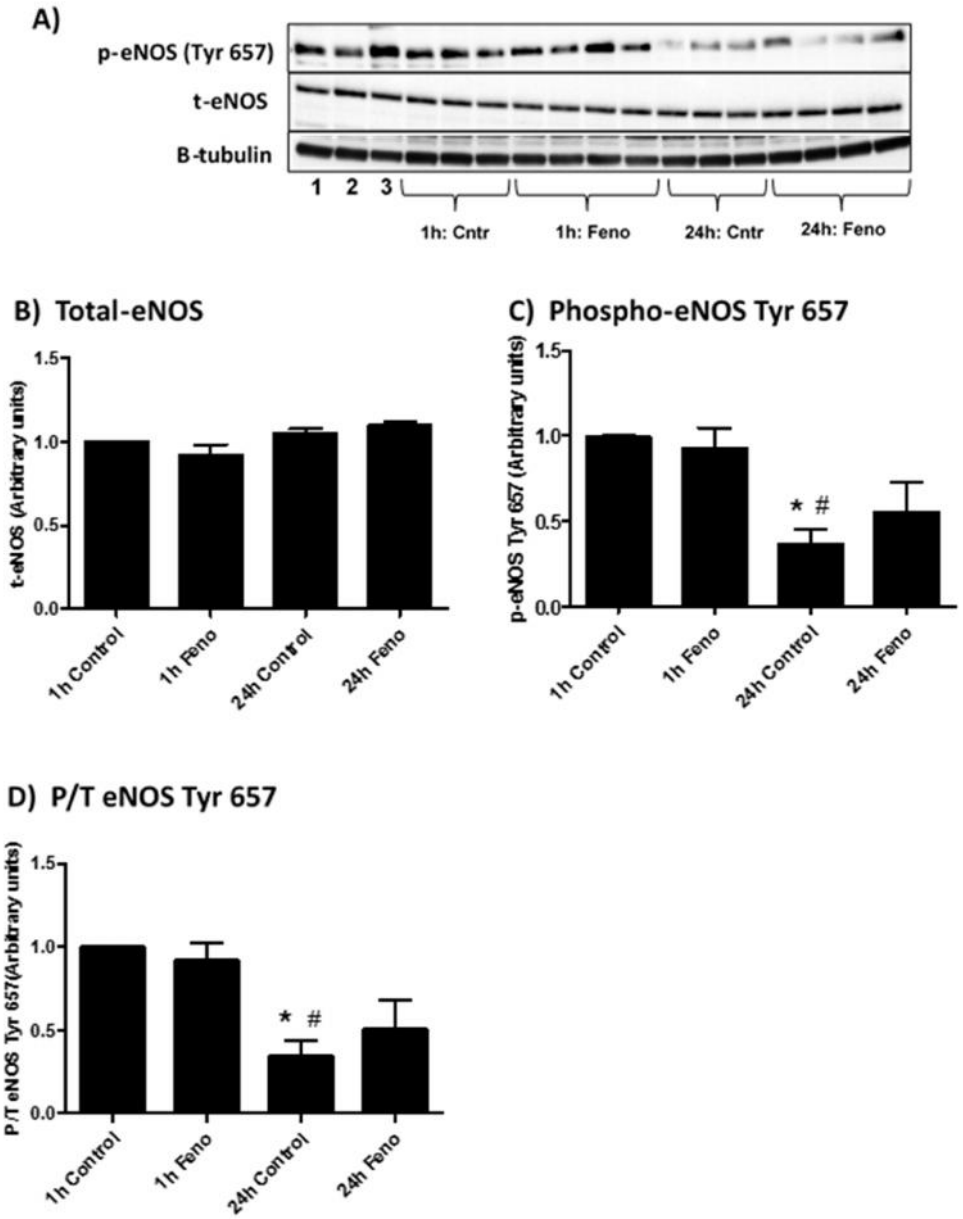

*Figure 3.33: Bar charts indicating changes in eNOS expression and phosphorylation (Tyr 657) of CMECs treated with fenofibrate (50 µM) for 1 and 24 hours A) Representative western blots indicating total-eNOS, phospho-eNOS (Tyr 657) and ß-tubulin; Lane 1: Interleukin-1ß; Lane 2: AICAR; Lane 3: OA – Okadiac acid. B) Analysed results for total-eNOS. C) Analysed results for phospho-eNOS (Tyr 657). D) Phosphorylated over total (P/T) ratio of eNOS Tyr 657. * p<0.05 vs Control; # p<0.05 vs 1h Feno. Cntr: Control; Feno: Fenofibrate. n=3-7*

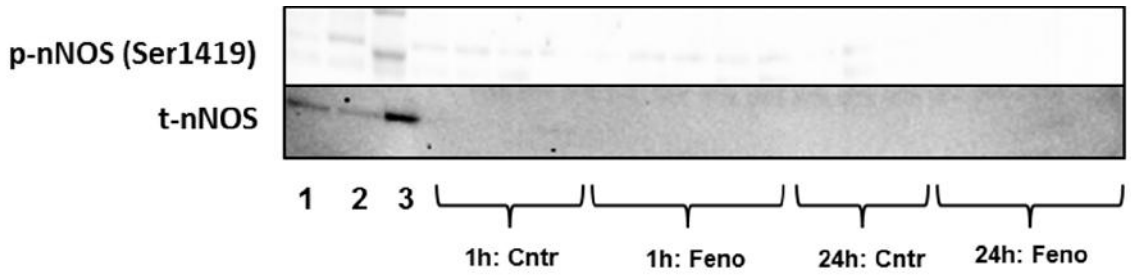

Figure 3.34: nNOS expression and phosphorylation (Ser 1417) of CMECs treated with fenofibrate (50 µM) for 1 and 24 hours. Total expression levels of nNOS and phospho-nNOS were too low to be detected and quantified. (1) Interleukin-1ß; (2) AICAR; (3) OA – Okadiac acid.

3.4.13.2 AMPK

No changes were detected in total-AMPK expression after 1 or 24 hour treatment (figure 3.35 B). 1 hour fenofibrate treatment did, however, significantly decrease phospho-AMPK at Thr 172 compared to 1 hour untreated controls (1h Control: 1; 1h Fenofibrate: 0.73 ± 0.04, $p<0.05$) (figure 3.35 C). The same trend was seen in the P/T ratio of AMPK, where 1 hour fenofibrate significantly decreased the P/T ratio compared to 1 hour untreated control group (1h Control: 1; 1h Fenofibrate: 0.64 ± 0.07, $p<0.05$) (figure 3.35 D). No differences were observed in the phospho-AMPK levels when subjected to 24 hours fenofibrate treatment compared to time-matched untreated controls. AICAR treated CMECs (loaded in lane 2) and okadiac acid (loaded in lane 3) showed to be potent inducers of AMPK phosphorylation, thereby serving as effective positive controls (figure 3.35 A)

3.4.13.3 PKB/Akt

No changes were detected in total-PKB/Akt expression levels after 1 or 24 hour treatment with fenofibrate (figure 3.36 B). Although the detection of phosphorylated PKB/Akt (Ser 473) levels was quite low, it was sufficient to be analysed and showed that 1 hour fenofibrate significantly reduced phospho-PKB/Akt compared to the 1 hour untreated control group (1h Control: 1; 1h Fenofibrate: 0.78 ± 0.05, $p<0.05$) (figure 3.36 C). 24 hour untreated controls showed reduced phosphorylation compared to the 1 hour untreated control group (1h Control: 1; 24h Control:

0.71 ± 0.05, $p<0.05$) (figure 3.36 C). These results were mirrored in the P/T ratio of PKB/Akt (1h Control: 1; 1h Fenofibrate: 0.83 ± 0.04, $p<0.05$) (1h Control: 1; 24h Control: 0.67 ± 0.02, $p<0.05$) (figure 3.36 D).

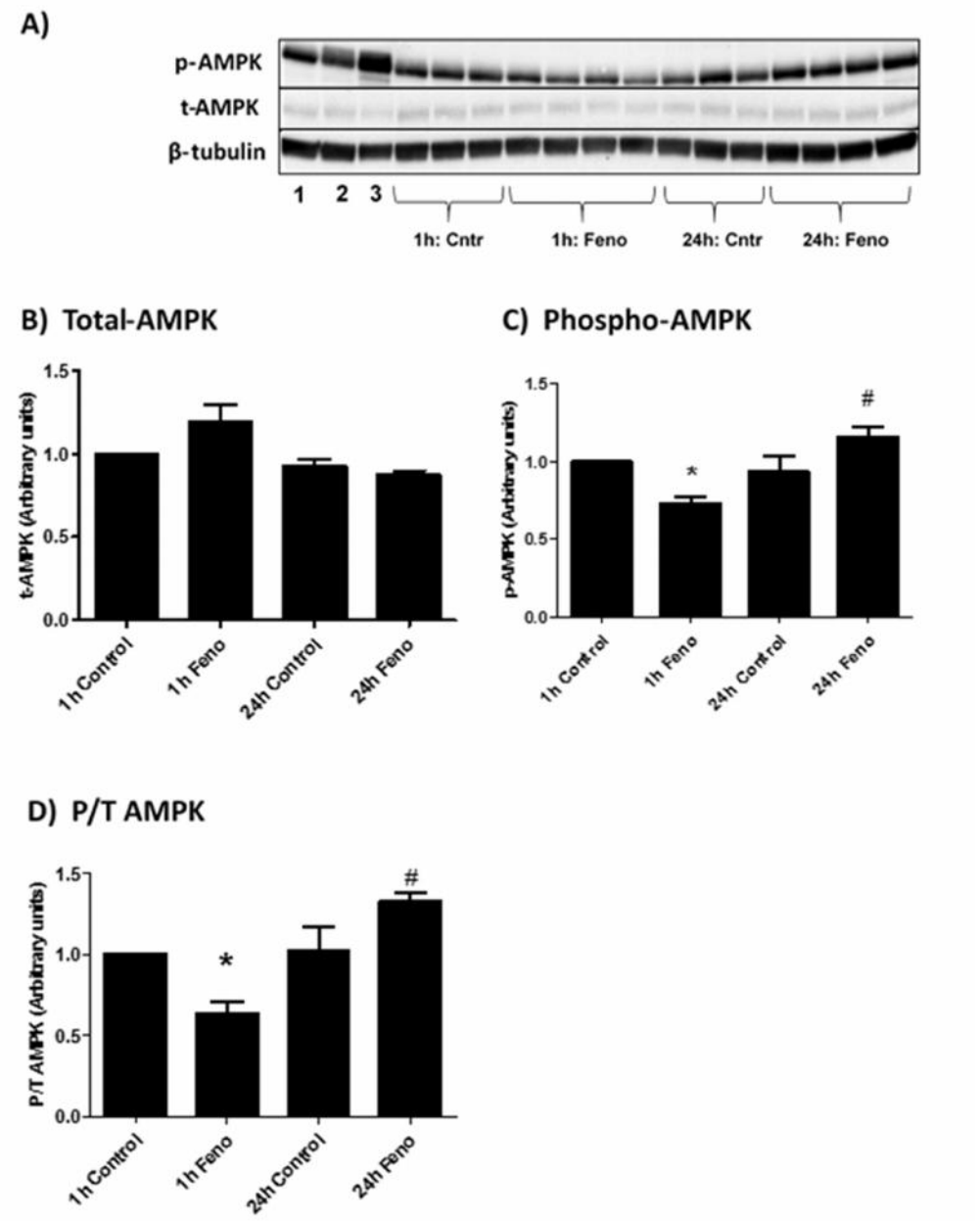

*Figure 3.35: Bar charts indicating changes in AMPK expression and phosphorylation (Thr 172) of CMECs treated with fenofibrate (50 µM) for 1 and 24 hours. A) Representative western blots showing total-AMPK, phospho-AMPK (Thr 172) and ß-tubulin; Lane 1: Interleukin-1ß; Lane 2: AICAR; Lane 3: OA – Okadiac acid. B) Analysed results for total-AMPK. C) Analysed results for phospho-AMPK (Thr 172). D) Phosphorylated over total (P/T) ratio of AMPK (Thr 172). * p<0.05 vs Control; # p<0.05 vs 1h Feno. ; Cntr: Control; Feno: Fenofibrate. n=3-7*

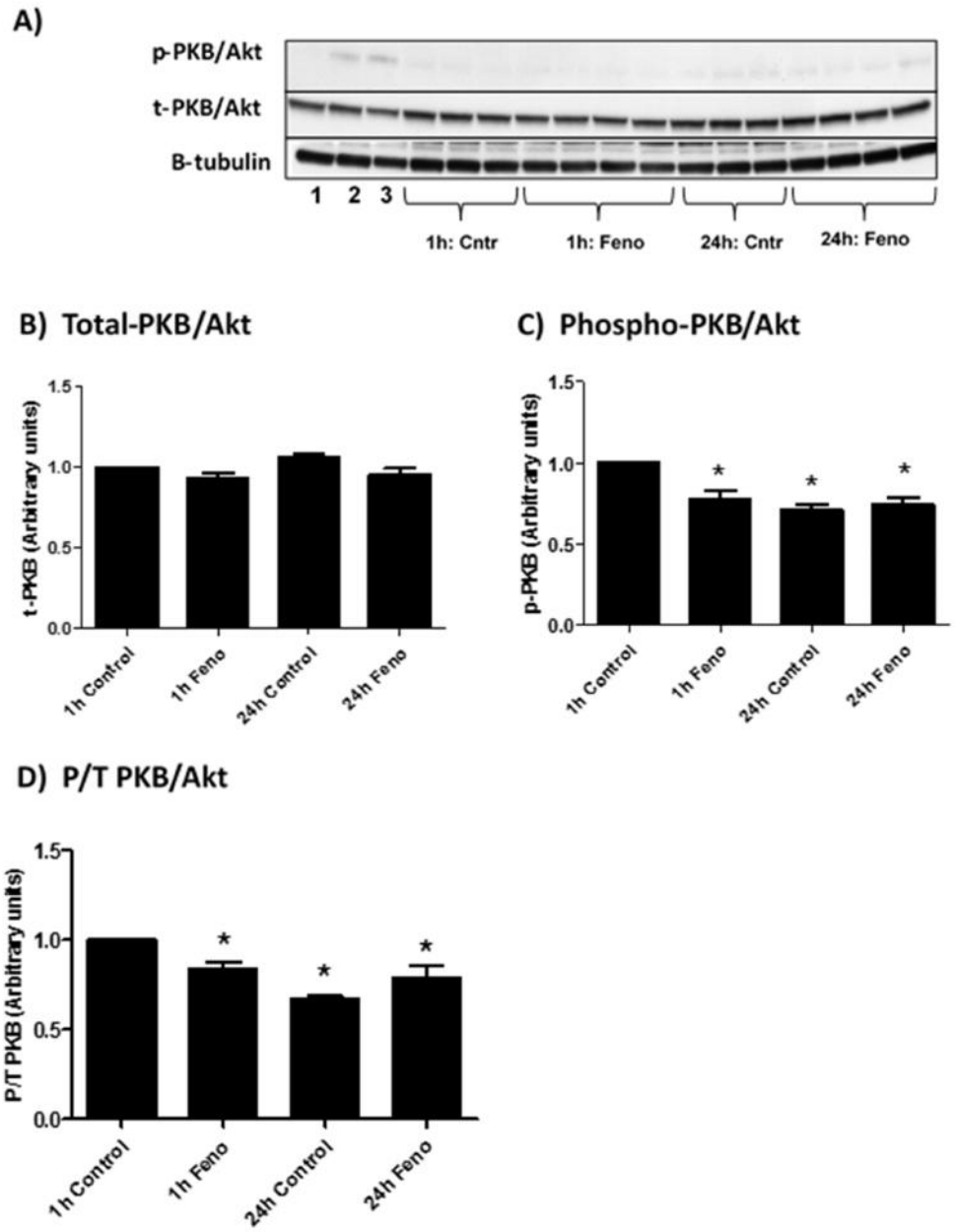

*Figure 3.36: Bar charts indicating changes in PKB/Akt expression and phosphorylation (Thr 172) of CMECs treated with fenofibrate (50 µM) for 1 and 24 hours. A) Representative western blots showing total-PKB/Akt, phospho-PKB/Akt (Ser 473) and ß-tubulin; Lane 1: Interleukin-1ß; Lane 2: AICAR; Lane 3: OA – Okadiac acid. B) Analysed results for total-PKB. C) Analysed results for phospho-PKB (Ser 473). D) Phosphorylated over total (P/T) ratio of PKB (Ser 473). * p<0.05 vs Control; Cntr: Control; Feno: Fenofibrate. n=3-7*

3.4.13.4 HSP 90

Neither 1 hour nor 24 hour treatment with fenofibrate altered HSP 90 expression levels compared to their respective time-matched untreated controls (figure 3.37 B).

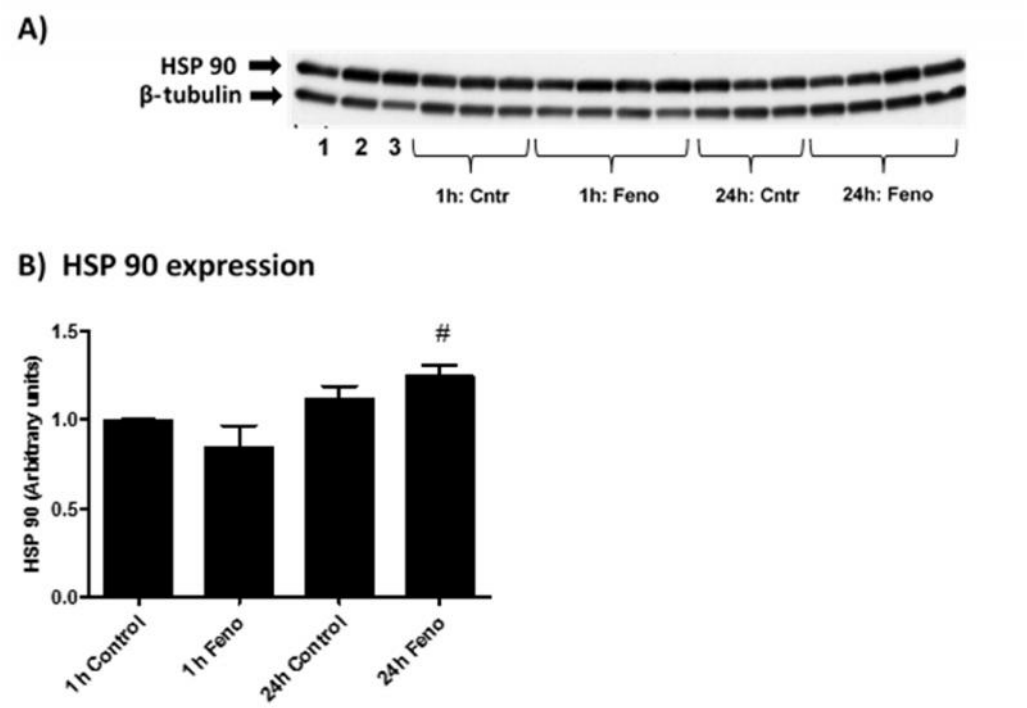

Figure 3.37: Bar charts indicating changes in HSP 90 expression of CMECs treated with fenofibrate (50 µM) for 1 and 24 hours. A) Representative western blots showing total HSP 90 and β-tubulin expression; Lane 1: Interleukin-1β; Lane 2: AICAR; Lane 3: OA – Okadiac acid. B) Analysed results for HSP 90. # p<0.05 vs 1h Feno. Cntr: Control; Feno: Fenofibrate. n=3-7

3.4.13.5 p22Phox and Nitrotyrosine

1 hour fenofibrate significantly increased p22Phox expression compared to the 1 hour untreated control group (1h Control: 1; 1h Fenofibrate: 1.20 ± 0.07, $p<0.05$) (figure 3.38 C). 24 hour fenofibrate treatment had no effect on p22Phox expression, however the 24 hour untreated control group showed significantly lower expression of p22Phox compared to 1 hour untreated controls (1h Control: 1; 24h Control: 0.75 ± 0.09, $p<0.05$). Neither 1 hour nor 24 hour fenofibrate treatment altered nitrotyrosine expression levels (figure 3.38 B and D).

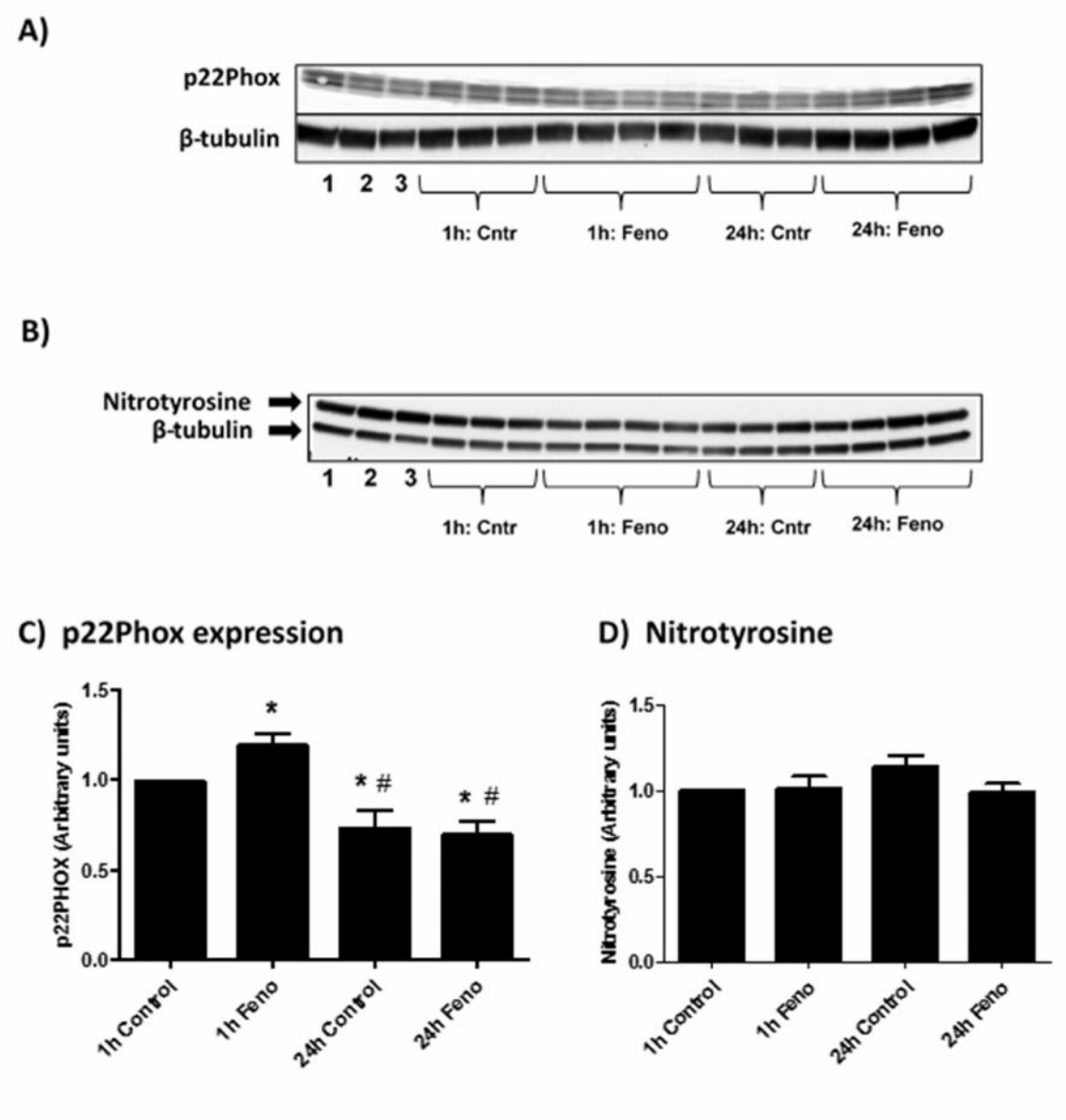

*Figure 3.38: Bar charts indicating changes in nitrotyrosine and p22Phox expression of CMECs treated with fenofibrate (50 µM) for 1 and 24 hours. A) Representative western blots showing total p22phox and β-tubulin expression. Lane 1: Interleukin-1β; Lane 2: AICAR; Lane 3: OA – Okadiac acid. B) Representative western blots indicating nitrotyrosine and β-tubulin expression; Lane 1: Interleukin-1β; Lane 2: AICAR; Lane 3: OA – Okadiac acid. C) Analysed results for p22phox. D) Analysed results for nitrotyrosine. * $p<0.05$ vs Control; # $p<0.05$ vs 1h Feno. Cntr: Control; Feno: Fenofibrate. n=3-7*

3.4.13.5 IκBα and Cleaved Caspase-3

Decreased total expression of IκBα is associated with increased NF-κB activity (Hayden & Ghosh 2008). 1 hour fenofibrate treatment significantly increased IκBα expression compared to untreated controls (1h Control: 1; 1h Fenofibrate: 1.17 ± 0.05, $p<0.05$) (figure 3.39 C). 24 hour fenofibrate treatment did not change IκBα expression.

Cleaved caspase-3 is a down-stream target of caspase-8 and indicative of apoptosis (Kuribayashi *et al*. 2006). Fenofibrate did not change cleaved caspase-3 levels after 1 hour or 24 hours compared to time-matched untreated controls (figure 3.39 D). However, the 24 hour untreated control group expressed significantly less cleaved caspase-3 compared to 1 hour untreated control group (1h Control: 1; 24h Control: 0.61 ± 0.16, $p<0.05$) (figure 3.39 D).

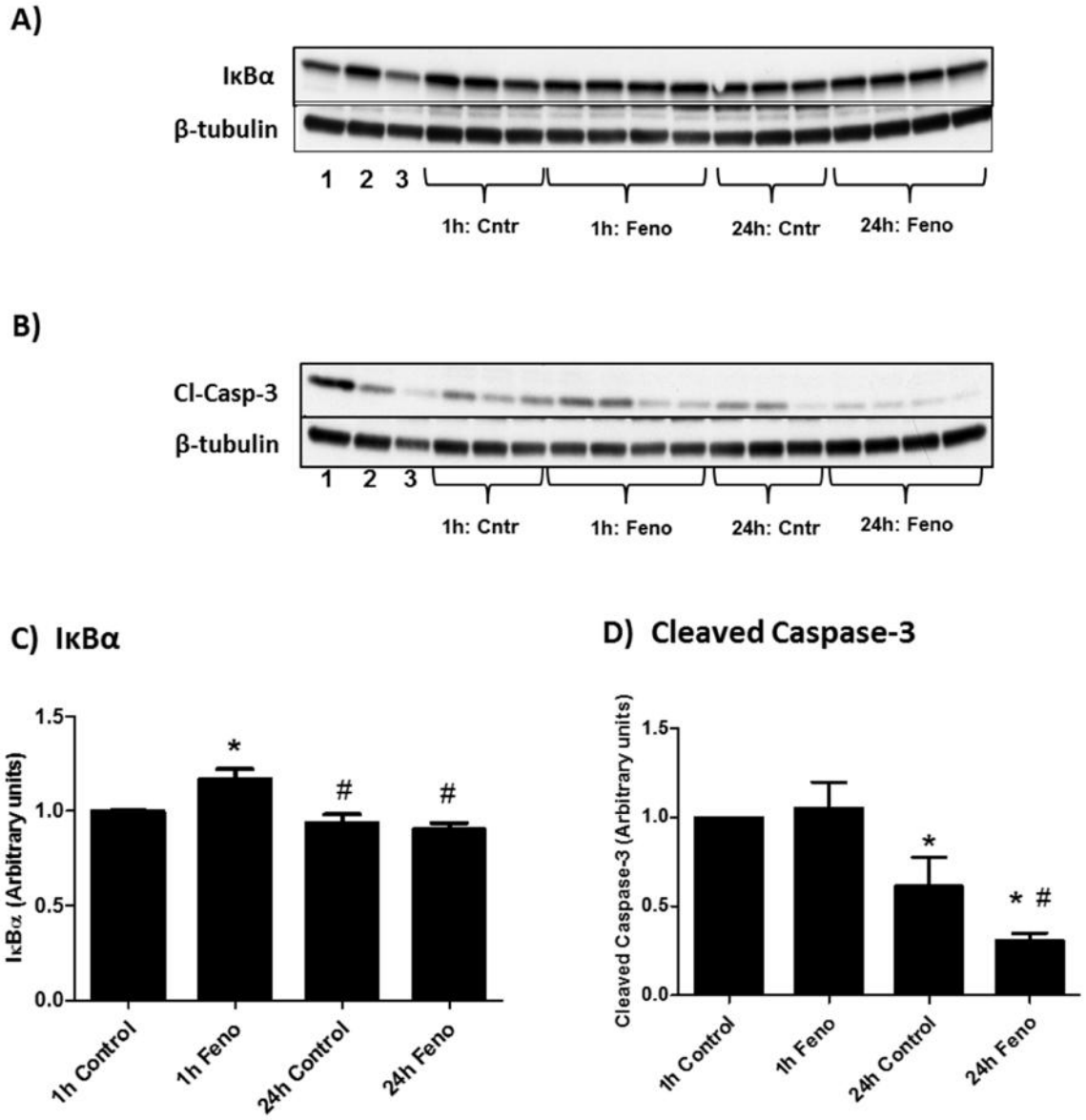

*Figure 3.39: Bar charts indicating changes in IκBα and cleaved Caspase-3 expression of CMECs treated with fenofibrate (50 µM) for 1 and 24 hours. A) Western blots showing total IκBα and β-tubulin expression; Lane 1: Interleukin-1β; Lane 2: AICAR; Lane 3: OA – Okadiac acid. B) Western blots indicating cleaved Caspase-3 and β-tubulin expression. Lane 1: Interleukin-1β; Lane 2: AICAR; Lane 3: OA – Okadiac acid. C) Analysed results for IκBα. D) Analysed results for cleaved Caspase-3. * p<0.05 vs Control; # p<0.05 vs 1h Feno. Cntr: Control; Feno: Fenofibrate. n=3-4*

3.4.14 Results: 5 min, 15 min and 30 min fenofibrate western blot analyses

In view of the fact that the findings of 1 and 24 hour fenofibrate treatment experiments were inconclusive with regards to which of the NOS isoforms were responsible for the increased NO production, we had to consider the possibility that enzyme activation could be a much earlier event. We therefore proceeded with experiments in which the fenofibrate treatment times were shortened.

3.4.14.1 NOS

Western blot analyses were performed on CMECs treated with fenofibrate for 5 min, 15 min and 30 min. Data showed that no changes occurred with respect to total eNOS expression at any of the time points (figure 3.40 B). 5 min fenofibrate treatment significantly reduced phosphorylation at Ser 1177 (Control: 1; 5 min: 0.86 ± 0.02, $p<0.05$) (figure 3.40 C) and the P/T ratio of eNOS Ser 1177 was also significantly reduced (Control: 1; 5 min: 0.80 ± 0.06, $p<0.05$) (figure 3.40 D). The inhibitory eNOS site, Thr 495 showed no changes in phosphorylation or P/T ratio at any of the time points (figure 3.41 B – D). With regards to nNOS, no changes in total nNOS expression were observed (figure 3.42 B). A significant decrease in nNOS phosphorylation (Ser 1417) occurred after 30 min of fenofibrate treatment (Control: 1; 30 min: 0.77 ± 0.18, $p<0.05$) (figure 3.42 C), however the P/T ratio of nNOS was only significantly reduced at the 5 min fenofibrate treatment time point (Control: 1; 5 min: 0.65 ± 0.11, $p<0.05$) (figure 3.42 D).

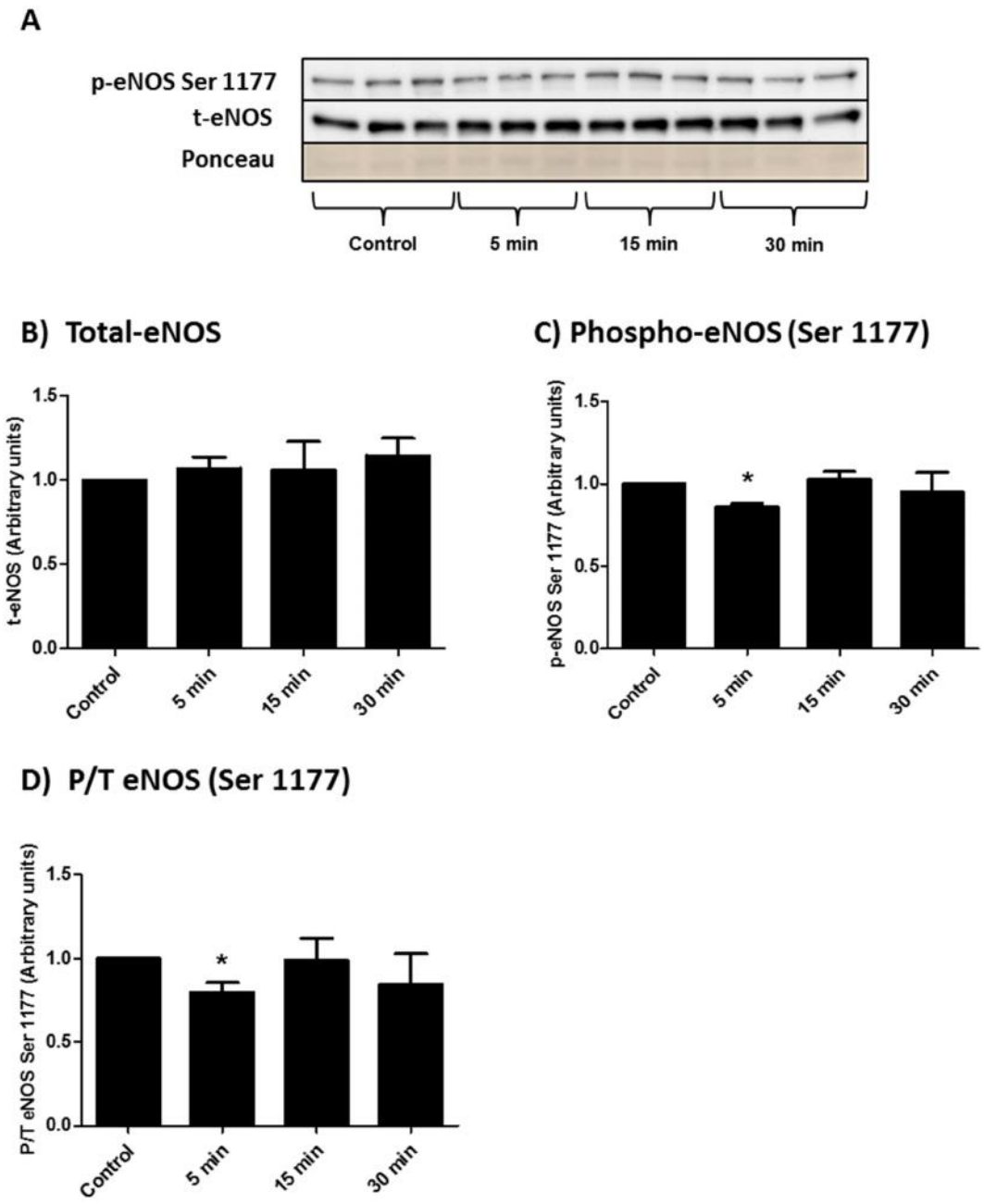

*Figure 3.40: Bar charts indicating changes in total and phosphorylated eNOS (Ser 1177) of CMECs treated with fenofibrate (50 µM) for for 5 min, 15 min and 30 min. A) Western blots showing total eNOS, phospho-eNOS (Ser 1177) and total protein loaded (ponceau stain). B) Analysed results for total-eNOS. C) Analysed results for phospho-eNOS (Ser 1177). D) Phosphorylated over total (P/T) ratio of eNOS (Ser 1177). * p<0.05 vs Control; n=3.*

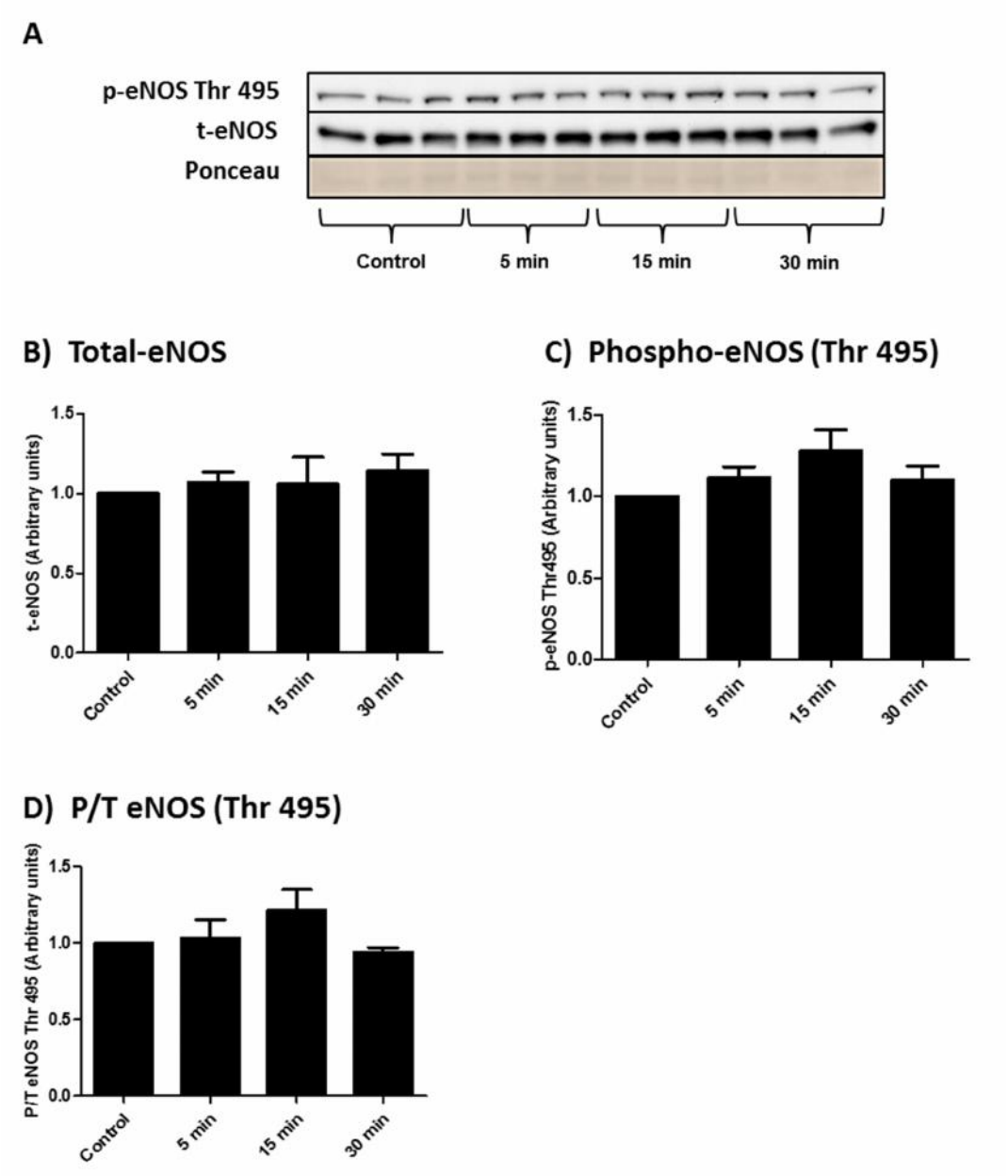

Figure 3.41: Bar charts indicating changes in total and phosphorylated eNOS (Thr 495) of CMECs treated with fenofibrate (50 µM) for for 5 min, 15 min and 30 min. A) Western blots showing total eNOS, phospho-eNOS (Thr 495) and total protein loaded (ponceau stain). B) Analysed results for total-eNOS. C) Analysed results for phospho-eNOS (Thr 495). D) Phosphorylated over total (P/T) ratio of eNOS (Thr 495). n=3.

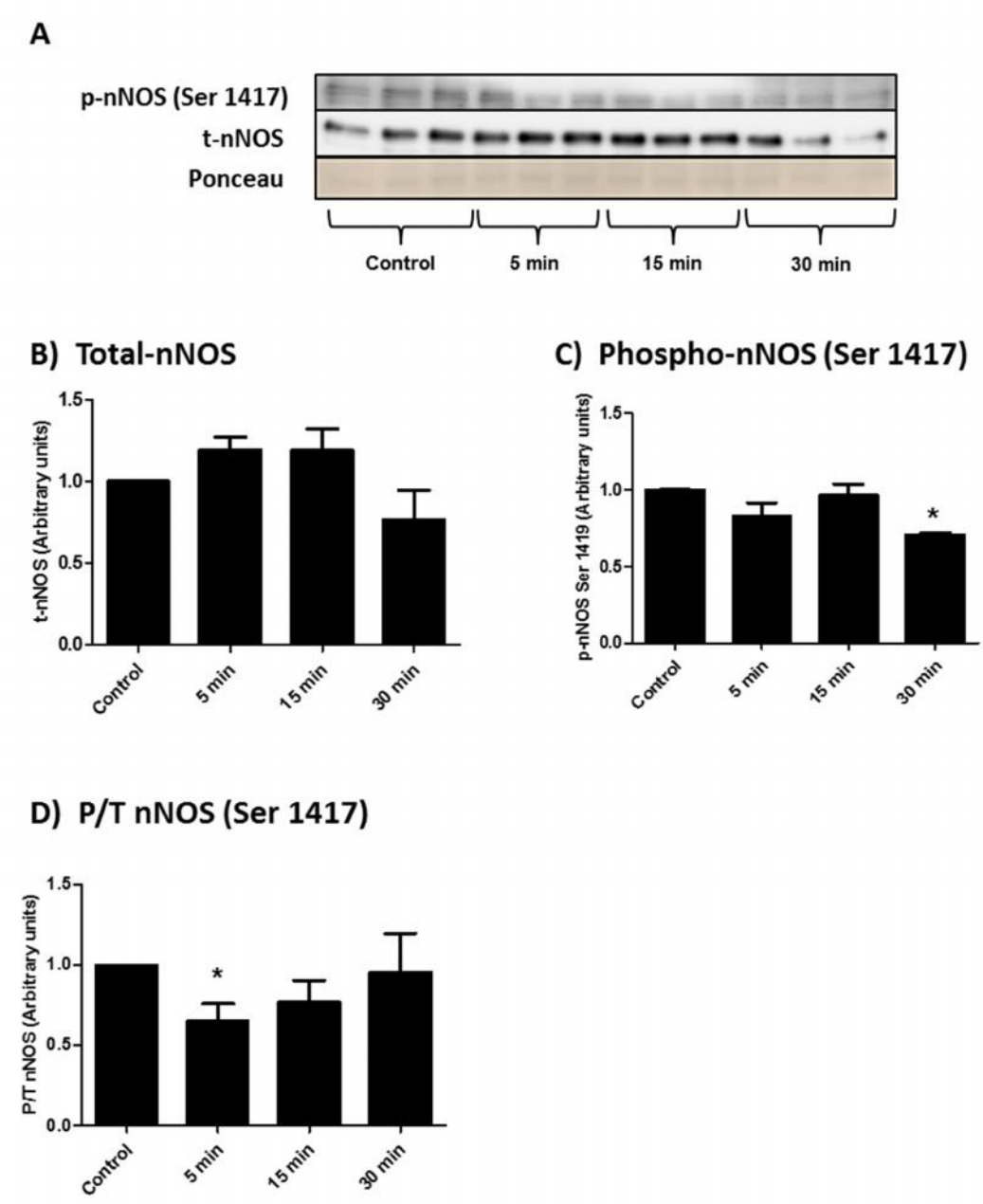

*Figure 3.42: Bar charts indicating changes in total and phosphorylated nNOS (Ser 1417) of CMECs treated with fenofibrate (50 µM) for for 5 min, 15 min and 30 min. A) Western blots showing total nNOS, phospho-nNOS (Ser 1417) and total protein loaded (ponceau stain). B) Analysed results for total-nNOS. C) Analysed results for phospho-nNOS (Ser 1419). D) Phosphorylated over total (P/T) ratio of nNOS (Ser 1419). * p<0.05 vs Control; n=3.*

3.4.14.2 AMPK

At 30 min fenofibrate treatment, total AMPK expression levels increased significantly (Control: 1; 30 min: 1.28 ± 0.01, $p<0.05$) (figure 3.43 B). However, 5 and 15 min of fenofibrate treatment resulted in significantly decreased AMPK phosphorylation (Thr 172) compared to the untreated control group (Control: 1; 5 min: 0.79 ± 0.05*; 15 min: 0.70 ± 0.08*, *$p<0.05$ vs Control) (figure 3.43 C). The P/T AMPK ratios were significantly lower at all three time points (Control: 1; 5 min: 0.67 ± 0.06*; 15 min: 0.66 ± 0.07*; 30 min: 0.65 ± 0.10*, *$p<0.05$ vs Control) (figure 3.43 D).

3.4.14.3 PKB/Akt

A significant increase in total PKB/Akt expression was observed at 30 min fenofibrate treatment (Control: 1; 30 min: 1.26 ± 0.06, $p<0.05$) (figure 3.44 B). Phosphorylated PKB/Akt (Ser 473) could not be detected.

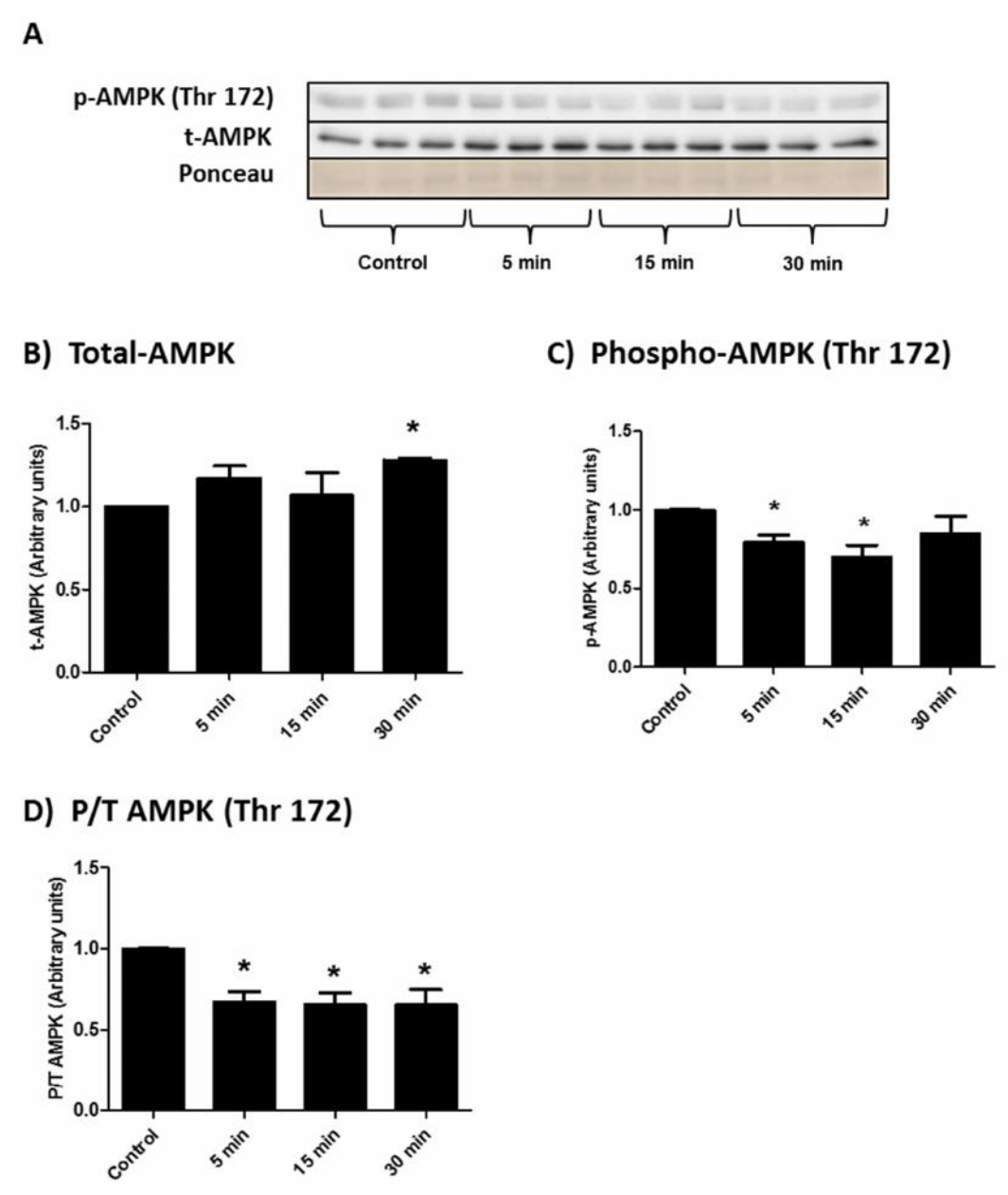

*Figure 3.43: Bar charts indicating changes in total and phosphorylated AMPK (Thr 172) of CMECs treated with fenofibrate (50 µM) for for 5 min, 15 min and 30 min. A) Western blots showing total-AMPK, phospho-AMPK (Thr 172) and total protein loaded (ponceau stain). B) Analysed results for total-AMPK. C) Analysed results for phospho-AMPK (Thr 172). D) Phosphorylated over total (P/T) ratio of AMPK (Thr 172). * p<0.05 vs Control; n=3.*

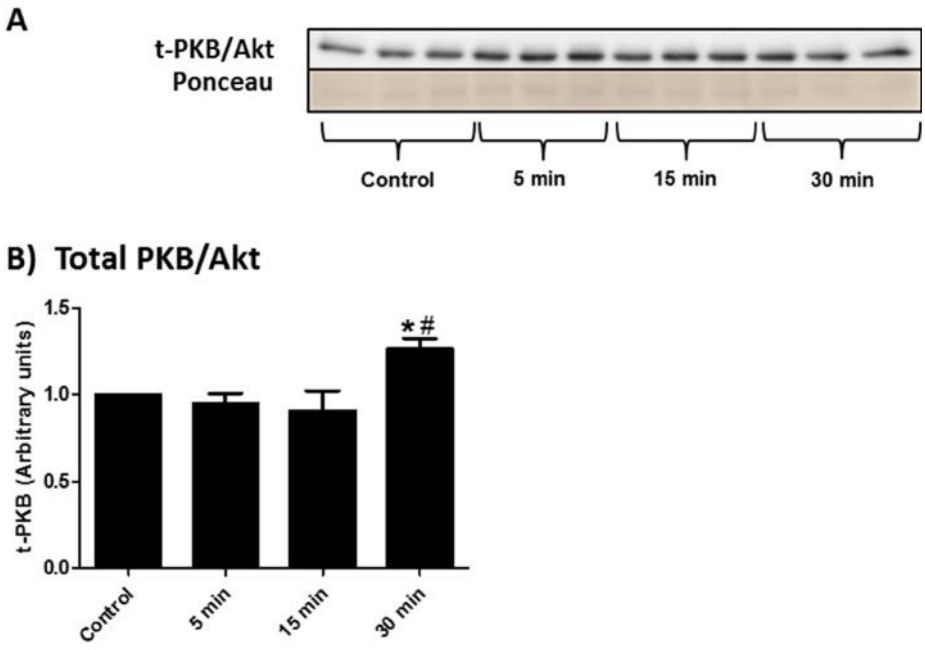

*Figure 3.44: Bar charts indicating changes in total and phosphorylated PKB/Akt (Ser 473) of CMECs treated with fenofibrate (50 µM) for for 5 min, 15 min and 30 min. A) Western blots showing total-PKB/Akt and total protein loaded (ponceau stain). Phospho-PKB/Akt could not be detected. B) Analysed results for total-PKB/Akt. * $p<0.05$ vs Control; $^{\#}p<0.05$ vs 5 min, n=3.*

3.4.15 Experimental protocol: Pretreatment with fenofibrate prior to TNF-α administration

In the next set of experiments, it was investigated whether pretreatment of CMECs with fenofibrate could protect the cells against the harmful effects of tumour necrosis factor alpha (TNF-α). TNF-α is one of the most common pro-inflammatory cytokines in the body, known to be a mediator of vascular/endothelial injury in disease conditions such as diabetes mellitus and obesity *(Picchi et al.,* 2006). CMECs were pretreated with 50 µM fenofibrate for 1 hour prior to administration of 20 ng/ml TNF-α for a further 24 hours (figure 3.45).

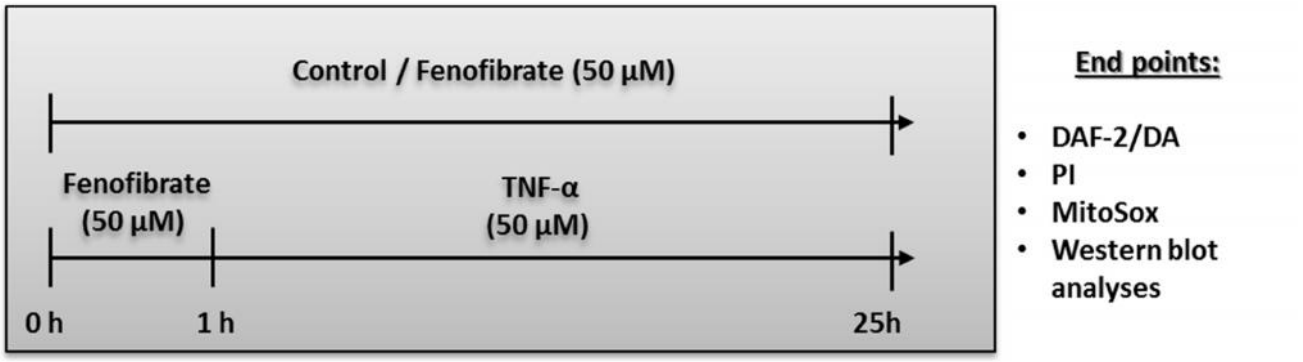

Figure 3.45: Experimental protocol followed to investigate the effects of fenofibrate pretreatment on TNF-α-treated CMECs. CMECs were pretreated with 50 µM fenofibrate for 1 hour prior to administration of 20 ng/ml TNF-α for a further 24 hours. End points included NO, necrosis and ROS production measurements by flow cytometric analysis of DAF-2/DA, PI and MitoSox fluorescence respectively. The expression and activation of important signalling proteins were measured by western blot analyses.

3.4.16 Results: Pretreatment with fenofibrate prior to TNF-α administration

3.4.16.1 NO measurements

Pretreatment of control CMECs (in the absence of TNF-α) with 50 µM fenofibrate (total treatment time: 25 hours) significantly increased DAF-2/DA fluorescence by ≈ 2.4-fold (Control: 100%; Fenofibrate: 235.7 ± 41.7%, $p<0.05$) (figure 3.46). CMECs treated with TNF-α only showed no change in DAF-2/DA fluorescence compared to untreated controls. Pretreatment of CMECs with TNF-α+fenofibrate significantly increased the fluorescence to the same extent as observed with fenofibrate treatment only (Control: 100%; TNF-α: 103.5 ± 14.73%; Fenofibrate + TNF-α: 219.2 ± 45.05%*#, * $p<0.05$ vs Control, # $p<0.05$ vs TNF-α) (figure 3.46).

3.4.16.2 MitoSox fluorescence

TNF-α had a robust increasing effect on mitochondrial ROS production (measured by MitoSox) (Control: 100%; TNF-α: 253.3 ± 59.6%; $p<0.05$) (figure 3.47). Even though large trends can be observed within the other groups, values did not reach significance.

3.4.16.3 Cell viability (necrosis): PI fluorescence

TNF-α increased PI fluorescence significantly compared to vehicle, fenofibrate and fenofibrate + TNF-α groups, and pretreatment with fenofibrate was able to prevent TNF- α induced necrosis (Fenofibrate vehicle: 58.6 ± 9.5%; Fenofibrate: 72 ± 4.8%; TNF-α: 127.4 ± 15.6%*#$^; Fenofibrate + TNF-α: 78.9 ± 5.8%; * $p<0.05$ vs Control; # $p<0.05$ vs Vehicle; $ $p<0.05$ vs Feno; @ $p<0.05$ vs TNF-α; ^ $p<0.05$ vs Feno + TNF-α) (figure 3.48).

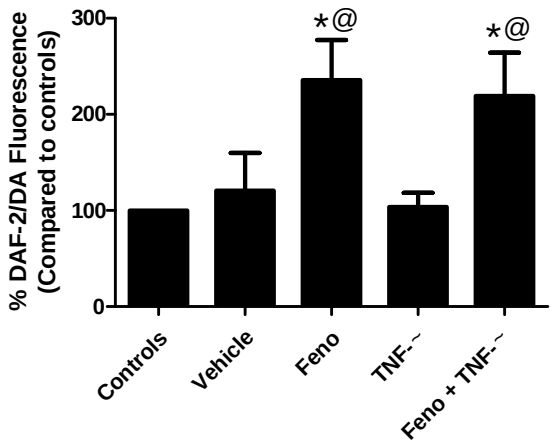

*Figure 3.46: Bar chart indicating DAF-2/DA fluorescence of CMECs pretreated with 50 µM fenofibrate for 1 hour prior to 20 ng/ml TNF-α for 24 hours. DAF-2/DA fluorescence significantly increased in response to fenofibrate treatment. In combination with TNF-α, fenofibrate still resulted in elevated DAF-2/DA levels. * p<0.05 vs Control; @ p<0.05 vs TNF-α. Vehicle: DMSO (for fenofibrate); Feno: Fenofibrate; TNF-α: Tumor necrosis factor α, n = 4 – 11.*

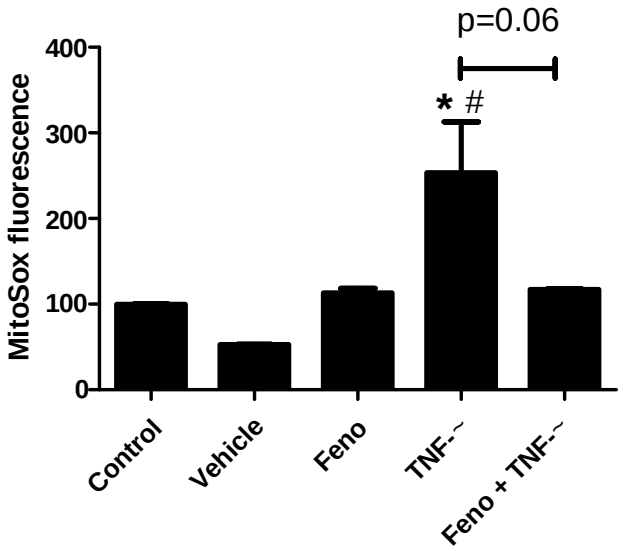

*Figure 3.47: Bar chart indicating MitoSox fluorescence of CMECs pretreated with 50 µM fenofibrate for 1 hour prior to 20 ng/ml TNF-α for 24 hours. TNF- α significantly increased MitoSox fluorescence compared to untreated control. Pretreatment with fenofibrate reduced MitoSox fluorescence back to control levels; the p-value of 0.06 was borderline significant. * p<0.05 vs Control; # p<0.05 vs (Fenofibrate) Vehicle, n = 3-4.*

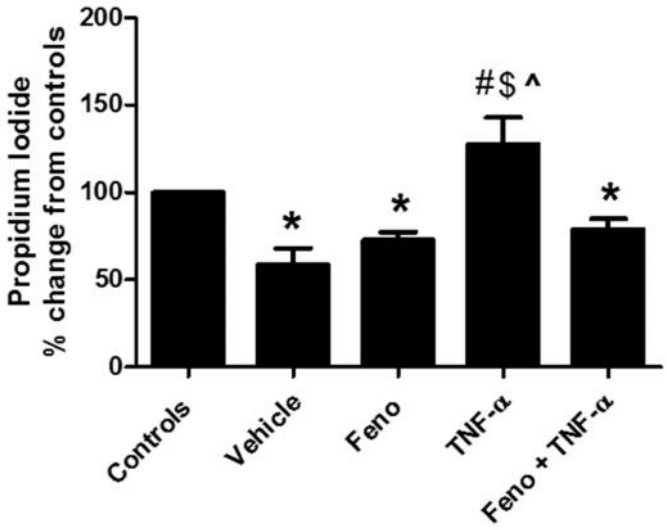

*Figure 3.48: Bar chart indicating changes in necrosis of CMECs pretreated with 50 µM fenofibrate for 1 hour prior to 20 ng/ml TNF-α for 24 hours. Graph illustrates % change in Propidium Iodide fluorescence compared to controls expressed as 100%. * p<0.05 vs Control; # p<0.05 vs Vehicle; $ p<0.05 vs Feno; @ p<0.05 vs TNF-α; ^ p<0.05 vs Feno + TNF-α; n = 9-15.*

3.4.16.4 Western blot analyses

NOS

Total eNOS expression remained at control levels in the fenofibrate only treated group, but was significantly reduced in the TNF-α-treated (with and without fenofibrate pretreatment) CMECs (Control: 1; TNF-α: 0.56 ± 0.02; Fenofibrate + TNF-α: 0.73 ± 0.05, $p<0.05$) (figure 3.49 B). Phosphorylated eNOS Ser 1177 levels were unchanged in all groups, except for a significant increase in the fenofibrate pretreatment + TNF-α group compared to TNF-α only group (TNF-α: 0.70 ± 0.08; Fenofibrate + TNF-α: 1.04 ± 0.06, $p<0.05$) (figure 3.49 C). This resulted in a significantly increased P/T eNOS (Ser 1177) ratio in the fenofibrate pretreatment + TNF-α group (Control: 1; Fenofibrate + TNF-α: 1.41 ± 0.10, $p<0.05$) (figure 3.49 D).

AMPK and PKB/Akt

The total protein expression of two upstream NOS activators, AMPK and PKB/Akt were unaffected by any of the treatments (figure 3.50 B and 3.51 B). Fenofibrate pretreatment did, however, result in a significant increase in AMPK phosphorylation compared to the TNF-α group without pretreatment (TNF-α: 0.76 ± 0.09; Fenofibrate + TNF-α: 1.14 ± 0.07, $p<0.05$) (figure 3.50 C).

IκBα

As expected, TNF-α robustly decreased total-IκBα expression, and fenofibrate pretreatment failed to change this (Control: 1; Vehicle: 1.08 ± 0.16; Fenofibrate: 1.12 ± 0.06; TNF- α: 0.64 ± 0.03$^{*\#\$}$; Fenofibrate + TNF-α: 0.51 ± 0.03$^{*\#\$}$, * $p<0.05$ vs Control; # $p<0.05$ vs Vehicle; $ $p<0.05$ vs Feno) (figure 3.52 B).

Cleaved PARP (poly ADP ribose polymerase) and Caspase-3

Both cleaved PARP and caspase-3 are indicators of apoptosis. Both the TNF-α only and fenofibrate pretreatment + TNF-α groups showed a pronounced up-regulation of PARP and cleaved caspase-3. Fenofibrate treatment resulted in a significant reduction in the expression of cleaved PARP and caspase-3 compared to TNF-α. The results were as follows: **PARP:** Control: 1; Vehicle: 0.79 ± 0.14; Fenofibrate: 0.76 ± 0.06; TNF- α: 1.65 ± 0.08$^{*\#\$}$; Fenofibrate + TNF-α:

1.28 ± 0.04*#$, and **Caspase-3:** Control: 1; Vehicle: 0.94 ± 0.17; Fenofibrate: 0.98 ± 0.11; TNF-α: 2.62 ± 0.22*#$; Fenofibrate + TNF-α: 1.60 ± 0.08*#$; * p<0.05 vs Control; # p<0.05 vs Vehicle; $ p<0.05 vs Fenofibrate (figure 3.53 B and C).

Nitrotyrosine and p22Phox

None of the treatments altered nitrotyrosine levels (figure 3.54 B). However, p22Phox expression was significantly reduced in the fenofibrate pretreatment + TNF-α group compared to the TNF-α only group (TNF-α: 1.59 ± 0.15; Fenofibrate + TNF-α: 0.78 ± 0.11; ^ p<0.05 vs fenofibrate + TNF-α) (figure 3.54 C).

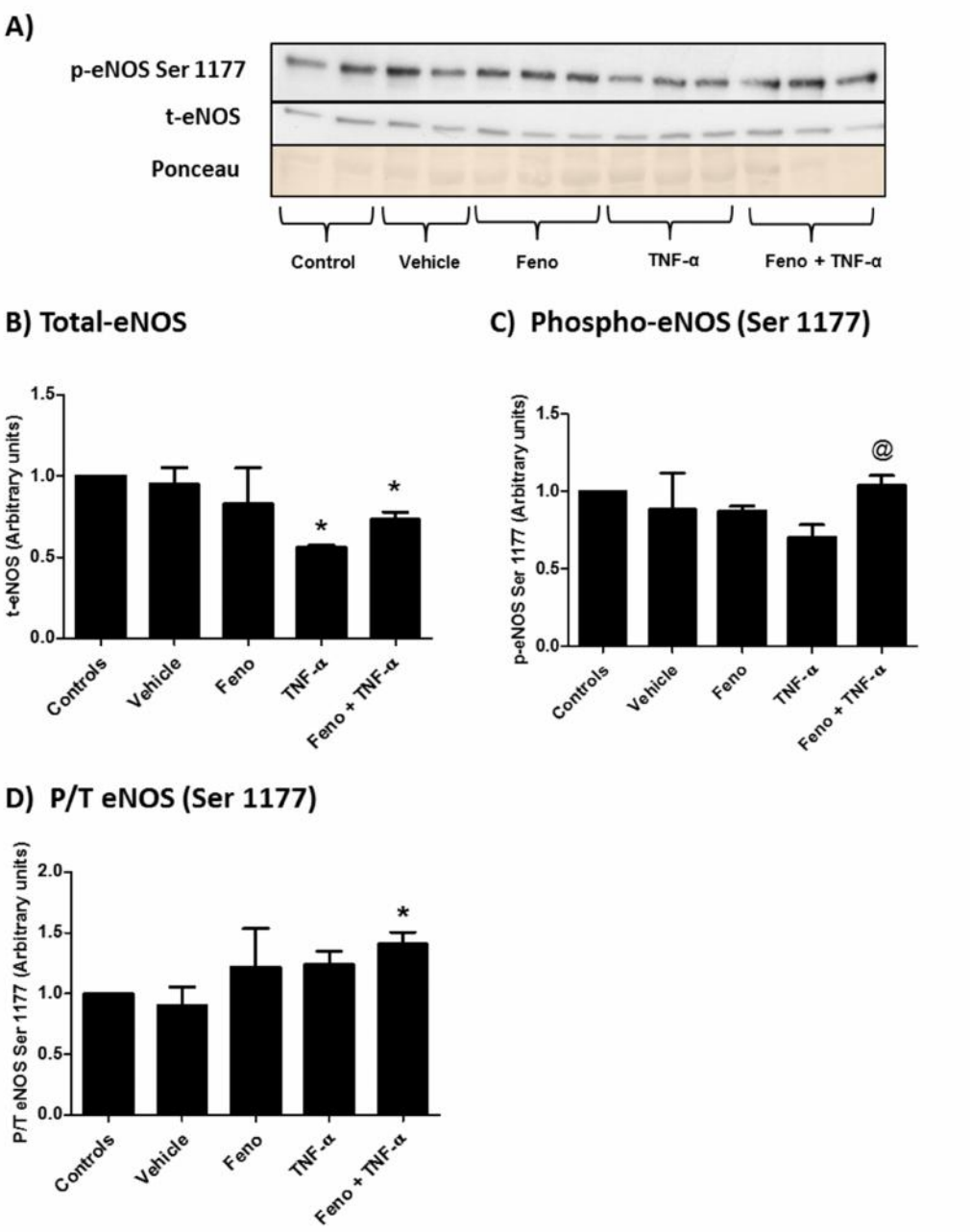

*Figure 3.49: Bar charts indicating changes in eNOS expression and phosphorylation (Ser 1177) of CMECs pretreated with 50 µM fenofibrate for 1 hour prior to 24 hour administration of 20 ng/ml TNF-α. A) Western blots showing total-eNOS, phospho-eNOS (Ser 1177) and total protein loaded (ponseau stain). B) Analysed results for total-eNOS. C) Analysed results for phospho-eNOS (Ser 1177). D) Phosphorylated over total (P/T) ratio of eNOS (Ser 1177). * $p<0.05$ vs Control, $^{@}$ $p<0.05$ vs TNF-α; n=3.*

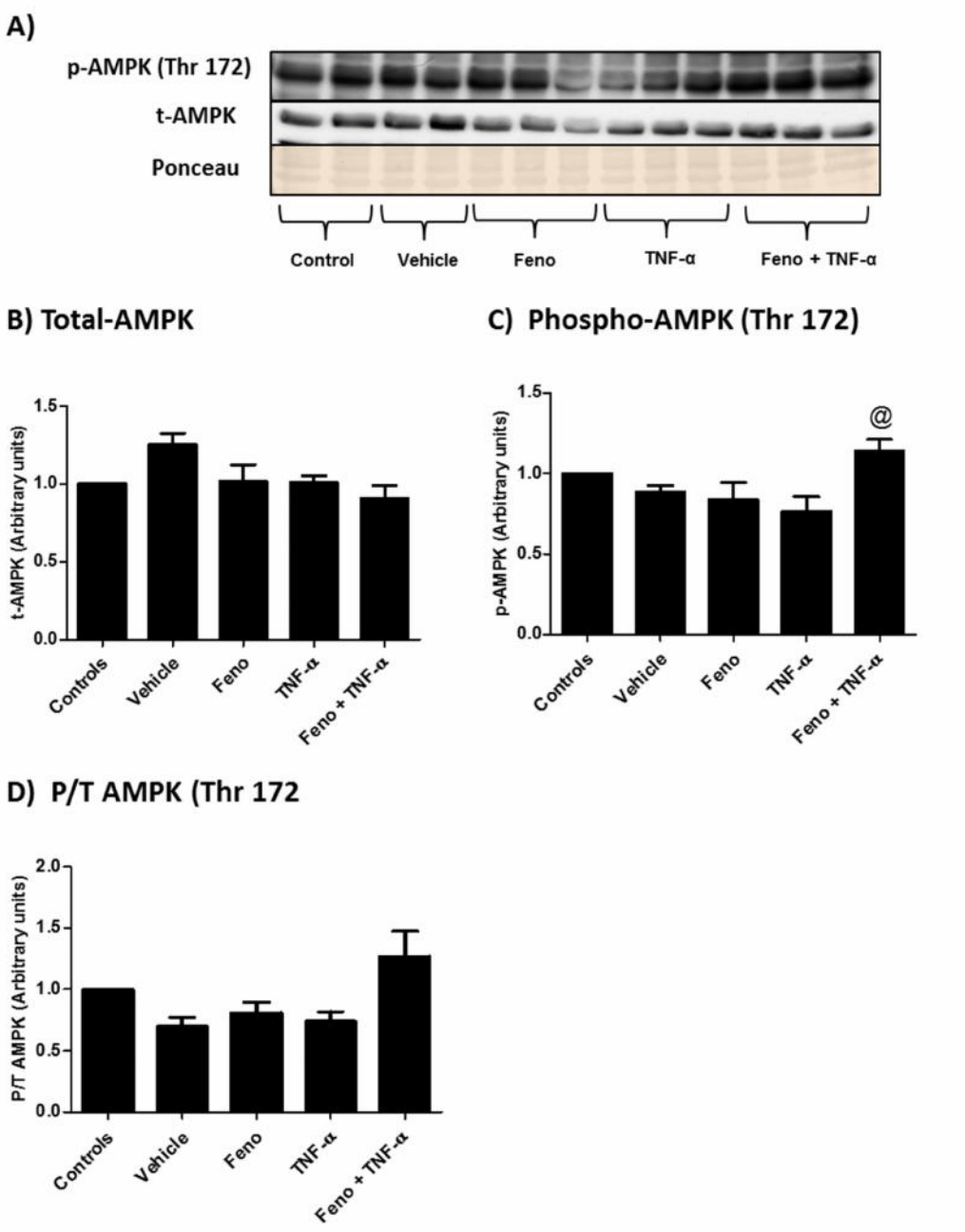

Figure 3.50: Bar charts indicating changes in AMPK expression and phosphorylation (Thr 172) of CMECs pretreated with 50 µM fenofibrate for 1 hour prior to 24 hour administration of 20 ng/ml TNF-α. A) Western blots showing total-AMPK, phospho-AMPK (Thr 172) and total protein loaded (ponseau stain). B) Analysed results for total-AMPK. C) Analysed results for phospho-AMPK (Thr 172). D) Phosphorylated over total (P/T) ratio of AMPK (Thr 172). @ p<0.05 vs TNF-α; n=3

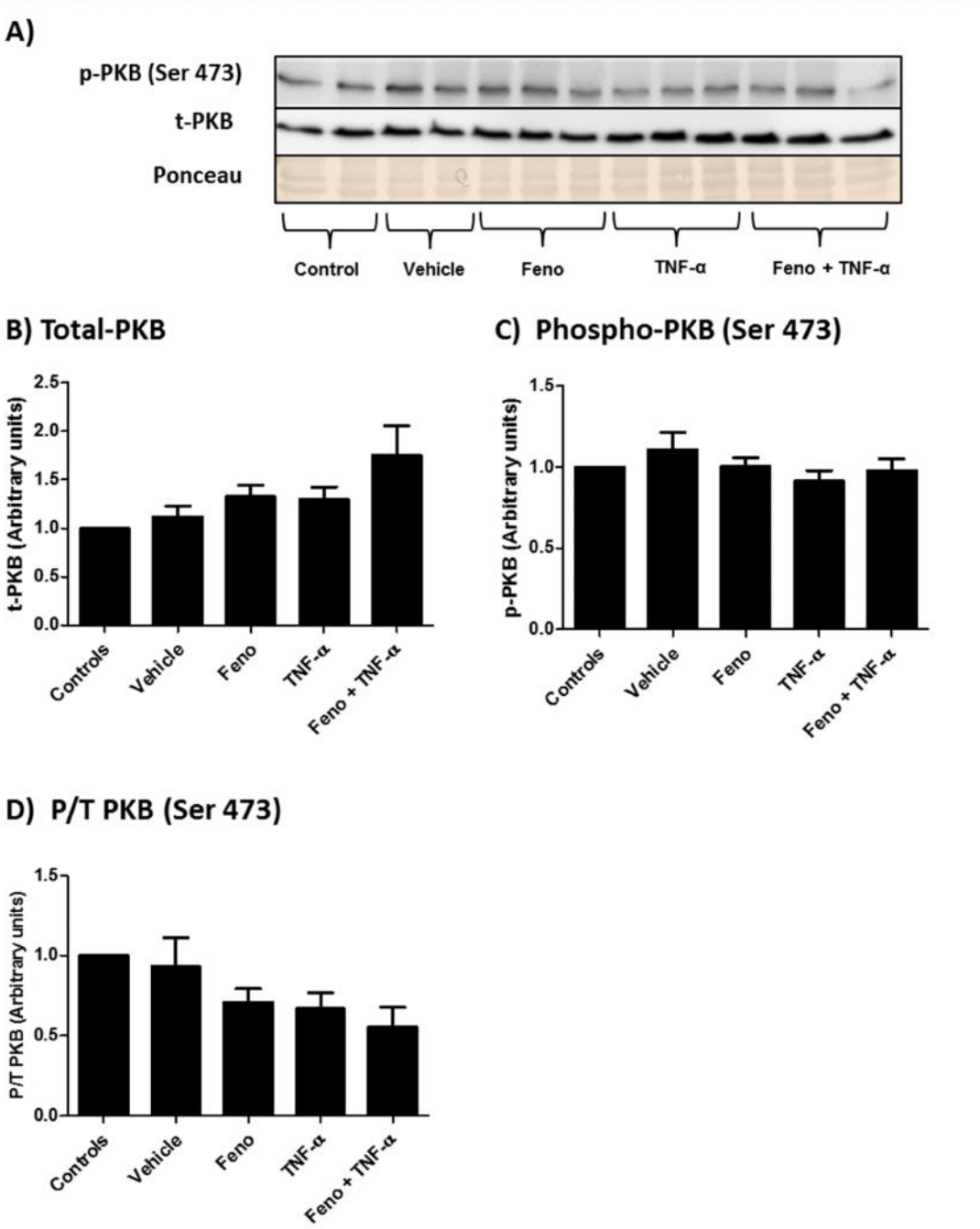

Figure 3.51: Bar charts indicating changes in PKB/Akt expression and phosphorylation (Ser 473) of CMECs pretreated with 50 µM fenofibrate for 1 hour prior to 24 hour administration of 20 ng/ml TNF-α. A) Western blots showing total-PKB/Akt, phospho- PKB/Akt (Ser 473) and total protein loaded (ponseau stain). B) Analysed results for total- PKB/Akt. C) Analysed results for phospho- PKB/Akt (Ser 473). D) Phosphorylated over total (P/T) ratio of PKB/Akt (Ser 473); n=3

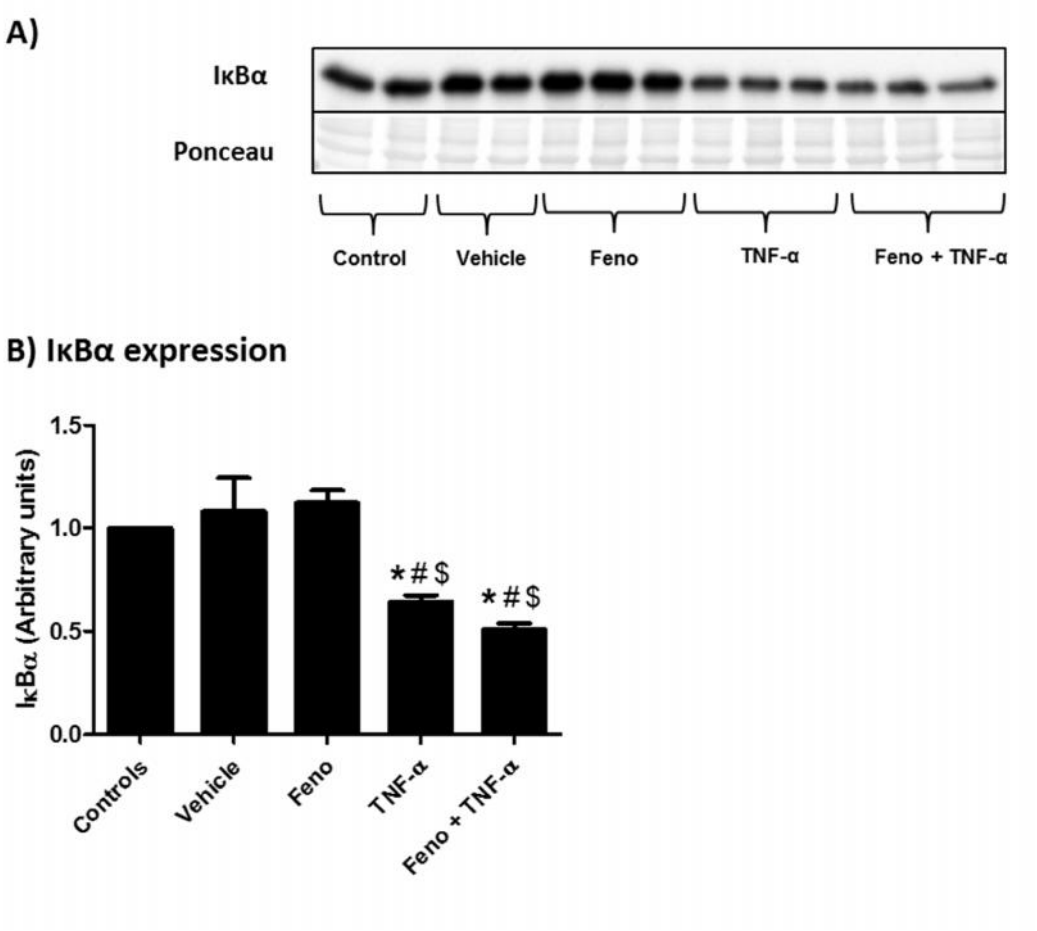

*Figure 3.52: Bar chart indicating changes in IκBα expression of CMECs pretreated with 50 µM fenofibrate for 1 hour prior to 24 hour administration of 20 ng/ml TNF-α. A) Western blots showing total-IκBα and total protein loaded (ponseau stain). B) Analysed results for total-IκBα. * p<0.05 vs Control; # p<0.05 vs Vehicle; $ p<0.05 vs Feno; n=3*

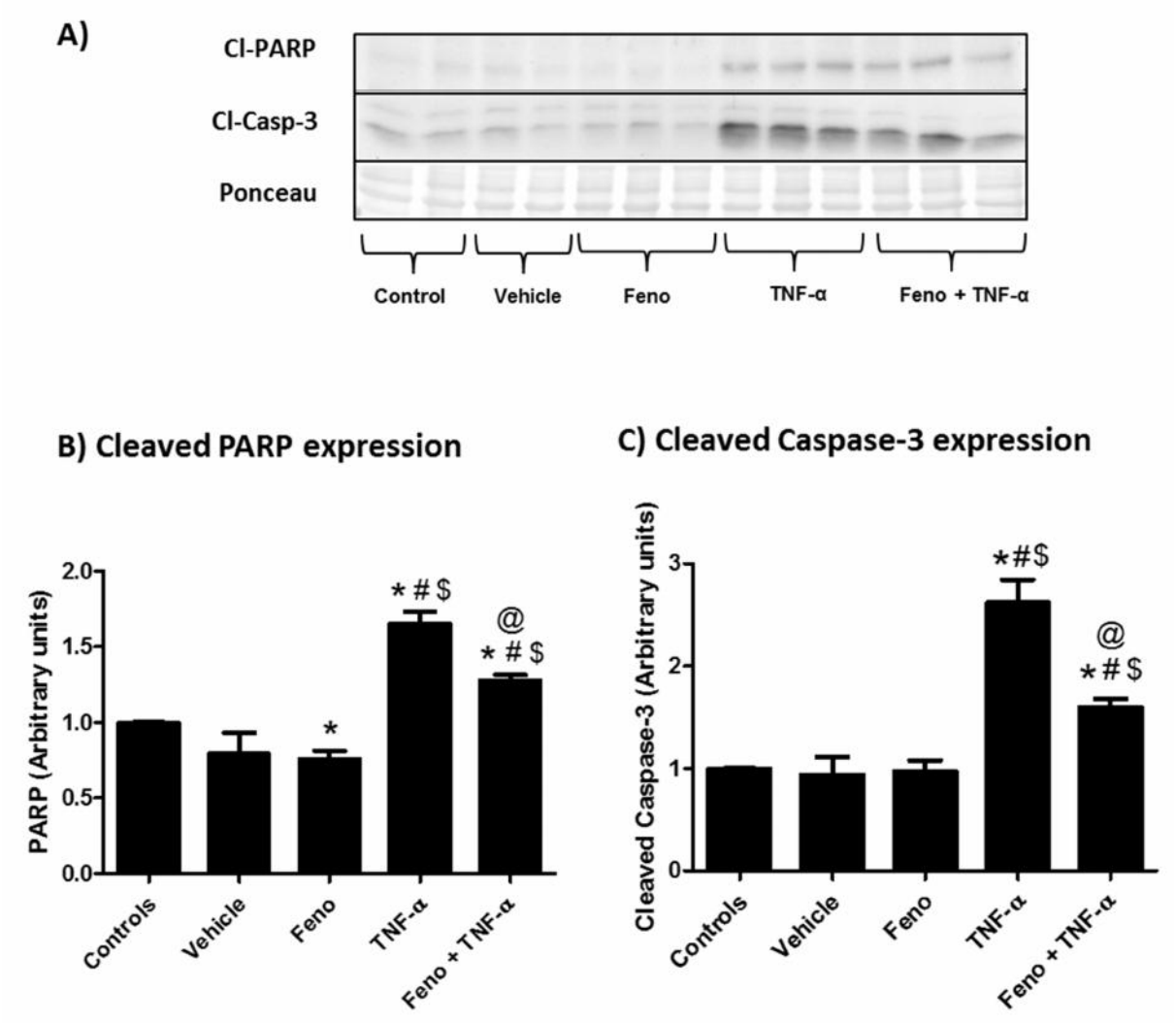

*Figure 3.53: Bar charts indicating changes in PARP and Caspase-3 expression of CMECs pretreated with 50 µM fenofibrate for 1 hour prior to 24 hour administration of 20 ng/ml TNF-α. A) Western blots showing cleaved PARP, cleaved Caspase-3 and total protein loaded (ponseau stain). B) Analysed results for cleaved-PARP. C) Analysed results for cleaved-Caspase-3. * p<0.05 vs Control; # p<0.05 vs Vehicle; $ p<0.05 vs Feno; @ p<0.05 vs TNF-α; n=3.*

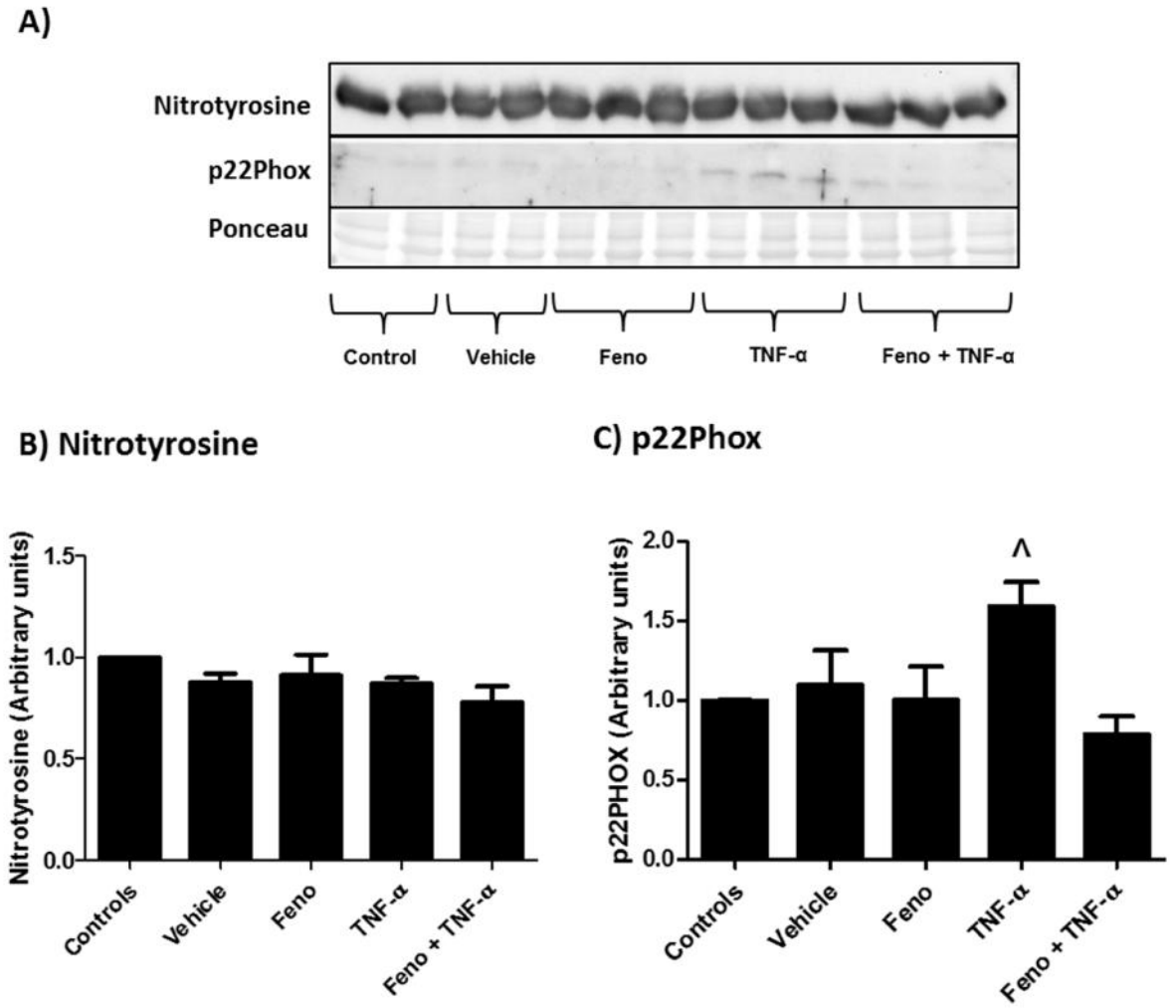

Figure 3.54: Bar charts indicating changes in nitrotyrosine and p22Phox expression of CMECs pretreated with 50 µM fenofibrate for 1 hour prior to 24 hour administration of 20 ng/ml TNF-α. A) Western blots showing nitrotyrosine, p22Phox and total protein loaded (ponceau stain). B) Analysed results for Nitrotyrosine. C) Analysed results for p22Phox. ^ $p<0.05$ vs Feno + TNF-α; n=3.

3.5 Discussion: *In vitro* findings of Fenofibrate

3.5.1 Intracellular NO production

In contrast to simvastatin, fenofibrate exerted pronounced increasing effects on NO production, especially at shorter treatment periods (1 hour and 4 hours). Based on the concentration and time response investigations, it was decided to continue with a concentration of 50 µM fenofibrate in further studies. This concentration falls well within ranges used in other *in vitro* experiments (Goya *et al*., 2004; Murakami *et al*., 2006) and compares well to the plasma concentrations achieved with 200 mg/day oral treatment (Zanetti *et al*., 2008). This was also the dosage used in the so-called FIELD trial, which according to the authors, resulted in beneficial microvascular effects (Keech *et al*., 2007).

Increases in NO production have been shown in fenofibrate treated HUVECs for periods as short as 2.5 minutes (Murakami *et al.,* 2006). In our hands, increased levels of NO could be observed after 5 min treatment in CMECs (data not shown). A previous study showed that fenofibrate (100 µM) treatment of human glomerular microvascular endothelial cells (HGMECs) resulted in a substantial increase in NO after 1 hour, however the effects waned at longer time periods (Tomizawa *et al.,* 2011). In the current study, a fenofibrate concentration of 50 µM significantly increased NO levels at 24 hours, but the response was not as robust as observed at 1 and 4 hours. These findings are in agreement with those observed by Tomizawa *et al.* (2011). Yang *et al*., (2005) could not demonstrate an increase in NO production in HUVECs treated with 30 µM fenofibrate for 24 hours. Goya *et al*., (2004) did not measure NO directly. They performed an eNOS activity assay (conversion of radiolabeled L-arginine to L-citrulline) and could not demonstrate increases in enzyme activity at 2 min, 5 min or 1 hour fenofibrate treatment. However, eNOS activity was increased at 24 - 48 hour fenofibrate (10 and 50 µM) treatment, therefore the current study contradicts the results of Goya *et al*. (2004). An interesting observation is that studies using short fenofibrate treatment periods resulted in profound NO increases of double the control values (Murakami *et al*., 2006; Tomizawa *et al*., 2011).

3.5.2 NOS inhibition investigations

Most of the *in vitro* studies that investigated the role of NOS, concluded that the fenofibrate-induced NO increases were mediated by eNOS (Goya *et al*., 2004; Murakami *et al*., 2006; Katayama *et al*., 2009; Tomizawa *et al*., 2011) Therefore, in order to confirm whether the fenofibrate-derived NO production observed after 1 hour treatment was due to eNOS we employed the use of L-NMMA. Although L-NMMA is relatively non-selective with regards to its NOS isoform specificity, many researchers use L-NMMA as a tool to investigate the contribution of the eNOS isoform (Tejedo *et al*., 2010). In our hands, inhibition studies with L-NMMA unexpectedly showed that NO production remained elevated at levels comparable with fenofibrate alone (figure 3.24 A), suggesting that NO was unlikely to be eNOS-derived. In an attempt to confirm the findings of the above experiments, we repeated the experiments by using a different NO measurement assay (Griess method) in CMECs, and a different, unrelated endothelial cell type, namely aortic endothelial cells (AECs). The data obtained from the Griess assay mirrored those of the DAF-2/DA fluorescence studies. Our NOS inhibition data are in contrast to those from a study by Murakami *et al.* (2006) who showed in HUVECs that fenofibrate-induced NO production was abolished in the presence of the NOS-inhibitor, N_{ω}-nitro-L-arginine methyl ester (L-NAME). In another *in vitro* study on HGMECs, eNOS was implicated indirectly as source of fenofibrate-induced NO by pharmacological inhibition of AMPK, one of the major upstream activators of eNOS (Tomizawa *et al*., 2011). A summary of previous fenofibrate treatment studies and their observations regarding NOS-NO biosynthesis appear in Table 1.2 (Chapter 1).

Pharmacological inhibition in experimental preparations does have shortcomings. It is often dose and time-dependent, in addition to almost never being 100% specific and often leads to other undesired and/or unknown biological effects unrelated to their intended application. In our hands, the L-NMMA experiments were unable to demonstrate contributions by NOS / eNOS to the fenofibrate-induced NO production. In view of this, comprehensive studies were conducted to investigate the expression and activation patterns of the NOS isoforms, and other related signalling proteins by means of western blotting.

3.5.3 NOS signalling pathway – Western blot results

eNOS Ser 1177 related pathways

Total eNOS expression was not altered by 1 or 24 hours fenofibrate treatment. These findings are in agreement with other studies, such as those by Murakami *et al*. (2006) in HUVECs, as well as Katayama *et al*. (2009) and Deplanque *et al.*, (2003) in aortic tissue. On the other hand, Goya *et al*. (2004) showed a significant increase in eNOS expression in cultured BAECs at 12 hours of fenofibrate treatment, and the trends were sustained at 48 hours. There were some shortcomings in the study by Goya and co-workers, namely the fact that they did not measure NO production as an important end-point, nor did they investigate the activation of eNOS (phosphorylation of eNOS Ser 1177). The study, however, did measure eNOS activity with an assay which measures the conversion of radiolabeled L-arginine to L-citrulline, and results were unchanged at 1 hour treatment with 50 µM fenofibrate. However, eNOS activity was significantly increased at 24 and 48 hour treatment periods.

As mentioned previously, the phosphorylation dynamics of kinases are highly complex and phosphorylation can occur within very short time periods. This phenomenon poses a challenge to the researcher when planning experimental protocols, and finding the optimal time-points of tissue collection for measurements is often a chance of occurrence (and a costly exercise!). Since no increases in the activation of eNOS via phosphorylation (Ser 1177) were observed at the initial time-points of 1 or 24 hours, it was decided to repeat the experiments at shorter treatment periods. Once again, fenofibrate treatment could not be linked to increased phosphorylation of eNOS at Serine 1177 at any of the shorter treatment periods; in fact, 5 min fenofibrate treatment resulted in decreased phosphorylation along with a reduced P/T ratio (figure 3.40 C and D). These results confirmed that, in our hands, the fenofibrate-derived NO produced by the CMECs was not mediated by arguably the most important kinase-dependent activation mechanism of eNOS, namely phosphorylation at Ser 1177, at any of the time points investigated (5 min, 15 min, 30 min, 1 hour and 24 hours).

Phosphorylation of eNOS Ser 1177 depends on the nature of the stimulus. Phosphorylation of Ser 1177 by means of shear stress results in sustained NO production (Dimmeler *et al*., 1999),

whereas stimulation by bradykinin results in transient increases in NO synthesis. Furthermore, various kinases have been reported to phosphorylate eNOS at the Ser 1177 residue. These include PKB/Akt (Dimmeler *et al*., 1999; Strijdom *et al.,* 2009b), PKA (Boo *et al*., 2002), PKC (Michell *et al*., 2001; Wang *et al.,* 2010b), AMPK and CaMKII (Chen *et al.,* 1999). Fenofibrate has been associated with increased phosphorylation of PKB/Akt (Thr 308) in HGMECs (Tomizawa *et al*., 2011) and PKB/Akt (Ser 473) in hepatocytes (Huang *et al*., 2008) and AMPK (Thr 172) (Murakami *et al*., 2006; Kim *et al.,* 2007; Tomizawa *et al*., 2011; Omae *et al*., 2012). In the above studies, experimental models of macrovascular and non-cardiac microvascular endothelial cells, as well as vascular tissue such as aortas, were used. As far as we are aware, no previous studies have been conducted on CMECs in the context of fenofibrate and NOS/NO biosynthesis. In the current study, reduced phosphorylation of eNOS Ser 1177 (1 hour treatment) was associated with a reduction in phospho-AMPK and phospho-PKB/Akt (Ser 473). It can therefore be speculated that eNOS Ser 1177 was simply not phosphorylated due to a lack of phosphorylated upstream kinases. Another mechanism may be the dephosphorylation of eNOS via the actions of phosphatases. Considering the large decrease in phosphorylation observed at 1 hour fenofibrate treatment, the latter could be a plausible explanation. In the western blot experiments, okadaic acid was employed as a positive control for eNOS phosphorylation. CMECs were treated with 500 µM okadaic acid and a large increase in the phosphorylation of eNOS Ser 1177 was observed. The mentioned concentration of okadaic acid has been reported to inhibit protein phosphatase 1 (PP1), protein phosphatase 2 A (PP2A) and protein phosphatase 2 B (PP2B) (Honkanan *et al*. 1994). These phosphatases could therefore be involved with rapid dephosphorylation of eNOS (Ser 1177). In separate studies in our laboratory, proteomic analysis of baseline CMECs demonstrated a high abundance of protein phosphatase 1F (2-fold higher expression in CMECs vs AECs), a known inhibitor of CAMK-II, which is one of the major upstream activators of eNOS. Future studies could be conducted to explore the possibility of protein phosphatase activation by fenofibrate.

HSP 90

eNOS can be post-translationally modified by protein-protein interactions with HSP 90. HSP 90 acts as chaperone protein and can enhance PKB/Akt induced phosphorylation of eNOS, by

enhancing kinase-substrate association and proximity, without interfering with the normal actions of PKB/Akt (Takahashi & Mendelsohn 2003). Similarly, HSP 90 can enhance eNOS activation via phosphorylation by AMPK (Fujimura *et al*. 2012). The present study found an increase in HSP 90 expression after 24 hour fenofibrate treatment compared to 1 hour fenofibrate treatment. Similar time-dependent trends were observed with the AMPK phosphorylation studies. From these findings, it can be speculated that HSP 90 recruited AMPK for eNOS phosphorylation, however, that it was insufficient to result in eNOS activation.

eNOS Ser 632 related signalling

Ser 1177 is not the only positive regulatory site of eNOS. The general understanding is that Ser 1177 is more involved with rapid agonist induced activation of eNOS providing a burst of NO. The phosphorylation of eNOS at Ser 632 is a slower process and eNOS activation via this residue contributes to a maintenance of NO levels after the initial burst (Mount *et al.,* 2007). However, 1 and 24 hour fenofibrate treatment did not affect eNOS Ser 632 phosphorylation, which excludes eNOS phosphorylation at this site as a possible mechanism of increased NO production.

The data thus far suggest that eNOS was not activated by fenofibrate treatment via the positive regulatory phosphorylation sites Ser 1177 and Ser 632. However, post-translational modification of eNOS involves positive and negative regulatory phosphorylation residues; therefore, the aim of the next series of experiments was to investigate the negative regulatory sites of eNOS. Even though no involvement of Thr 495 or Tyr 657 was found in the 1 hour treatment groups, fenofibrate significantly inhibited eNOS via elevated phosphorylation at Thr 495 after 24 hours. To the best of our knowledge, this is a novel finding. The major upstream kinase involved with Thr 495 phosphorylation is protein kinase C (Mount *et al.* 2007). Chen *et al.* (1999) also found that in the absence of Ca^{2+}/CaM, AMPK is able to phosphorylate eNOS Thr 495, resulting in inhibition of the enzyme. However, in our hands, activation and phosphorylation of AMPK were not observed at 24 hours. eNOS Tyr 657, associated with reduced enzyme activity (Fisslthaler *et al*., 2008; Loot *et al*., 2009), also failed to undergo any changes in response to fenofibrate at any of the given time points.

nNOS

In the current study, the other constitutive NOS isoform, nNOS, was also investigated. Del Campo *et al.* (2011) showed that fenofibrate increased neuronal release of NO by increased phosphorylation of nNOS in mesenteric arteries of diabetic rats. However, the data showed that in our hands, this isoform did not seem to play a significant role in CMECs. Furthermore, from a technical point of view, the detection of nNOS and phosphorylated nNOS was inconsistent (figure 3.34 and figure 3.42). nNOS expression and phosphorylation were detected in the 5, 15 and 30 minute treatments with fenofibrate and these experiments indicated a decrease in phosphorylation. nNOS was therefore also excluded as source for fenofibrate-derived NO.

iNOS

The third major NOS isoform, is the inducible NOS (iNOS). Few studies have investigated the effects of fenofibrate treatment on iNOS. One study showed that fenofibrate increased pancreatic iNOS expression in monosodium glutamate-induced obese rats, which was associated with an increase in NFκB activity (Liu *et al*. 2011). Another study on rat aortic tissue showed that fenofibrate induced endothelial dysfunction (observed as a diminished vasodilatory response) in a time-dependent fashion, and although iNOS expression was measured, they failed to show any changes in iNOS expression (Blanco-Rivero *et al*. 2007). In the current study, the NO response to 1 hour fenofibrate was particularly robust (≈2-fold increase; figure 3.13 A), therefore we speculated that it could be suggestive of iNOS induction (particularly in view of the eNOS findings). We therefore repeated the experiments with the iNOS-selective inhibitor, 1400W. Again two different NO-detection methods (DAF-2/DA fluorescence and Griess method) (figure 3.26 B and C) were used in both CMECs and AECs; however, the findings were similar to those of the L-NMMA studies, with no reduction in the fenofibrate-induced NO production. DAF-2/DA fluorescent results however showed a modest, yet statistically insignificant (≈15%) decreasing trend in the NO production of the 1400W + fenofibrate group. Even though this reduction was not significant, the lack of eNOS and nNOS phosphorylation prompted us to further investigate this finding by means of targeted mRNA and protein expression measurements. The pro-inflammatory cytokine, interleukin-1β served as a positive control for iNOS induction (Lowry *et al*., 2013). Results indicated that CMECs did not express iNOS on protein or mRNA level under

control conditions, however interleukin-1β was able to significantly increase iNOS mRNA and protein expression (figure 3.28) while a ~50% knock-down was confirmed with two constructs of iNOS silencing RNA. This is in agreement with a study by Balligand *et al*. (1995) who showed similar findings in CMECs. Furthermore, the mRNA and protein expression data indicated that fenofibrate did not induce iNOS after 1 hour treatment and was therefore an unlikely candidate responsible for increased NO levels in this scenario.

Summary: NOS-NO studies

In summary, 50 µM fenofibrate resulted in a large increase in NO after 1 hour incubation in CMECs. The elevated levels of NO were associated with a lack of phosphorylation at the positive regulatory site of eNOS Ser 1177 after 5 min, 15 min, 30 min, 1 hour and 24 hours. Another positive regulatory eNOS residue (Ser 632), was also excluded as a mechanism of increased NO production at 1 and 24 hours. The eNOS inhibitory site Thr 495, was significantly phosphorylated after 24 hours of fenofibrate treatment, suggesting an inhibition of eNOS at this time-point. Two of the major upstream activating kinases of eNOS, namely AMPK and PKB/Akt showed no signs of activation, and the expression of HSP 90, associated with recruitment of PKB/Akt and AMPK in activating eNOS, was only increased compared to 1 hour fenofibrate treatment. iNOS was not detected at mRNA or protein level in reponse to fenofibrate treatment and nNOS was inconsistently detected, and therefore unlikely to be involved with the consistent increase in NO found in this study. After 24 hours some trends started to emerge suggestive of AMPK activation along with increased HSP 90 expression, however it did not result in eNOS activation. It is therefore proposed that in our hands, the fenofibrate-derived effect on NO in CMECs is more likely to be due to NOS-independent mechanisms.

NO synthesis: NOS-independent mechanisms

Fisslthaler *et al*. (1999) and Fichtlscherer *et al*. (2004) reported that endothelium-dependent pro-vasodilation mechanisms exist in many arterial beds in response to stimuli, even after NOS inhibition. In the present study, an *in vitro* model of cultured CMECs was used, which to the best of our knowledge, has never been used in previous *in vitro* investigations with fenofibrate. Zhao

et al. (2013) showed that aortic ring contractions of spontaneously hypertensive rats were decreased via an endothelium-dependent mechanism compared to normal Wistar-Kyoto rats. Administration of the NOS inhibitors L-NAME and 1400W (directly to the organ bath) had no effect on the contractile responses; however, when treated with diphenyleneiodonium (inhibitor of flavonoid proteins including cytochrome P450 reductase) and clotrimazole (cytochrome P450 inhibitor), the contractile responses were abolished. This effect was accompanied by increased levels of nitrates and nitrites in plasma as well as aortic tissue. They further showed by means of DAF-FM diacetate fluorescence and human aortic endothelial cells (HAEC) that nitrate and nitrite levels were reduced in the presence of the above mentioned cytochrome P450 inhibitors. They therefore concluded that the NO, which reversed the impaired contractile responses in the aortic rings, was produced by an NOS- independent mechanism. In view of the cytochrome P450 inhibition studies, they suggested that the NO was synthesised via the reduction of nitrates and nitrites to NO by cytochrome P450 reductase. It has been known for many years that NO can be generated via NOS-independent mechanisms; however, the phenomenon of nitrate and nitrite reduction to form NO has exclusively been described in the context of hypoxia or ischaemia (Kitakaze et al. 2001; Webb et al. 2004; Duranski et al. 2005) when there is a shortage of oxygen, an essential substrate for NOS activity. However, in the studies of Zhao *et al*. (2013), experiments were conducted in an aerobic environment.

The family of cytochrome P450 enzymes are involved with the metabolism of xenobiotics and vascular homeostasis (Campbell & Harder 1999) and is located in the membrane of the endoplasmic reticulum (microsomes) (Roos & Jakubowski 2008; Pandey & Flück 2013). The tissue-selective distribution and regulation of cytochrome P450 is controlled by different nuclear receptors, such as Pregnane X Receptor (PXR), Glucocorticoid receptor (GR) and Constitutive Androstane Receptor (CAR). Upon activation by a xenobiotic ligand, PXR forms a heterodimer with retinoid X receptor (RXR) which can bind to response elements in the regulatory regions of the induced genes (Bertrand-Thiebault *et al*. 2007). Fenofibrate is a synthetic ligand for PPAR-α, and upon binding also forms a heterodimer complex with RXR before binding to response elements (Berger & Moller 2002). PPAR-α has further been reported to participate with PXR in metabolizing xenobiotics (Barbier *et al*., 2004). It is therefore proposed that one possibility to

explain the NOS-independent increases observed in our study with fenofibrate, could be via its putative effects on cytochrome P450. Fenofibrate binds as a synthetic ligand to PPAR-α, which in conjuction with PXR, could activate cytochrome P450 reductase. Cytochrome P450 reductase can utilise nitrites (as was found in figure 3.24 B and C; Griess assay) and produce NO by a NOS-independent mechanism. In separate studies in our laboratory, proteomic analysis of CMECs showed abundant expression of the cytochrome P450 enzyme (unpublished data). A summary of the hypothetical pathways is depicted in figure 3.55.

3.5.4 ROS and cell viability

One of fenofibrate's pleiotropic effects includes antioxidant activities. Fenofibrate treatment has previously been associated with decreased superoxide production derived from high glucose treatment in HUVECs, which was also associated with decreased apoptosis (Zanetti *et al*., 2008). Decreased superoxide production in aortic tissue of nicotine treated rats (Kaur *et al.,* 2010) pretreated with fenofibrate has also been reported. In vivo, fenofibrate was shown to increase superoxide dismutase activity in rat brain microvessels (Wang *et al.,* 2010a). It seems, however, as if the antioxidant activities of fenofibrate are more evident during diseased states or pathological conditions than under basal conditions. The current study showed increased expression of p22Phox after 1 hour treatment (figure 3.38 C). P22Phox is the subunit of NADPH oxidase, responsible for superoxide production (Ambasta *et al.,* 2004). Even though results showed increased p22Phox expression, DHE data (figure 3.14 A) showed no changes in intracellular superoxide production. In the event of increased levels of NO as well as increased levels of superoxide, superoxide can scavenge NO resulting in the formation of harmful peroxynitrite (Ferdinandy & Schulz 2003). 30 µM and 50 µM fenofibrate resulted in decreased levels of mitochondrial ROS/peroxynitirite at 1 and 4 hours. As far as we are aware, no previous studies used DHR-123 in order to assess oxidative stress. Furthermore, fenofibrate has previously been reported to decrease nitrotyrosine in renal tissue when administered to control and diabetic animals (Chen & Quilley 2008). The current study did, however, not find any changes in nitrotyrosine after 1 or 24 hours.

NO can exert pro-apoptotic or anti-apoptotic effects. As previously mentioned, if excessive amounts of NO are produced, it can combine with superoxide anions to form peroxynitrite. Peroxynitrite formation results in increased lipid peroxidation along with DNA breakage and consequently a decrease in cell viability (Virág *et al.,* 2003; Razavi *et al.* 2005). In the current study, 24 hour treatment with fenofibrate resulted in a decrease in apoptosis as shown by the Annexin-V data as well as decreased expression of cleaved-Caspase-3, which could be due to the modest increase in NO. NO can inhibit apoptosis by S-nitrosylation of the executer caspase, caspase-3 (Rossig *et al.,* 1999), rendering it inactive. This is an interesting finding, since it seems as if most of the robust pleiotropic effects found in the current study were observed at the shorter treatment periods, however a decrease in apoptosis was only seen after 24 hours treatment.

3.5.5 Pro-inflammatory pathways

Fenofibrate has previously been shown to possess anti-inflammatory properties, which was demonstrated *in vivo* in human studies (Belfort *et al*., 2010), as well as *in vitro* by decreasing nuclear factor kappa B (NF-κB) activity of endothelial cells (Yang *et al*. 2005; Tomizawa *et al.* 2011). NF-κB has emerged as a key cellular regulator of inflammation and is activated in many chronic inflammatory diseases and cancers (Wolfrum *et al*., 2007; Gyrd-Hansen & Meier 2010; Ben-Neriah & Karin 2011; Cao *et al.*, 2013;). IκBα plays an important inhibitory role on NF-κB activity. Whilst bound to NF-κB, the latter remains inactivated; however, upon phosphorylation, IκBα dissociates from NF-κB, and is subsequently broken down via proteasomal processes. The dissociation step provides the stimulus for NF-κB to become activated and to translocate to the nucleus and perform its role as a transcription factor. Therefore, a decrease in total IκBα protein expression is associated with increased NF-κB activity. In the present study, 1 hour fenofibrate treatment resulted in a significant increase in IκBα expression, suggestive of lower levels of NF-κB activity and hence reduced activation of NF-κB-dependent pro-inflammatory pathways. Our data are in agreement with those of Tomizawa *et al.,* (2011), who showed that fenofibrate (30 and 100 μM) increased IκBα expression in advanced glycated end-product (AGE)–bovine serum albumin (BSA) treated HGMECs. These changes were observed after only 30 minutes of fenofibrate treatment. The authors suggested decreased levels of NF-κB activity to be due to

AMPK (Thr 172) activation. The study of Yang *et al*. (2005) pretreated HUVECs with fenofibrate prior to administration of oxidized-low density lipoprotein (ox-LDL) and found fenofibrate to inhibit ox-LDL induced endothelial damage as a result of decreased levels of asymmetric dimethylarginine (ADMA) (an endogenous inhibitor of NOS; partakes in the vascular inflammatory reaction). These results were associated with decreased NF-κB activity, an effect that was PPARα dependent. Considering these studies and the fact that the present study did not find increased AMPK activation after 1 hour treatment, it is proposed that increased expression of IκBα is directly related to PPARα receptor activation.

3.5.6 1 hour untreated controls versus 24 hour untreated controls

An interesting observation was made with regards to the differences in phosphorylation between the 1 hour control and 24 hour control groups. Phosphorylation was significantly decreased in the 24 hour control group compared to 1 hour in phospho-eNOS (Ser 1177), phospho-eNOS (Thr 495), phospho-eNOS (Tyr 657) and phospho-PKB/Akt. Furthermore, p22Phox expression and cleaved-caspase 3 formation was decreased. These observations highlighted the importance of including time-controls for treatments. It can be speculated that these effects are due to supplemental depletion of the growth media. CMECs were cultured in growth media containing vascular endothelial growth factor (VEGF), human epidermal growth factor (hEGF), human fibroblastic growth factor (hFGF), long chain human insulin-like growth factor (R3-IGF-1), ascorbic acid, hydrocortisone and antibiotics gentamicin and amphotericin. VEGF (Yang *et al*. 2014) and R3-IGF-1 (Imrie *et al*., 2009) have been shown to increase eNOS activity in endothelial cells and that after 1 hour the effects of these supplements were still ongoing while after 24 hours supplements have been depleted and the effects abolished.

3.5.7 Fenofibrate pretreatment studies

In the previous sections, the pleiotropic effects of fenofibrate in normal, baseline CMECs were discussed, and indeed it was shown that fenofibrate could exert pleiotropic effects in a non-diseased environment. The next step was to establish whether the effects of fenofibrate were able to protect against the endothelial cell injury induced by the harmful, pro-inflammatory stimulus, TNF-α. As discussed in chapter 1, inflammation is not only associated with

cardiovascular risk factors such as diabetes or obesity, but also with atherosclerosis from the initial to the end stages when thrombotic complications occur (Libby 2006). Once inflammatory cells (e.g. macrophages) have infiltrated the area of vascular injury, they release cytokines such as TNF-α, proteases, and ROS, which trigger vasoconstriction or vasodilation (Groth *et al.*, 2014), thrombus formation (Carter 2005; Libby 2006), angiogenesis and tissue remodelling (Wilensky *et al*., 1995). TNF-α has been shown to result in endothelial activation and dysfunction with oxidative stress regarded as the likely common mechanism (Genis *et al*., 2014). The effects of TNF-α are very much concentration-dependent. In a separate study from our laboratory, it was confirmed that 20 ng/ml TNF-α resulted in upregulation of pro-apoptotic pathways as measured by proteomic analysis (Genis *et al.*, 2014). Our aim was therefore to investigate whether the beneficial baseline effects of fenofibrate that were observed in normal CMECs (increased NO production, decreased mitochondrial/peroxynitrite formation, anti-apoptotic and anti-NF-KB pro-inflammatory signalling) would be sustained and possibly even protect endothelial cells against a harmful, pro-inflammatory microenvironment induced by TNF-α treatment.

eNOS-NO biosynthesis

Fenofibrate treatment alone significantly increased NO levels observed in the previous experiments, whilst TNF-α treatment alone did not change NO levels. However, when TNF-α-treated CMECs were pretreated with fenofibrate, the NO production increased significantly to reach the levels observed in fenofibrate only groups (figure 3.46). The effects of TNF-α on the NOS-NO biosynthesis pathway are quite variable, and are time, concentration and even cell type specific (Genis, Stellenbosch University, 2014). On the one hand, TNF-α has been shown to result in an up-regulation of the NOS/NO pathway (Yoshizumi *et al*., 1993; De Palma *et al*., 2006), whilst others demonstrated the opposite effects (Ahmad 2002; Picchi *et al*., 2006; Gao *et al*., 2007). Decreased bio-availability of NO is considered a hallmark of endothelial dysfunction (Bonetti 2003). In the current study, the NO production in the TNF-α treatment group remained at untreated control levels, while pretreatment with TNF-α increased NO levels approximately 120%; furthermore, total eNOS expression was decreased in the TNF-α-treated cells, and fenofibrate pretreatment could not alter this (figure 3.49B). However, interestingly, fenofibrate pretreatment did significantly increase the phosphorylated eNOS (Ser 1177) levels compared to

the TNF-α only group; in fact, the phospho / total eNOS ratio of the pretreatment group was the only experimental intervention that was significantly increased compared to untreated control samples. This is an intriguing finding, considering the lack of eNOS activation seen with fenofibrate treatment in previous *in vitro* studies of this chapter. Additionally, the fenofibrate pretreatment group also showed increased AMPK phosphorylation, which coincided with the increased eNOS phosphorylation, suggesting that the AMPK-eNOS pathway was activated only when fenofibrate was pre-administered to TNF-α-treated cells.

ROS production, apoptosis and NF-κB signalling

Although, in our hands, treatment of CMECs with 20 ng/ml TNF-α (24 hours) did not result in reduced NO production (one of the hall-marks of endothelial dysfunction), it did result in the manifestation of other major markers of endothelial cell injury, namely increased levels of mitochondrial ROS (figure 3.47), increased levels of NADPH oxidase activity as seen in p22phox expression (figure 3.54 C), as well as increased apoptosis (cleaved caspase-3 and PARP) (figure 3.53 B and C). The pronounced effects of TNF-α treatment on ROS production failed to translate into increased necrosis compared to untreated control samples, however, necrosis was significantly higher in the TNF-α group compared to the fenofibrate only and fenofibrate pretreatment groups (figure 3.48). The effects of TNF-α on ROS generation and cell death have been described by many others (reviewed in Zhang *et al*., 2009). Increased ROS production is one of the mechanisms of NF-κB activation, which can result in target gene activation for TNF-α protein synthesis (De Martin *et al*., 2000). In the present study, the TNF-α treatment and fenofibrate pretreatment groups both showed reduced IκBα expression (i.e. increased NF-κB activity) (figure 3.52). The data also showed that the increased ROS production in the TNF-α group was abolished by fenofibrate pretreatment (figure 3.54 C). Interestingly, these findings were associated with reduced levels of necrosis and apoptosis. PARP can be cleaved by caspase-3 and is considered a prominent marker of apoptosis. It is preferable not to observe PARP cleavage in isolation since PARP-1 proteolysis has previously been found due to technical reasons (Soldani & Scovassi 2002). In the current study similar results were found for both markers of apoptosis. Cleaved PARP (89 kDa) expression correlated well with cleaved-caspase-3 expression and both these apoptotic markers showed a similar trend to necrosis levels observed in figure

3.48. Fenofibrate pretreatment therefore improved cell viability by decreasing, although not abolishing, the pro-apoptotic and pro-necrotic effects of TNF-α, possibly due to decreased levels of ROS.

The marker of peroxynitrite damage, namely nitrotyrosine, showed no changes and it therefore seems that TNF-α did not exert its detrimental effects through peroxynitrite formation, but rather via increased ROS levels from the mitochondria and the NADPH oxidase system. Peroxynitrite is generated as a result of the chemical reaction between NO and superoxide (Ferdinandy & Schulz 2003). Even though increased levels of superoxide were present, increased NO levels were not, thus making peroxynitrite formation unlikely. Pretreatment with fenofibrate showed a strong anti-oxidant effect compared to TNF-α only samples, which could be due to the up-regulation of anti-oxidant systems. In previous studies we also showed that 1 and 4 hour treatment with fenofibrate decreased mitochondrial ROS/peroxynitrite levels measured by DHR-123 fluorescence (figure 3.15), which is suggestive of increased anti-oxidant mechanisms. Fenofibrate has previously been reported to result in the up-regulation of superoxde dismutase (SOD) as well as catalase (Toyama *et al.*, 2004; Olukman *et al.,* 2010; Wang *et al.,* 2010a) and it is proposed that up-regulation of these anti-oxidants resulted in decreased levels of ROS. The anti-oxidant effects of fenofibrate seemed more robust than its effects on the pro-inflammatory NF-κB pathway in the CMECs. As expected, the pro-inflammatory cytokine TNF-α resulted in increased NF-κB activity in the CMECs as observed by a reduction in IκBα expression. Fenofibrate pretreatment was, however, not able to attenuate this effect. A summary of findings is depicted in figure 3.56.

3.5.8 Summary of the *in vitro* effects of fenofibrate

Fenofibrate exerted pleiotropic effects in CMECs under basal conditions. The effects on NO production were more robust for shorter treatment periods and were associated with decreased mitochondrial ROS/peroxynitrite. NO seems to be produced via a NOS independent pathway, it is proposed to be via cytochrome P450 reductase. Pretreatment of CMECs with fenofibrate resulted in beneficial effects with regards to NO production, ROS and cell viability. Even though fenofibrate increased NO after 1 hour via a NOS-independent mechanism, its seems as the micro-

environment changed by adding TNF-α CMECs started to switch toward eNOS-prevalent mechanisms. Final conclusions will follow later in the dissertation.

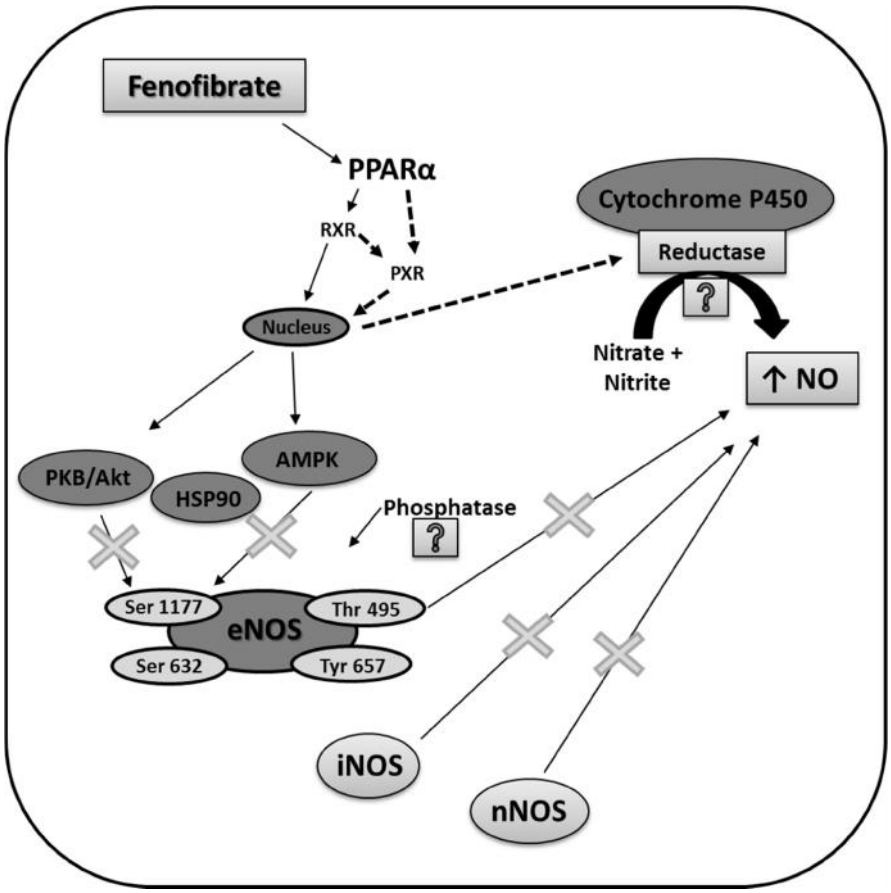

Figure 3.55: A cartoon depicting proposed mechanisms involved with fenofibrate-derived NO production after 1 hour treatment. Our findings provided no evidence in favour of NOS-dependent NO synthesis. It is proposed that fenofibrate bound as ligand to PPAR-α which formed a complex with RXR. RXR can either directly result in transcription of genes responsible for stimulating cytochrome P450 reductase or RXR can via PXR result in gene transcriptions. It is proposed that cytochrome P450 reductase converted nitrates and nitrites to NO; all of these mechanisms were NOS-independent. Significant down-regulation of eNOS could possibly be due to increased phosphatase activity. PPAR-α: Peroxisome proliferator activated receptor; RXR: Retinoid-X-receptor; PXR: Pregnane-X-receptor; AMPK: AMP-activated protein kinase; PKB/Akt: Protein kinase B; HSP 90: Heat shock protein 90; eNOS: Endothelial nitric oxide synthase; nNOS: neuronal nitric oxide synthase; iNOS: inducible nitric oxide synthase.

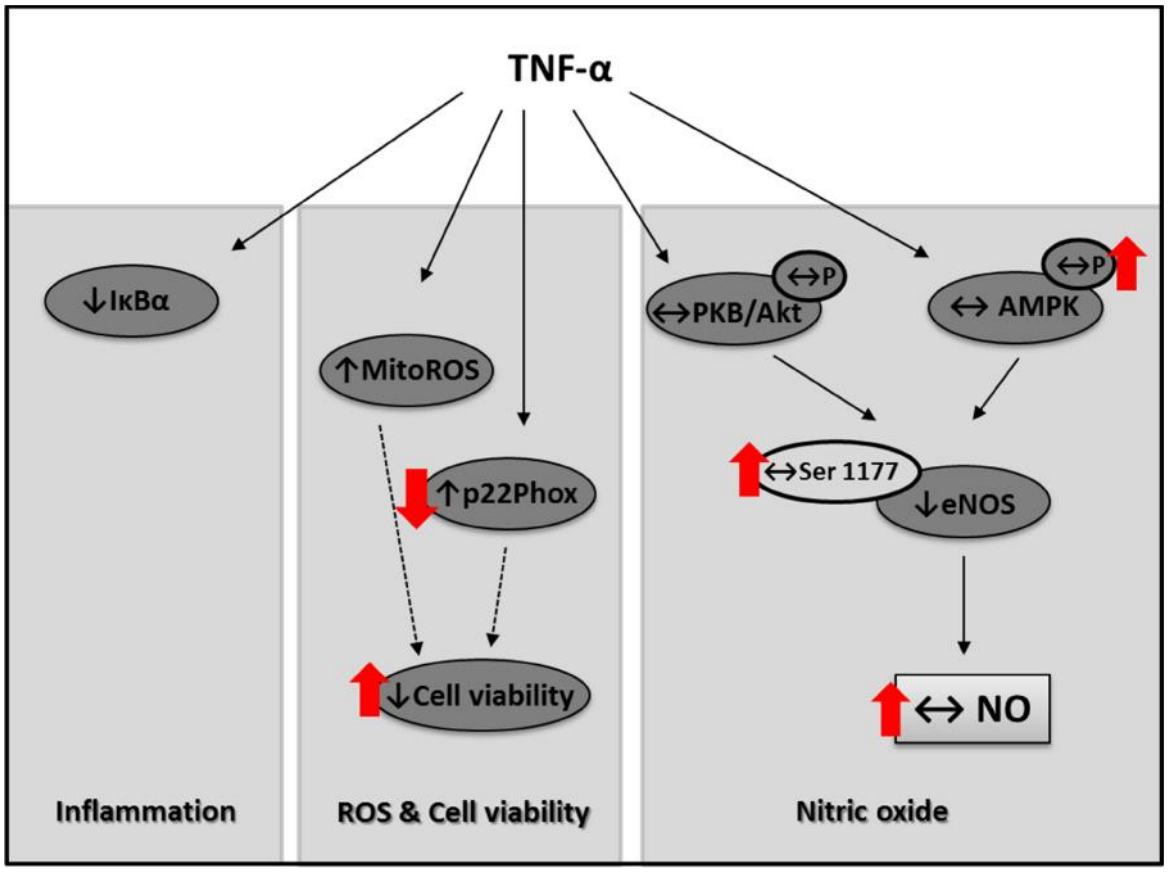

Figure 3.56: A cartoon depicting the effect of 1 hour fenofibrate pre-treatment on TNF-α. The effects of TNF-α is indicated in black arrows, while changes brought about by fenofibrate pre-treatment are indicated in red. TNF-α: Tumor necrosis factor alpha; AMPK: AMP-activated protein kinase; PKB/Akt: Protein kinase B; HSP 90: Heat shock protein 90; eNOS: Endothelial nitric oxide synthase; MitoROS: Mitochondrial reactive oxygen species; P: Phosphorylation.

Chapter 4

Materials and Methods: Ex vivo and In vivo studies

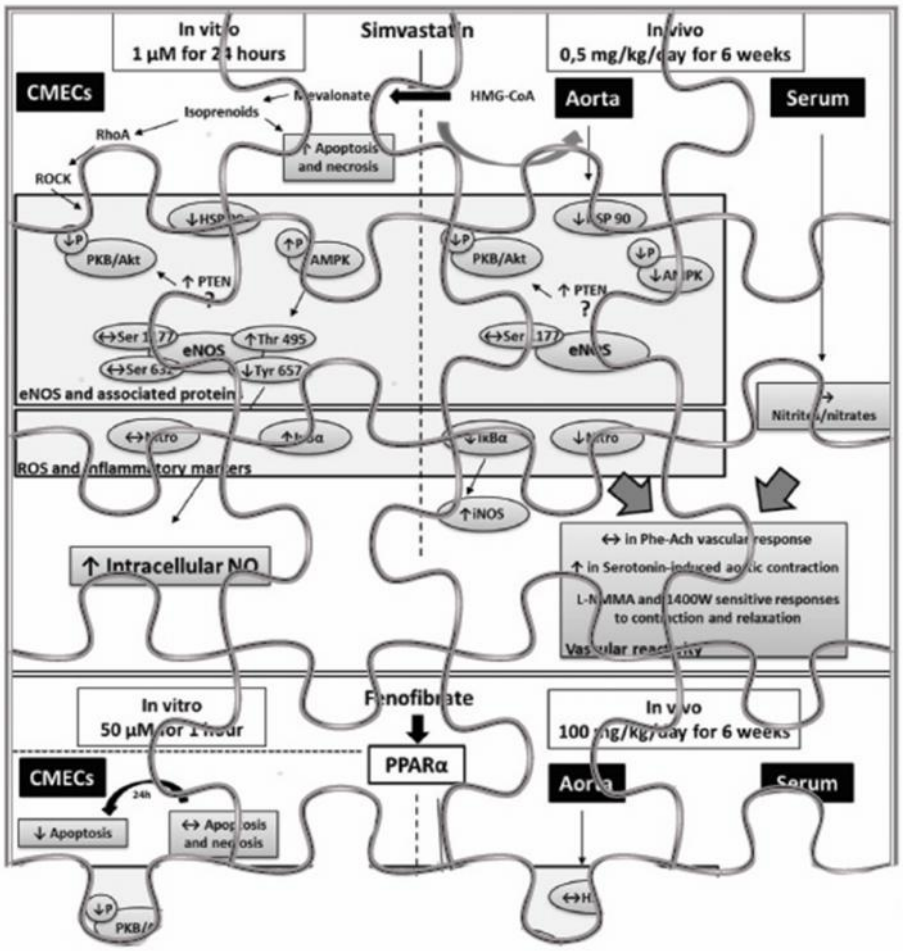

Chapter 4: Materials and Methods – *Ex vivo and in vivo* studies

4.1 Introduction

Chapter 4 describes the experimental methods and protocols followed for the *ex vivo* and *in vivo* studies. The ***ex vivo*** studies consisted of investigations into the organ bath-based vascular contraction-relaxation function of aortas obtained from healthy male Wistar rats. In these studies, fenofibrate was administered directly to the aortic rings mounted in the organ bath, and acute vascular and endothelium-dependent responses measured. The ***in vivo*** studies comprised a 6-week period of oral treatment with fenofibrate or simvastatin, followed by organ bath-based investigations into the vascular contraction-relaxation function of the aortas obtained from the treated animals.

4.2 Materials

N^G-Monomethyl-L-arginine monoacetate (L-NMMA) was from Calbiochem (San Diego, CA, USA). Dimethyl sulfoxide (DMSO), 1400W dichloride, nitrite/nitrate colorimetric kit, acetylcholine, serotonin and phenylephrine were from Sigma-Aldrich (St Louis, Mo, USA). All other chemicals and buffer reagents were purchased from Merck (Darmstadt, Germany).

4.3 Animal care

Experiments were conducted according to "The Revised South African National Standard for the Care and Use of Animals for Scientific Purposes (South African Bureau of Standards, SANS 10386, 2008)". Ethics approval was received from the University of Stellenbosch (Project number: SU-ACUM11-00002 and SU-ACUM13-00041). Male Wistar rats weighing between 200 - 250 g were housed at room temperature in the Animal Housing Unit of the Faculty of Medicine and Health Sciences of Stellenbosch University. Animals were subjected to normal 12 hour light and dark cycles and had free access to standard rat chow and water. Animals were anaesthetized with pentobarbital (160 mg / kg) before excision of the aortas.

4.4 Excision and mounting of aortic rings

As soon as the rat stopped reacting to a toe-pinch test, an incision was made through skin and muscle layers across the ventral side of the rat, just below the thoracic region. The diaphragm was cut and ribcage cut in a cranial direction as to expose the thoracic cavity. Heart, lungs, trachea and oesophagus were removed. The thoracic aorta (above the diaphragm to distal end of the aortic arch) was excised and immediately placed in ice cold Krebs Henseleit buffer (KHB; composition in mM: NaCl 119, $NaHCO_3$ 25, KCl 4.75, KH_2PO_4 1.2, $MgSO_4.7H_2O$ 0.6, Na_2SO_4 0.6, $CaCl_2.H_2O$ 1.25, and glucose 10). Perivascular fat and connective tissue were removed (figure 4.1) and the aorta cut into a 3-4 mm ring segment that was subsequently mounted onto two stainless steel hooks in a 25 ml organ bath (AD Instruments, Bella Vista, New South Wales, Australia) (figure 4.2) containing oxygenated (95% O_2 and 5% CO_2) KHB (figure 4.3). Aortic ring tension was recorded with an isometric force transducer (TRI202PAD, Panlab, lCornellà, BCN, Spain) and data analysed with LabChart 7 sofware (Dunedin, New Zealand).

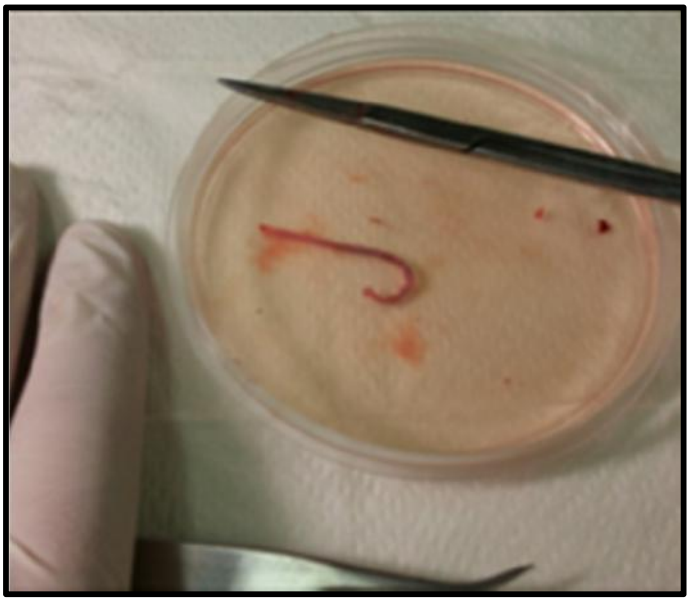

Figure 4.1: A thoracic aorta excised and cleaned of connective tissue and perivascular fat (from Loubser D, M.Sc thesis, Stellenbosch University, April 2014).

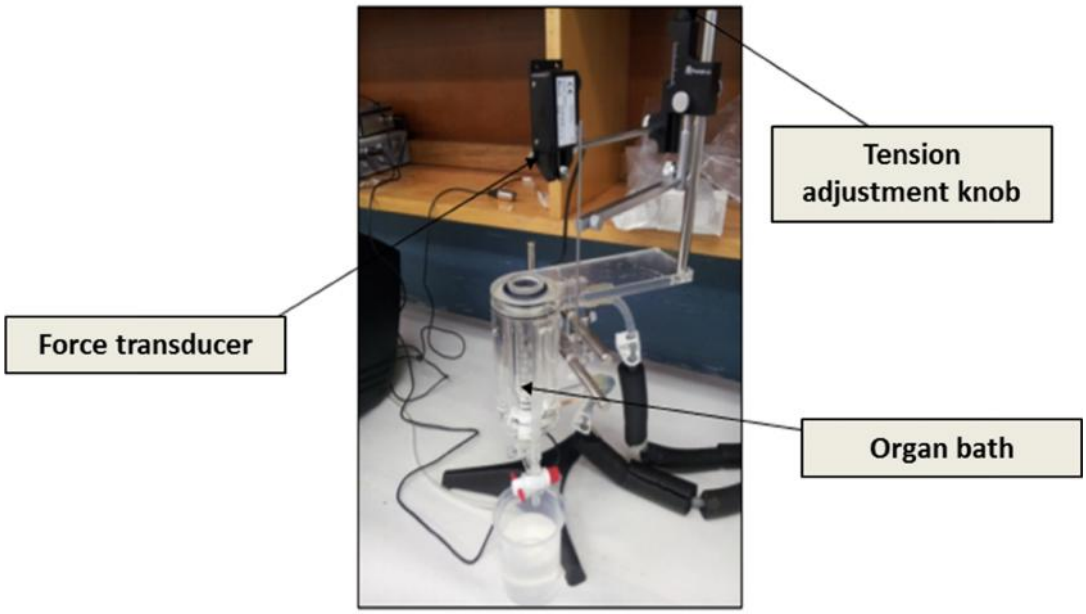

Figure 4.2: Tissue organ bath with force transducer (modified from Loubser D, M.Sc thesis, Stellenbosch University, April 2014)

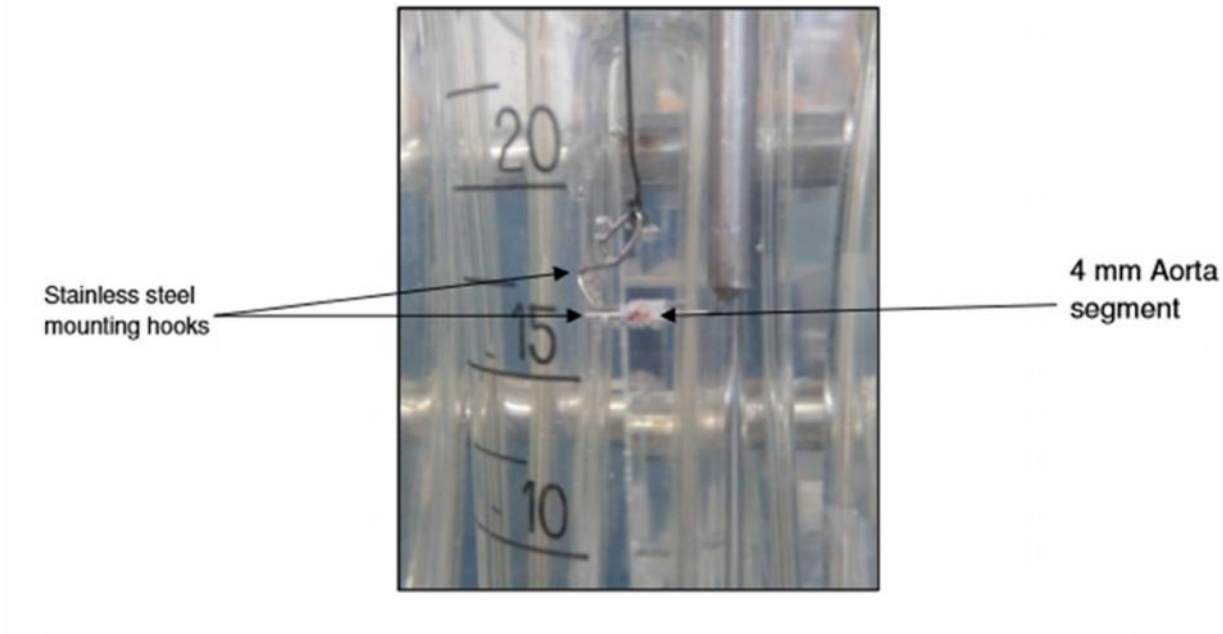

Figure 4.3: Organ bath with an aorta ring segment suspended between two 2 steel hooks (from Loubser D, M.Sc thesis, Stellenbosch University, April 2014).

4.5 Experimental protocol: *ex vivo* studies

Pilot studies were performed to investigate the effect of *ex vivo* administration of fenofibrate and simvastatin on vasodilation of a pre-contracted aortic ring. Simvastatin administration did not result in vasorelaxation of the aortic rings and it was decided to only continue with fenofibrate for *ex vivo* studies.

The isometric tension measurement protocol was based on a modification of a previously described technique (Privett *et al*., 2004). Mounted aortic rings were stabilised under a resting tension of 1.5 g for 30 minutes during which time the KHB in the organ bath was changed every 10 minutes with pre-warmed (37 ^{o}C) KHB. Functionality of the endothelium was tested with a first round of contraction with phenylephrine (100 nM) and acetylcholine induced (10 µM) relaxation. Phenylephrine is an α-adrenergic receptor agonist which acts directly on the vascular smooth muscle cells leading to contraction. Acetylcholine binds to endothelial surface receptors resulting in an increase in intracellular calcium and consequently eNOS activation, NO release and smooth muscle cell relaxation. Rings that showed at least a 70% relaxation of maximum phenylephrine-induced contraction were deemed viable, and included for further investigations. Following the first round of contraction-relaxation induction, the organ bath was rinsed with fresh KHB and rings were stabilised for a further 30 minutes at 1.5 g tension, replacing the KHB every 10 minutes. Aortic ring contraction was induced with the administration of 1 µM phenylephrine until a plateau was reached. As a positive control for endothelium-dependent relaxation, aortic rings were subsequently exposed to cumulative concentrations of acetylcholine (30 nM – 10 µM), and experimental aortic rings to cumulative concentrations of fenofibrate (50 µM – 125 µM) added *ex vivo* to the organ bath. In order to investigate whether the observations were due to endothelial-derived eNOS-NO release, aortic rings were pre-treated with the NOS inhibitor, L-NMMA (100 µM) for 15 min prior to the phenylephrine-acetylcholine and phenylephrine-fenofibrate protocols (figure 4.4).

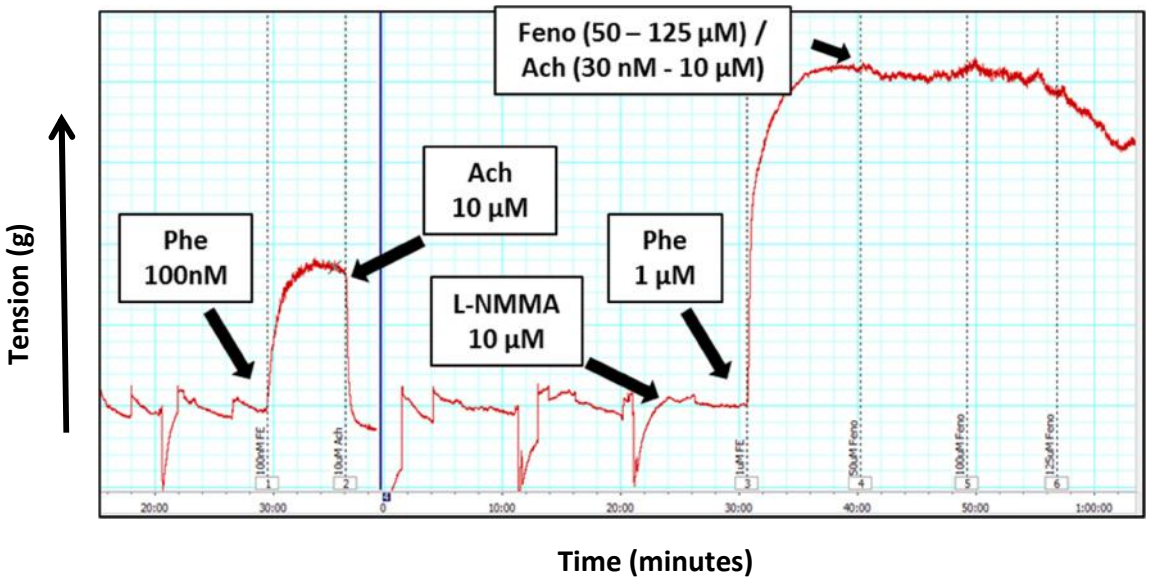

Figure 4.4: A representative LabChart recording showing the aortic ring responses to the experimental protocol followed for the ex vivo studies. Phe: Phenylephrine; Ach: Acetylcholine; Feno: Fenofibrate; L-NMMA: N^G-Monomethyl-L-arginine monoacetate..

4.6 Experimental protocol: *in vivo* studies

For the *in vivo* studies, 60 male Wistar rats were divided into 3 groups: Control (untreated), Fenofibrate and Simvastatin (figure 4.5). Rats were included in the study with a starting weight of approximately 140 – 160g. They were housed 3 per cage according to conditions mentioned in 4.3.

4.6.1 Drug administrations

Fenofibrate was retrieved from Lipanthyl® 200 mg (Abbott, Illinois, USA) capsules, while simvastatin was retrieved from Zocor® 10 mg tablets (MSD), after crushing and powdering the tablets. Drugs were set in jelly cubes and administered to the animals daily (figure 4.6). The untreated control animals received jelly cubes without any drugs. Fenofibrate was administered at a dose of 100 mg/kg/day (Blanco-Rivero *et al*., 2007; Alvarez de Sotomayor *et al.,* 2007; Katayama *et al.,* 2009) and simvastatin was administered at 0.5 mg/kg/day (Lefer et al., 2001) for 6 weeks. A week before treatment started, animals received plain jelly cubes to familiarise them with the taste and feeding process. Animals received treatments in the morning and all animals were monitored until their jelly cube was consumed. Food and water intake were carefully monitored and animals were weighed each week in order to adjust treatments according to increasing body-weight.

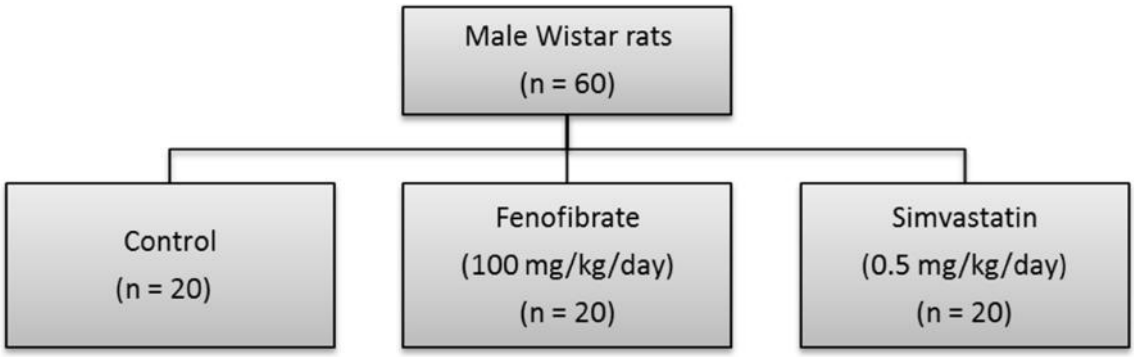

Figure 4.5: Flow chart indicating in vivo treatment groups.

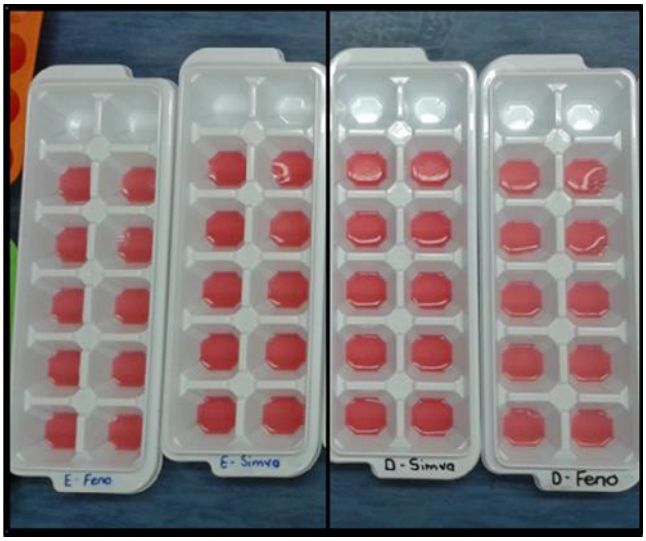

Figure 4.6: Photo of drug treatments made up in jelly cubes set in ice trays. Each animal received 1 cube per day for 6 weeks.

4.6.2 Nitrite/nitrate colorimetric assay

Once animals were sacrificed, blood was collected from the thoracic cavity and placed in serum separation tubes (BD VacutainerR). Blood was left on ice for 30 minutes before being centrifuged for 10 minutes at 3000 rpm. Serum was removed and stored at -80 ^{o}C for nitrite/nitrate analysis.

For these investigations, serum samples were transferred to a 96-well plate, and the nitrite/nitrate concentrations measured with the Griess colorimetric assay (Sigma-Aldrich, St Louis, Mo, USA) in a standard microplate reader (FLUOstar Omega platereader from BMG Labtech, Ortenberg, Germany). Standard curves were prepared by serial dilutions (0; 25; 50; 100 µM) of $NaNO_3$ standard solution which were included on the 96-well plate. Each standard was assayed in duplicate.

All blood serum samples were ultra-filtrated (500 rpm, 4 ^{o}C for 1 hour) using Amicon 10 (Millipore) tubes in order to remove haemoglobin and proteins. Following this, each sample was added to the 96-well plate in duplicate. In order to determine the combined nitrate + nitrite concentrations, samples and standards were incubated with nitrate reductase solution and enzyme co-factors (received with kit) to convert all nitrates to nitrites. Griess reagent was then added and nitrite concentrations determined by the colour reaction measured at 540 nM in the microplate reader. The concentration nitrates+nitrites in each sample were determined from the standard curve (figure 4.7).

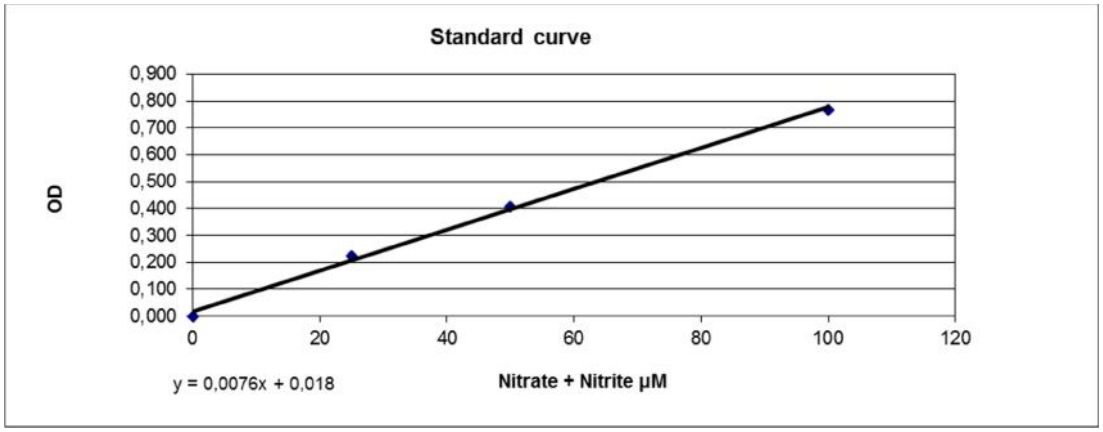

Figure 4.7: Nitrate and nitrite standard curve.

4.6.3 Liver weight measurements

Fenofibrate acts as a synthetic agonist of the peroxisome proliferator-activated receptor alpha (PPAR-α) which ultimately regulates the cholesterol-dependent and independent effects (Despre 2001; Goya *et al*., 2004; Ali *et al.,* 2009). PPAR-α is especially strongly expressed in the liver (Ferre 2004). There is also an ongoing debate regarding the effect of statins on hepatotoxicity (Lewis 2012), and therefore liver weights from all groups were determined. Livers were quickly removed and weighed, as increased liver weight has been shown to be an indicator of liver toxicity (Smyth *et al.*, 2008).

4.6.4 Aortic ring investigations

The thoracic aorta was excised, cleaned of connective tissue and suspended in the organ bath as described under section 4.4. Two rings were cut out from each aorta and mounted immediately in separate organ baths (figure 4.8), which allowed two simultaneous experiments to be performed at a time. Rings were subjected to the same protocol as mentioned in section 4.4. Following the first round of phenylephrine-acetylcholine experiments, each group was subjected to the following four isometric tension protocols (figure 4.9 and 4.10):

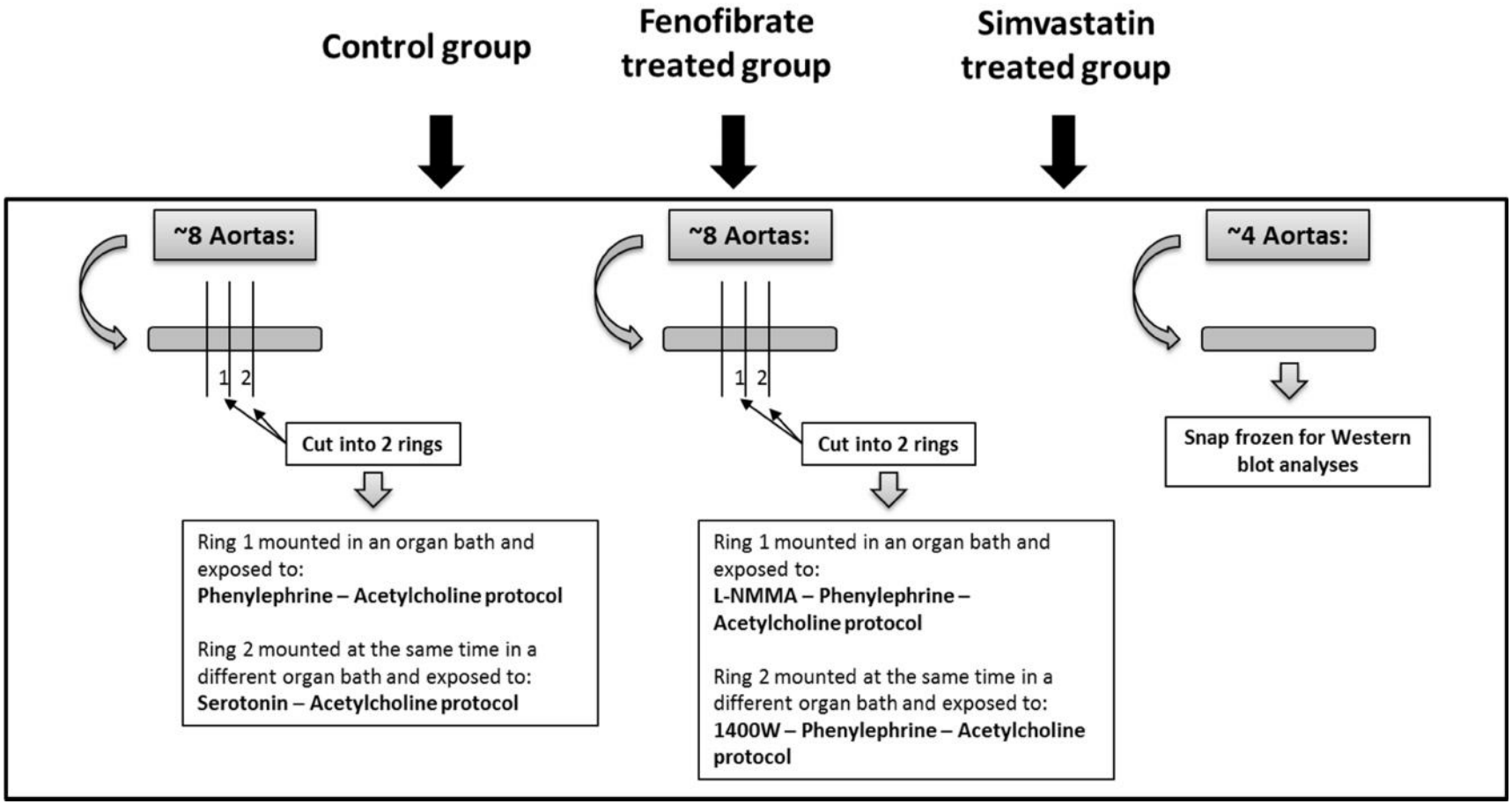

Figure 4.8: Scheme indicating procedures performed on cleaned aortic tissue to obtain aortic rings for isometric tension studies. L-NMMA: N^G-Monomethyl-L-arginine monoacetate.

1) **Cumulative phenylephrine-induced contraction followed by cumulative acetylcholine-induced relaxation:** This protocol was executed by cumulative aortic ring contractions induced with phenylephrine (administration of phenylephrine in a cumulative fashion resulting in a step-wise increase in the total concentration as follows: 100 nM; 300 nM; 500 nM; 800 nM; 1 µM). Each phenylephrine aliquot was administered directly to the organ bath as soon as maximum contraction was reached with the previous administration. Once maximum contraction was reached at the final phenylephrine concentration of 1 µM, acetylcholine was administered in a cumulative manner in order to induce relaxation (step-wise increases in acetylcholine concentrations: 30 nM; 100 nM; 300 nM; 1 µM; 10 µM). The experimental protocol was terminated once the final acetylcholine administration (final concentration: 10 µM) resulted in maximum % relaxation of contraction (figure 4.9 A).

2) **Cumulative serotonin-induced contraction:** This protocol was executed by cumulative aortic ring contractions induced with serotonin (administration of serotonin in a cumulative fashion resulting in a step-wise increase in the total concentration as follows: 100 nM; 1 µM; 10 µM; 100 µM). Serotonin (5-hydroxytriptamine; 5-HT) was used as an alternative pro-contractile agent as it binds to a different vascular smooth muscle cell receptor (5-HT_{2A} receptor) (Bae *et al*., 2007) than phenylephrine (figure 4.9 B).

3) **L-NMMA pretreatment, followed by cumulative phenylephrine-induced contraction and cumulative acetylcholine-induced relaxation:** In this protocol, the role of NOS-derived NO was manipulated by pre-administration of the NOS-inhibitor, L-NMMA (100 µM) 15 minutes prior to the cumulative phenylephrine - acetylcholine protocol (figure 4.10 A).

4) **1400W pretreatment, followed by cumulative phenylephrine-induced contraction and cumulative acetylcholine-induced relaxation:** In this protocol, the role of iNOS-derived NO was manipulated by pre-administration of the iNOS-inhibitor, 1400W (80 µM) 30 minutes prior to the cumulative phenylephrine - acetylcholine protocol (figure 4.10 B).

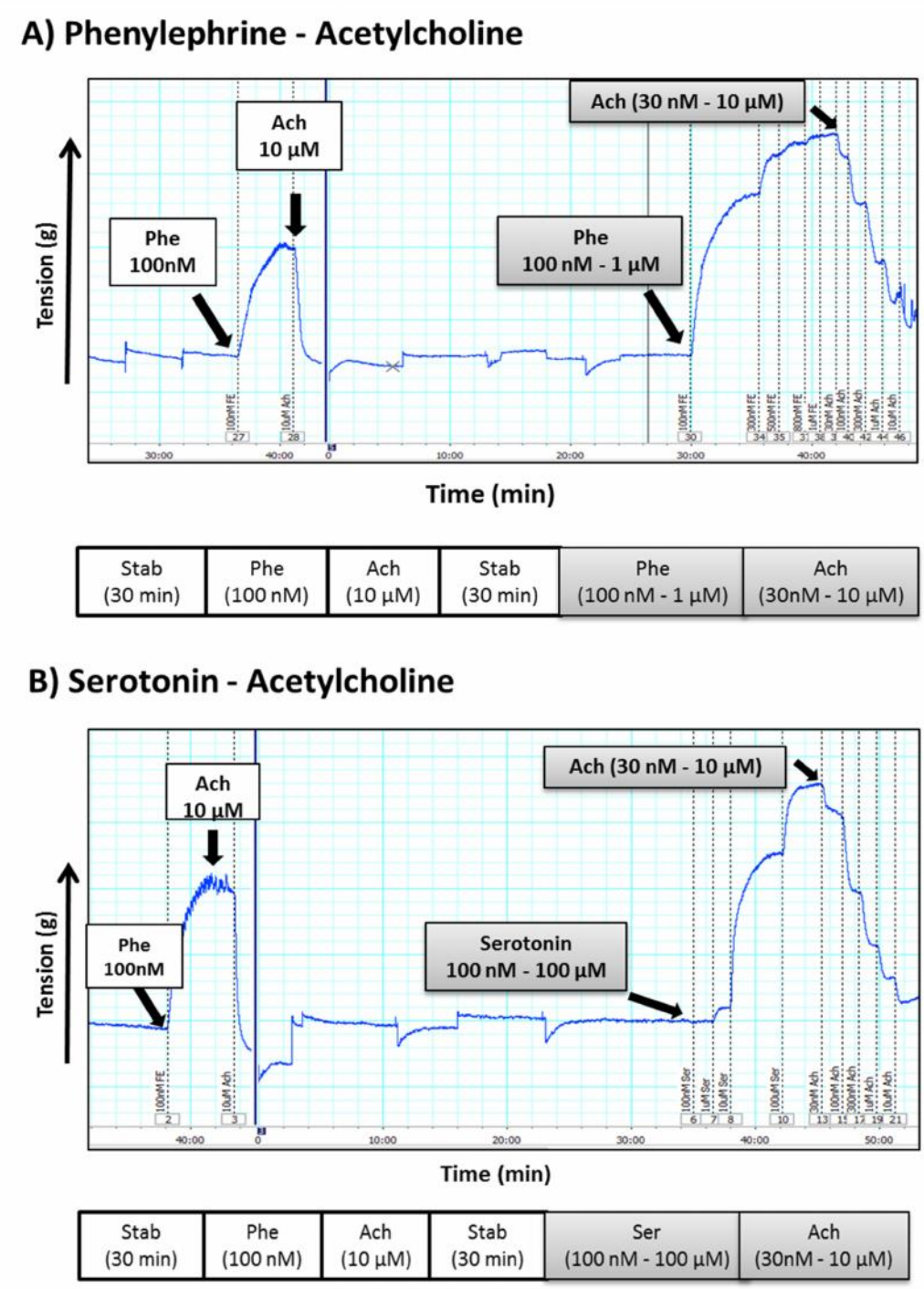

Figure 4.9: Representative LabChart recordings showing the aortic ring responses to the experimental protocols for A) Phenylephrine administration followed by acetylcholine and B) Serotonin administration followed by acetylcholine. These two protocols were performed on aortic rings from the same aorta mounted at the same time in separate organ baths. Phe: Phenylephrine; Ach: Acetylcholine.

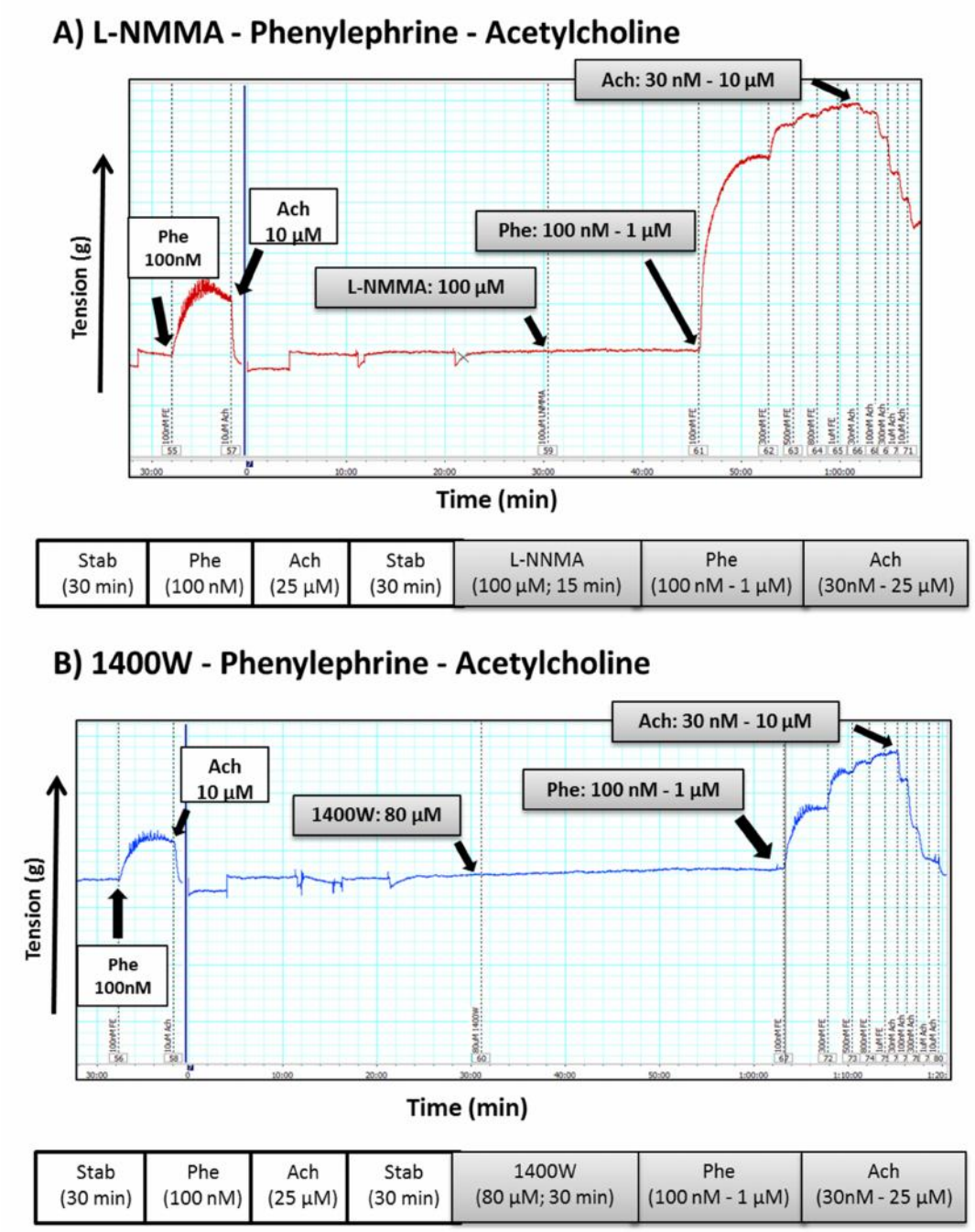

Figure 4.10: Representative LabChart recordings showing the aortic ring responses to the experimental protocols for A) L-NMMA pre-incubation followed by phenylephrine and acetylcholine administration and B) 1400W pre-incubation followed by phenylephrine and acetylcholine administration. These two protocols were performed on aortic rings from the same aorta mounted at the same time in separate organ baths. Phe: Phenylephrine; Ach: Acetylcholine; L-NMMA: N^G-Monomethyl-L-arginine monoacetate.

4.7 Signalling investigations - Western blot analyses

4.7.1 Materials

Similar materials were used as mentioned in Chapter 2, section 2.6.1.

4.7.2 Aortic tissue homogenisation

Aortic tissue stored in liquid nitrogen was thawed and rinsed with 500 µL of PBS. Tissue was then cut into smaller aortic rings. 120 mg of aortic tissue was added to 120 mg of 1.6 mm stainless steel beads and 400 µL of lysis buffer (modified from Hou *et al.,* 2008). Lysis buffer consisted of 20 mM Tris; 1mM EGTA; 150 mM NaCl; 1mM β-glycerophosphate; 1 mM sodium orthovanadate; 2.5 mM tetra-sodium diphosphate; 1 mM PMSF; 0.1 % sodium dodecylsulfate (SDS); 10 µg/ml aprotinin; 10 µg/ml leupeptin; 50 nM NaF and 1 % triton-X100. Tissue was homogenized in a Bullet Blender™ (Next Advance, Inc., NY, USA) by the following steps:

- 3 minutes at speed selection 8
- 2 minutes at speed selection 10
- 5 minutes at speed selection 8
- 3 minutes at speed selection 8

In between the homogenisation cycles, samples were cooled on ice. After homogenisation, samples remained on ice for a further 30 minutes and were then centrifuged for 15 minutes at 14 000 rpm at 4 ^{o}C. Protein content was determined by the Bradford assay (Bradford, 1976) as mentioned in Chapter 2, section 2.6.2.1. Samples were made to yield a final protein content of 15 µg/15 µl of sample.

4.7.3 SDS-polyacrylamide gel and membrane

Loading of samples on a SDS-polyacrylamide gel, subsequent transfer to membrane as well as antibody conditions and protein band visualization was conducted as described in chapter 2.

4.8 Statistical analyses

Data were analysed using GraphPad Prism 5 software (GraphPad Software, San Diego, CA, USA). All aortic ring isometric tension data are expressed as the % contraction from a resting tension of 1.5 g or % relaxation of maximum contraction. Data were statistically analysed by means of two-way analysis of variance followed by Bonferroni post-test. Overall differences in contraction or relaxation of treatment groups were calculated by the area under the curve (AUC). Differences with a p-value < 0.05 were considered statistically significant.

For the western blot data, controls were adjusted to the value of 1. Student's t-tests or one-way analysis of variance (with Bonferroni multiple comparison test) were used to determine statistical significance. Differences with a p-value < 0.05 were considered statistically significant.

Chapter 5

Results and discussions on the ex vivo and in vivo pleiotropic effects of Simvastatin and Fenofibrate

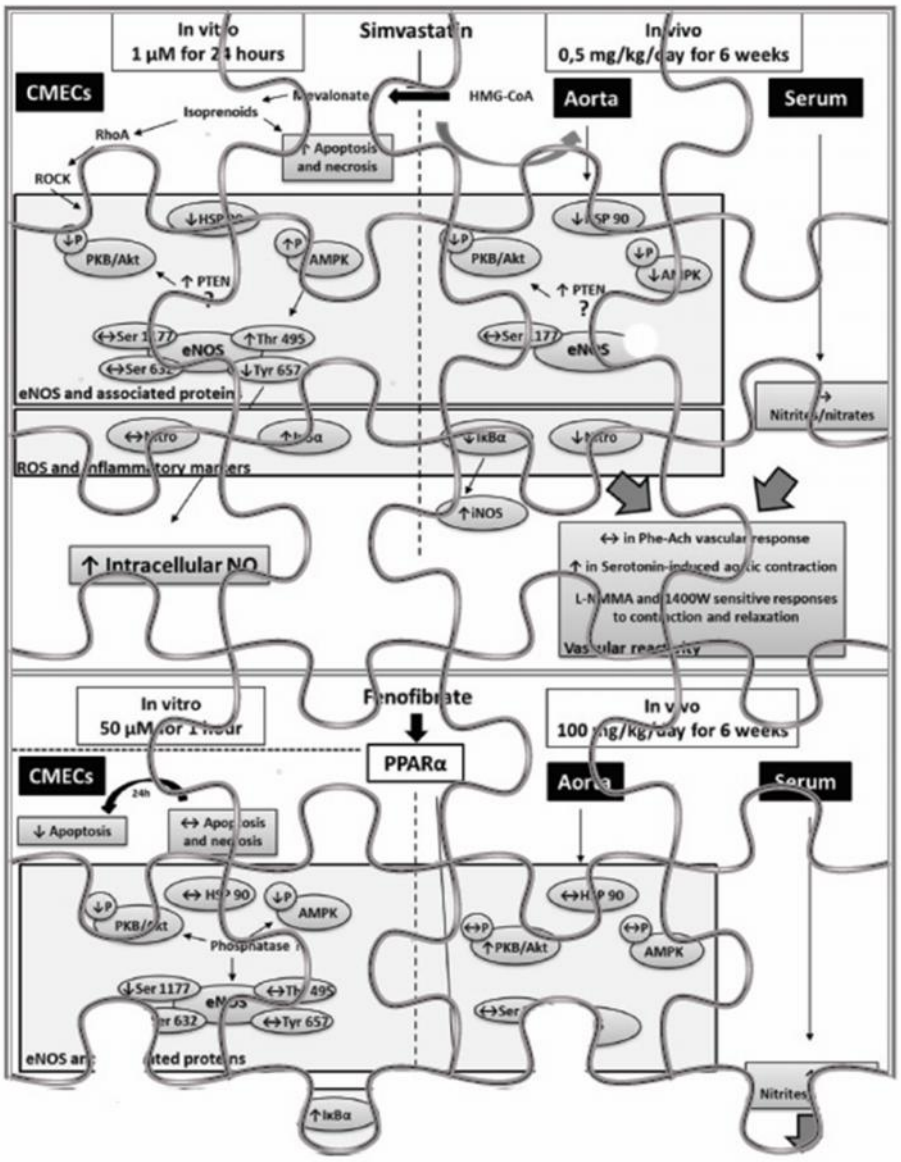

Chapter 5: Results and discussions on the ex vivo and in vivo pleiotropic effects of Simvastatin and Fenofibrate

5.1 Introduction

In vivo, simvastatin is taken up by the liver where it inhibits the rate limiting step in the *de novo* cholesterol synthesis pathway and hence exerts the cholesterol-dependent and independent effects explained in chapter 1 (Rikitake & Liao 2005). *In vivo,* fenofibrate acts as a synthetic ligand for peroxisome proliferator-activated receptor alpha (PPAR-α)thereby activating PPAR-α to form heterodimers with retinoid-X receptor resulting in translocation of PPAR-α from the cytosol to the nucleus where it transcribes genes involved with lipid metabolism (Berger & Moller 2002). The *in vitro* results from chapter 3 indicated that although treatment with simvastatin resulted in a modest increase in nitric oxide (NO) production, no other pleiotropic (cholesterol-independent) effects were observed with regards to the end-points of interest to the current study. Conversely, fenofibrate showed pleiotropic effects under both basal and pro-inflammatory conditions as demonstrated by the following observations: increased NO production, reduced ROS levels, and selective anti-apoptotic effects. Although *in vitro* investigations such as with simvastatin and fenofibrate in the current study form an important foundation in research, it has to be acknowledged that such treatments could exert different effects when metabolised in an *in vivo* environment, especially with regards to simvastatin. Simvastatin is a pro-drug and is metabolized in the liver to its active form, whereas in the *in vitro* setting, it is converted to its active form before administration to cells.

The endothelium plays an important role in maintaining vascular tone by regulating the balance between vasodilating and vasoconstricting factors. During pathological conditions a decrease in vasodilating substances such as nitric oxide (NO) is found with (relative or absolute) increased levels of vasoconstrictors such as the prostanoids (Davignon & Ganz 2004; Vanhoutte *et al*., 2009). Vascular tension investigations have proven to be a valuable experimental tool to explore endothelial and vascular function (Dhanakoti *et al*., 2000; Streefkerk *et al*., 2002; Cordaillat *et al.,* 2007). The endothelium is the main vascular site of NO-production, which results in

hyperpolarisation of underlying vascular smooth muscle cells and subsequent vasodilation (Félétou & Vanhoutte 2009). Therefore the current study undertook a drug treatment programme whereby rats were treated with fenofibrate and simvastatin over a period of 6 weeks, allowing us to measure *in vivo* changes in protein expression and phosphorylation over time, in addition to measuring the effects of the drugs on vasoreactivity using an aortic ring model.

5.2 Specific aims

This chapter aimed to investigate the pleiotropic effects of fenofibrate and simvastatin in vascular tissue by means of the following:

(i) To investigate the effects of *in vivo* and *ex vivo* treatment with simvastatin and fenofibrate on vascular responses by means of aortic ring isometric tension studies.

(ii) By determining Signalling proteins in the aortic tissue involved with these responses by means of Western blotting.

5.3 Results: Ex vivo fenofibrate administration

In chapter 3, *in vitro* studies with fenofibrate treatment showed a robust and large response with regards to NO production, especially during shorter treatment periods. The first phase of the studies in this chapter was aimed at investigating the ability of fenofibrate to acutely dilate pre-contracted aortic rings from healthy Wistar rats by direct administration in an *ex vivo* organ bath – isometric tension model. In order to elicit an endothelium / eNOS – dependent vasodilatory response, phenylephrine precontracted rings were dilated with acetylcholine.

5.3.1 Vascular relaxation: Ach and L-NMMA

Figure 5.1 indicates the normal vasodilatory response in aortas from healthy rats elicited by cumulative concentrations of acetylcholine, expressed as % of maximum phenylephrine-pre-contraction (% Relaxation at 10 µM cumulative acetylcholine concentration: 70.1 ± 3.44 %). Vasodilation was significantly attenuated by pre-administration of the NOS inhibitor N^G-Monomethyl-L-arginine monoacetate (L-NMMA) as seen by an overall reduction in the area

under the curve (Control: 6136; L-NMMA: 3431; p<0.0001). Additionally, relaxation was significantly inhibited by L-NMMA at the following cumulative Ach concentrations: **100 nM** (Control: 26.13 ± 3.01 %; L-NMMA: 7.65 ± 1.50 %; p<0.01), **300 nM** (Control: 41.88 ± 4.02 %; L-NMMA: 16.80 ± 3.22 %; p<0.001), **1 µM** (Control: 56.79 ± 4.17 %; L-NMMA: 31.47 ± 7.45 %; p<0.001) and **10 µM** (Control: 70.10 ± 3.44 %; L-NMMA: 40.40 ± 8.05 %; p<0.001).

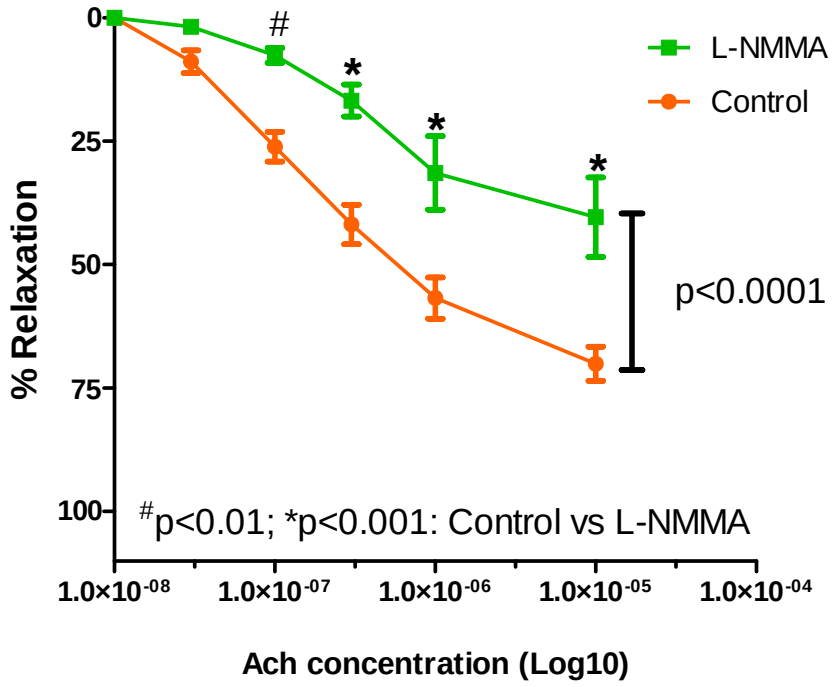

Figure 5.1: Graph indicating the % relaxation of aortic rings harvested from normal rats induced by cumulative acetylcholine (Ach) concentrations ("Control" on the graph) and the attenuation of relaxation by pre-incubation with the NOS-inhibitor, L-NMMA (n = 6 / group).

5.3.2 Vascular relaxation: DMSO, fenofibrate and L-NMMA

In the next series of *ex vivo* experiments, fenofibrate was added directly to aortic rings from healthy rats pre-contracted with 1 µM of phenylephrine in a single administration. Although the DMSO administrations exerted a small pro-relaxation response, fenofibrate significantly increased the maximum recorded % relaxation of the aortic rings compared to DMSO (Fenofibrate: 22.88 ± 2.24 % vs. DMSO vehicle: 9.93 ± 2.75%; $p<0.001$) (figure 5.2 A). In order to contextualise the % relaxation obtained with fenofibrate, a separate series of the standard Ach-induced relaxation protocol was included, and from the data it is clear that the pro-relaxation effects of fenofibrate were significantly less robust than those of Ach (figure 5.2 B).

Pre-incubation of the aortic rings with L-NMMA (prior to phenylephrine induced contraction) abolished the vasodilatory response induced by fenofibrate (Fenofibrate: 22.88 ± 2.24 %; L-NMMA + fenofibrate: 7.90 ± 4.16 %; $p<0.05$) (figure 5.3).

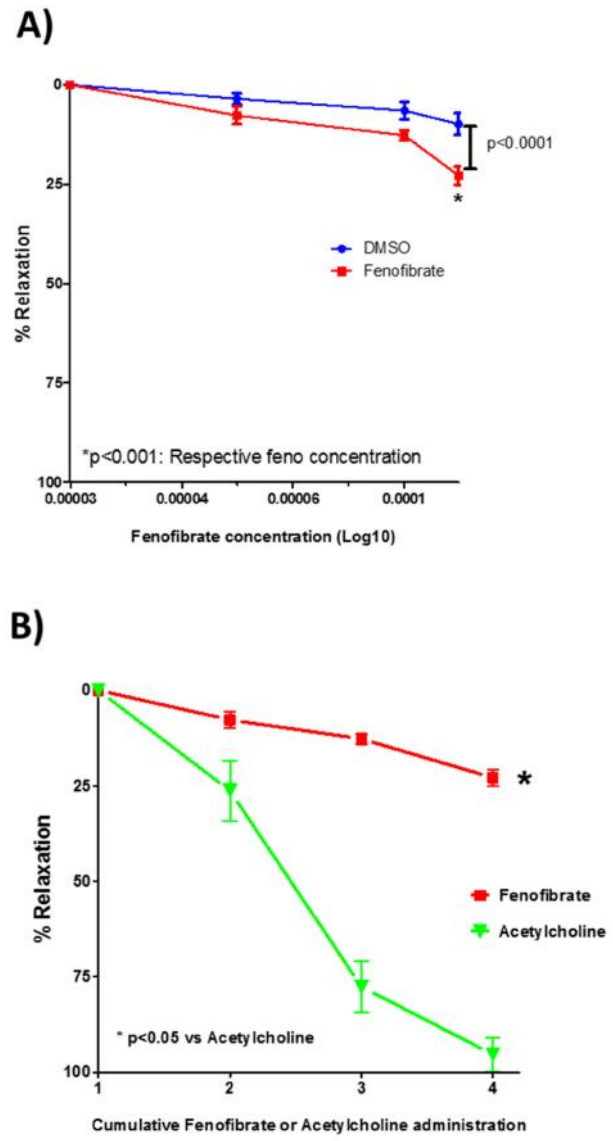

Figure 5.2: Graphs indicating vascular ring-relaxations induced by cumulative concentrations of fenofibrate or DMSO and Ach (n = 4-5). A) Shows relaxation induced by ex vivo administration of fenofibrate and its vehicle, DMSO. B) Graph illustrating the difference in % dilation by fenofibrate and acetylcholine. (Acetylcholine concentrations – 1: 0 nM; 2: 300 nM; 3: 1 µM; 4: 10 µM; Fenofibrate concentrations - 1: 0 µM; 2: 50 µM; 3: 100 µM; 4: 125 µM); n = 4-6

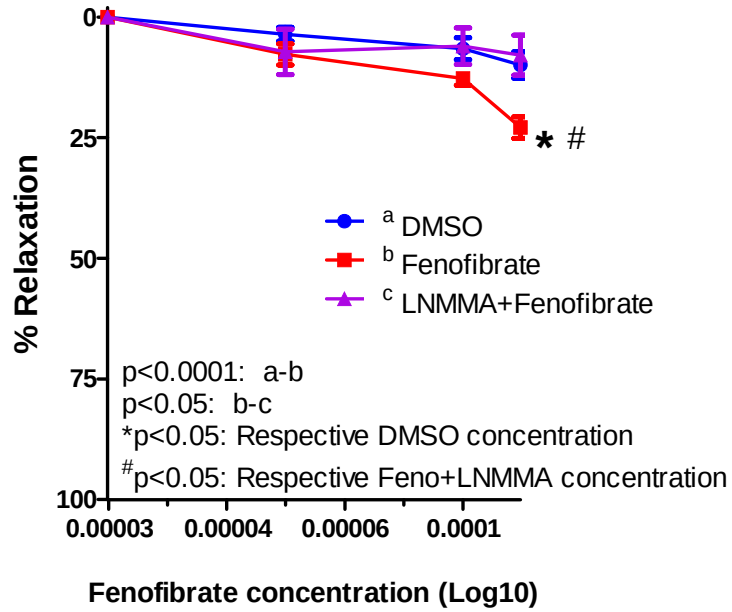

Figure 5.3: Graph indicating vascular ring-relaxations induced by cumulative concentrations of fenofibrate, with and without pre-incubation with L-NMMA.

5.4 Results: *In vivo* administration of fenofibrate and simvastatin

For the *in vivo* studies, 60 male Wistar rats were divided into control, fenofibrate (100 mg/kg/day) and simvastatin (0.5 mg/kg/day) groups and received the respective treatments for 6 weeks. After 6 weeks animals were sacrificed and the following data were obtained.

5.4.1 Biometric data

5.4.1.1 Body weights

No differences in body weight were found between groups at the start or end of the 6 weeks treatment programme (Table 5.1).

Table 5.1: Average body weights of Wistar rats at the beginning and end of study.

Group	Start: Body weight	End: Body weight
Control	183,2 ± 2,7 g	326,4 ± 7,2 g
Fenofibrate	187,9 ± 3,8 g	318,9 ± 6,4 g
Simvastatin	189,3 ± 4,1 g	347,0 ± 12,2 g

5.4.1.2 Liver weights

At the end of the six weeks feeding programme, untreated, control animals had an average liver weight of 12.79 ± 0.39 g. Fenofibrate significantly increased liver weight to an average of 23.48 ± 0.71*# g (*$p<0.05$ vs control; #$p<0.05$ vs simvastatin) while simvastatin did not significantly alter liver weight (14.75 ± 0.92 g) (figure 5.4). The ratio of liver weight/body weight expressed in figure 5.5 showed similar trends.

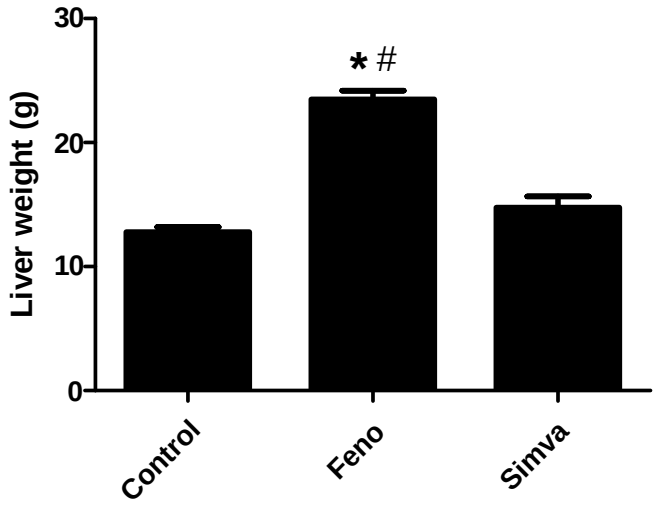

*Figure 5.4: Bar chart showing average rat liver weights of the three groups at the end of the 6 week feeding period. * p<0.05 vs control; # p<0.05 vs simvastatin (n = 20 per group).*

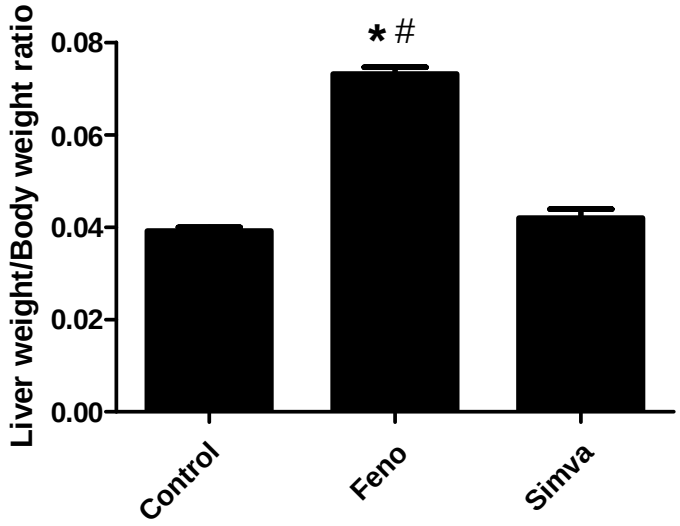

*Figure 5.5: Bar chart showing average rat liver weight/body weight ratio of the three groups at the end of the 6 week feeding period. * p<0.05 vs control; # p<0.05 vs simvastatin (n = 20 per group).*

5.4.1.3 Food and Water intake

The average food (figure 5.6) and water (figure 5.7) intake were measured per cage/day for 24 rats. Three rats were housed per cage. Simvastatin treated animals showed a small, but significantly greater food intake than control animals. Fenofibrate treated animals also showed a modest, but significantly higher food and water intake compared to control and simvastatin treated animals: **Food** – Control: 65.17 ± 0.54 g; Fenofibrate: 73.22 ± 0.69 g*#; Simvastatin: 67.85± 0.67 g; *p<0.05 vs control; #p<0.05 vs simvastatin; **Water** - Control: 97.13 ± 2.26 ml; Fenofibrate: 110.80 ± 2.20 ml*#; Simvastatin: 92.18 ± 2.40 ml; *p<0.05 vs control; #p<0.05 vs simvastatin.

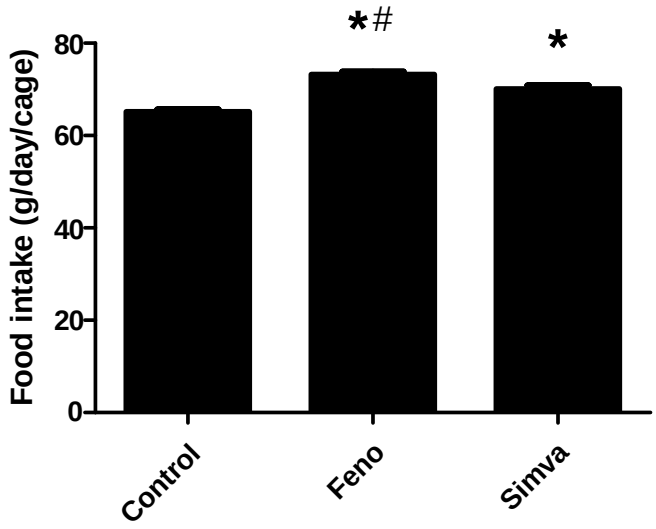

*Figure 5.6: Bar chart showing average food intake of the three groups for the duration of the 6 week feeding period, * p<0.05 vs control; # p<0.05 vs simvastatin (n = 24 rats per group).*

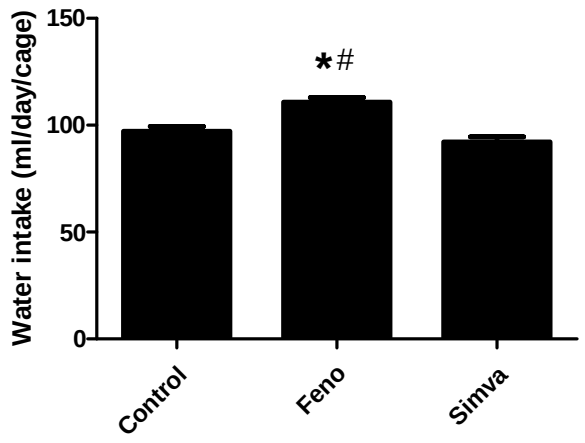

*Figure 5.7: Bar chart showing average water intake of the three groups for the duration of the 6 week feeding period, * p<0.05 vs control; # p<0.05 vs simvastatin (n = 20 rats per group).*

5.4.2 Serum: Nitrites and nitrates

In order to investigate whether the 6 week drug treatment regimens would result in detectable increases in blood NO levels, the concentration of the major downstream metabolites of NO, nitrites and nitrates was measured in the serum of the animals. Fenofibrate significantly increased the concentration of nitrites and nitrates compared to the untreated, control groups (Control: 0.50 ± 1.43 µM; Fenofibrate: 6.20 ± 1.43 µM; p<0.05). Although simvastatin treatment increased the nitrites and nitrates in the serum, it failed to reach statistical significance (figure 5.8).

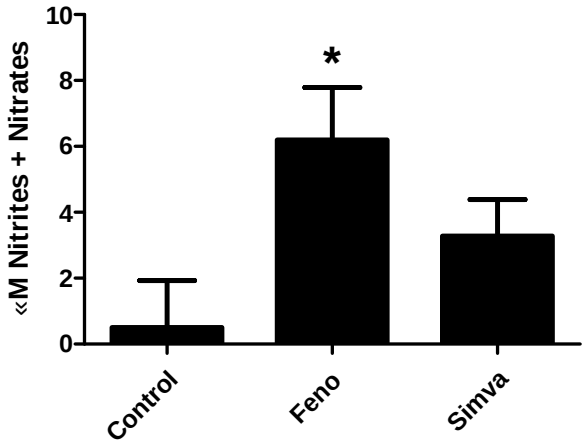

*Figure 5.8: Bar chart indicating the concentration of nitrites + nitrates in serum of the three groups (n = 6 / group; in duplicate); *p<0.05 vs control.*

5.4.3 Aortic ring investigations

Results are presented in the same order as indicated in chapter 4, figure 4.9 and 4.10.

5.4.3.1 Protocol 1: Phenylephrine – Acetylcholine

Cumulative contractions with phenylephrine (Phe) showed no changes in any of the treatment groups compared to untreated control groups (figure 5.9 A). Similarly, acetylcholine (Ach) induced relaxations were similar in untreated control, fenofibrate and simvastatin treated groups (figure 5.9 B).

5.4.3.2 Protocol 2: Serotonin

Cumulative contractions were also induced with a different vasoconstrictor, serotonin and figure 5.10 A, C and D show that 100 µM of serotonin induced a significant pro-contractile response in aortic rings from simvastatin treated animals compared to untreated control and fenofibrate groups (Control: 115.84 ± 3.44 %; Fenofibrate: 112.23 ± 6.19 %; Simvastatin: 137.80 ± 9.83*$ %; *$p<0.05$ vs control; $^{\$}p<0.05$ vs fenofibrate). Fenofibrate showed no changes in contraction compared to untreated controls (figure 5.10 B).

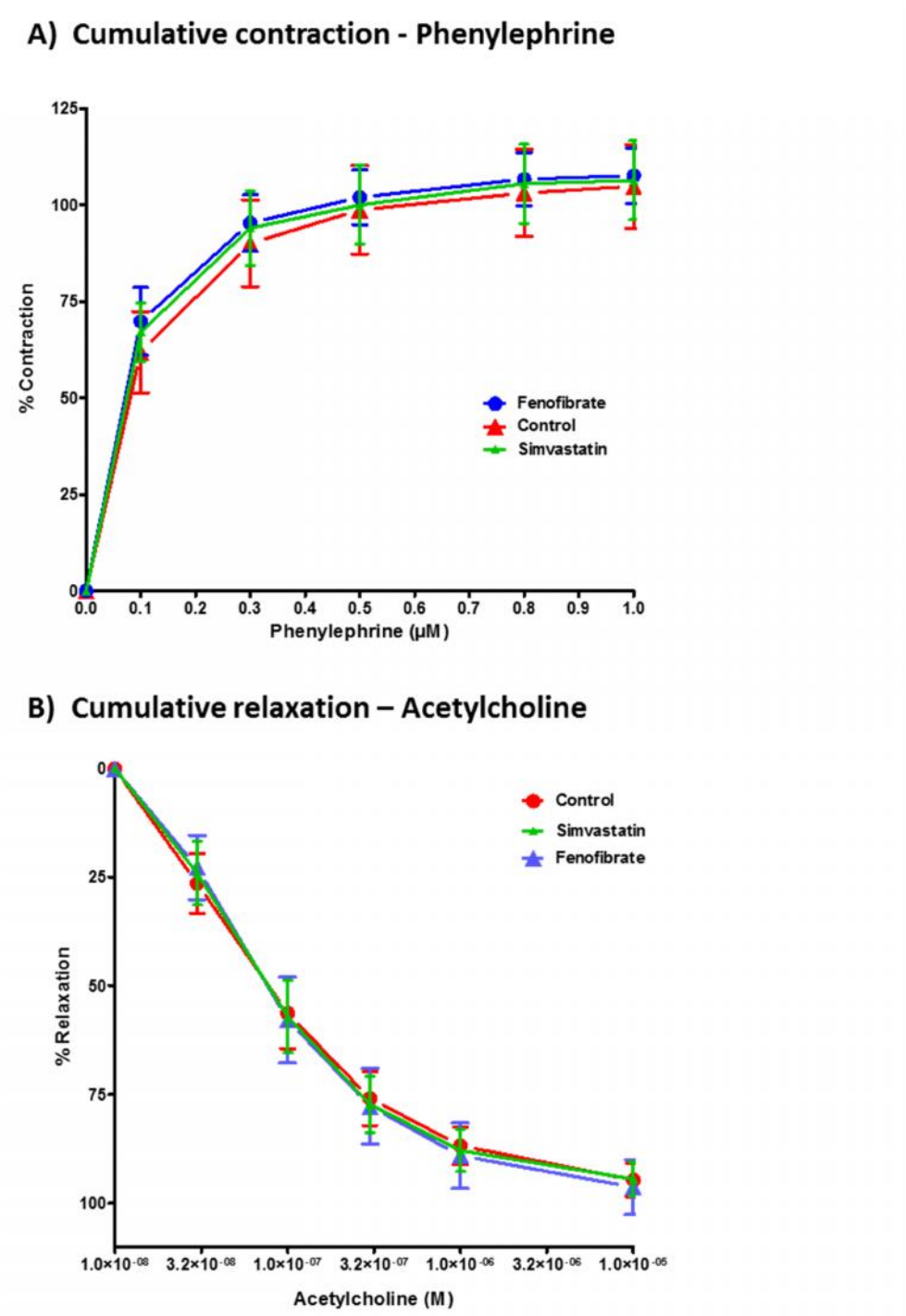

Figure 5.9: Graphs indicating the effects of in vivo fenofibrate and simvastatin treatment on phenylephrine induced contraction and acetylcholine induced relaxation. A) Aortic ring contractions in response to cumulative concentrations of phenylephrine followed by B) cumulative concentrations of acetylcholine (n = 7-8 per group).

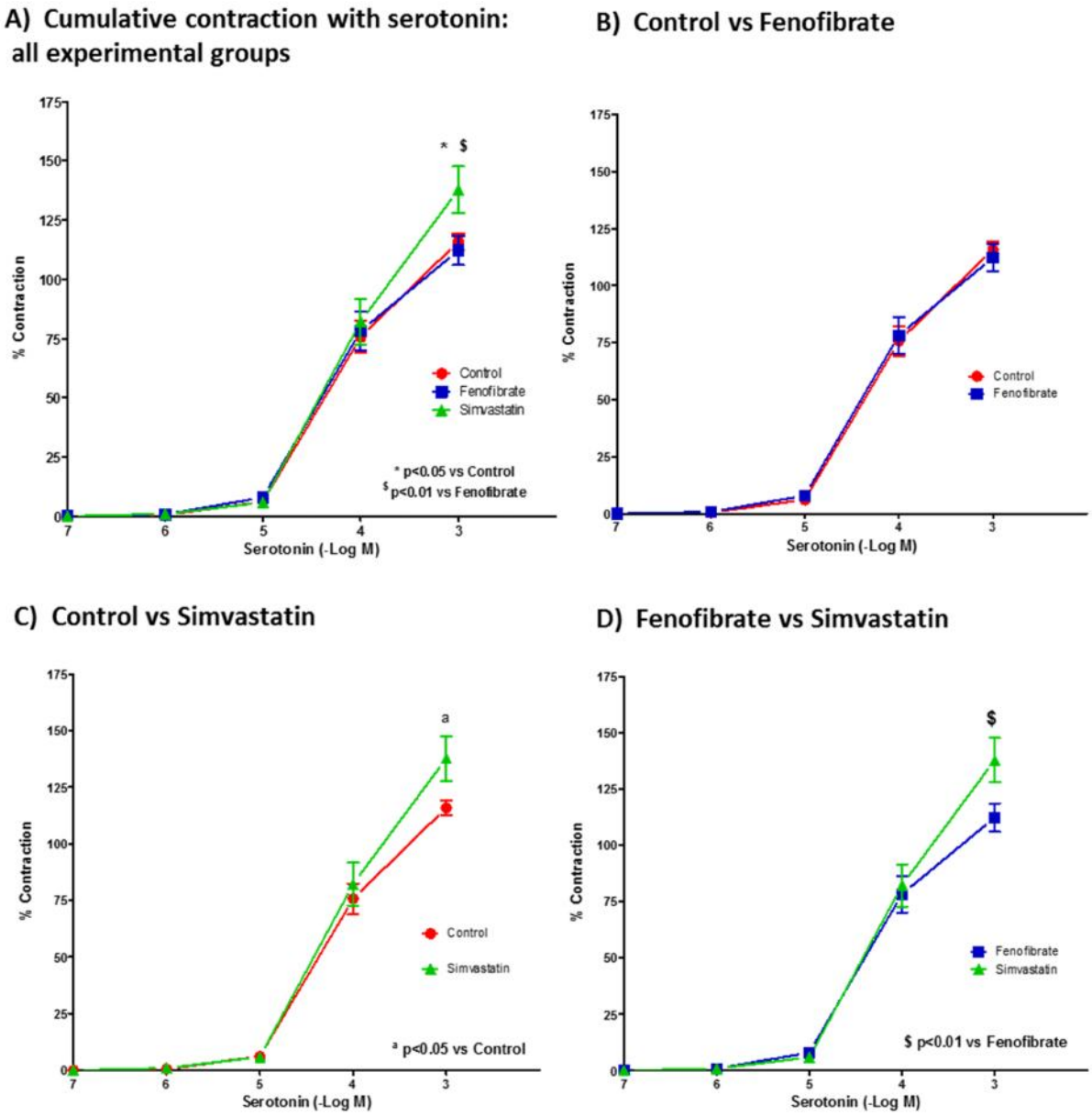

Figure 5.10: Graphs indicating the effects of in vivo fenofibrate and simvastatin treatment on serotonin induced contraction. A) Aortic ring contractions of all experimental groups, in response to cumulative concentrations of Serotonin. The experimental group results are further separated in B) for control and fenofibrate groups, C) control and simvastatin groups and D) simvastatin and fenofibrate groups (n = 5 per group).

5.4.3.3 Protocol 3: L-NMMA – Phenylephrine – Acetylcholine

Contraction studies

Figure 5.11 A clearly illustrates the outstanding pro-contractile effects exerted by 100 µM L-NMMA pre-administration in all the groups. L-NMMA pre-treatment significantly increased contraction in untreated control rings: **AUC** (**Control**: 88.2; **L-NMMA+Control**: 146.0; $p<0.001$), which was further underscored by measuring a 64% increase in contraction at the maximum cumulative Phe concentration in the L-NMMA+Control vs control groups (figure 5.11 A). Similar pro-contractile effects were observed in aortic rings from fenofibrate treated (**AUC**: **Fenofibrate**: 92.45; **L-NMMA+Fenofibrate**: 154.2; $p<0.0001$) (figure 5.11 A) and simvastatin treated (**AUC**: **Simvastatin:** 90.88; **L-NMMA+Simvastatin**: 171.0; $p<0.0001$) (figure 5.11 A). In the presence of L-NMMA, aortas from fenofibrate and simvastatin treated animals showed a 63% and 84% increase in contraction at the maximum cumulative Phe concentration respectively compared to rings without L-NMMA (figure 5.11 A).

In the next set of analyses, the three L-NMMA pre-treated groups were compared with each other. Comparisons of the **AUC** indicated that L-NMMA pre-administration exerted a significant pro-contractile response in the aortic rings from simvastatin treated rats compared to control groups (L-NMMA+Control: 146.0; L-NMMA+Simvastatin: 171.0; $p<0.05$) (figure 5.11 C). These findings were further underscored when the data at the first three cumulative Phe concentrations were compared: **100 nM** (L-NMMA+Control: 121.86 ± 7.33 %; L-NMMA+Simvastatin: 155.73 ± 9.69 %; $p<0.05$ vs control), **300 nM** (L-NMMA+Control: 150.01 ± 6.194 %; L-NMMA+Simvastatin: 176.68 ± 7.8 %; $p<0.05$ vs control) and **500 nM** (L-NMMA+Control: 158.53 ± 6.04 %; L-NMMA+Simvastatin: 184.18 ± 7.41 %; $p<0.05$ vs control) (figure 5.11 C). Furthermore, the AUC of aortic rings from simvastatin-treated animals was significantly greater than that of fenofibrate-treated animals (L-NMMA+Simvastatin: 171.0; L-NMMA+Fenofibrate: 152.4; $p<0.05$) (figure 5.11 D). No differences in contraction were found between untreated control + L-NMMA and fenofibrate treated + L-NMMA (figure 5.11 B).

Relaxation studies

As expected, figure 5.12 A clearly illustrates the anti-relaxation effects exerted by L-NMMA pre-administration in all groups. Aortic rings from control animals showed a significant reduction in

vasorelaxation in the presence of L-NMMA as calculated by the **AUC** (**Control:** 8903; **L-NMMA+Control**: 4139; $p<0.0001$) (figure 5.12 A), further underscored by the fact that L-NMMA pre-treatment resulted in a 50% reduction in relaxation at the maximum cumulative Ach concentration (figure 5.12 A). Similar results were observed in the fenofibrate treated groups (**AUC**: **Fenofibrate:** 8592; **L-NMMA+Fenofibrate**: 3427; $p<0.0001$) (figure 5.12 A) and simvastatin treated groups (**AUC: Simvastatin**: 8950; **L-NMMA+Simvastatin**: 2239; $p<0.0001$) (figure 5.12 A). In the presence of L-NMMA, aortic rings from fenofibrate and simvastatin treated animals resulted in a 51% and 68% decrease in relaxation at the maximum cumulative Ach concentration (figure 5.12 A).

With regards to Ach-induced relaxation following L-NMMA pre-incubation, the simvastatin-group showed an overall significant anti-relaxation response to Ach compared to the other groups as calculated by the **AUC** (L-NMMA+Control: 4139; L-NMMA+Fenofibrate: 3427; L-NMMA+Simvastatin: 2239*$^{\$}$; *$p<0.0001$ vs L-NMMA+Control; $^{\$}$ $p<0.05$ vs L-NMMA+Fenofibrate) (figure 5.12A). L-NMMA pre-incubation of aortic rings from the simvastatin group further exerted Ach concentration specific differences in relaxation compared to the L-NMMA+control group at the following cumulative Ach concentrations: **300 nM** (L-NMMA+Control: 32.27 ± 4.73 %; L-NMMA+Simvastatin: 13.63 ± 2.019 %; $p<0.01$ vs L-NMMA+Control), **1 µM** (L-NMMA+Control: 39.28 ± 5.35 %; L-NMMA+Simvastatin: 19.562 ± 2.49 %; $p<0.01$ vs L-NMMA+Control) and **10 µM** (L-NMMA+Control: 45.69 ± 5.78 %; L-NMMA+Simvastatin: 27.04 ± 3.09 %; $p<0.01$ vs L-NMMA+Control) (figure 5.12 C) as calculated by the two-way ANOVA test. The AUC of simvastatin-treated aortic rings was significantly less than that of fenofibrate-treated rings (L-NMMA+Simvastatin: 2239; L-NMMA+Fenofibrate: 3427; $p<0.05$) (figure 5.12 D). No differences in relaxation were found between untreated control + L-NMMA and fenofibrate treated + L-NMMA (figure 5.12 B).

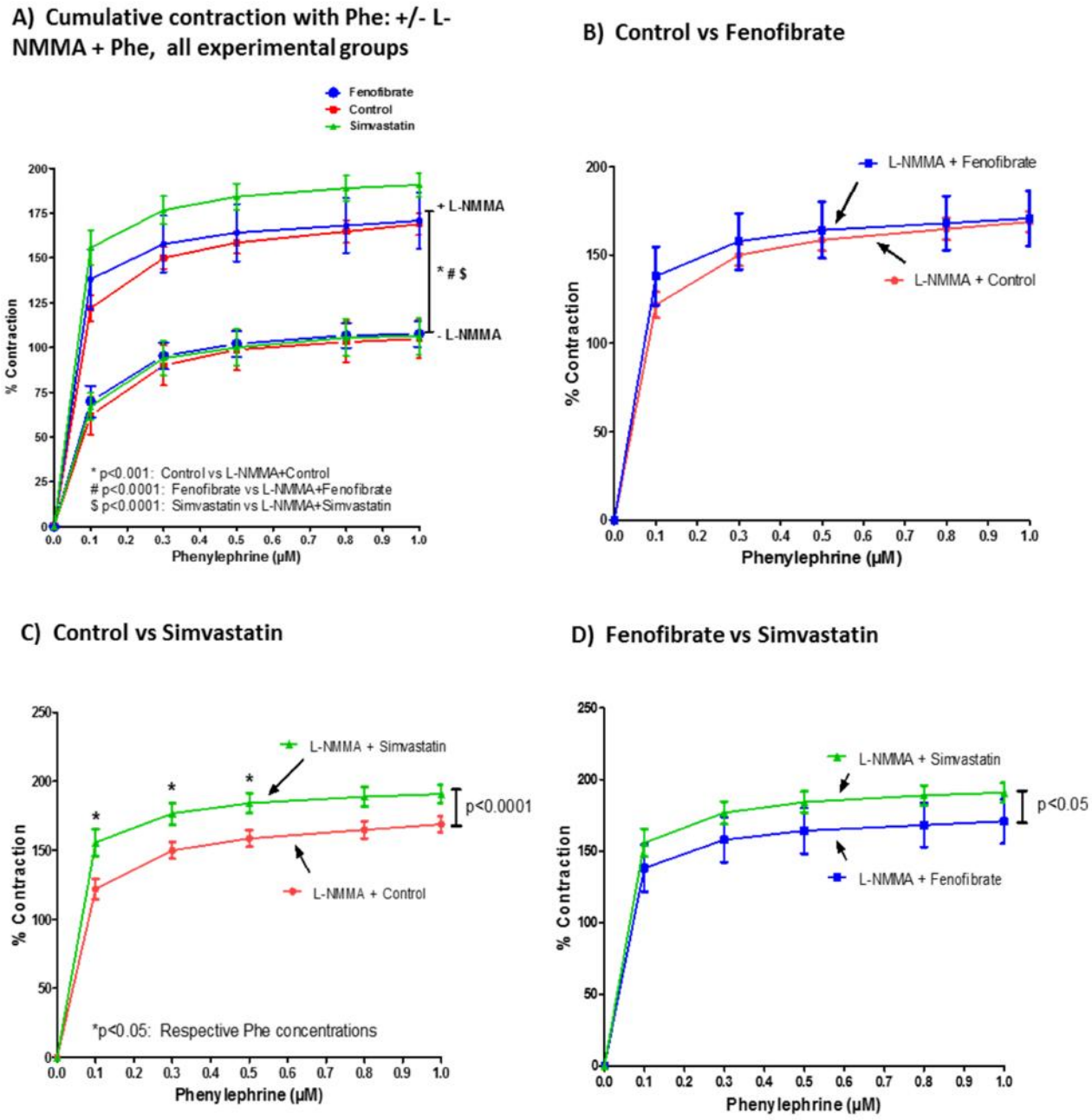

Figure 5.11: Graphs showing the effects of L-NMMA pre-administration on Phe-induced contraction. A) Graph indicates differences in contraction of aortic rings between control, fenofibrate and simvastatin treated groups incubated with or without L-NMMA. Results are further separated, showing aortic ring contractions from the B) L-NMMA+Control group versus L-NMMA+Fenofibrate group, C) L-NMMA+Control group versus L-NMMA+Simvastatin group and D) L-NMMA+Fenofibrate versus L-NMMA+Simvastatin; n = 6-7 per group.

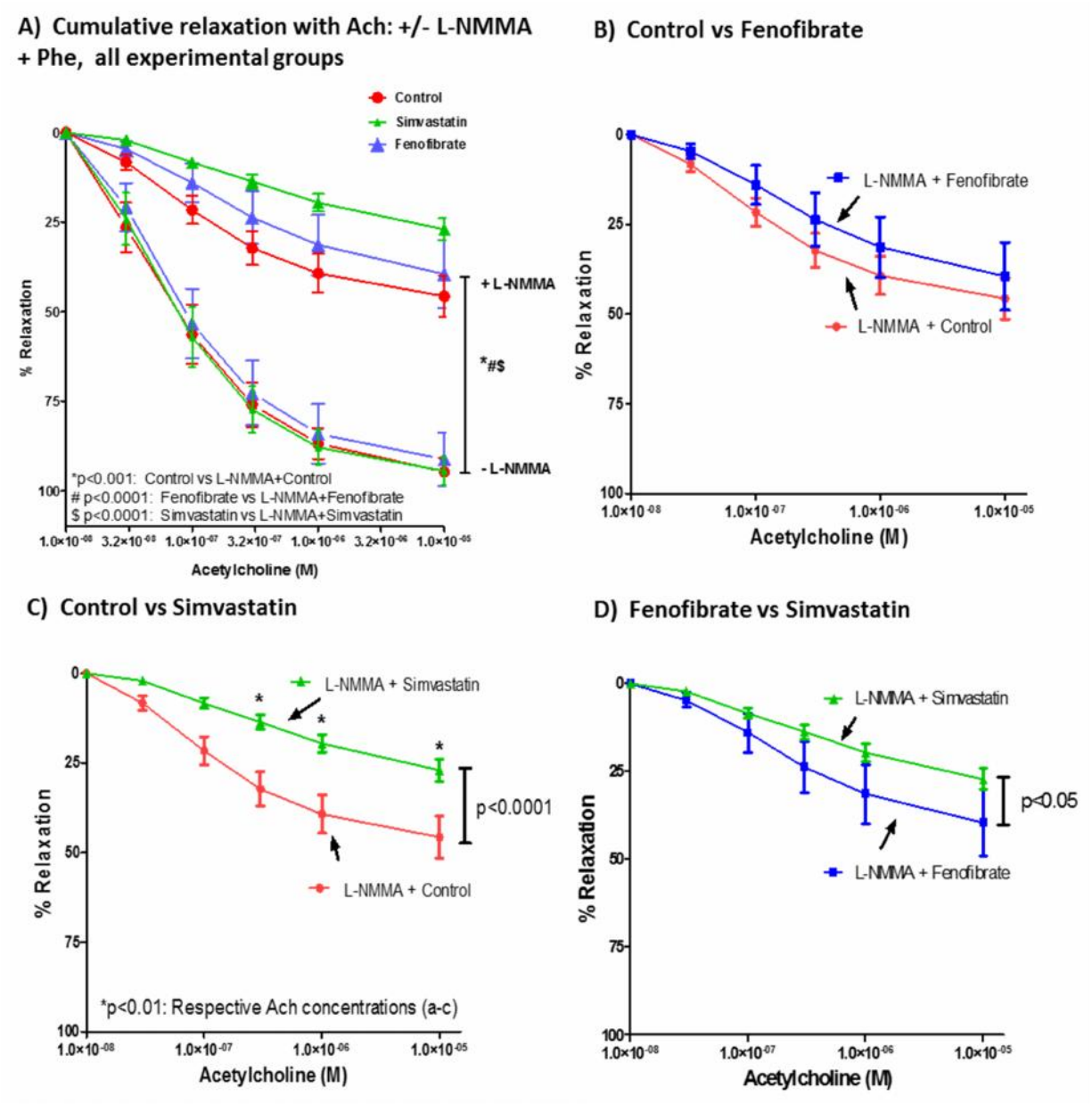

Figure 5.12: Graphs showing the effects of L-NMMA pre-administration on Ach-induced relaxation. A) Graph indicates differences in relaxation of aortic rings between control, fenofibrate and simvastatin treated groups incubated with or without L-NMMA. Results are further separated, showing aortic ring relaxations from the B) L-NMMA+Control group versus L-NMMA+Fenofibrate group, C) L-NMMA+Control group versus L-NMMA+Simvastatin group and D) L-NMMA+Fenofibrate versus L-NMMA+Simvastatin; n = 6-7 per group.

5.4.3.4 Protocol 4: 1400W – Phenylephrine – Acetylcholine

Contraction studies

Figure 5.13 (A and F) shows the significant pro-contractile effect exerted by pre-administration of the iNOS inhibitor, 1400W (80 µM) in the aortic rings from simvastatin treated animals; **AUC**: Simvastatin: 90.88; 1400W+Simvastatin: 120.8; $p<0.0001$). In the next set of analyses, the three 1400W pre-treated groups were compared with each other. 1400W pre-incubation elicited a pronounced overall pro-contractile effect on aortic rings from simvastatin-treated animals as shown by the **AUC** (1400W+Control: 79.45; 1400W+Fenofibrate: 75.09; 1400W+Simvastatin: 120.8*$^{\$}$; *$p<0.0001$ vs 1400W+Control; $^{\$}$ $p<0.05$ vs 1400W+Fenofibrate) (figure 5.13 B and C). 1400W pre-incubation did not change the contractile responses of aortic rings in the fenofibrate-treated group compared to control aortic rings. 1400W pre-incubation in the simvastatin treated aortic rings further exerted Phe-induced concentration specific differences in contraction compared to control and fenofibrate groups at the following cumulative Phe concentrations: **500 nM** (1400W+Control: 88.41 ± 12.69 %; 1400W+Fenofibrate: 85.08 ± 11.88 %; 1400W+Simvastatin: 133.50 ± 15.33*$^{\$}$ %; *$p<0.05$ vs Control; $^{\$}$ $p<0.05$ vs Fenofibrate), **800 nM** (1400W+Control: 95.87 ± 12.87 %; 1400W+Fenofibrate: 90.65 ± 12.07 %; 1400W+Simvastatin: 140.58 ± 15.54*$^{\$}$ %; *$p<0.05$ vs Control; $^{\$}$ $p<0.05$ vs Fenofibrate) and **1 µM** (1400W+Control: 97.45 ± 12.79 %; 1400W+Fenofibrate: 91.29 ± 12.69 %; 1400W+Simvastatin: 141.92 ± 15.64*$^{\$}$ %; *$p<0.05$ vs Control; $^{\$}$ $p<0.05$ vs Fenofibrate) (figure 5.13 C and D) as calculated by a two-way ANOVA .

The contraction of aortic rings from control animals was not affected by the presence or absence of 1400W (figure 5.13 D). Aortic rings from fenofibrate treated animals showed a significant pro-contractile response to Phe in the absence of 1400W pre-incubation; AUC: Fenofibrate: 92.45; 1400W+Fenofibrate: 75.09; $p<0.01$) (figure 5.13 E).

Relaxation studies

With regards to Ach induced relaxation, pre-administration of the iNOS inhibitor, 1400W did not exert any effects on aortic ring relaxation in any of the groups when compared to their treatment-matched controls without 1400W pre-administration (figure 5.14 A). Pre-incubation with 1400W

in the simvastatin aortic rings did however result in an overall anti-relaxation response to Ach as calculated by the AUC compared to the other groups pre-incubated with 1400W (1400W+Control: 9379; 1400W+Fenofibrate: 9652; 1400W+Simvastatin: 8380*$; *p<0.0001 vs 1400W+Control; $ p<0.01 vs 1400W+Fenofibrate) (figure 5.14 B, C and D). The 1400W+simvastatin group further showed Ach concentration specific differences in relaxation compared to control rings pre-incubated with 1400W at the following cumulative Ach concentrations: **30 nM** (1400W+ Control: 37.82 ± 3.05 %; 1400W+Simvastatin: 16.45 ± 1.86 %; p<0.05), **100 nM** (1400W+Control: 73.02 ± 3.52 %; 1400W+Simvastatin: 50.71 ± 3.76 %; p<0.05) and **300 nM** (1400W+Control: 88.00 ± 3.30 %; 1400W+Simvastatin: 72.03 ± 4.57 %; p<0.05 vs control) (figure 5.14 C) as calculated by a two-way ANOVA .

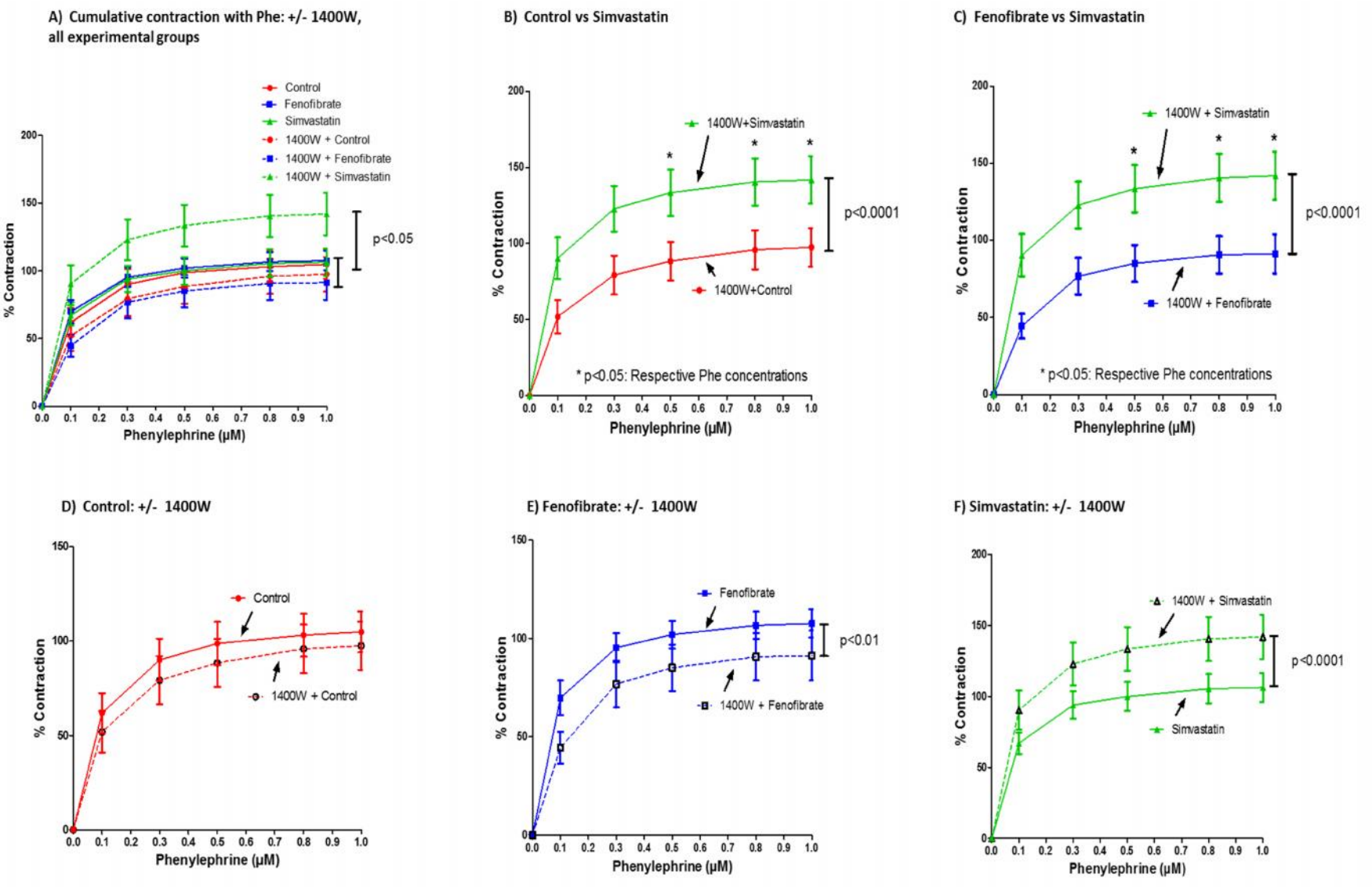

Figure 5.13: Graphs showing the effects of 1400W pre-administration on Phe-induced contraction. A) Graph indicates differences in contraction of aortic rings between control, fenofibrate and simvastatin treated groups incubated with or without 1400W. Results are further

separated, showing aortic ring contractions from the B) 1400W+Simvastatin group and 1400W+Control group, C) 1400W+Fenofibrate and 1400W+Simvastatin group, D) Control group with or without 1400W; E) Fenofibrate group with or without 1400W; F) Simvastatin group with or without 1400W;n = 6-7 per group.

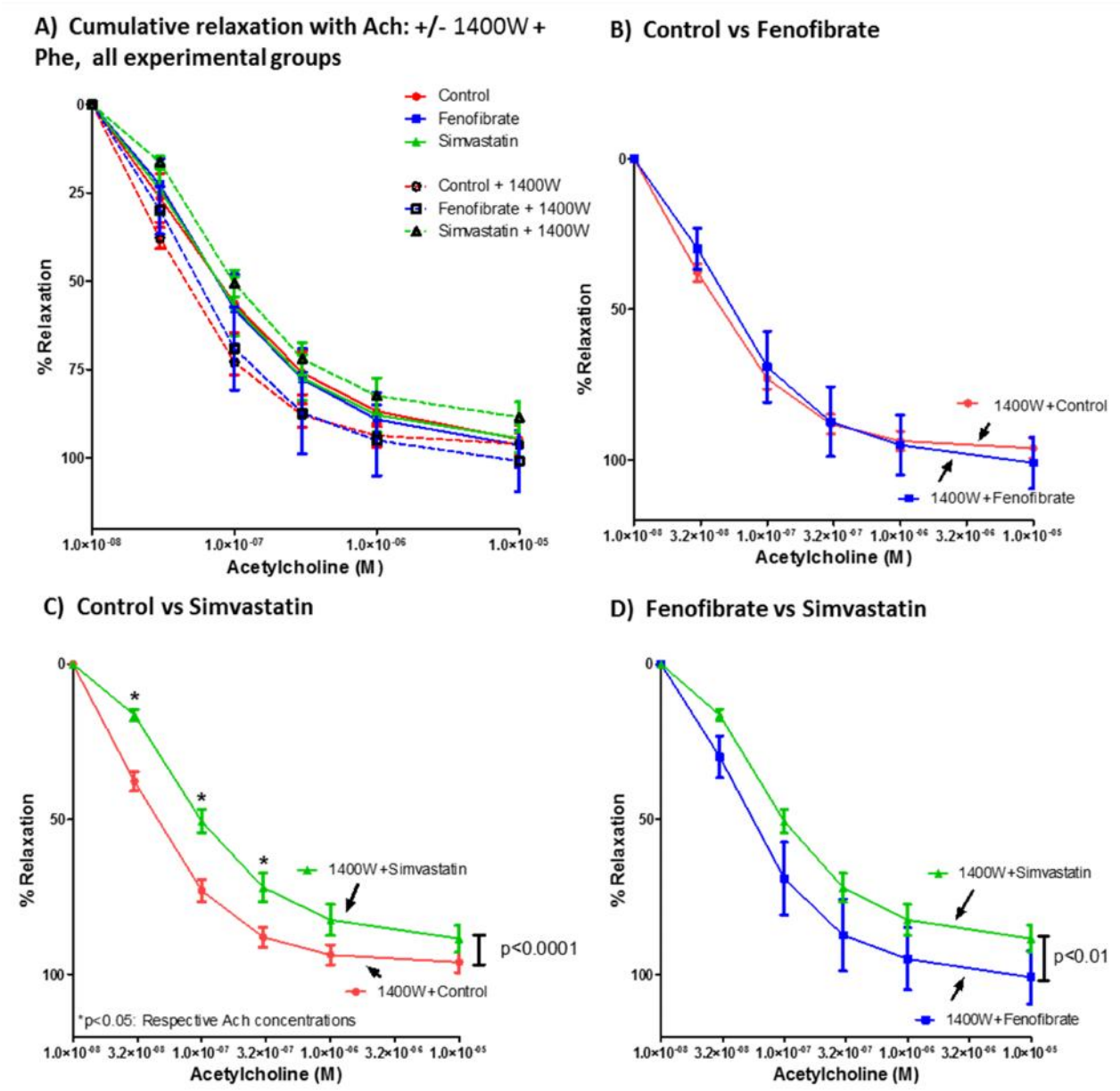

Figure 5.14: Graphs showing the effects of 1400W pre-administration on Ach-induced relaxation. A) Graph indicates effects on relaxation of aortic rings between control, fenofibrate and simvastatin treated groups incubated with or without 1400W. Results are further separated, showing aortic ring relaxations from the B) 1400W+control group and 1400W+Fenofibrate group, C) 1400W+Control group and 1400W+Simvastatin group, D) 1400W+Fenofibrate group and 1400W+Simvastatin group,; n = 6-7 per group.

5.4.4 Signalling investigations

In order to observe whether the functional data of the vascular reactivity investigations could be explained by changes in intracellular signal transduction pathways, western blot analyses were performed on frozen aortic tissue of control, fenofibrate and simvastatin treated animals. Total protein expression is expressed as a ratio of loading control (β-tubulin) and these values were used to calculate the phosphorylation/total ratio. Controls are expressed as 1.

5.4.4.1 NOS

No statistically significant changes were found in total-eNOS expression, phospho-eNOS Ser 1177 or the ratio of P/T eNOS in any of the experimental groups (figure 5.15 B - D).

With regards to iNOS expression, fenofibrate and simvastatin significantly increased iNOS expression in aortic tissue (Control: 1; Fenofibrate: 1.42 ± 0.15*; Simvastatin: 1.84 ± 0.06*; *p<0.05 vs Control) (figure 5.16).

nNOS expression could not be detected.

5.4.4.2 AMPK

Fenofibrate as well as simvastatin treated aortic tissue showed significantly lower expression of AMPK (Control: 1 Fenofibrate: 0.74 ± 0.02*; Simvastatin: 0.78 ± 0.05*; *p<0.05 vs Control) (figure 5.17 B). Simvastatin treated aortic tissue further showed lower levels of phospho-AMPK (Thr 172) (Control: 1; Simvastatin: 0.62 ± 0.07; p<0.05) (figure 5.17 C). No changes were found in the phospho/total ratio of AMPK (figure 5.17 D).

5.4.4.3 PKB/Akt

Fenofibrate treatment significantly increased PKB/Akt expression (Control: 1; Fenofibrate: 1.33 ± 0.04; p<0.05) (figure 5.18 B). Simvastatin treatment significantly decreased phosphorylation of PKB/Akt (Control: 1; Simvastatin: 0.37 ± 0.04; p<0.05) (figure 5.18 C) while both treatments resulted in a significantly reduced phospho/total ratio of PKB/Akt (Control: 1; Fenofibrate: 0.35 ± 0.17*; Simvastatin: 0.28 ± 0.05*; *p<0.05 vs Control) (figure 5.18 D).

5.4.4.4 HSP 90

Fenofibrate treatment did not change HSP 90 expression in aortic tissue, however simvastatin treatment significantly reduced HSP 90 expression (Control: 1; Simvastatin: 0.50 ± 0.01; $p<0.05$) (figure 5.19 B).

5.4.4.5 Nitrotyrosine and IκBα expression

Fenofibrate treatment did not change nitrotyrosine levels, however simvastatin treatment significantly reduced nitrotyrosine levels compared to untreated controls (Control: 1; Simvastatin: 0.59 ± 0.05; $p<0.05$) (figure 5.20 C). Similarly, fenofibrate treatment had no effect on IκBα expression, however simvastatin treatment significantly reduced IκBα expression compared to untreated controls and the fenofibrate treated group (Control: 1; Fenofibrate: 1.12 ± 0.22; Simvastatin: 0.47 ± 0.06; $p<0.05$) (figure 5.20 D)

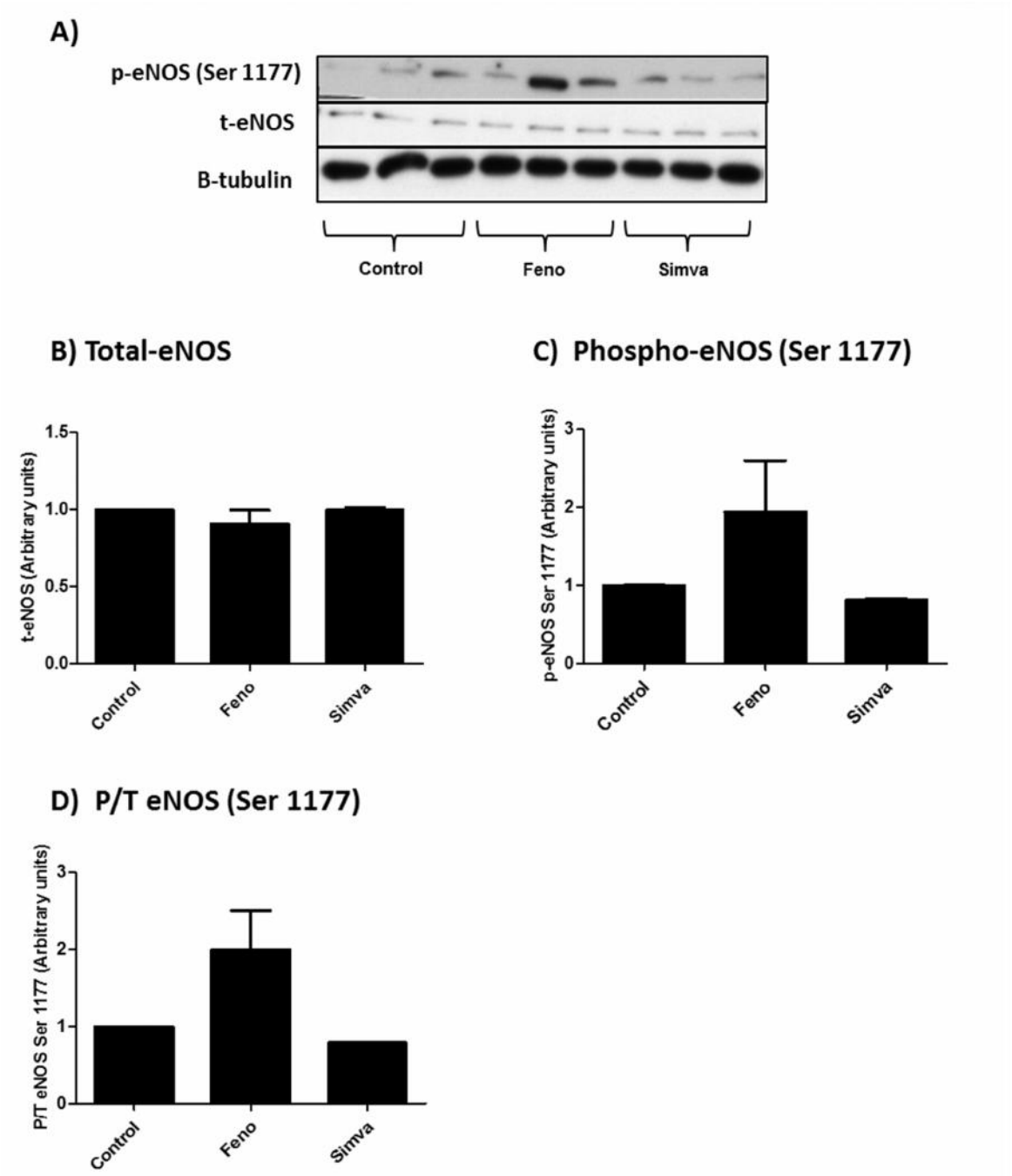

*Figure 5.15: Bar charts indicating changes in eNOS expression and phosphorylation (Ser 1177) in aortic tissue from rats receiving fenofibrate and simvastatin treatment in vivo. A) Representative western blots indicating total-eNOS, phospho-eNOS (Ser 1177) and β-tubulin. B) Analysed data for total-eNOS. C) Analysed data for phospho-eNOS (Ser 1177). D) Phosphorylated over total (P/T) ratio of eNOS Ser 1177. * $p<0.05$ vs Control; $n = 3$.*

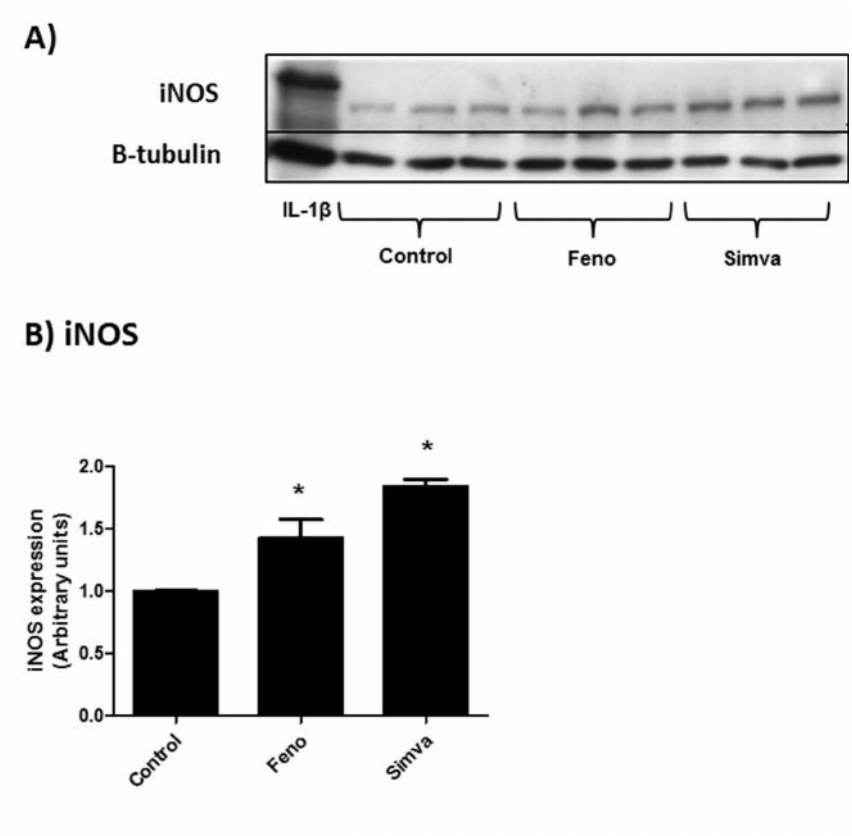

*Figure 5.16: Bar charts indicating changes in iNOS expression in aortic tissue from rats receiving fenofibrate and simvastatin treatment in vivo. A) Representative western blots indicating iNOS expression and β-tubulin. B) Analysed data for HSP 90. Interleukin-1β (IL-1β) included as positive control for iNOS. * $p<0.05$ vs Control, $n = 3$.*

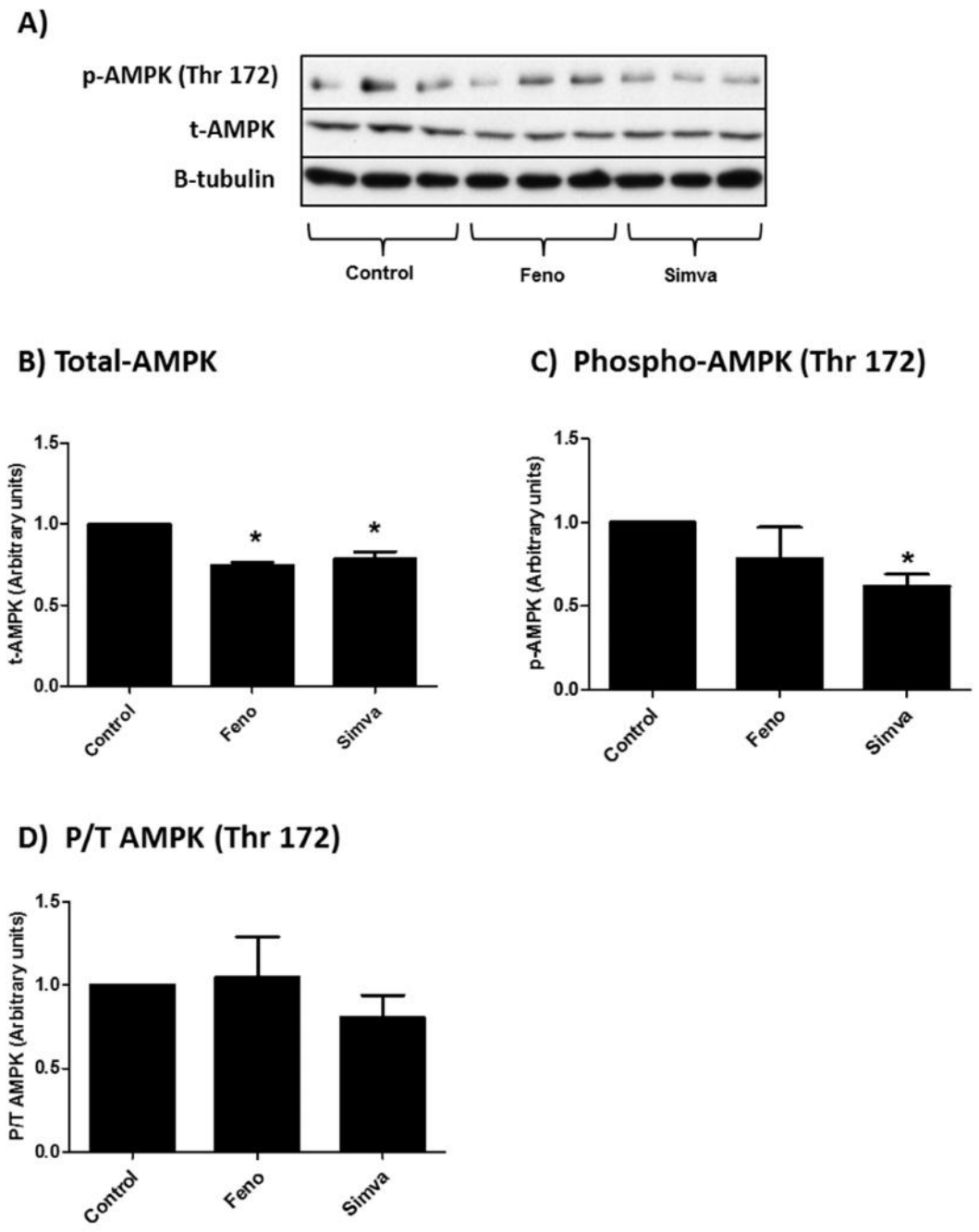

*Figure 5.17: Bar charts indicating changes in AMPK expression and phosphorylation (Thr 172) in aortic tissue from rats receiving fenofibrate and simvastatin treatment in vivo. A) Representative western blots indicating total-AMPK, phospho-AMPK (Thr 172) and β-tubulin. B) Analysed data for total-AMPK. C) Analysed results for phospho-AMPK (Thr 172). D) Phosphorylated over total (P/T) ratio of AMPK (Thr 172). * p<0.05 vs Control; n = 3.*

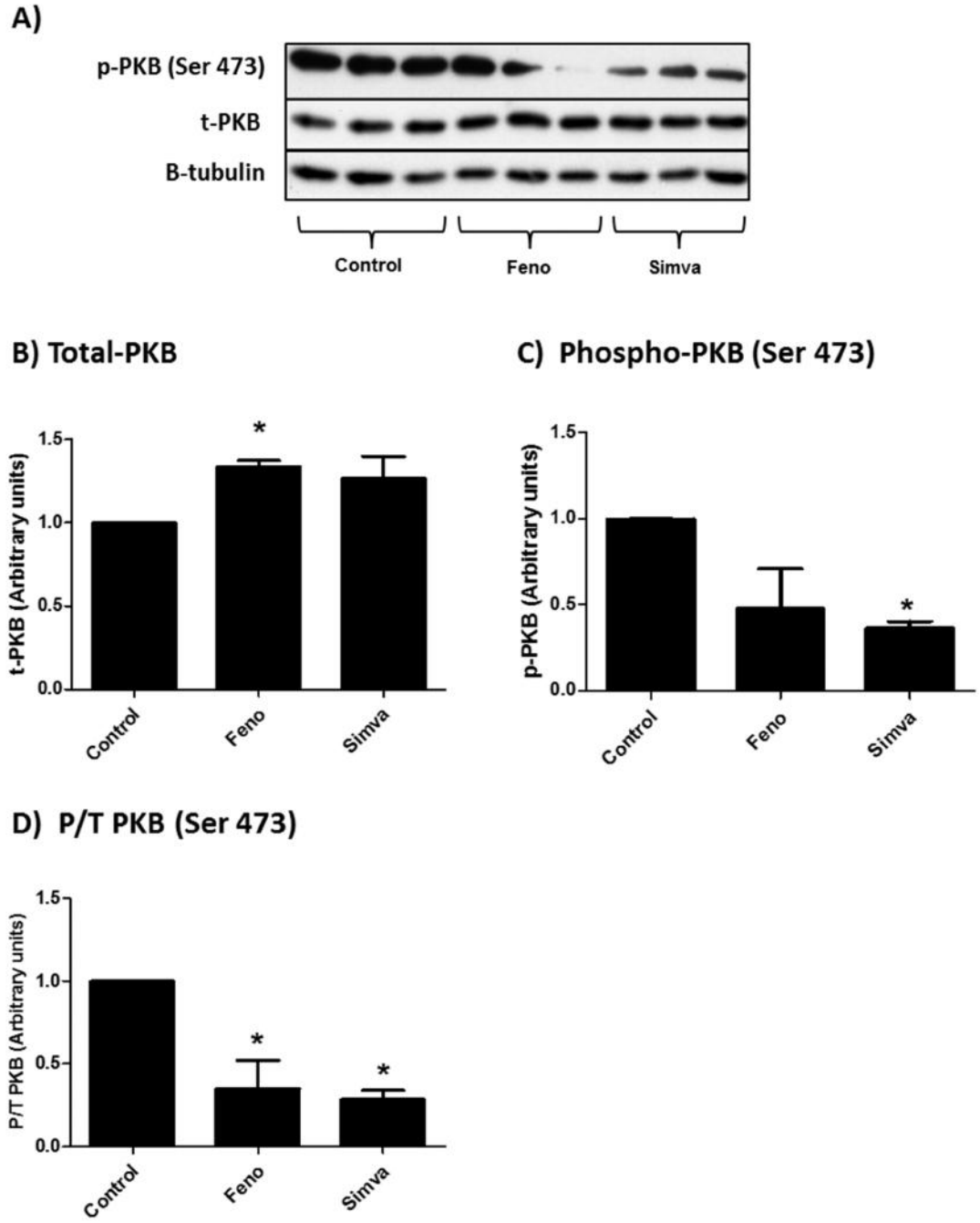

*Figure 5.18: Bar charts indicating changes in PKB expression and phosphorylation (Ser 473) in aortic tissue from rats receiving fenofibrate and simvastatin treatment in vivo. A) Representative western blots indicating total-PKB, phospho-PKB (Ser 473) and β-tubulin. B) Analysed data for total-PKB. C) Analysed results for phospho-PKB (Ser 473). D) Phosphorylated over total (P/T) ratio of PKB (Ser 473). * $p<0.05$ vs Control; $n = 3$.*

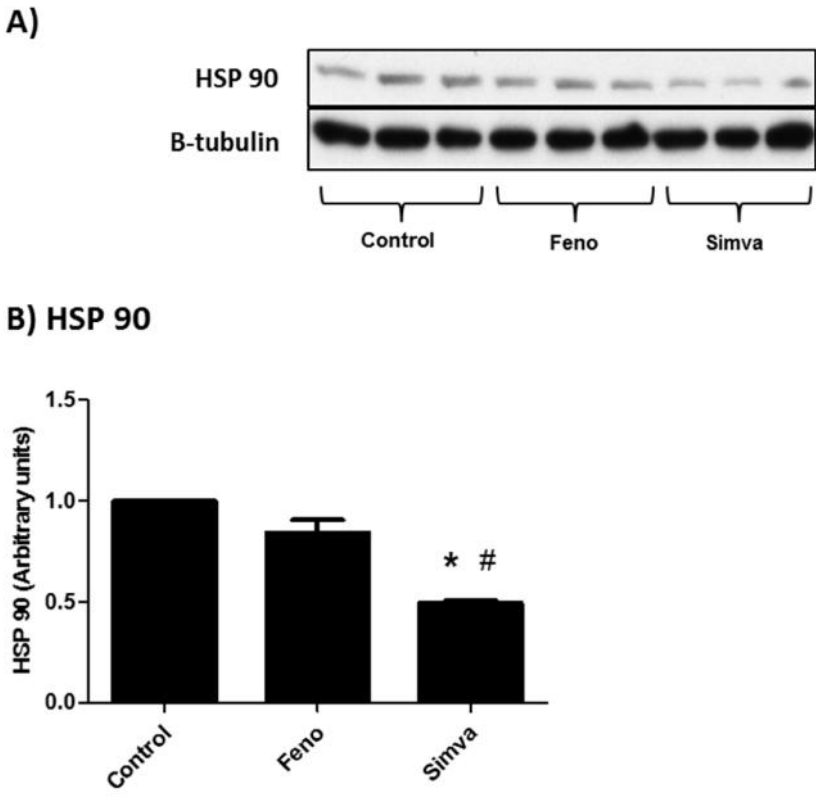

*Figure 5.19: Bar charts indicating changes in HSP 90 expression in aortic tissue from rats receiving fenofibrate and simvastatin treatment in vivo. A) Representative western blots indicating HSP 90 expression and β-tubulin. B) Analysed data for HSP 90. * $p<0.05$ vs Control, # $p<0.05$ vs Fenofibrate; n = 3.*

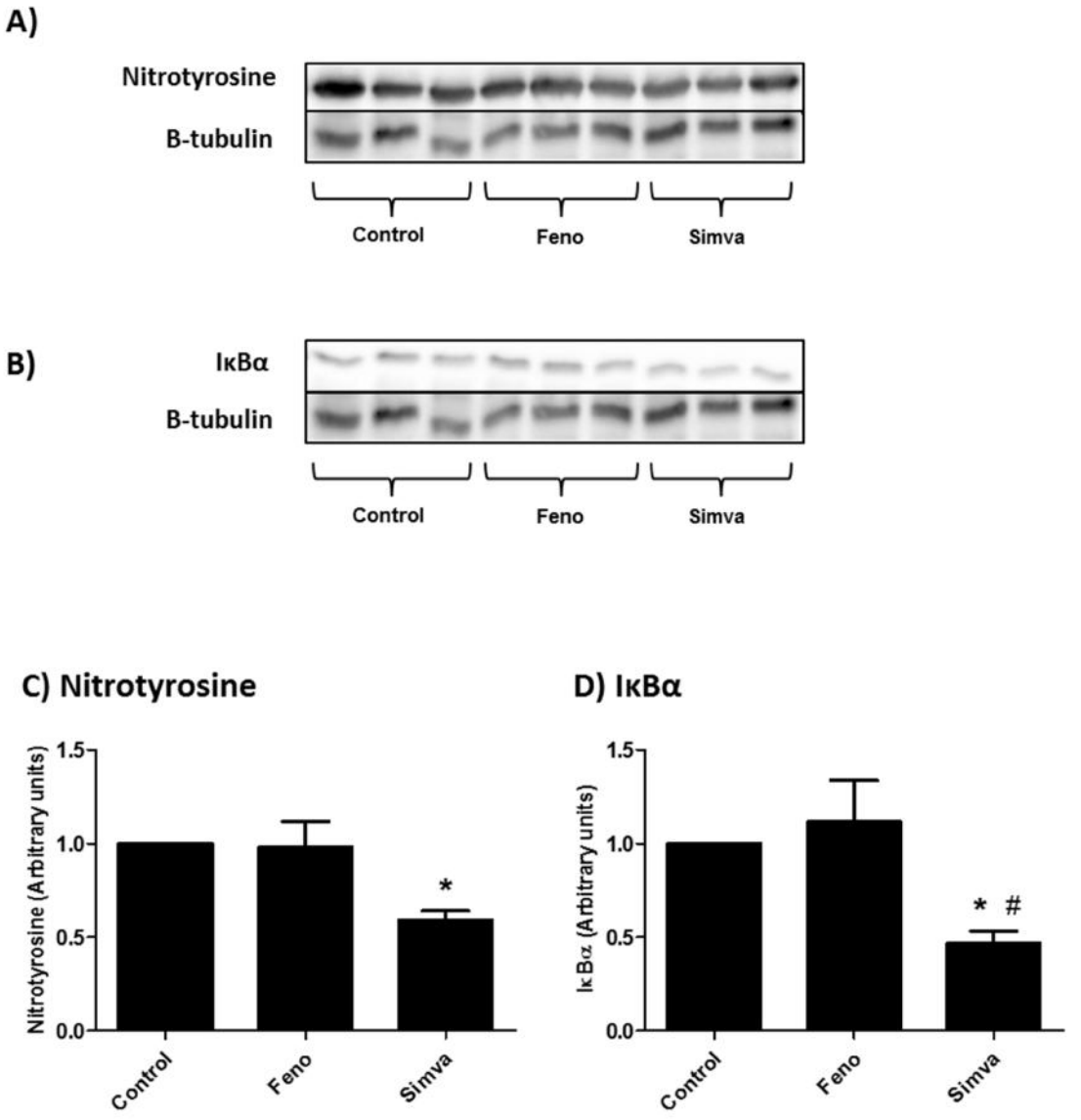

*Figure 5.20: Bar charts indicating changes in nitrotyrosine and IκBα expression in aortic tissue from rats receiving fenofibrate and simvastatin treatment in vivo. A) Representative western blots indicating nitrotyrosine and β-tubulin. B) Representative western blots indicating IκBα expression and β-tubulin. C) Analysed data for nitrotyrosine. D) Analysed data for IκBα expression. * $p<0.05$ vs Control; $^{\#}p<0.05$ vs Fenofibrate; $n = 3$.*

5.5 Discussion

5.5.1 Ex vivo fenofibrate administration

Figure 5.1 shows aortic rings from healthy rats, precontracted with phenylephrine (Phe), to relax in a concentration-dependent manner in response to acetylcholine (Ach). Cumulative concentrations of Ach resulted in ~ 75% maximum relaxation of aortic rings. Pre-treatment with the NOS-inhibitor, L-NMMA resulted in a significant inhibition of relaxation, confirming the involvement of NOS-derived NO to relaxation. These experiments confirmed that the vascular isometric tension model was functional.

In these experiments, fenofibrate was added *ex vivo* directly to the aortic rings in the organ bath. The acute ability of fenofibrate to induce vaso-relaxation was investigated by pre-contracting aortic rings with the α-adrenergic stimulant, Phe, followed by cumulative concentrations (50 µM – 125 µM) of fenofibrate (figure 5.2). The results from the *in vitro* experiments in chapter 3 demonstrated that 1 hour treatment with 50 µM fenofibrate increased NO production by ~ 50 – 60% in cardiac microvascular endothelial cells (CMECs) (figure 3.13A, 3.24A and 3.26A). Similar increases in NO were shown in aortic endothelial cells (AECs) as measured by the Griess assay (figure 3.24C and 3.26C). In the current chapter, we showed that *ex vivo* administration of fenofibrate elicited a modest, yet significant ~ 22% vasodilatory response in the aortic rings, which was mediated by NO as confirmed by the L-NMMA inhibition studies (figure 5.2A). However, the effect of fenofibrate should be seen in context when compared to the pro-relaxation effects elicited by Ach (~75%) (figure 5.2B). Although Liu *et al*. (2012) showed a ~ 73% relaxation in Sprague–Dawley rat aortic rings exposed to *ex vivo* administration of fenofibrate, this was achieved with a very high concentration (2.2 mM), 17-fold higher than the maximum cumulative concentration used in the current study.

Although both fenofibrate and Ach resulted in NOS-dependent vasodilation, a pronounced difference was observed in the time response. Ach showed an instantaneous vasodilatory effect after administration of the cumulative concentrations, and the maximum relaxation was observed within an average of ~ 3-5 minutes. Maximum relaxation with cumulative fenofibrate administration was only reached after ~ 30 minutes. These differences can be explained by diverse mechanistic actions of Ach and fenofibrate. Acetylcholine binds to receptors on the

endothelial cell surface (Davignon & Ganz 2004) resulting in increased levels of intracellular calcium, followed by eNOS activation and NO-production (Bredt & Snyder 1990). Fenofibrate on the other hand, binds to PPAR-α which forms a complex with retinoid-X-receptor and translocates to the nucleus to perform transcriptional actions, a relatively time-consuming process that is unlikely to lend itself to immediate detectable changes. Furthermore, previous studies on endothelial cells have shown that fenofibrate increases AMPK activation, resulting in down-stream activation of eNOS *ex vivo* (Qu *et al.* 2012) and *in vitro* (Murakami *et al*. 2006). In summary, compared to Ach, e*x vivo* administration of fenofibrate resulted in a slower and smaller NO response in the aortic rings.

5.5.2 In vivo fenofibrate and simvastatin treatments

5.5.2.1 Biometric data

Both fenofibrate and simvastatin treatment groups showed higher food intake than untreated control rats (figure 5.6). Additionally, fenofibrate treated animals had a higher water intake (figure 5.7). Amidst these observations, no statistical differences in body weight were found between groups (table 5.1). Fenofibrate binds to PPAR-α which is involved with transcription of genes involved in lipid metabolism and energy expenditure (Larsen *et al*., 2003) and has been shown to increase basal metabolic rate in rats (Mancini *et al.*, 2001). These factors can explain the higher food intake in the fenofibrate-treated animals. Increased food intake could have resulted in increased thirst and thus increased water intake. Simvastatin has not previously been associated with increased food intake or body weight gain in animal models (Carneado *et al*., 2002; Wang *et al*., 2013) which makes the higher food intake observed in this study interesting. Even though body weights were not statistically different, simvastatin treated animals were on average 25 g heavier than untreated controls and could possibly account for the small but significant increase in food intake.

5.5.2.2 Liver weight

Fenofibrate treatment increased average liver weights of the treated rats by ≈11 g (figure 5.4). Fruchart *et al.* (1999) and Deplanque *et al*. (2003) ascribed this phenomenon to peroxisome proliferation associated with fenofibrate treatment. Peroxisomes are subcellular organelles and in the liver they are usually about 0.5 – 1 microns in size. Peroxisomes are involved with break-

down of long-chain fatty acids and many chemicals are known to increase the number and size of peroxisome organelles in hepatocytes from rats and mice. This process is associated with replicative DNA synthesis and subsequent hepatocyte growth (Bently *et al*., 1993). Deplanque *et al.* (2003) further stated that enlarged livers are actually an indication of fenofibrate showing pharmacological activity. Increased liver weight can, however, also be due to signs of liver toxicity (Smyth *et al*., 2008). Therefore, histological analyses of the fenofibrate-induced enlarged livers will have to be performed in order to confirm or exclude this possibility. Simvastatin did not alter liver weight.

5.5.2.3 Serum nitrite and nitrate concentration

True to the *in vitro* and *ex vivo* results indicating increased NO production following fenofibrate treatment, the 6 weeks *in vivo* fenofibrate treatment programme resulted in increased levels of serum nitrites and nitrates (figure 5.8). Similar results have been found in pre-diabetic C57BL/6J mice treated with 100 mg/kg/day fenofibrate (Katayama *et al*., 2009) as well as in diabetic animals (Balakumar *et al*., 2009), and nicotine treated rats (Kaur *et al.*, 2010; Chakkarwar 2011) receiving 32 mg/kg/day fenofibrate. These results demonstrate the pleiotropic effects of fenofibrate on NO synthesis, and indicate an overall increase in NOS activity, resulting in increased levels of NO.

Simvastatin did not significantly alter the nitrite and nitrate levels in serum, although there was an increasing trend (figure 5.8). Similar results were shown by Carneado *et al.* (2002) who found that 1 mg/kg/day and 2 mg/kg/day simvastatin treatment did not alter the levels of the NO break-down products in Wistar Kyoto rats. The same study showed that reduced levels of nitrites and nitrates in spontaneously hypertensive rats were significantly increased by simvastatin treatment. Conversely, Perez-Guerrero *et al.* (2003) showed that normotensive Wistar rats had increased serum nitrite and nitrate levels after 1 mg/kg/day simvastatin treatment for 8 weeks. The NOS-inhibitor L-NAME significantly attenuated the levels, thereby confirming that increased NOS activation was the mechanism.

5.5.2.4 Vascular ring investigations

Phenylephrine - Acetylcholine

No differences were found in Phe-induced contractions (figure 5.9A) or Ach-induced relaxations (figure 5.9B) in any of the treatment groups. It is important to note that the aortic rings were harvested from healthy Wistar rats, in the absence of any pathophysiological changes. Changes brought about by experimental treatments are therefore expected to be less robust. Both fenofibrate (Qu *et al*., 2012) and simvastatin (Carneado *et al*., 2002) treatment in healthy animals failed to show changes in Phe induced contractions and Ach-induced relaxations of aortic rings from Wistar Kyoto or Wistar rats. Other studies did, however, show that fenofibrate treatment at a similar concentration used in the current study, resulted in improved vasodilatory effects in spontaneously hypertensive rats (SHR) (Qu *et al*., 2012) and aged (113 – 114 week) rats (Alvarez de Sotomayor *et al.,* 2007). Lower concentrations of fenofibrate such as 32 mg/kg/day (Chakkarwar 2011) and 30 mg/kg/day (Kaur *et al*., 2010) have similarly shown improvements in relaxation of nicotine treated rats. Simvastatin (1 mg/kg/day) also improved the vaso-dilatory response in SHR and at 2 mg/kg/day resulted in an anti-contractile effect (Carneado *et al.*, 2002). It further restored relaxation inhibited by the NOS-inhibitor L-NAME in Wistar rats (Perez-Guerrero *et al.*, 2003) and improved vascular relaxation of hereditary hyperglyceridemic rats at a concentration of 10 mg/kg/day (Török *et al*. 2007). It has to be noted that these studies used higher concentrations than the 0.5 mg/kg/day simvastatin used in the current study.

Serotonin

Aortic rings from fenofibrate treated animals showed no changes in contraction when stimulated with 100 µM serotonin. However, in contrast to the Phe-induced contraction studies, serotonin induced pro-contractile effects in aortic rings from simvastatin treated animals (figure 5.10 C). Serotonin was used as an alternative inducer of vasoconstriction, as it binds to a different vascular smooth muscle cell receptor (5-HT_{2A} receptor) (Bae *et al*., 2007) than phenylephrine and therefore provides the investigator with a different receptor-induced mechanism to study the contractility of the aortic rings. A possible explanation for the pro-contractile effects of serotonin in the simvastatin treated aortas could be related to RhoA. RhoA and its downstream kinase, RhoA kinase/ROCK, play an important role in vascular smooth muscle cell contraction and inhibition thereof shows promising results in the prevention of vascular diseases (Dong *et al*.,

2010; Nunes *et al*., 2010). ROCK activation results in dephosphorylation of myocin light chain phosphatase, and consequently increased phosphorylation of myocin light chain and increased contractility of smooth muscle cells (Yao *et al*., 2010) Simvastatin treatment results in inhibition of RhoA due to inhibition of its upstream isoprenoid, however RhoA can also be activated via 5-HT receptor activation. Guilluy *et al*. (2007) showed that 5-HT-receptors co-immunoprecipitated with RhoA *in vitro* and *in vivo,* a pathway independent of isoprenoid formation. The study showed that 5-HT results in activation of RhoA and if activation is prolonged (72 hours), RhoA will be depleted. It is proposed that the short period of the serotonin protocol (approximately 5-10 minutes of serotonin administration in the organ bath) was sufficient to activate RhoA and subsequent contraction of aortic rings.

L-NMMA, 1400W and NOS related signalling

Inhibition of NOS with L-NMMA resulted in increased pro-contractile (figure 5.11) and reduced vasodilatory responses (figure 5.12) in aortic rings from simvastatin treated rats compared to the responses observed in control and fenofibrate treated aortic rings. Although only simvastatin treated aortic rings showed these differences mentioned, it is important to note that contraction responses of untreated controls and fenofibrate treated rats were significantly increased and relaxation responses were significantly reduced by NOS inhibition with L-NMMA compared to control and fenofibrate rings without L-NMMA (figure 5.11 and 5.12). These results demonstrate the importance and involvement of NOS and NOS-derived NO in anti-contractile and vasodilatory responses of the vasculature. From the data, it appears as if simvastatin treated aortic rings were more susceptible to NOS inhibition compared to the other groups. The functional observations were not supported by western blot data of eNOS measurements, as the analyses showed no changes in eNOS protein expression or phosphorylation in aortic tissue in any of the treatment groups (figure 5.15). However, both fenofibrate and simvastatin treatment did increase iNOS expression compared to untreated control (figure 5.16). The involvement of iNOS-derived NO in anti-contractile responses was evident in figure 5.13 F. When iNOS was inhibited with 1400W, simvastatin treated aortic rings showed increased contraction compared to untreated control and fenofibrate groups (figure 5.13 B and C). While iNOS inhibition resulted in impaired dilation of simvastatin aortic rings compared to untreated controls and fenofibrate (figure 5.14 C and D), figure 5.14 B showed that there were no differences in the relaxation of simvastatin aortic rings

in the presence or absence of 1400W. iNOS expression was also significantly increased in the fenofibrate group, however inhibition thereof did not affect any of the vascular responses (figure 5.13 and 5.14). Long term (12 weeks) fenofibrate treatment has previously been shown to result in increased iNOS expression in pancreatic tissue. This was however associated with increased NF-κB activity (Liu *et al.,* 2011). The current study did not find increased NF-κB activity, which excludes this pathway as the mediator of increased iNOS expression. A similar finding was reported by Krishna *et al*. (2012) who found that fenofibrate increased iNOS expression in mouse aortic tissue.

Vascular tissue has been shown to express nNOS (Del Campo *et al*., 2011), however in the current study expression levels in aortic tissue were too low to be detected and therefore nNOS was unlikely to play an important role in vascular responses.

eNOS associated proteins

Fenofibrate treatment did not change eNOS expression in the aortic tissue, and although phospho-eNOS (Ser 1177) did not increase significantly, there appears to be an increasing trend (figure 5.15 C). Other studies were also not able to show any changes in eNOS expression in vascular tissue of rats or mice treated *in vivo* with fenofibrate (Deplanque *et al*., 2003; Alvarez de Sotomayor *et al.,* 2007). Katayama *et al*., (2009) showed increased phosphorylation of Ser 1177 in aortic tissue from mice treated with 100 mg/kg/day fenofibrate for 28 days and Becker *et al*. (2012) also showed increased phosphorylation in mice lung tissue. Considerably fewer studies investigated the phosphorylation status of eNOS in vascular tissue, and most were interested in eNOS expression. Associated with unchanged eNOS expression and activation, the upstream activator AMPK showed significantly decreased levels of expression (figure 5.17B). On the other hand, PKB/Akt expression was increased in aortic tissue after fenofibrate treatment (figure 5.18 B). HSP 90 showed no changes (figure 5.19B). Previous studies in vascular endothelial cells showed that fenofibrate treatment resulted in the up-regulation of AMPK and eNOS and thus increase NO production *in vitro* (Kim *et al.,* 2007; Tomizawa *et al*., 2011) and *in vivo* (Omae *et al*., 2012). The results of the current study contradict those of the mentioned studies.

Simvastatin similarly did not change eNOS expression or phosphorylation in aortic tissue and additionally resulted in significant down-regulation of the eNOS upstream molecules, AMPK,

PKB/Akt, as well as the chaperone HSP 90. Considering the greater vascular responsiveness of simvastatin aortic rings to inhibition of NOS (L-NMMA), this is an interesting finding. Simvastatin has been shown *in vivo* in Wistar rats to increase AMPK activation, resulting in increased eNOS (Ser 1177) activation and resultant vaso-dilation of aortas (Rossoni *et al*., 2011). Additionally, simvastatin has been shown in *in vivo* investigations of mouse aortic and myocardial tissue and *in vitro* in HUVECs, BAECs and human capillary derived endothelial cells (Sun *et al*., 2006) and human iliac artery endothelial cells (Xenos *et al*., 2005) to increase AMPK (Thr 172) phosphorylation. Due to the mechanistic action of simvastatin, namely inhibition of the RhoA/ROCK pathway it has been shown to result in increased PKB/Akt phosphorylation (Rikitake & Liao 2005); therefore our finding of PKB/Akt down-regulation was unexpected and difficult to explain.

ROS and inflammatory proteins

Nitrotyrosine expression was investigated as a marker of oxidative stress, and our data showed that fenofibrate had no effect on nitrotyrosine levels (figure 5.20 C). Simvastatin, however, decreased nitrotyrosine levels, demonstrating a potentially anti-oxidant effect. Numerous reports have been published showing the anti-oxidant effects of simvastatin *in vivo* (Girona *et al*., 1999; Alvarez De Sotomayor *et al*., 2000; Carneado *et al*., 2002; Heeba *et al*., 2007).

Fenofibrate treatment could also not alter the expression of the inflammatory marker IκBα, whereas simvastatin significantly decreased its expression, thereby indicating increased NF-κB activity (figure 5.20 D). The increase in NF-κB activity could explain increased iNOS expression as this association has previously been shown (Aktan 2004). Simvastatin is mostly associated with increased eNOS activity although it has been reported to increase iNOS expression in human brain microvascular endothelial cells (Pinzón-Daza *et al*., 2012). iNOS has been found to be upregulated in atherosclerotic lesions, however contrary to the traditional view of increased iNOS expression being associated with harmful effects, recent studies have shown that iNOS up-regulation was protective against thrombotic occlusion (Upmacis *et al*., 2011). Krishna *et al*., (2012) showed increased expression of iNOS in supra-renal aortas of mice associated with a protective effect against abdominal aortic aneurysm. These studies attest to the fact that

increased iNOS expression can contribute to protective mechanisms in the vasculature. Findings are summarized in figure 5.21 and 5.22.

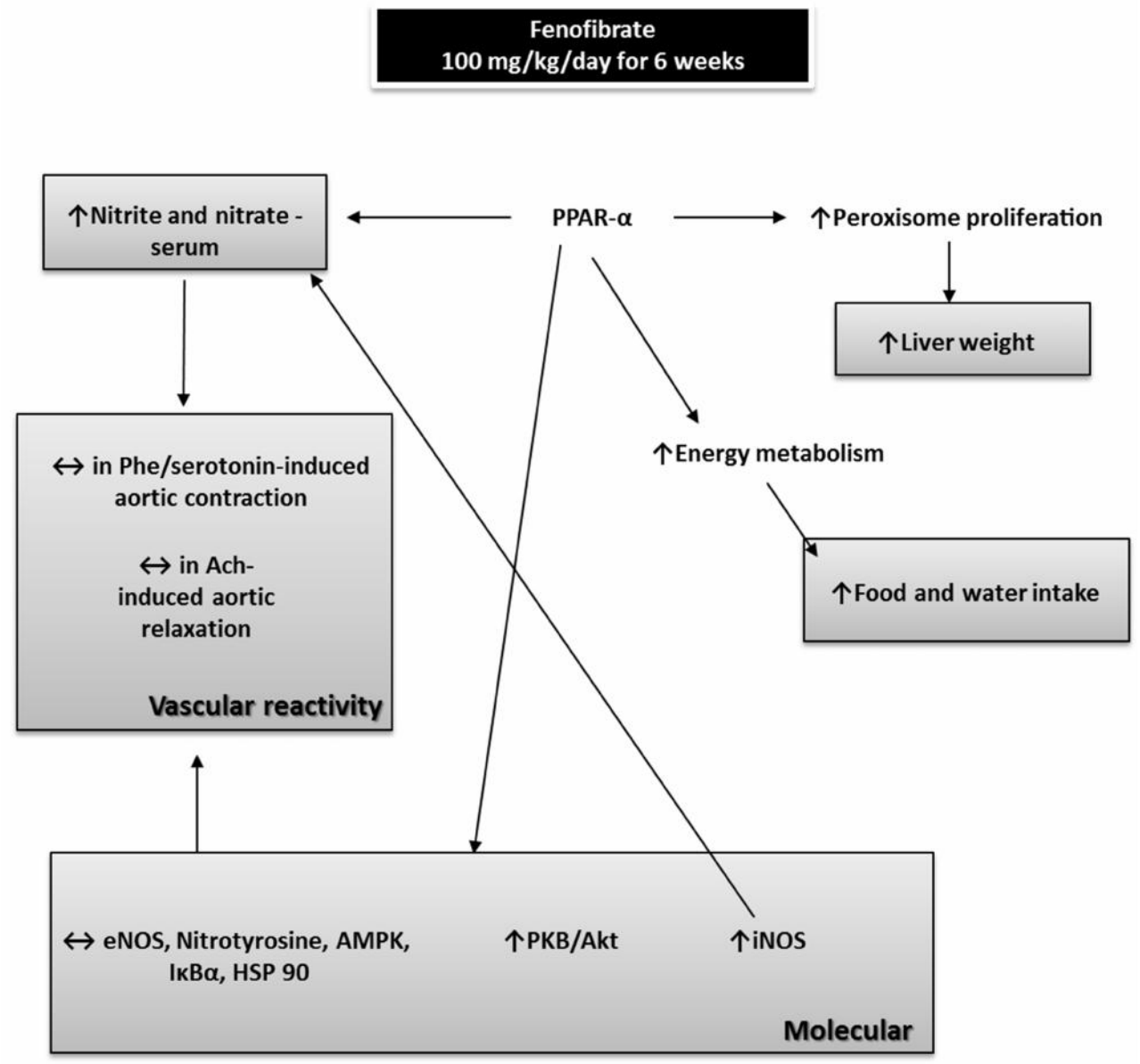

Figure 5.21: Summary of findings after 6 weeks treatment with 100 mg/kg/day fenofibrate treatment.

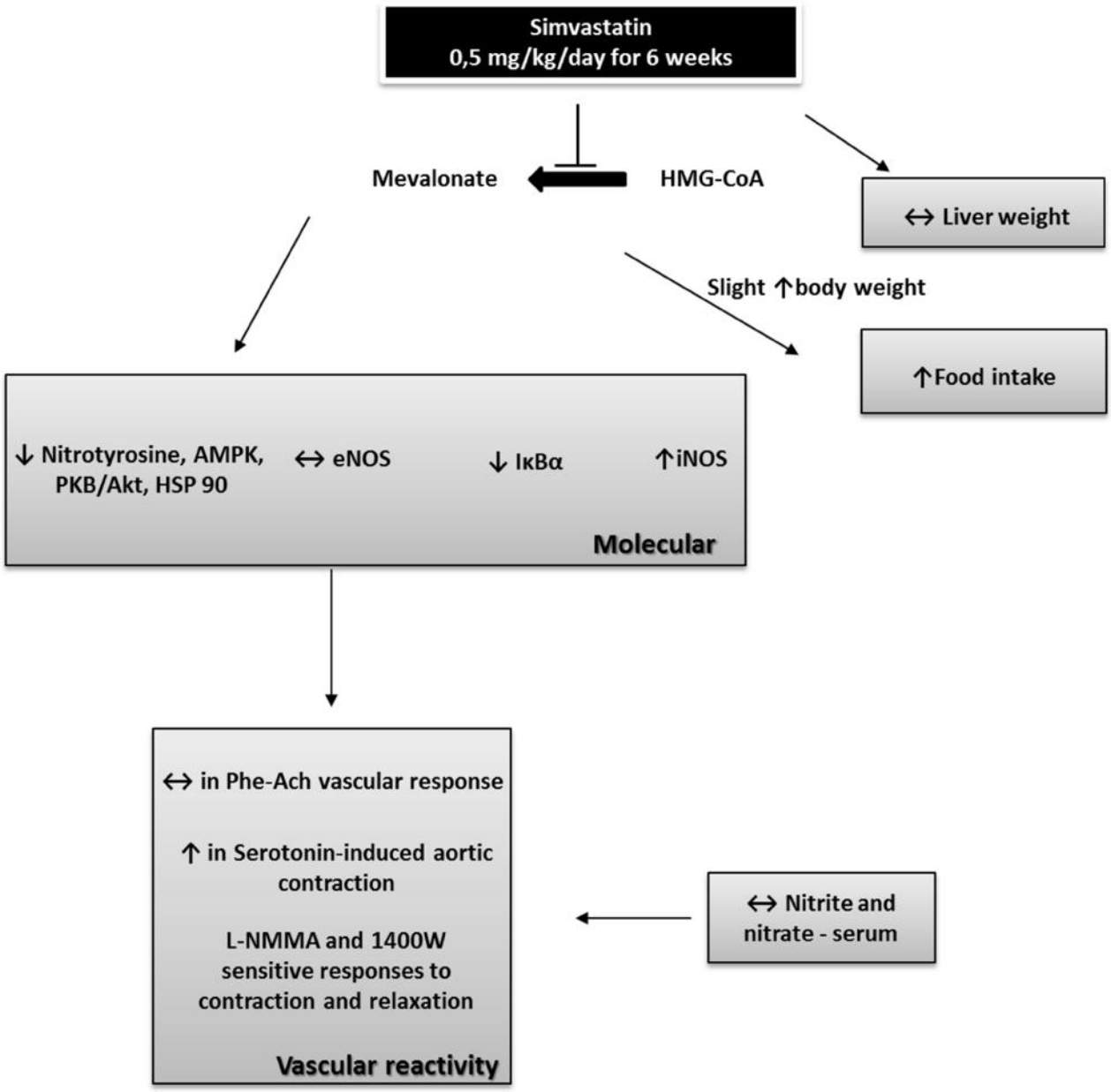

Figure 5.22: Summary of findings after 6 weeks treatment with 0.5 mg/kg/day simvastatin treatment.

Chapter 6:

Conclusion

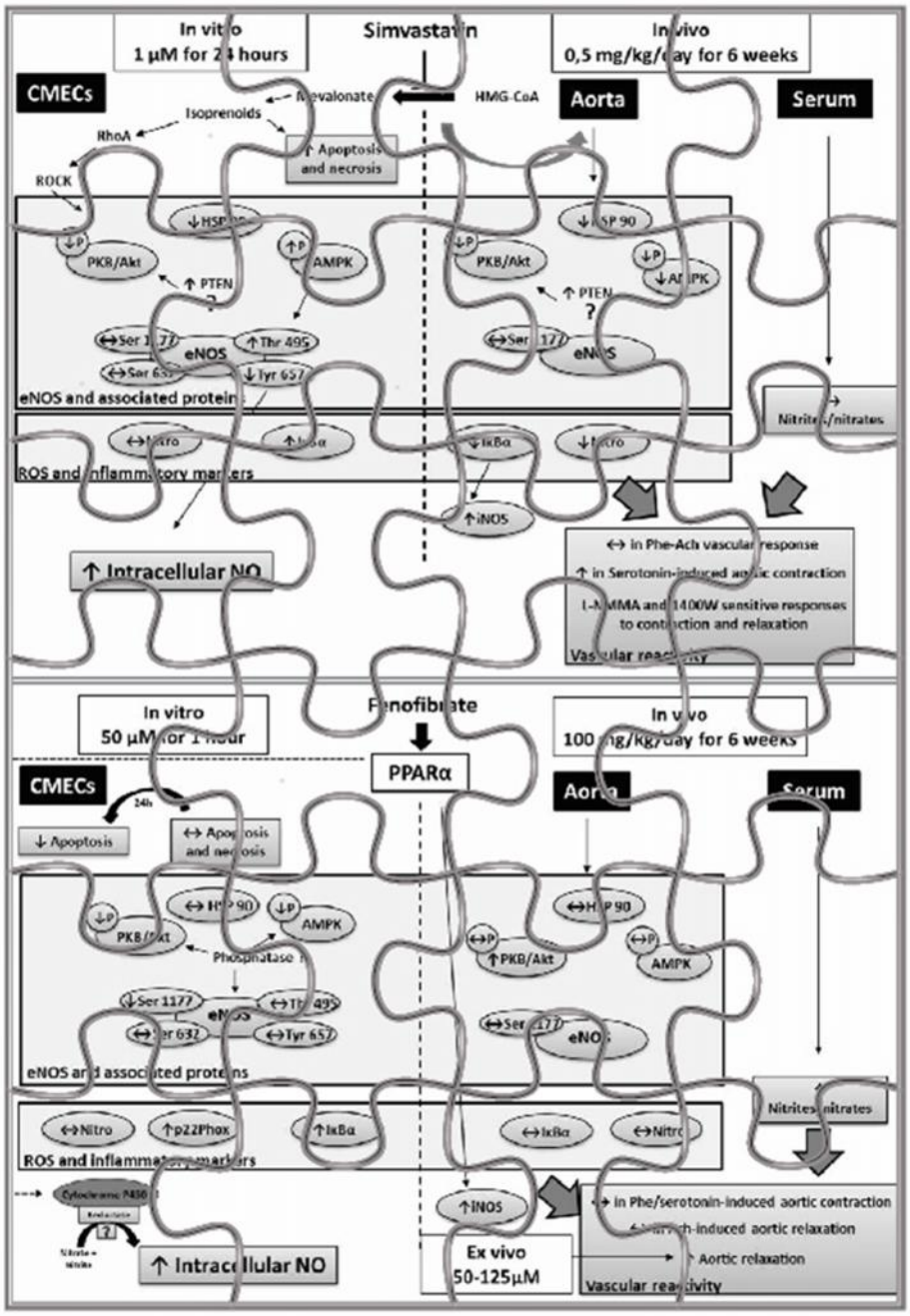

Chapter 6: Conclusion

6.1 Introduction

This dissertation investigated the pleiotropic (i.e. cholesterol-independent) effects in vascular cells and tissue, particularly with regards to the NOS-NO biosynthesis and related pathways of two commonly prescribed anti-dyslipidaemic drugs. Simvastatin and fenofibrate were investigated in different experimental models, making use of *in vitro, ex vivo* and *in vivo* techniques. The results of these investigations have been reported and discussed separately in chapters 3 and 5. The aim of the current chapter is an attempt to integrate the results, and provide some proposals as to how the data from the various experiments and experimental models could fit together to form a whole. Due to very distinct differences in drug concentrations and treatment periods within the *in vitro, ex vivo* and *in vivo* models, results cannot always be compared directly, however overall trends will be discussed. The final section of this chapter deals with the main conclusions.

6.2 Simvastatin

Statins have been prescribed to patients suffering from dyslipidaemia for decades. The statin drug family has proved its efficacy in clinical trials to improve cholesterol parameters as well as result in improved primary outcomes e.g. reduction in coronary events or slowing of atherosclerotic processes. Recently, the focus has shifted from the cholesterol dependent effects to the cholesterol-independent effects of statins. Numerous reviews have been published discussing these pleiotropic effects of statins (LaRosa 2001; Davignon *et al*. 2004; Greenwood & Mason 2007; Ii & Losordo 2007; Blum & Shamburek 2009). The current study focussed on the pleiotropic effects of one of the most frequently prescribed statins, namely simvastatin, on the following parameters: NO production, ROS production and oxidative stress status, inflammatory pathways, apoptosis and necrosis. A summary of findings is presented in figure 6.1.

6.2.1 NO producing abilities

In vitro results demonstrated that simvastatin exerted modest increasing effects on NO production in CMECs. Subsequent signalling investigations could however not shed further light on underlying NOS-derived sources of NO synthesis. It is proposed that reduced phosphorylation

of eNOS Tyr 657 (providing a mechanism for reduced inhibition of eNOS), could have resulted in an increased NO output emanating from eNOS. Besides an increase in the activation of a major protein kinase upstream from eNOS, namely AMPK (Thr 172), no other indication of eNOS activation or upstream activating molecules could be detected. Pilot studies with *ex vivo* administration of simvastatin to pre-contracted aortic rings failed to elicit vasodilatory responses and thus further *ex vivo* investigations were terminated. *In vivo* treatment of rats with simvastatin for 6 weeks failed to significantly increase the serum bioavailability of NO, as measured by a nitrite and nitrate assay. Furthermore, six weeks treatment with simvastatin failed to alter the vasoactive responses (phenylephrine-induced contractility followed by acetylcholine-induced relaxation) in aortic rings compared to untreated control groups. However, interestingly, the aortic rings from simvastatin-treated animals did show a pro-contractile response when contracted with serotonin; furthermore, it appeared that the aortic rings in this group were more susceptible to NOS inhibition, compared to the rings from control or fenofibrate treated animals. Overall the results suggest that in our hands, simvastatin did activate NO synthesis, however the effects were relatively modest.

An interesting finding of the study is the fact that iNOS inhibition with *ex vivo* administration of 1400W resulted in an anti-contractile response of fenofibrate and untreated control aortic rings, while similar inhibition of iNOS in simvastatin treated rings resulted in a pro-contractile response. These differences in responses were amidst increased iNOS expression in both fenofibrate and simvastatin treated aortic tissue. Even though values were not statistically different between levels of iNOS expression in fenofibrate and simvastatin groups, simvastatin treated animals showed a trend of higher expression. Increased iNOS expression is commonly associated with increased contractility of vascular tissue (Mathewson & Wadsworth 2004; Korkmaz *et al*., 2011) and it is fascinating that simvastatin treatment would alter aortic tissue in such a way that it utilizes iNOS in an anti-contractile manner, while untreated controls and fenofibrate treated animals did not.

The lack of response in the signalling molecules eNOS and PKB/Akt could be due to insufficient inhibition of the rate limiting step in cholesterol synthesis, namely HMG-CoA to mevalonate, thus still yielding isoprenoids that would activate RhoA and ROCK, thereby attenuating the activation

of PKB/Akt and eNOS. The lack of robust responses from the *in vivo* experiments could be time and concentration dependent. The present study aimed to explore the effects of simvastatin treatment at a lower rather than higher dosage, as many authors fall in the trap of increasing drug dosages to achieve maximum effect. The chosen dosage in the current study of 0.5 mg/kg/day (Lefer *et al*. 2001) has previously been reported to be cardioprotective. In hindsight, however, it can be speculated that the concentration of simvastatin was perhaps not sufficient to effectively inhibit formation of isoprenoids. Under ideal circumstances, it would have been appropriate to measure the serum levels of simvastatin in the animals, but such investigations are very expensive and exceeded our budget. Signalling data from the aortic tissue samples strongly suggested inhibition of PKB/Akt and eNOS. The cholesterol-dependent and pleiotropic effects of statins are ascribed to the very important inhibition of HMG-CoA to mevalonate along with inhibition of downstream targets, therefore a lack of pleiotropic effects suggest a lack of proper inhibition.

An editorial comment by Schulz (2005) suggested that statins exert measurable cardioprotective effects in the acute/subacute setting. The protective effects of simvastatin and other statins are dependent on the modulation of kinase activity and over longer treatment periods, these effects are lost. A study by Mensah *et al.* (2005) found that treatment with atorvastatin resulted in an up-regulation of phosphatase and tensin homolog deleted on chromosome 10 (PTEN) resulting in a lower level of phosphorylation of PKB/Akt. Recently simvastatin was shown to upregulate PTEN activity in human breast cancer cells (Ghosh-choudhury *et al.,* 2010). Phosphatase activity was not measured in the current study, however it could explain the lack of kinase activity in the *in vitro* and *in vivo* studies.

6.2.2 Decreased ROS production

In vitro, simvastatin failed to show any reduction in ROS levels. In fact, 100 nM simvastatin increased mitochondrial/peroxynitrite ROS. *In vivo* treatment did however result in decreased levels of nitrotyrosine formation, which is a marker of intracellular nitrosative stress. The pro-vasodilatory effect of simvastatin found in other studies has been proposed to be due to increased expression and activation of superoxide dismutase (Alvarez de Sotomayor *et al*., 2001;

Carneado *et al*., 2002). The current study did not investigate antioxidant enzymes and can therefore not relate any improvements in ROS to any specific antioxidant system. Comparing the *in vitro* and *in vivo* results suggest that a longer treatment period might result in improved anti-oxidant activities and decreased ROS formation.

6.2.3 Inflammatory pathways

In contrast to the effect of simvastatin on ROS, *in vitro* treatment with simvastatin resulted in reduced activation of the pro-inflammatory transcription factor, NF-KB, as observed by increased levels of IκBα expression. However *in vivo* treatment showed the opposite effect. Decreased IκBα expression was also associated with increased iNOS expression. iNOS expression was not measured *in vitro* in CMECs, and this is one of the shortcomings of the study. Further investigations will have to be performed to investigate to what extent simvastatin induced inflammatory responses *in vivo*.

6.2.4 Anti-apoptotic and anti-necrotic properties

Unfortunately apoptosis and necrosis were only evaluated in *in vitro* experiments. Simvastatin treatment resulted in increased apoptosis and necrosis, and it is proposed to be due to increased isoprenoid formation resulting in inhibition of the anti-apoptotic protein, Bcl-2.

6.3 Fenofibrate

Fenofibrate is the most recent member of the fibrate family to appear on the pharmaceutical market. It has been shown to be very effective in increasing HDL-cholesterol levels as well as leading to modest decreases in LDL-cholesterol and triglyceride levels. Despite these improvements in lipid parameters it has failed to improve primary outcomes such as cardiovascular disease events in clinical trials. Similar to simvastatin, fenofibrate has gained attention due to its ability to exert pleiotropic effects. The current study aimed to investigate the pleiotropic effects of fenofibrate in vascular cells and tissue with an emphasis on the NOS-NO synthesis and related pathways. A summary of these effects are presented in figure 6.2.

6.3.1 NO producing abilities

In vitro measurements of NO showed robust responses to fenofibrate treatment. The responses were, however, more profound at shorter treatment periods (1 hour and 4 hours), after which

they wore off as treatment periods increased. This finding was confirmed by the *ex vivo* vaso-dilatory effects of fenofibrate. The involvement of eNOS, iNOS and nNOS in the increased levels of NO were investigated rigorously, but despite an exhaustive array of experiments, concentration-time investigations, pharmacological inhibition studies, and application of different experimental models, in our hands, results failed to show a NOS-dependent mechanism. *In vivo* treatment with fenofibrate significantly increased serum nitrite and nitrate levels, indicating an overall increase in NO bio-availability in the circulation of the animals. However, western blot data performed on the aortic tissue from the *in vivo* treated rats failed to show increased levels of eNOS expression and phosphorylation. Previous *in vitro* studies have shown that fenofibrate increased NO via eNOS-dependent mechanisms (Goya *et al.,* 2004; Murakami *et al*., 2006; Becker *et al*., 2012) and *in vivo* (Kaur *et al*., 2010; Chakkarwar 2011; Omae *et al*., 2012). In the current study, we investigated eNOS activation by phosphorylation at various time points in the endothelial cell models; however, increased activation by phosphorylation could not be demonstrated. The difference in results compared to other studies could be due to endothelial cell type-specific reasons. There is no evidence of any other studies that investigated the effects of fenofibrate on the NOS-NO biosynthesis system in cardiac derived microvascular endothelial cells.

On the other hand, the isometric tension model in the current study did show that fenofibrate exerted modest vasodilatory effects on aortic rings from healthy animals via acute *ex vivo* administration, and that this effect was abolished in the presence of L-NMMA, thus confirming that the vasodilatory response was a result of NOS-derived NO release. Six week treatment with fenofibrate did result in increased iNOS expression in aortic tissue, but not eNOS, although the phosphorylated eNOS (Ser 1177) levels increased by ~ 2-fold (not statistically significant). Vascular reactivity results do not suggest increased iNOS expression to have had any detrimental effects with regards to contraction or relaxation. iNOS showed no involvement in *in vitro* studies.

6.3.2 Decreased ROS production

Fenofibrate failed to show anti-oxidant effects after a 6 week *in vivo* treatment regimen. Limited markers of ROS were included in these investigations and anti-oxidant enzymes such as catalase and superoxide dismutase were not investigated, therefore it is impossible to fully conclude

about the anti-oxidant effects. *In vitro* fenofibrate treatment did however decrease mitochondrial ROS/peroxynitrite after 1 hour.

6.3.3 NF-KB inflammatory pathway

Fenofibrate did not show any cellular pro-inflammatory effects in any of the experimental models with regards to the NF-KB pathway. *In vitro* investigations showed increased IκBα expression suggesting that the pro-inflammatory NF-KB pathway was not activated. This observation was not reflected in the aortic tissue after prolonged *in vivo* treatment. PPAR-α activation, the major mechanism of fenofibrate actions, is commonly associated with anti-inflammatory effects in humans (Belfort *et al.*, 2010; Krysiak *et al*., 2013) and our *in vitro* results support these findings.

6.3.4 Anti-apoptotic and anti-necrotic properties

Markers of apoptosis and necrosis were only investigated in the *in vitro* studies. Acute treatment with fenofibrate did not show anti-apoptotic or necrotic effects, however after 24 hours an anti-apoptotic effect was seen in CMECs. It is important to note that these investigations were performed in cells harvested from healthy rats. These results therefore indicate that fenofibrate showed baseline pleiotropic effects, which contributed to cellular protection against a harmful stimulus such as TNF-α. Pre-treatment with fenofibrate resulted in decreased apoptosis and necrosis, induced by the pro-inflammatory cytokine TNF-α.

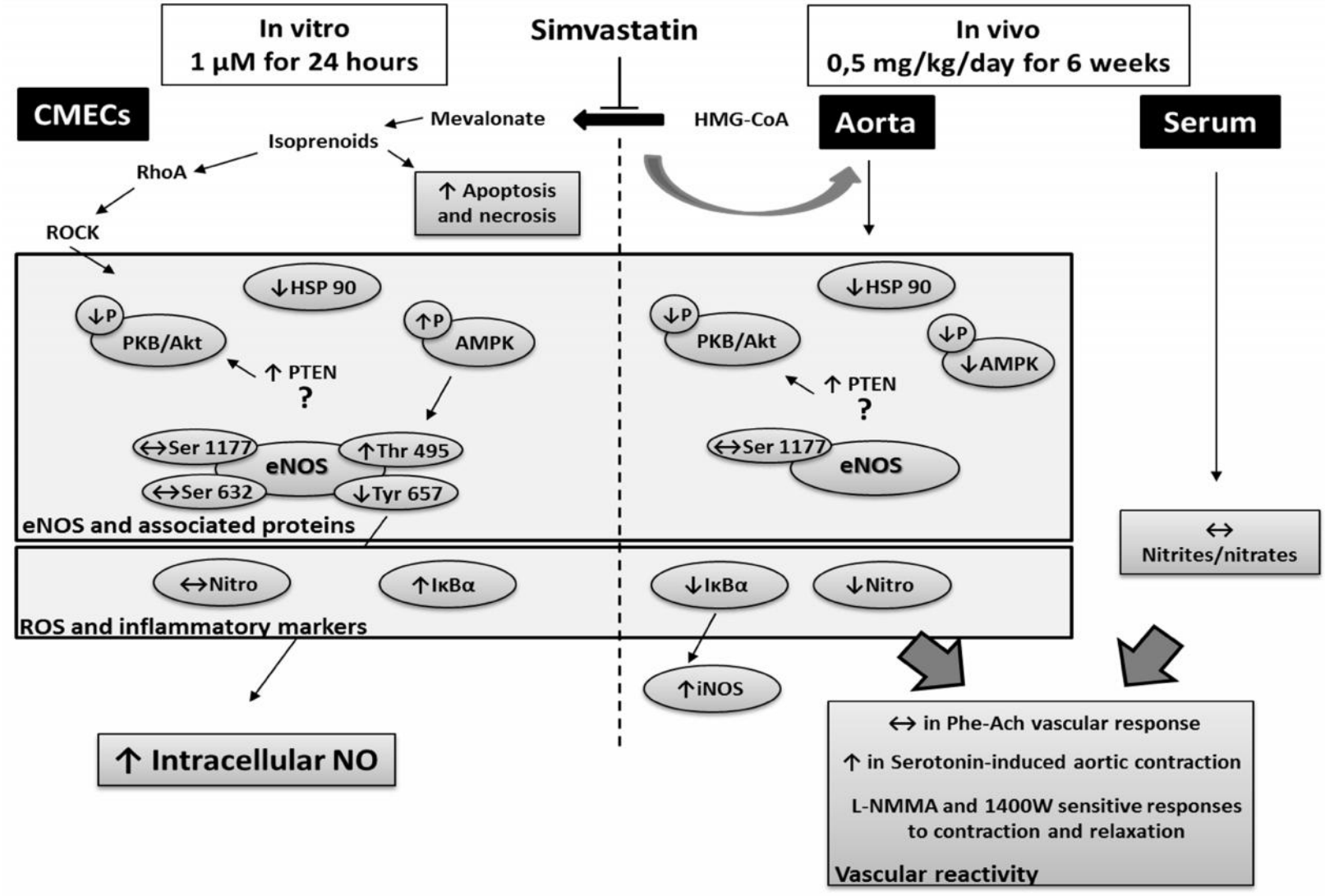

Figure 6.1: Summary of findings from in vitro and in vivo treatment with simvastatin.

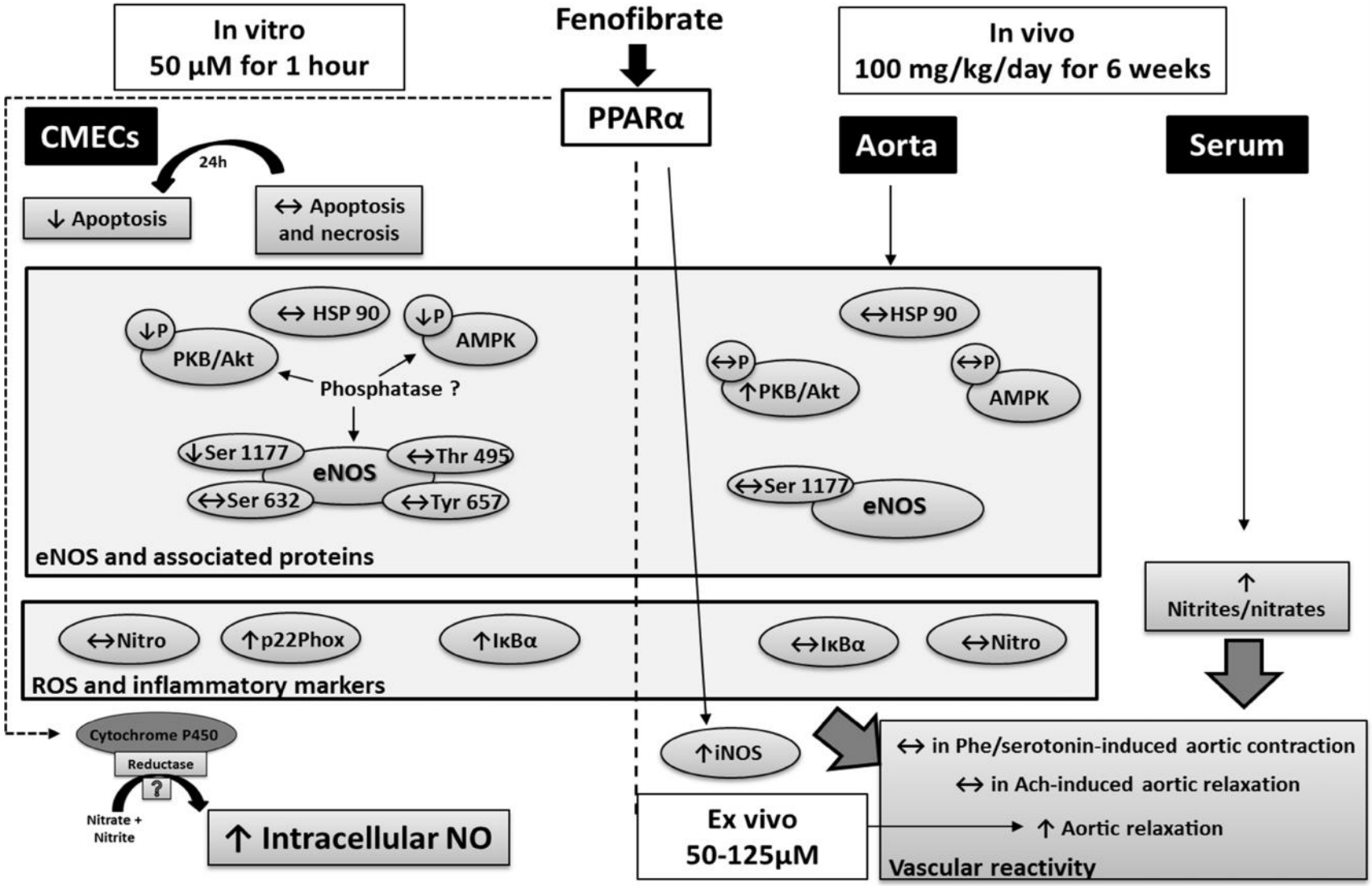

Figure 6.2: Summary of findings form in vitro and in vivo treatment with fenofibrate.

6.4. Final conclusions

Simvastatin

This study aimed to investigate the pleiotropic effects of two anti-dyslipidaemic agents, namely simvastatin and fenofibrate on vascular tissue, particularly with regards to the NOS-NO and other related pathways. Considering the reputation of statins in general, it was unexpected to find the relative lack of robust, detectable pleiotropic effects in this study, either *in vitro* or *in vivo*. Compared to fenofibrate, simvastatin only managed to result in a modest increase in NO *in vitro* and although simvastatin treated rat aortic rings showed a greater susceptibility when NOS was inhibited, no improvements were found in contractile and vaso-dilation responses. In our hands, involvement of eNOS in the actions of simvastatin could not be demonstrated in any of the experimental models and conditions, which is indeed surprising. In aortic tissue, increased iNOS expression was observed, and the isometric tension studies demonstrated that iNOS played an important anti-contractile role in the aortic rings from simvastatin-treated animals. As far as we are aware, this observation is novel and has not been reported elsewhere, and investigations are required to further elucidate this interesting finding.

Although simvastatin failed to improve the vaso-active responses in the aortic rings, there was, at the same time, no indication that it was harmful (e.g. inducing endothelial dysfunction). Considering the mechanism that has previously been described for the pleiotropic effects of simvastatin, it can be concluded from our own data that simvastatin, at the dose utilized, probably failed to effectively inhibit HMG-CoA to mevalonate; if this was the case, an inhibitory effect on PKB/Akt phosphorylation due to ROCK could be a likely scenario. This argument could also help explain the *in vitro* findings of increased apoptosis and necrosis. In both *in vitro* and *in vivo* studies a significant down-regulation of HSP 90 was observed. HSP 90 plays an essential role in PKB/Akt and AMPK related phosphorylation of eNOS and could possibly have been inhibited by ROCK. A possible explanation for the weak effect of simvastatin *in vitro* could be that the drug was ineffectively metabolised. As for the *in vivo* situation (6 weeks treatment programme), it has previously been shown that statin-related protective effects are abolished over longer treatment periods. Additionally, the dosage of simvastatin used in the current study could have been too

low to induce proper inhibition of ROCK. These factors may have constrained the study to show the full potential of simvastatin with regards to pleiotropic effects in vascular tissue.

Overall, it can be concluded that simvastatin did not show endothelio-protective effects in a model of CMECs or after 6 weeks *in vivo* treatment in aortic tissue.

Fenofibrate

Although it was not necessarily the intention at the outset, the current study evolved in such a way that considerably more experiments were performed with fenofibrate than simvastatin. On the whole, considerably less data are available in the literature on fenofibrate's effects and underlying mechanisms in the context of vascular biology compared to simvastatin. Furthermore, pilot studies with fenofibrate in our laboratory quickly revealed very interesting data with regards to acute NO production, which had to be pursued further. Reports from the fenofibrate clinical trial (FIELD) suggested that fenofibrate treatment resulted in improved outcomes with respect to microvascular disease conditions. This prompted us to further investigate fenofibrate in a model of cardiac derived microvascular endothelial cells. In our hands, fenofibrate was very effective in increasing NO in CMECs after acute treatments, however subsequent efforts to identify the NOS isoform involved with these effects turned out to be a challenging task. The vast majority of previous studies have shown that eNOS is associated with fenofibrate-induced NO production in one way or another, with only a handful of studies suggesting contributions from iNOS and nNOS.

In the current study, eNOS activation was investigated by measuring phosphorylation at multiple time points (5, 15, 30, 60 min and 24 hours), however we failed to demonstrate increased phosphorylation of eNOS Ser 1177, the most well described phosphorylation site for activation, at any of the time points. The search for the involvement of alternative phosphorylation sites revealed interesting data, but failed to show activation of eNOS. Additionally, inhibition of NOS with L-NMMA and iNOS with 1400W prior to fenofibrate administration did not reverse or abolish elevated NO levels. In order to confirm these results an alternative NO-detection technique (Griess method) was used, which mirrored the DAF-2/DA flow cytometry data. It can therefore only be concluded that, in our hands, fenofibrate treatment in a model of cardiac microvascular endothelial cells resulted in acute increases of intracellular nitric oxide via a NOS-independent

mechanism. Two mechanisms are proposed for these results. One being that fenofibrate treatment, most likely due to ligand binding to PPAR-α, activated the cytochrome P450 reductase enzyme, which in turn converted nitrites and nitrates to NO. Cytochrome P450 is involved with xenobiotic metabolism and it is speculated that fenofibrate activated this system and bypassed NOS completely. The second proposed mechanism is that fenofibrate treatment resulted in the up-regulation of an, as yet unknown, phosphatase, which could have resulted in the dephosphorylation of eNOS and possibly also one or more of its upstream kinase activators; however, this hypothesis only explains why we failed to show eNOS activation, but does not address where the increased NO production originated. Further investigations will however have to be conducted to test these hypotheses.

Another significant finding was the fact that acute, short-term treatment with fenofibrate down-regulated intracellular pro-inflammatory pathways by reducing the activation of NF-KB, an effect that disappeared after 24 hours. This was associated with a significant up-regulation of p22Phox, subunit of the important endothelial ROS generating enzyme, NADPH-oxidase. Apart from this, no other signs of oxidative stress could be demonstrated; in fact, a reduction in mitochondrial ROS/peroxynitrite was observed. Since most of the investigations in this study were performed on healthy CMECs, the relative lack of robust and detectable effects of fenofibrate can be ascribed to the fact that the baseline status of the cells was associated with optimal homeostasis and protection, and it can therefore be speculated that they were less receptive to any additional pleiotropic effects exerted by the drug. It came as no surprise therefore, that the protective effects (anti-oxidant, anti-apoptosis and anti-necrosis) of fenofibrate were considerably more pronounced and detectable when fenofibrate was pre-administered to endothelial cells exposed to the pro-inflammatory cytokine, TNF-α. This underlines the importance of incorporating models of injury when performing experimental planning of studies investigating drug effects. In this regard, 1 hour pre-treatment with fenofibrate resulted in increased NO even in the presence of TNF-α, as well as reduction in oxidative stress and apoptosis. The PI data additionally showed that pre-treatment with fenofibrate attenuated necrosis induced by TNF-α. The *in vitro* pretreatment with fenofibrate prior to TNF-α administration was the only set of experiments in the current study that could demonstrate a significant increase in phosphorylation of eNOS (Ser 1177).

Our model of *in vivo* treatment of healthy rats with fenofibrate could also not show robust pleiotropic effects. Although 6 weeks of fenofibrate treatment increased the bioavailability of NO in the blood, no anti-inflammatory or anti-oxidant effects were detected in the aortic tissue. Despite the increased NO levels in the circulation of these animals, the *ex vivo* aortic ring studies failed to show an improvement in their vaso-active properties compared to untreated control groups; on the other hand, however, neither did fenofibrate treatment cause any harmful effects on the aortas. Increased iNOS expression was detected in aortic tissue and inhibition studies with 1400W suggested iNOS to exert a pro-contractile effect in these vascular rings. It would be interesting to investigate the protective effects of these baseline pleiotropic effects on animals with a pathological condition, similar to the pre-treatment studies performed *in vitro*.

Ex vivo administration of fenofibrate to pre-contracted aortic rings further confirmed the ability of fenofibrate to induce NO production. Even though the vasodilatory effect was not as pronounced or rapid compared to the effect of acetylcholine, it was still evident within 30 minutes. These were also some experiments in the current study that definitely linked fenofibrate-derived NO to NOS, as observed when the vasodilatory response was abolished in the presence of L-NMMA.

It can therefore be concluded that, in our hands, fenofibrate showed pleiotropic effects in vascular endothelial cells and tissue, with increased NO production being the most pronounced effect, confirmed *in vitro, ex vivo* and *in vivo*. Only modest, and at times inconsistent anti-oxidant and anti-inflammatory effects were demonstrated. Acute administrations of fenofibrate were also sufficient to protect endothelial cells against the harmful effects of stimuli, such TNF-α, associated with vascular diseases.

Finally, this study showed for the first time that the mechanisms responsible for the pleiotropic effects of fenofibrate on vascular NOS-NO pathways may not be as straight-forward as previously thought. In contrast to many other studies, the *in vitro* experiments of the present study showed that fenofibrate exerted its actions via a NOS-independent mechanism, resulting in large increases of NO after acute treatment. It has to be noted, however, that these experiments were conducted on healthy endothelial cells. The mechanisms were investigated in detail in a model of cardiac microvascular endothelial cells, and could very well be a cell-specific response,

however in light of the beneficial clinical outcomes seen in studies where fenofibrate treatment was associated with improvement in microvascular diseases, our data may shed light on the mechanisms. The present study further showed that fenofibrate treatment was not detrimental to cell and tissue models from healthy animals, in *in vitro* or *in vivo* experimental conditions, and furthermore, that acute treatment resulted in more robust pleiotropic effects than longer treatments. These acute treatments were also sufficient to protect endothelial cells from the effects of TNF-α by showing improvements in cell viability parameters measured with different techniques. Along with these findings, fenofibrate treatment was able to prevent the large increases in ROS associated with TNF-α treatment, possibly suggesting an up-regulation of anti-oxidant systems already after 1 hour. It is also important to note that even though concentrations and time-frames of fenofibrate treatment varied between the *in vitro, ex vivo* and *in vivo* models, a prominent and common observation between these models was the pronounced ability of fenofibrate to increase NO levels. It is by far the most robust and consistent finding of the study and shows that if an effect of a drug is biologically relevant it will be robust enough to be evident independent of a specific model.

Comparing the two anti-dyslipidaemic agents, fenofibrate and simvastatin, fenofibrate showed greater pleiotropic effects *in vitro*, *ex vivo* and *in vivo*. Simvastatin treatment resulted in inconsistent results and it seems as though the inhibition of isoprenoid synthesis is truly the most important and possibly the only pathway related to pleiotropic effects of simvastatin, making fenofibrate more diverse in its pleiotropic actions. The study also demonstrated the novel finding of increased iNOS expression and functioning in simvastatin-treated, anti-contractile aortic responses. The relatively small role eNOS played in *in vitro* and *in vivo* investigations possibly highlights the strong relationship between ROCK and eNOS. ROCK, an upstream inhibitor of eNOS, is one of the main role players of simvastatin related mechanisms, and if the lack of robust pleiotropic effects found with simvastatin treatment was indeed due to insufficient inhibition of mevalonate and consequently ROCK, these results suggest ROCK to have a potent eNOS inhibitory action under baseline conditions. Therefore, in as much as upstream activators of eNOS, such as PKB/Akt and AMPK were included in normal baseline investigations of eNOS (even using other therapies than statins), the role of ROCK should not be underestimated in these

scenarios. In conclusion, this study contributed to valuable insights and mechanisms underlying the pleiotropic effects of two commonly used anti-dyslipidaemic agents.

6.5 Shortcomings of the study

In hindsight, the following investigations would have added great value to this study, however due to time and cost-constraints it could not be performed:

a) Repeating Western blots with all the eNOS phosphorylation site antibodies in *in vitro* and *in vivo* investigations of fenofibrate and simvastatin. Some of the antibodies were only purchased later in the study, thus creating gaps in signalling results between different models.
b) In addition to measuring iNOS mRNA levels following fenofibrate treatment, it would have been interesting to also perform qPCR analysis on eNOS and nNOS mRNA.
c) Should time have allowed, the involvement of cytochrome P450 reductase in fenofibrate-derived NO production could have been investigated.
d) With regards to simvastatin treatment in *in vitro* and *in vivo* models, the extent of ROCK activation would have provided valuable information and answers to the lack of PKB/Akt, and possibly further downstream eNOS activity.
e) *In vivo* treatment with simvastatin could have been performed using a higher dosage, thus possibly resulting in more robust pleiotropic effects.
f) Along with investigations on kinase activity involved in changes brought about by fenofibrate and simvastatin treatments, investigating phosphatase contributions would have added great value to the study.
g) In light of the beneficial outcomes of fenofibrate pre-treatment studies prior to TNF-α administration, additional investigations with fenofibrate as post-treatment would also have added great value to the study.

6.6 Future directions

Future investigations are mostly based on the shortcomings of the present study and would aim to address the following issues:

- Explore and investigate the NOS-independent mechanisms resulting in acute fenofibrate-derived NO production, including cytochrome P450 reductase and phosphatase role-players in this scenario.
- Perform NOS gene expression investigations on all three isoforms from endothelial cell cultures and *in vivo* treated animals.
- Investigate the fascinating finding of iNOS expression contributing to the anti-contractile effect of simvastatin *in vivo*. Also, repeat *in vivo* investigations using different dosages of simvastatin and also shorter treatment periods.
- To further investigate changes in contraction of simvastatin treated aortic rings and its susceptibility to serotonin as vaso-constrictor.

6.7 Outputs

The following outputs derived directly or indirectly from the study:

Book chapter

Genis A, Smit S, **Westcott C**, Mthethwa M, Strijdom H. Attenuation of eNOS-NO biosynthesis, up-regulation of antioxidant proteins and differential protein regulation in TNF-alpha-treated cardiac endothelial cells: Early signs of endothelial dysfunction. In: Endothelial Dysfunction: Risk Factors, Role in Cardiovascular Diseases and Therapeutic Approaches (Nova Scientific Publishers, Hauppauge, NY, USA) 2014.

Peer reviewed published conference proceedings

1. **Westcott C**, Genis A, Mthethwa M, Strijdom H. Short term fenofibrate treatment increases nitric oxide production in cardiac endothelial cells through a nitric oxide synthase-independent mechanism. Cardiovascular Research Supplements (2014) 103, S9–S463.
2. **Westcott C,** Strijdom H. Fenofibrate causes nitric oxide production from an unknown source. Scientific Research and Essays April 2012; 7: 48.

Conference contributions

1. Smith T, Van Vuuren D, **Westcott C**, Strijdom H. Simvastatin and Fenofibrate in myocardial ischaemia/reperfusion. Poster presentation at the 58th Annual Academic Day of Stellenbosch University's Faculty of Medicine and Health Sciences, 13 August 2014.
2. **Westcott C**, Loubser D, Genis A, Mudau M, Strijdom H. Fenofibrate and the vasculature: The NOS-tastic journey to underlying mechanisms. Oral presentation at the the 41st Annual Physiology Society of South Africa congress, held at Roodevallei Conference lodge, South Africa, 15-18 September 2013.

3. **Westcott C**, Van Wyk WA, Genis A, Mudau M, Strijdom H. Fenofibrate and endothelial cells: Building the NOS puzzle. Oral presentation at the Faculty's Annual Academic Day, held at Tygerberg campus, Stellenbosch University, South Africa, 14-15 August 2013.

   **** Received second prize in the Basic Sciences division.***

4. **Westcott C**, Strijdom H. The pleiotropic effects of fenofibrate on microvascular level. Oral presentation at the Medical Research Council Annual research day, Parow, South Africa, 23-24 October 2012.

5. **Westcott C**, Strijdom H. Fenofibrate and nitric oxide: what happens on microvascular level? Poster presentation at the 40th Annual Conference of the Physiology society of Southern Africa, hosted by the University of Stellenbosch, South Africa, 11-13 September2012.

6. Graham R, Mudau M, **Westcott C**, Strijdom H. Investigating the pro-injury properties of ADMA and TNF-α, and endothelioprotective effects of oleanolic acid and fenofibrate in cardiac microvascular endothelial cells (CMECs). Oral presentation at the Physiology Society of Southern Africa Congress, Stellenbosch, September 2012

   ****One of the winning presentations in the Honours student category.***

7. **Westcott C**, Strijdom, H. Fenofibrate causes large amounts of nitric oxide, but where does it come from? Oral presentation at the annual academic day of the Faculty of Health Sciences, Stellenbosch University, 17-18 August 2011.

   **** Received second prize in the Basic Sciences division.***

8. **Westcott C**, Strijdom, H. Fenofibrate causes large amounts of nitric oxide from an unknown source. Poster presentation at the 39th Annual Conference of the Physiology society of Southern Africa, hosted by the University of Western Cape, South Africa, 29-31 August 2011.

Student supervision

Honours student supervision:

Ms Roxy Graham – Graduated 2012

> Ms Graham successfully finished her B.Sc Honours degree (*cum laude*) and her research project was graded with the highest marks in her group.

Mr Wiehan van Wyk – Graduated 2013

Successful applications for research grants

This project was successful in funding applications from the following funding bodies:

National Research Foundation, Thuthuka 2012 – 2014.

Harry Crossley foundation, 2011 – 2014.

References

References

Adak, S. *et al*., 2001. Neuronal nitric-oxide synthase mutant (Ser-1412 --> Asp) demonstrates surprising connections between heme reduction, NO complex formation, and catalysis. The Journal of biological chemistry, 276(2), pp.1244–52.

Ahmad, M., 2002. Role of Isoprenylcysteine Carboxyl Methyltransferase in Tumor Necrosis Factor-alpha Stimulation of Expression of Vascular Cell Adhesion Molecule-1 in Endothelial Cells. Arteriosclerosis, Thrombosis, and Vascular Biology, 22(5), pp.759–764.

Ahmed, T., 2013. High dose simvastatin as a potential anticancer therapy in leukemia patients, PhD thesis, University of Kentucky.

Aird, W.C., 2007. Phenotypic heterogeneity of the endothelium: I. Structure, function, and mechanisms. Circulation research, 100(2), pp.158–73.

Aktan, F., 2004. iNOS-mediated nitric oxide production and its regulation. Life sciences, 75(6), pp.639–53.

Alagona, P., 2010. Fenofibric acid: a new fibrate approved for use in combination with statin for the treatment of mixed dyslipidemia. Vascular health and risk management, 6, pp.351–62.

Alderton, W.K., Cooper, C.E. & Knowles, R.G., 2001. Nitric oxide synthases: structure, function and inhibition. The Biochemical journal, 357, pp.593–615.

Ali, F.Y. *et al*., 2009. Antiplatelet actions of statins and fibrates are mediated by PPARs. Arteriosclerosis, thrombosis, and vascular biology, 29(5), pp.706–11.

Alvarez de Sotomayor, M. *et al*., 2000. Characterization of endothelial factors involved in the vasodilatory effect of simvastatin in aorta and small mesenteric artery of the rat. British Journal of Pharmacology, 131, pp.1179-1187.

Alvarez de Sotomayor, M. *et al*., 2001. Effect of simvastatin on vascular smooth muscle responsiveness: involvement of Ca(2+) homeostasis. European journal of pharmacology, 415(2-3), pp.217–24.

Alvarez de Sotomayor, M., Mingorance, C. & Andriantsitohaina, R., 2007. Fenofibrate improves age-related endothelial dysfunction in rat resistance arteries. Atherosclerosis, 193(1), pp.112–20.

Ambasta, R.K. *et al.,* 2004. Direct interaction of the novel Nox proteins with p22phox is required for the formation of a functionally active NADPH oxidase. The Journal of biological chemistry, 279(44), pp.45935–41.

Anderson, H.D.I., Rahmutula, D. & Gardner, D.G., 2004. Tumor necrosis factor-alpha inhibits endothelial nitric-oxide synthase gene promoter activity in bovine aortic endothelial cells. The Journal of biological chemistry, 279(2), pp.963–9.

Andrew, P.J. & Mayer, B., 1999. Enzymatic function of nitric oxide synthases. Cardiovascular research, 43(3), pp.521–31.

Angelone, T. *et al*., 2012. Nitrite is a positive modulator of the Frank-Starling response in the vertebrate heart. American journal of physiology. Regulatory, integrative and comparative physiology, 302(11), pp.R1271–81.

Arany, I. *et al*., 1996. Regulation of inducible nitric oxide synthase mRNA levels by differentiation and cytokines in human keratinocytes. Biochemical and biophysical research communications, 220(3), pp.618–22.

Arciszewski, M.B., 2007. Expression of neuronal nitric oxide synthase in the pancreas of the sheep. Anatomia, histologia, embryologia, 36(5), pp.375–81.

Armitage, J. *et al*., 2010. Intensive lowering of LDL cholesterol with 80 mg versus 20 mg simvastatin daily in 12,064 survivors of myocardial infarction: a double-blind randomised trial. Lancet, 376(9753), pp.1658–69.

Arora, R., Hare, D.L. & Zulli, A., 2012. Simvastatin reduces endothelial NOS: caveolin-1 ratio but not the phosphorylation status of eNOS in vivo. Journal of atherosclerosis and thrombosis, 19(8), pp.705–11.

Ascer, E. *et al.,* 2004. Atorvastatin reduces proinflammatory markers in hypercholesterolemic patients. Atherosclerosis, 177(1), pp.161–6.

Assmann, G. *et al*., 1996. High-density lipoprotein cholesterol as a predictor of coronary heart disease risk. The PROCAM experience and pathophysiological implications for reverse cholesterol transport. Atherosclerosis, 124(Suppl.), pp.S11–S20.

Bae, Y.M. *et al*., 2007. Serotonin-induced ion channel modulations in mesenteric artery myocytes from normotensive and DOCA-salt hypertensive rats. J Smooth Muscle Res, 43(3), pp.85–97.

Balakumar, P., Chakkarwar, V.A. & Singh, M., 2009. Ameliorative effect of combination of benfotiamine and fenofibrate in diabetes-induced vascular endothelial dysfunction and nephropathy in the rat. Molecular and cellular biochemistry, 320(1-2), pp.149–62.

Balakumar, P., Rohilla, A. & Mahadevan, N., 2011. Pleiotropic actions of fenofibrate on the heart. Pharmacological research : the official journal of the Italian Pharmacological Society, 63(1), pp.8–12.

Balligand, J.L. *et al*., 1995. Induction of NO synthase in rat cardiac microvascular endothelial cells by IL-1β and IFN-γ. American Physiological Society, 268 (Heart Circ. Physiol. 37): H1293-H1303.

Barbier, O. *et al*., 2004. Genomic and non-genomic interactions of PPARalpha with xenobiotic-metabolizing enzymes. Trends in endocrinology and metabolism: TEM, 15(7), pp.324–30.

Barrett, B. *et al*., 2006. Validated HPLC-MS/MS method for simultaneous determination of simvastatin and simvastatin hydroxy acid in human plasma. Journal Pharmaceutical & Biomedical Analysis;41(2):517–526.

Bates, T.E. *et al*., 1995. Immunocytochemical evidence for a mitochondrially located nitric oxide synthase in brain and liver. Biochemical and biophysical research communications, 213(3), pp.896–900.

Bates, T.E. *et al.,* 1996. Mitochondrial nitric oxide synthase: a ubiquitous regulator of oxidative phosphorylation? Biochemical and biophysical research communications, 218(1), pp.40–4.

Bauer, P.M. *et al.,* 2003. Compensatory phosphorylation and protein-protein interactions revealed by loss of function and gain of function mutants of multiple serine phosphorylation sites in endothelial nitric-oxide synthase. The Journal of biological chemistry, 278(17), pp.14841–9.

Bays, H.E. *et al*., 2001. Effectiveness and tolerability of ezetimibe in patients with primary hypercholesterolemia: pooled analysis of two phase II studies. Clinical therapeutics, 23, pp.1209–30.

Becker, J. *et al.,* 2012. The peroxisome proliferator-activated receptor α agonist fenofibrate decreases airway reactivity to methacholine and increases endothelial nitric oxide synthase phosphorylation in mouse lung. Fundamental & clinical pharmacology, 26(3), pp.340–6.

Bedard, K. & Krause, K., 2007. The NOX Family of ROS-Generating NADPH Oxidases : Physiology and Pathophysiology. Physiological reviews, 87, pp.245–313.

Belfort, R. *et al.,* 2010. Fenofibrate reduces systemic inflammation markers independent of its effects on lipid and glucose metabolism in patients with the metabolic syndrome. The Journal of clinical endocrinology and metabolism, 95(2), pp.829–36.

Bender, A.T. *et al.,* 1999. Neuronal Nitric-oxide Synthase Is Regulated by the hsp90-based Chaperone System in Vivo. Journal of Biological Chemistry, 274(3), pp.1472–1478.

Ben-Neriah, Y. & Karin, M., 2011. Inflammation meets cancer, with NF-κB as the matchmaker. Nature immunology, 12(8), pp.715–23.

Bentley, P. *et al*, 1993. Hepatic peroxisome proliferation in rodents and its significance for humans. Food Chem Toxicol., Nov;31(11):857-907.

Berger, J & Moller, D.E., 2002. Mechanisms of PPARs. Annu Rev Med, 53, pp.409-435.

Bers, D. & Ziolo, M.T., 2014. When Is cAMP Not cAMP?: Effects of Compartmentalization. Circulation research, 89(5), pp.373–375.

Bertrand-Thiebault, C. *et al*., 2007. Effect of HMGCoA reductase inhibitors on cytochrome P450 expression in endothelial cell line. Journal of cardiovascular pharmacology, 49(5), pp.306–15.

Bian, K. & Murad, F., 2008. Vascular System : Role of Nitric Oxide in Cardiovascular Diseases. , 10(4), pp.304–310.

Birjmohun, R.S. *et al.,* 2005. Efficacy and safety of high-density lipoprotein cholesterol-increasing compounds: a meta-analysis of randomized controlled trials. Journal of the American College of Cardiology, 45(2), pp.185–97.

Blanchette, J., Jaramillo, M. & Olivier, M., 2003. Signalling events involved in interferon-gamma-inducible macrophage nitric oxide generation. Immunology, 108(4), pp.513–22.

Blanco-Colio, L.M. *et al.,* 2002. 3-Hydroxy-3-methyl-glutaryl coenzyme A reductase inhibitors, atorvastatin and simvastatin, induce apoptosis of vascular smooth muscle cells by downregulation of Bcl-2 expression and Rho A prenylation. Atherosclerosis, 161(1), pp.17–26.

Blanco-Rivero, J. *et al.,* 2007. Long-term fenofibrate treatment impairs endothelium-dependent dilation to acetylcholine by altering the cyclooxygenase pathway. Cardiovascular research, 75(2), pp.398–407.

Blum, A & Shamburek, R., 2009. The pleiotropic effects of statins on endothelial function, vascular inflammation, immunomodulation and thrombogenesis. Atherosclerosis, 203(2), pp.325–30.

Boer, R. *et al.,* 2000. The inhibitory potency and selectivity of arginine substrate site nitric-oxide synthase inhibitors is solely determined by their affinity toward the different isoenzymes. Molecular pharmacology, 58(5), pp.1026–34.

Bogdan, C., Röllinghoff, M. & Diefenbach, A, 2000. The role of nitric oxide in innate immunity. Immunological reviews, 173(1), pp.17–26.

Bogdan, C., 2001. Nitric oxide and the immune response. Nature immunology, 2(10), pp.907–16.

Boissel, J.-P. *et al*., 2004. The Neuronal Nitric Oxide Synthase Is Upregulated in Mouse Skin Repair and in Response to Epidermal Growth Factor in Human HaCaT Keratinocytes. Journal of investigational Dermatology, 123, pp.132–139.

Bonetti, P.O., 2003. Endothelial Dysfunction: A Marker of Atherosclerotic Risk. Arteriosclerosis, Thrombosis, and Vascular Biology, 23(2), pp.168–175.

Boo, Y.C. *et al*., 2003. Endothelial NO synthase phosphorylated at SER635 produces NO without requiring intracellular calcium increase. Free Radical Biology and Medicine, 35(7), pp.729–741.

Boo, Y.C. *et al.,* 2006. Coordinated regulation of endothelial nitric oxide synthase activity by phosphorylation and subcellular localization. Free radical biology & medicine, 41(1), pp.144–53.

Boo, Y.C., Sorescu, G., *et al.,* 2002. Shear stress stimulates phosphorylation of endothelial nitric-oxide synthase at Ser1179 by Akt-independent mechanisms: role of protein kinase A. The Journal of biological chemistry, 277(5), pp.3388–96.

Bouloumié, A, Schini-Kerth, V.B. & Busse, R., 1999. Vascular endothelial growth factor up-regulates nitric oxide synthase expression in endothelial cells. Cardiovascular research, 41(3), pp.773–80.

Braam, B. & Verhaar, M.C., 2007. Understanding eNOS for pharmacological modulation of endothelial function: a translational view. Current pharmaceutical design, 13(17), pp.1727–40.

Bradford, M., 1976. A Rapid and Sensitive Method for the Quantitation of Microgram Quantities of Protein Utilizing the Principle of Protein-Dye Binding. Anal. Biochem.; 72: 248-254.

Brandes, R.P., Weissmann, N. & Schröder, K., 2010. NADPH oxidases in cardiovascular disease. Free radical biology & medicine, 25, pp.459–461.

Bredt, D.S. *et al.,* 1991. Cloned and expressed nitric oxide synthase structurally resembles cytochrome P-450 reductase. Nature;351: 714 – 718.

Bredt, D.S. & Snyder, S.H., 1990. Isolation of nitric oxide synthetase, a calmodulin-requiring enzyme. Proceedings of the National Academy of Sciences of the United States of America, 87(2), pp.682–5.

Brenman, J.E. *et al.,* 1996. Interaction of nitric oxide synthase with the postsynaptic density protein PSD-95 and alpha1-syntrophin mediated by PDZ domains. Cell, 84(5), pp.757–67.

Brevetti, G., Schiano, V. & Chiariello, M., 2008. Endothelial dysfunction: a key to the pathophysiology and natural history of peripheral arterial disease? Atherosclerosis, 197(1), pp.1–11.

Bryan, N.S. *et al.,* 2004. Cellular targets and mechanisms of nitros(yl)ation: an insight into their nature and kinetics in vivo. Proceedings of the National Academy of Sciences of the United States of America, 101(12), pp.4308–13.

Bryan, N.S., 2006. Nitrite in nitric oxide biology: cause or consequence? A systems-based review. Free radical biology & medicine, 41(5), pp.691–701.

Buchwalow, I.B. *et al*., 2001. Inducible nitric oxide synthase in the myocard. Molecular and cellular biochemistry, 217, pp.73–82.

Butcher, E.C., 1991. Leukocyte-endothelial cell recognition: Three (or more) steps to specificity and diversity. Cell, 67(6):1033-36.

Butt, E. et al., 2000. Endothelial Nitric-oxide Synthase (Type III) Is Activated and Becomes Calcium Independent upon Phosphorylation by Cyclic Nucleotide-dependent Protein Kinases. Journal of Biological Chemistry, 275(7), pp.5179–5187.

Campbell, W.B. & Harder, D.R., 1999. Endothelium-Derived Hyperpolarizing Factors and Vascular Cytochrome P450 Metabolites of Arachidonic Acid in the Regulation of Tone. Circulation Research, 84(4), pp.484–488.

Cao, C. *et al.,* 2013. IKKε knockout prevents high fat diet induced arterial atherosclerosis and NF-κB signaling in mice. PloS one, 8(5), p.e64930.

Carneado, J. *et al.,* 2002. Simvastatin improves endothelial function in spontaneously hypertensive rats through a superoxide dismutase mediated antioxidant effect. Journal of hypertension, 20(3), pp.429–37.

Carter, A.M., 2005. Inflammation, thrombosis and acute coronary syndromes. Diabetes & vascular disease research : official journal of the International Society of Diabetes and Vascular Disease, 2(3), pp.113–21.

Castelli, W.P. *et al*., 1986. Incidence of coronary heart disease and lipoprotein cholesterol levels. The Framingham Study. JAMA: the journal of the American Medical Association; Vol. 256(20):2835-8.

Castro, L., Rodriguez, M. & Radi, R., 1994. Aconitase Is Readily Inactivated by Peroxynitrite , but Not by its Precursor, Nitric Oxide. The Journal of biological chemistry, 269(47), pp.29409–29415.

Chakkarwar, V.A., 2011. Fenofibrate attenuates nicotine-induced vascular endothelial dysfunction in the rat. Vascular pharmacology, 55(5-6), pp.163–8.

Chan, D.K. & Miskimins, W.K., 2012. Metformin and phenethyl isothiocyanate combined treatment in vitro is cytotoxic to ovarian cancer cultures. Journal of ovarian research, 5(1), p.19.

Channon, K.M., 2004. Tetrahydrobiopterin: Regulator of Endothelial Nitric Oxide Synthase in Vascular Disease. TCM, 14(8), pp.323–327.

Chen, M. *et al.,* 2008. Involvement of CAPON and nitric oxide synthases in rat muscle regeneration after peripheral nerve injury. Journal of molecular neuroscience : MN, 34(1), pp.89–100.

Chen, X. *et al.,* 2010. Simvastatin combined with nifedipine enhances endothelial cell protection by inhibiting ROS generation and activating Akt phosphorylation. Acta pharmacologica Sinica, 31(7), pp.813–20.

Chen, Y.-J. & Quilley, J., 2008. Fenofibrate treatment of diabetic rats reduces nitrosative stress, renal cyclooxygenase-2 expression, and enhanced renal prostaglandin release. The Journal of pharmacology and experimental therapeutics, 324(2), pp.658–63.

Chen, Z.P. *et al.,* 1999. AMP-activated protein kinase phosphorylation of endothelial NO synthase. FEBS letters, 443(3), pp.285–9.

Chiasson, V.L. *et al.,* 2011. Protein Kinase C ι II -Mediated Phosphorylation of Endothelial Nitric Oxide Synthase Threonine 495 Mediates the Endothelial Dysfunction Induced by FK506 (Tacrolimus). The Journal of pharmacology and experimental therapeutics, 337(3), pp.718–723.

Chinetti, G. *et al*., 1998. Activation of Proliferator-activated Receptors and Induces Apoptosis of Human Monocyte-derived Macrophages. Journal of Biological Chemistry, 273(40), pp.25573–25580.

Cho, H.J. *et al.,* 1992. Calmodulin is a subunit of nitric oxide synthase from macrophages. The Journal of experimental medicine, 176(2), pp.599–604.

Cordaillat, M. *et al*., 2007. Nitric oxide pathway counteracts enhanced contraction to membrane depolarization in aortic rings of rats on high-sodium diet. American journal of physiology. Regulatory, integrative and comparative physiology, 292(4), pp. R1557-62.

Cosby, K. *et al.,* 2003. Nitrite reduction to nitric oxide by deoxyhemoglobin vasodilates the human circulation. Nature medicine, 9(12), pp.1498–505.

Cosentino, F. *et al*, 1998. Tetrahydrobiopterin alters superoxide and nitric oxide release in prehypertensive rats. J Clin Invest; 101(7):1530–1537.

Cotton, J.M*. et al.,* 2001. Effects of Nitric Oxide Synthase Inhibition on Basal Function and the Force-Frequency Relationship in the Normal and Failing Human Heart In Vivo. Circulation, 104(19), pp.2318–2323.

Coughlan, K. A. *et al*., 2014. AMPK activation: a therapeutic target for type 2 diabetes? Diabetes, metabolic syndrome and obesity : targets and therapy, 7, pp.241–53.

Crabtree, M.J. *et al*., 2009. Quantitative regulation of intracellular endothelial nitric-oxide synthase (eNOS) coupling by both tetrahydrobiopterin-eNOS stoichiometry and biopterin redox status: insights from cells with tet-regulated GTP cyclohydrolase I expression. The Journal of biological chemistry, 284(2), pp.1136–44.

Crow, J.P., Beckman, J.S. & McCord, J.M., 1995. Sensitivity of the essential zinc-thiolate moiety of yeast alcohol dehydrogenase to hypochlorite and peroxynitrite. Biochemistry; 34(11):3544-52.

Cui, H. *et al*., 2007. PDZ protein interactions underlying NMDA receptor-mediated excitotoxicity and neuroprotection by PSD-95 inhibitors. The Journal of neuroscience : the official journal of the Society for Neuroscience, 27(37), pp.9901–15.

Daff, S., 2010. NO synthase: structures and mechanisms. Nitric oxide : biology and chemistry / official journal of the Nitric Oxide Society, 23, pp.1–11.

Davidson, M.H., 2005. Reducing residual risk for patients on statin therapy: the potential role of combination therapy. The American journal of cardiology, 96, p.3K–13K.

Davidson, S.M. & Duchen, M.R., 2007. Endothelial mitochondria: contributing to vascular function and disease. Circulation research, 100(8), pp.1128–41.

Davignon, J. & Ganz, P., 2004. Role of endothelial dysfunction in atherosclerosis. Circulation, 109(23 Suppl 1), pp.III27–32.

Davignon, J., Jacob, R.F. & Mason, R.P., 2004. The antioxidant effects of statins. Coronary Artery Disease, 15(5), pp.251–258.

Davis, M.E. *et al.,* 2001. Shear Stress Regulates Endothelial Nitric Oxide Synthase Expression Through c-Src by Divergent Signaling Pathways. Circulation Research, 89(11), pp.1073–1080.

Davis, M.E. *et al.,* 2004. Shear stress regulates endothelial nitric-oxide synthase promoter activity through nuclear factor kappaB binding. The Journal of biological chemistry, 279(1), pp.163–8.

De Martin, R. *et al*., 2000. The Transcription Factor NF- B and the Regulation of Vascular Cell Function. Arteriosclerosis, Thrombosis, and Vascular Biology, 20(11), pp.e83–e88.

De Palma, C. *et al.,* 2006. Endothelial nitric oxide synthase activation by tumor necrosis factor alpha through neutral sphingomyelinase 2, sphingosine kinase 1, and sphingosine 1 phosphate receptors: a novel pathway relevant to the pathophysiology of endothelium. Arteriosclerosis, thrombosis, and vascular biology, 26(1), pp.99–105.

Deanfield, J.E., Halcox, J.P. & Rabelink, T.J., 2007. Endothelial function and dysfunction: testing and clinical relevance. Circulation, 115(10), pp.1285–95.

Del Campo, L., Blanco-Rivero, J. & Balfagon, G., 2011. Fenofibrate increases neuronal vasoconstrictor response in mesenteric arteries from diabetic rats: role of noradrenaline,

neuronal nitric oxide and calcitonin gene-related peptide. European journal of pharmacology, 666(1-3), pp.142–9.

Demyanets, S. *et al*., 2006. Hydroxymethylglutaryl-coenzyme A reductase inhibitors induce apoptosis in human cardiac myocytes in vitro. Biochemical pharmacology, 71(9), pp.1324–30.

Deplanque, D. *et al*., 2003. Peroxisome proliferator-activated receptor-alpha activation as a mechanism of preventive neuroprotection induced by chronic fenofibrate treatment. The Journal of neuroscience : the official journal of the Society for Neuroscience, 23(15), pp.6264–71.

Despre, J., 2001. Cholesterol : An Update on Fenofibrate. The American journal of cardiology, 88(12A), pp.30–36.

Dhanakoti, S.N. *et al*., 2000. Involvement of cGMP-dependent protein kinase in the relaxation of ovine pulmonary arteries to cGMP and cAMP contraction Involvement of cGMP-dependent protein kinase in the relaxation of ovine pulmonary arteries to cGMP and cAMP. Journal of Applied Physiology, 88, pp. 1637-1642.

Diebold, B.A., Bokoch, G.M., 2001. Molecular basis for Rac2 regulation of phagocyte NADPH oxidase. Nat Immunol; 2: 211–215.

Dimmeler, S. *et al.,* 1999. Activation of nitric oxide synthase in endothelial cells by Akt-dependent phosphorylation. Nature, 399(6736), pp.601–5.

Dimmeler, S., Dernbach, E. & Zeiher, A. M., 2000. Phosphorylation of the endothelial nitric oxide synthase at ser-1177 is required for VEGF-induced endothelial cell migration. FEBS letters, 477, pp.258–62.

Dong, M. *et al*., 2010. Rho-kinase inhibition: a novel therapeutic target for the treatment of cardiovascular diseases. Drug Discovery Today, 15(15-16), pp. 622-629.

Downs, J.R. *et al.,* 1998. Primary Prevention of Acute Coronary Events With Lovastatin in Men and Women With Average Cholesterol Levels: results of AFCAPS/TexCAPS, Air Force/Texas Coronary Atherosclerosis Prevention Study. JAMA : the journal of the American Medical Association, 279, pp.1615–1622.

Doyle, M.P. & Hoekstra, J.W., 1981. Oxidation of nitrogen oxides by bound dioxygen in hemoproteins. Journal of inorganic biochemistry, 14(4), pp.351–8.

Drew, B.G. *et al*., 2004. High-density lipoprotein and apolipoprotein AI increase endothelial NO synthase activity by protein association and multisite phosphorylation. Proceedings of the National Academy of Sciences of the United States of America, 101(18), pp.6999–7004.

Dreyer, J. *et al.,* 2004. Nitric oxide synthase (NOS)-interacting protein interacts with neuronal NOS and regulates its distribution and activity. The Journal of neuroscience : the official journal of the Society for Neuroscience, 24(46), pp.10454–65.

Dudzinski, D. & Michel, T., 2007. Life history of eNOS: Partners and pathways. Cardiovascular research, 75(2), pp.247–260.

Dudzinski, D.M. *et al.,* 2006. The regulation and pharmacology of endothelial nitric oxide synthase. Annual review of pharmacology and toxicology, 46, pp.235–76.

Duranski, M.R. *et al.,* 2005. Cytoprotective effects of nitrite during in vivo ischemia-reperfusion of the heart and liver. The Journal of clinical investigation, 115(5), pp.1232–40.

El-Azab, M.F., Hazem, R.M. & Moustafa, Y.M., 2012. Role of simvastatin and/or antioxidant vitamins in therapeutic angiogenesis in experimental diabetic hindlimb ischemia: effects on capillary density, angiogenesis markers, and oxidative stress. European journal of pharmacology, 690(1-3), pp.31–41.

El-Mlili, N. *et al.,* 2008. Chronic hyperammonemia reduces the activity of neuronal nitric oxide synthase in cerebellum by altering its localization and increasing its phosphorylation by calcium-calmodulin kinase II. Journal of neurochemistry, 106(3), pp.1440–9.

Endo, A., 2004. The origin of the statins. 2004. Atherosclerosis. Supplements, 5(3), pp.125–30.

Erwin, P.A. *et al.,* 2005. Receptor-regulated dynamic S-nitrosylation of endothelial nitric-oxide synthase in vascular endothelial cells. The Journal of biological chemistry, 280(20), pp.19888–94.

Falk, E., 2006. Pathogenesis of atherosclerosis. Journal of the American College of Cardiology, 47(8 Suppl), pp.C7–12.

Fan, J.-S. *et al.,* 1998. Protein Inhibitor of Neuronal Nitric-oxide Synthase, PIN, Binds to a 17-Amino Acid Residue Fragment of the Enzyme. Journal of Biological Chemistry, 273(50), pp.33472–33481.

Farnier, M., 2008. Update on the clinical utility of feno fi brate in mixed dyslipidemias : mechanisms of action and rational prescribing. Vascular health and risk management, 4(5), pp.991–1000.

Félétou, M. & Vanhoutte, P.M., 2009. EDHF: an update. Clinical science, 117(4), pp.139–55.

Ferdinandy, P. & Schulz, R., 2003. Nitric oxide, superoxide, and peroxynitrite in myocardial ischaemia-reperfusion injury and preconditioning. British journal of pharmacology, 138(4), pp.532–43.

Fichtlscherer, S. *et al*., 2004. Inhibition of cytochrome P450 2C9 improves endothelium-dependent, nitric oxide-mediated vasodilatation in patients with coronary artery disease. Circulation, 109(2), pp.178–83.

Fisslthaler, B. *et al*., 1999. Cytochrome P450 2C is an EDHF synthase in coronary arteries. Nature, 401(6752), pp.493–7.

Fisslthaler, B. *et al.,* 2000. Phosphorylation and activation of the endothelial nitric oxide synthase by fluid shear stress. Acta physiologica Scandinavica, 168(1), pp.81–8.

Fisslthaler, B. *et al.,* 2008. Inhibition of endothelial nitric oxide synthase activity by proline-rich tyrosine kinase 2 in response to fluid shear stress and insulin. Circulation research, 102(12), pp.1520–8.

Fleming, I., Bara, A.T. & Busse, R., 1996. Calcium signalling and autacoid production in endothelial cells are modulated by changes in tyrosine kinase and phosphatase activity. J Vasc Res;33(3):225-34.

Fleming, I. & Busse, R., 1999. Signal transduction of eNOS activation. Cardiovascular research, 43(3), pp.532–41.

Fleming, I. & Busse, R., 2003. Molecular mechanisms involved in the regulation of the endothelial nitric oxide synthase. American journal of physiology, Regulatory, integrative and comparitive physiology, 284, pp.R1–R12.

Fleming, I. *et al*., 1998. Ca2+-Independent Activation of the Endothelial Nitric Oxide Synthase in Response to Tyrosine Phosphatase Inhibitors and Fluid Shear Stress. Circulation Research, 82(6), pp.686–695.

Fleming, I. *et al*., 2001. Phosphorylation of Thr495 Regulates Ca2+/Calmodulin-Dependent Endothelial Nitric Oxide Synthase Activity. Circulation Research, 88(11), pp.e68–e75.

Folkman, J. & Shing, Y., 1992. Angiogenesis. The Journal of biological chemistry, 267(16), pp.10931–10934.

Förstermann, U., Boissel, J.-P. & Kleinert, H., 1998. Expressional control of the “constitutive” isoforms of nitric oxide synthase (NOS I and NOS III). FASEB Journal, 12, pp.773–790.

Förstermann, U. & Sessa, W.C., 2011. Nitric oxide synthases: regulation and function. European heart journal, 33(7), pp.829–37, 837a–837d.

Fridolfsson, H.N. *et al*., 2014. Regulation of intracellular signaling and function by caveolin. FASEB journal : official publication of the Federation of American Societies for Experimental Biology, 28, pp.1–9.

Fruchart, J-C., Duriez, P. & Staels, B., 1999. Peroxisome proliferator-activated receptor-alpha activators regulate genes governing lipoprotein metabolism, vascular inflammation and atherosclerosis. Current Opinion in Lipidology, 10, pp.245-257.

Fuentes, E. & Palomo, I., 2014. Mechanism of antiplatelet action of hypolipidemic, antidiabetic and antihypertensive drugs by PPAR activation: PPAR agonists: New antiplatelet agents. Vascular pharmacology.

Fujimura, N. *et al.,* 2012. Geranylgeranylacetone, heat shock protein 90/AMP-activated protein kinase/endothelial nitric oxide synthase/nitric oxide pathway, and endothelial function in humans. Arteriosclerosis, thrombosis, and vascular biology, 32(1), pp.153–60.

Fukata, M. *et al.,* 2004. Identification of PSD-95 Palmitoylating Enzymes University of California at San Francisco. Neuron, 44, pp.987–996.

Fukuda, Y. *et al.,* 2002. Tetrahydrobiopterin restores endothelial function of coronary arteries in patients with hypercholesterolaemia. (Basic Research) Heart; Vol.87(3), p.264(6)

Fulton, D., Gratton, J.P. & Sessa, W.C., 2001. Post-translational control of endothelial nitric oxide synthase: why isn't calcium/calmodulin enough? The Journal of pharmacology and experimental therapeutics, 299(3), pp.818–24.

Fulton, D. *et al*., 2005. Src kinase activates endothelial nitric-oxide synthase by phosphorylating Tyr-83. The Journal of biological chemistry, 280(43), pp.35943–52.

Furchgott, R.F. & Zawadzki, J.V., 1980. The obligatory role of endothelial cells in the relaxation of arterial smooth muscle by acetylcholine. Nature;299: 373–376.

Furchgott R.F., 1988. Studies on relaxation of rabbit aorta by sodium nitrite: the basis for the proposal that acid-activable inhibitory factor from bovine retractor penis is inorganic nitrite and the endothelium-derived relaxing factor is nitric oxide. In Vanhoutte PM, Ed. Vasodilatation: Vascular Smooth Muscle Peptides, Autonomic Nerves, and Endothelium. New York: Raven Press, 23,pp.401–414.

Galley, H.F. & Webster, N.R., 2004. Physiology of the endothelium. British journal of anaesthesia, 93(1), pp.105–13.

Gallis, B. *et al.,* 1999. Identification of Flow-dependent Endothelial Nitric-oxide Synthase Phosphorylation Sites by Mass Spectrometry and Regulation of Phosphorylation and Nitric Oxide Production by the Phosphatidylinositol 3-Kinase Inhibitor LY294002. Journal of Biological Chemistry, 274(42), pp.30101–30108.

Gao, X. *et al.,* 2007. Tumor necrosis factor-alpha induces endothelial dysfunction in Lepr(db) mice. Circulation, 115(2), pp.245–54.

Garcia-Cardena, G. *et al*., 1996. Endothelial Nitric Oxide Synthase Is Regulated by Tyrosine Phosphorylation and Interacts with Caveolin-1. Journal of Biological Chemistry, 271(44), pp.27237–27240.

Garg, C.U. & Hassid, A., 1989. Nitric oxide-generating vasodilators and 8-Bromo-Cyclic Guanosine Monophosphate inhibit mitogenesis and proliferation of cultured rat vascular smooth muscle cells. J. Clin. Invest., 83(May), pp.1774–1777.

Garvey, E.P. *et al*., 1997. 1400W is a slow, tight binding, and highly selective inhibitor of inducible nitric-oxide synthase in vitro and in vivo. The Journal of biological chemistry, 272(8), pp.4959–63.

Genis, A., 2014. Exposure of cardiac microvascular endothelial cells to harmful stimuli: A study of the cellular responses and mechanisms. PhD thesis, University of Stellenbosch.

Ghafourifar, P. & Richter, C., 1997. Nitric oxide synthase activity in mitochondria. FEBS Letters, 418(3), pp.291–296.

Ghosh, D.K., Abu-Soud, H.M. & Stuehr, D.J., 1996. Domains of macrophage N(O) synthase have divergent roles in forming and stabilizing the active dimeric enzyme. Biochemistry, 35(5), pp.1444–9.

Ghosh-choudhury, N. *et al.,* 2010. Simvastatin induces derepression of PTEN expression via NFkappaB to inhibit breast cancer cell growth. Cell Signal., 22(5), pp.749–758.

Girona, J. *et al*., 1999. Simvastatin decreases aldehyde production derived from lipoprotein oxidation. Am J Cardiol, 83, pp.846–851.

Giustarini, D. *et al.,* 2008. Nitrite and nitrate measurement by Griess reagent in human plasma: evaluation of interferences and standardization. Methods in enzymology, 440(07), pp.361–80.

Glass, C.K. & Witztum, J.L., 2001. Atherosclerosis : The Road Ahead Review. Cell, 104(February), pp.503–516.

Gomez Sandoval, Y.-H. & Anand-Srivastava, M.B., 2011. Enhanced levels of endogenous endothelin-1 contribute to the over expression of Giα protein in vascular smooth muscle cells from SHR: Role of growth factor receptor activation. Cellular signalling, 23(2), pp.354–62.

Gordon, T. *et al.,* 1977. High density lipoprotein as a protective factor against coronary heart disease. The Framingham Study. Am J Med; May;62(5):707-14.

Gorren, A.C.F. & Mayer, B., 2007. Nitric-oxide synthase: a cytochrome P450 family foster child. Biochimica et biophysica acta, 1770(3), pp.432–45.

Gotto, A.M. & Farmer, J. A., 2006. Drug insight: the role of statins in combination with ezetimibe to lower LDL cholesterol. Nature clinical practice. Cardiovascular medicine, 3(12), pp.664–72.

Govers, R. & Rabelink, T.O.N.J., 2001. Cellular regulation of endothelial nitric oxide synthase. American journal of physiology, Renal Physiology, 280, pp.F193–F206.

Goya, K. *et al*., 2004. Peroxisome proliferator-activated receptor alpha agonists increase nitric oxide synthase expression in vascular endothelial cells. Arteriosclerosis, thrombosis, and vascular biology, 24(4), pp.658–663.

Greenwood, J. & Mason, J.C., 2007. Statins and the vascular endothelial inflammatory response. Trends in immunology, 28(2), pp.88–98.

Griendling, K.K. & FitzGerald, G.A., 2003. Oxidative stress and cardiovascular injury: Part I: basic mechanisms and in vivo monitoring of ROS. Circulation, 108(16), pp.1912–6.

Griess, P., 1879. Bermerkungen zu der Abhandlung der HH. Weselsky and Benedict "Ueber einige Azoverbindungen. Ber. Dtsch. Chem. Ges., 12, pp426-428.

Groemping, Y. & Rittinger, K., 2005. Activation and assembly of the NADPH oxidase : a structural perspective. Biochem. J., 386, pp.401–416.

Groth, A. *et al*., 2014. Inflammatory cytokines in pulmonary hypertension. Respiratory research, 15(1), p.47.

Grover-Páez, F. & Zavalza-Gómez, A.B., 2009. Endothelial dysfunction and cardiovascular risk factors. Diabetes research and clinical practice, 84(1), pp.1–10.

Grumbach, I.M. *et al.,* 2005. A negative feedback mechanism involving nitric oxide and nuclear factor kappa-B modulates endothelial nitric oxide synthase transcription. Journal of molecular and cellular cardiology, 39(4), pp.595–603.

Gryglewski, R.J., Palmer, R.M.J. & Moncada S., 1986. Superoxide anion is involved in the breakdown of endothelium-derived vascular relaxing factor. Nature; 320:454-456.

Guilluy, C. *et al*., 2007. Transglutaminase-dependent RhoA Activation and Depletion by Serotonin in Vascular Smooth Muscle Cells. The Journal of Biological Chemistry, 282(5), pp. 2918-28.

Guyton, A.C. & Hall, J.E., 2000. The textbook of Medical Physiology. 10th ed. WB Saunders company, USA, Philadelphia.

Gyrd-Hansen, M. & Meier, P., 2010. IAPs: from caspase inhibitors to modulators of NF-kappaB, inflammation and cancer. Nature reviews. Cancer, 10(8), pp.561–74.

Haas, M.J. & Mooradian, A.D., 2010. Regulation of high-density lipoprotein by inflammatory cytokines: establishing links between immune dysfunction and cardiovascular disease. Diabetes/Metabolism Research and Reviews, 26 (2): 90–99.

Halliwell, B., 1997. What nitrates tyrosine? Is nitrotyrosine specific as a biomarker of peroxynitrite formation in vivo? FEBS Letters, 411, pp.157–60.

Han, C.-H. *et al.,* 1998. Regulation of the Neutrophil Respiratory Burst Oxidase. IDENTIFICATION OF AN ACTIVATION DOMAIN IN p67phox. Journal of Biological Chemistry, 273(27), pp.16663–16668.

Harris, M.B. *et al.,* 2001. Reciprocal phosphorylation and regulation of endothelial nitric-oxide synthase in response to bradykinin stimulation. The Journal of biological chemistry, 276(19), pp.16587–91.

Harris, M.B. *et al.,* 2004. Acute activation and phosphorylation of endothelial nitric oxide synthase by HMG-CoA reductase inhibitors. American journal of physiology. Heart and circulatory physiology, 287(2), pp.H560–6.

Haslinger, B. *et al.,* 2003. Simvastatin suppresses tissue factor expression and increases fibrinolytic activity in tumor necrosis factor-alpha-activated human peritoneal mesothelial cells. Kidney international, 63(6), pp.2065–74.

Hattori, Y. *et al.,* 1996. Tetrahydrobiopterin and GTP cyclohydrolase I in a rat model of endotoxic shock: relation to nitric oxide synthesis. Experimental physiology, 81(4), pp.665–71.

Hausenloy, D.J. & Yellon, D.M., 2008. Targeting residual cardiovascular risk: raising high-density lipoprotein cholesterol levels. Heart, 94, pp.706–714.

Hayden, M.S. & Ghosh, S., 2008. Shared principles in NF-kappaB signaling. Cell, 132(3), pp.344–62.

Head, B.P., Patel, H.H. & Insel, P. A., 2014. Interaction of membrane/lipid rafts with the cytoskeleton: impact on signaling and function: membrane/lipid rafts, mediators of cytoskeletal arrangement and cell signaling. Biochimica et biophysica acta, 1838(2), pp.532–45.

Heeba, G. *et al*., 2007. Adverse balance of nitric oxide/peroxynitrite in the dysfunctional endothelium can be reversed by statins. Journal of cardiovascular pharmacology, 50(4), pp.391–8.

Heemskerk, N., van Rijssel, J. & van Buul, J.D., 2014. Rho-GTPase signaling in leukocyte extravasation: An endothelial point of view. Cell adhesion & migration, 8(2), pp.67–75.

Heitzer, T. *et al*., 2000. Tetrahydrobiopterin improves endothelium-dependent vasodilation by increasing nitric oxide activity in patients with Type II diabetes mellitus. Diabetologia; 43: 1435-8.

Heitzer, T. *et al.,* 2001. Endothelial Dysfunction, Oxidative Stress, and Risk of Cardiovascular Events in Patients With Coronary Artery Disease. Circulation, 104(22), pp.2673–2678.

Hoffmann, A., Natoli, G. & Ghosh, G., 2006. Transcriptional regulation via the NF-kappaB signaling module. Oncogene, 25(51), pp.6706–16.

Honkanan, R.E. *et al.,* 1994. Characterization of natural toxins with inhibitory activity against serine/threonine protein phosphatases. Toxicon, 32(3), pp.339–350.

Hou, C.J.-Y. *et al*., 2008. Diabetes reduces aortic endothelial gap junctions in ApoE-deficient mice: simvastatin exacerbates the reduction. The journal of histochemistry and cytochemistry : official journal of the Histochemistry Society, 56(8), pp.745–52.

Hou, R. & Goldberg, A.C., 2009. Lowering low-density lipoprotein cholesterol: statins, ezetimibe, bile acid sequestrants, and combinations: comparative efficacy and safety. Endocrinology and metabolism clinics of North America, 38, pp.79–97.

Huang, Z. *et al.,* 2008. Activation of peroxisome proliferator-activated receptor-alpha in mice induces expression of the hepatic low-density lipoprotein receptor. British journal of pharmacology, 155(4), pp.596–605.

Huisamen, B. *et al.*, 2011. ANG II type I receptor antagonism improved nitric oxide production and enhanced eNOS and PKB/Akt expression in hearts from a rat model of insulin resistance. Molecular and cellular biochemistry, 349(1-2), pp.21–31.

Hulsmans, M. *et al*., 2012. Decrease of miR-146b-5p in monocytes during obesity is associated with loss of the anti-inflammatory but not insulin signaling action of adiponectin. PloS one, 7(2), p.e32794.

Igarashi, J., Bernier, S.G. & Michel, T., 2001. Sphingosine 1-phosphate and activation of endothelial nitric-oxide synthase. differential regulation of Akt and MAP kinase pathways by EDG and bradykinin receptors in vascular endothelial cells. The Journal of biological chemistry, 276(15), pp.12420–6.

Ii, M. & Losordo, D.W., 2007. Statins and the endothelium. Vascular pharmacology, 46(1), pp.1–9.

Iliodromitis, E.K. *et al*., 2010. Simvastatin in contrast to postconditioning reduces infarct size in hyperlipidemic rabbits: possible role of oxidative/nitrosative stress attenuation. Basic research in cardiology, 105(2), pp.193–203.

Imrie, H. *et al.,* 2009. Vascular Insulin-Like Growth Factor-I Resistance and Diet-Induced Obesity. Endocrinology, Vol.150(10), pp.4575-4582.

Ischiropoulos, H. *et al*., 1999. Detection of reactive nitrogen species using 2.7-Dichlorodihydrofluorescein and dihydrorhodamine 123. Methods in enzymology, 301, pp.367–373.

Ishii, M. *et al*., 1997. Acceleration of oxidative stress-induced endothelial cell death by nitric oxide synthase dysfunction accompanied with decrease in tetrahydrobiopterin content. Life sciences, 61(7), pp.739–47.

Istvan, E.S. *et al.*, 2000. Crystal structure of the catalytic portion of human HMG-CoA reductase: insights into regulation of activity and catalysis. The EMBO journal, 19(5), pp.819–30.

Jang IK, Lassila R & Fuster V., 1993. Atherogenesis and inflammation. Eur. Heart J.; 14 (Suppl K:2-6).

Jones, S.P. & Bolli, R., 2006. The ubiquitous role of nitric oxide in cardioprotection. Journal of molecular and cellular cardiology, 40(1), pp.16–23.

Jones, S.P. *et al*., 1999. Myocardial ischemia-reperfusion injury is exacerbated in absence of endothelial cell nitric oxide synthase. The American journal of physiology, 276(5 Pt 2), pp.H1567–73.

Junquero, D.C. *et al*., 1992. Inhibition of cytokine-induced nitric oxide production by transforming growth factor-B1 in human smooth muscle cells. Journal of Physiology, 454, pp.451–465.

Kaneta, S. *et al.,* 2003. All hydrophobic HMG-CoA reductase inhibitors induce apoptotic death in rat pulmonary vein endothelial cells. Atherosclerosis, 170(2), pp.237–243.

Kanno, S. *et al.,* 2000. Attenuation of Myocardial Ischemia/Reperfusion Injury by Superinduction of Inducible Nitric Oxide Synthase. Circulation, 101(23), pp.2742–2748.

Kapur, N.K. & Musunuru, K., 2008. Clinical efficacy and safety of statins in managing cardiovascular risk. Vascular health and risk management, 4(2), pp.341–53.

Kashani, A. *et al*., 2006. Risks associated with statin therapy: a systematic overview of randomized clinical trials. Circulation, 114(25), pp.2788–97.

Katayama, A. *et al.,* 2009. Fenofibrate enhances neovascularization in a murine ischemic hindlimb model. Journal of cardiovascular pharmacology, 54(5), pp.399–404.

Katsiki, N. *et al.,* 2010. Effect of HMG-CoA reductase inhibitors on vascular cell apoptosis: beneficial or detrimental? Atherosclerosis, 211(1), pp.9–14.

Kaur, J., Reddy, K. & Balakumar, P., 2010. The novel role of fenofibrate in preventing nicotine- and sodium arsenite-induced vascular endothelial dysfunction in the rat. Cardiovascular toxicology, 10(3), pp.227–38.

Kawanabe, Y. & Nauli, S.M., 2011. Endothelin. Cellular and molecular life sciences : CMLS, 68(2), pp.195–203.

Keech, A.C. *et al.*, 2007. Effect of fenofibrate on the need for laser treatment for diabetic retinopathy (FIELD study): a randomised controlled trial. Lancet, 370(9600), pp.1687–97.

Keech, A. *et al.,* 2005. Effects of long-term fenofibrate therapy on cardiovascular events in 9795 people with type 2 diabetes mellitus (the FIELD study): randomised controlled trial. Lancet, 366(9500), pp.1849–61.

Kiechl, S. *et al.,* 2012. Subclinical Atherosclerosis, Markers of Inflammation, and Oxidative Stress. Ultrasound and Carotid Bifurcation Atherosclerosis; 4:487-509.

Kim, J. *et al*., 2007. Fenofibrate regulates retinal endothelial cell survival through the AMPK signal transduction pathway. Experimental Eye Research, 84(5), 886–93.

Kin, H. *et al*., 2006. Neutrophil depletion reduces myocardial apoptosis and attenuates NFkappaB activation/TNFalpha release after ischemia and reperfusion. The Journal of surgical research, 135(1), pp.170–8.

Kitakaze, M. *et al.,* 2001. Role of cellular acidosis in production of nitric oxide in canine ischemic myocardium. Journal of molecular and cellular cardiology, 33, pp.1727–37.

Kleinbongard, P. *et al*., 2003. Plasma nitrite reflects constitutive nitric oxide synthase activity in mammals. Free Radical Biology and Medicine, 35(7), pp.790–796.

Kon Koh, K. *et al.,* 2006. Additive Beneficial Effects of Fenofibrate Combined With Candesartan in the Treatment of Hypertriglyceridemic. Diabetes Care, 29, pp.195–201.

Korkmaz, B. *et al*., 2011. Activation of MEK1/ERK1/2/iNOS/sGC/PKG pathway associated with peroxynitrite formation contributes to hypotension and vascular hyporeactivity in endotoxemic rats. *Nitric oxide : biology and chemistry / official journal of the Nitric Oxide Society*, 24(3), pp.160–72.

Kou, R., Greif, D. & Michel, T., 2002. Dephosphorylation of endothelial nitric-oxide synthase by vascular endothelial growth factor. Implications for the vascular responses to cyclosporin A. The Journal of biological chemistry, 277(33), pp.29669–73.

Krishna, S.M. *et al*., 2012. Fenofibrate increases high-density lipoprotein and sphingosine 1 phosphate concentrations limiting abdominal aortic aneurysm progression in a mouse model. The American Journal of Pathology, 181(2), pp. 706-718.

Krysiak, R., Gdula-Dymek, A. & Okopien, B., 2013. The effect of fenofibrate on lymphocyte release of proinflammatory cytokines and systemic inflammation in simvastatin-treated patients with atherosclerosis and early glucose metabolism disturbances. Basic & clinical pharmacology & toxicology, 112(3), pp.198–202.

Kubota, T. *et al*., 2005. Fenofibrate induces apoptotic injury in cultured human hepatocytes by inhibiting phosphorylation of Akt. Apoptosis : an international journal on programmed cell death, 10(2), pp.349–58.

Kureishi, Y. *et al.,* 2000. The HMG-CoA reductase inhibitor simvastatin activates the protein kinase Akt and promotes angiogenesis in normocholesterolemic animals. Nature medicine, 6(9), pp.1004–10.

Kuribayashi, K., Mayes, P.A. & El-deiry, W.S., 2006. What are Caspases 3 and 7 Doing Upstream of the Mitochondria? Cancer Biology & Therapy, 5(7), pp.763–765.

Laemmli, U.K., 1970. Cleavage of Structural Proteins during the Assembly of the Head of Bacteriophage T4. Nature; 227: 680 – 685.

La Sala, A. *et al.,* 2012. Regulation of collateral blood vessel development by the innate and adaptive immune system. Trends in molecular medicine, 18(8), pp.494–501.

Lacza, Z. *et al.,* 2006. Mitochondrial NO and reactive nitrogen species production: does mtNOS exist? Nitric oxide : biology and chemistry / official journal of the Nitric Oxide Society, 14(2), pp.162–8.

Lahoz, C. & Mostaza, J.M., 2007. Atherosclerosis as a systemic disease. Rev Esp Cardiol, 60(2), pp.184–95.

Lamas, S. *et al*., 1992. Endothelial nitric oxide synthase: molecular cloning and characterization of a distinct constitutive enzyme isoform. Proceedings of the National Academy of Sciences of the United States of America, 89(14), pp.6348–52.

Larsen, P.J. *et al*., 2003. Differential Influences of Peroxisome Proliferator – Activated Receptors gamma and alpha on Food Intake and Energy Homeostasis. Diabetes, 52, pp. 2249-2259.

LaRosa, J.C. *et al*., 2005. Intensive lipid lowering with atorvastatin in patients with stable coronary disease. The New England journal of medicine, 352(14), pp.1425–35.

LaRosa, J.C., 2001. Pleiotropic effects of statins and their clinical significance. The American journal of cardiology, 88(3), pp.291–3.

Lee, J.-J. *et al*., 2009. Antithrombotic and antiplatelet activities of fenofibrate, a lipid-lowering drug. Atherosclerosis, 206(2), pp.375–82.

Lefer, D.J. *et al.,* 2001. HMG-CoA reductase inhibition protects the diabetic myocardium from ischemia-reperfusion injury. FASEB journal : official publication of the Federation of American Societies for Experimental Biology, 15(8), pp.1454–6.

Lei, J. *et al.,* 2013. Nitric oxide, a protective molecule in the cardiovascular system. Nitric oxide : biology and chemistry / official journal of the Nitric Oxide Society, 35, pp.175–85.

Lepore, D.A., 2000. Nitric oxide synthase-independent generation of nitric oxide in muscle ischemia--reperfusion injury. Nitric oxide : biology and chemistry / official journal of the Nitric Oxide Society, 4(6), pp.541–5.

Lewis, J.H., 2012. Clinical perspective: statins and the liver--harmful or helpful? Digestive diseases and sciences, 57(7), pp.1754–63.

Li, X. *et al*., 2012. Phosphorylation of endothelial NOS contributes to simvastatin protection against myocardial no-reflow and infarction in reperfused swine hearts: partially via the PKA signaling pathway. Acta pharmacologica Sinica, 33(7), pp.879–87.

Liao, J.K. & Laufs, U., 2005. Pleiotropic effects of statins. Annual review of pharmacology and toxicology, 45(4), pp.89–118.

Libby, P., 2006. Inflammation and cardiovascular disease mechanisms. The American journal of clinical nutrition, 83(2), p.456S–460S.

Lin, W.-H., Zhang, H. & Zhang, Y.-T., 2013. Investigation on Cardiovascular Risk Prediction Using Physiological Parameters. Computational and mathematical methods in medicine, pp.1–21.

Liu, S. *et al.,* 2011. Long-term fenofibrate treatment impaired glucose-stimulated insulin secretion and up-regulated pancreatic NF-kappa B and iNOS expression in monosodium

glutamate-induced obese rats: is that a latent disadvantage? Journal of translational medicine, 9(1), p.176.

Liu, A. *et al*., 2012. Relaxation of rat thoracic aorta by fibrate drugs correlates with their potency to disturb intracellular calcium of VSMCs. Vascular Pharmacology, 56(3-4), pp. 168-75.

Loot, A.E. *et al*., 2009. Angiotensin II impairs endothelial function via tyrosine phosphorylation of the endothelial nitric oxide synthase. The Journal of experimental medicine, 206(13), pp.2889–96.

Loubser, D.J., 2014. Nitric Oxide and the Endothelium: Characterisation of in vitro Nitric Oxide Detection Techniques and an ex vivo Method of Measuring Endothelial Function. M.Sc dissertation, Stellenbosch University.

Lowry, J.L. *et al*., 2013. Endothelial nitric-oxide synthase activation generates an inducible nitric-oxide synthase-like output of nitric oxide in inflamed endothelium. The Journal of biological chemistry, 288(6), pp.4174–93.

Lüscher, T.F. & Vanhoutte, P.M., 1990 The endothelium: modulator of cardiovascular function. CRC, Boca Raton, pp 1–228.

Lyons, C.R., Orloff, J. & Cunningham, J.M., 1992. Molecular cloning and functional expression of an inducible nitric oxide synthase from a murine macrophage cell line. The Journal of biological chemistry, 267(9), pp.6370–6374.

MacMicking, J.D. *et al*., 1995. Altered responses to bacterial infection and endotoxic shock in mice lacking inducible nitric oxide synthase. Cell, 81(4), pp.641–50.

Maiolino, G. *et al.,* 2013. The role of oxidized low-density lipoproteins in atherosclerosis: the myths and the facts. Mediators of inflammation, 2013, p.714653.

Malek, A.M. *et al.*, 1999. Induction of nitric oxide synthase mRNA by shear stress requires intracellular calcium and G-protein signals and is modulated by PI 3 kinase. Biochemical and biophysical research communications, 254(1), pp.231–42.

Mancini, F.P.Y., 2001. Fenofibrate prevents and reduces body weight gain and adiposity in diet-induced obese rats. FEBS Letters, 491, pp. 154-158.

Marletta, M.A., 1993. Nitric oxide synthase structure and mechanism. The Journal of biological chemistry, 268(17), pp.12231–4.

Mas, M., 2009. A Close Look at the Endothelium: Its Role in the Regulation of Vasomotor Tone. European Urology Supplements, 8(2), pp.48–57.

Massaro, M. *et al.,* 2010. Statins inhibit cyclooxygenase-2 and matrix metalloproteinase-9 in human endothelial cells: anti-angiogenic actions possibly contributing to plaque stability. Cardiovascular research, 86(2), pp.311–20.

Massion, P.B. *et al*., 2003. Nitric oxide and cardiac function: ten years after, and continuing. Circulation research, 93(5), pp.388–98.

Mathewson, A.M. & Wadsworth, R.M., 2004. Induction of iNOS restricts functional activity of both eNOS and nNOS in pig cerebral artery. *Nitric oxide : biology and chemistry / official journal of the Nitric Oxide Society*, 11(4), pp.331–9.

Matsuno, H. *et al*., 2004. Simvastatin enhances the regeneration of endothelial cells via VEGF secretion in injured arteries. Journal of cardiovascular pharmacology, 43(3), pp.333–40.

McNeill, E. & Channon, K.M., 2012. The role of tetrahydrobiopterin in inflammation and cardiovascular disease. Thrombosis and haemostasis, 108(5), pp.832–9.

Meininger, C.J. *et al*., 2000. Impaired nitric oxide production in coronary endothelial cells of the spontaneously diabetic BB rat is due to tetrahydrobiopterin deficiency. Biochemistry Journal, 349, pp.353–356.

Mendis, S. *et al*., 2011. Global Atlas on cardiovascular disease prevention and control 2011. World Health Organization.

Mensah, K., Mocanu, M.M. & Yellon, D.M., 2005. Failure to protect the myocardium against ischemia/reperfusion injury after chronic atorvastatin treatment is recaptured by acute atorvastatin treatment: a potential role for phosphatase and tensin homolog deleted on chromosome ten? Journal of the American College of Cardiology, 45(8), pp.1287–91.

Michel, J.B. *et al.,* 1997. Reciprocal Regulation of Endothelial Nitric-oxide Synthase by Ca2+-Calmodulin and Caveolin. Journal of Biological Chemistry, 272(25), pp.15583–15586.

Michel, T. & Vanhoutte, P.M., 2010. Cellular signaling and NO production. Pflügers Archiv : European journal of physiology, 459(6), pp.807–16.

Michell, B.J. *et al.,* 2001. Coordinated control of endothelial nitric-oxide synthase phosphorylation by protein kinase C and the cAMP-dependent protein kinase. The Journal of biological chemistry, 276(21), pp.17625–8.

Michell, B.J. *et al*., 2002. Identification of regulatory sites of phosphorylation of the bovine endothelial nitric-oxide synthase at serine 617 and serine 635. The Journal of biological chemistry, 277(44), pp.42344–51.

Michiels, C., 2003. Endothelial cell functions. Journal of cellular physiology, 196, pp.430–43.

Miller, M.R. & Megson, I.L., 2007. Recent developments in nitric oxide donor drugs. British journal of pharmacology, 151(3), pp.305–21.

Mishra, O.P., Ashraf, Q.M. & Delivoria-Papadopoulos, M., 2009. Tyrosine phosphorylation of neuronal nitric oxide synthase (nNOS) during hypoxia in the cerebral cortex of newborn piglets: the role of nitric oxide. Neuroscience letters, 462(1), pp.64–7.

Mochizuki, M. *et al.,* 2010. Effect of Sesame Lignans on TNF-α-Induced Expression of Adhesion Molecules in Endothelial Cells. Bioscience, Biotechnology and Biochemistry, 74(8), pp.1539–1544.

Moore, P.K. & Handy, R.L., 1997. Selective inhibitors of neuronal nitric oxide synthase--is no NOS really good NOS for the nervous system? Trends in pharmacological sciences, 18(6), pp.204–11.

Mori, M. & Gotoh, T., 2000. Regulation of nitric oxide production by arginine metabolic enzymes. Biochemical and biophysical research communications, 275(3), pp.715–9.

Mount, P.F., Kemp, B.E. & Power, D.A., 2007. Regulation of endothelial and myocardial NO synthesis by multi-site eNOS phosphorylation. Journal of molecular and cellular cardiology, 42(2), pp.271–9.

Mpe, M.T., 2010. Are we doing enough to prevent a heart disease epidemic? Journal of the South African Heart Association; 7:146-149.

Mraiche, F. *et al*., 2005. Effects of statins on vascular function of endothelin-1. British journal of pharmacology, 144(5), pp.715–26.

Mudau, M. *et al.,* 2012. Endothelial dysfunction: the early predictor of atherosclerosis. Cardiovascular journal of Africa, 23(4), pp.222–31.

Mulhaupt, F. *et al*., 2003. Statins (HMG-CoA reductase inhibitors) reduce CD40 expression in human vascular cells. Cardiovascular research, 59(3), pp.755–66.

Münzel, T. *et al.,* 2005. Vascular consequences of endothelial nitric oxide synthase uncoupling for the activity and expression of the soluble guanylyl cyclase and the cGMP-dependent protein kinase. Arteriosclerosis, thrombosis, and vascular biology, 25, pp.1551–7.

Murakami, H. *et al*., 2006. Fenofibrate activates AMPK and increases eNOS phosphorylation in HUVEC. Biochemical and biophysical research communications, 341(4), pp.973–8.

Musial, A., and Eissa, N.T., 2001. Inducible nitric-oxide synthase is regulated by the proteasome degradation pathway. The Journal of biological chemistry;276(26):24268-73.

Natarajan, P., Ray, K.K. & Cannon, C.P., 2010. High-density lipoprotein and coronary heart disease: current and future therapies. Journal of the American College of Cardiology, 55(13), pp.1283–99.

Navarro-Antolín, J. *et al*., 2001. Formation of peroxynitrite in vascular endothelial cells exposed to cyclosporine A. FASEB journal : official publication of the Federation of American Societies for Experimental Biology, 15(7), pp.1291–3.

Nazarewicz, R.R., Bikineyeva, A. & Dikalov, S.I., 2013. Rapid and specific measurements of superoxide using fluorescence spectroscopy. Journal of biomolecular screening, 18(4), pp.498–503.

Ni, X.-Q. *et al*., 2013. Statins suppress glucose-induced plasminogen activator inhibitor-1 expression by regulating RhoA and nuclear factor-κB activities in cardiac microvascular endothelial cells. Experimental biology and medicine (Maywood, N.J.), 238(1), pp.37–46.

Nicholls, S.J. *et al.,* 2007. Statins, High-Density Lipoprotein Cholesterol and Regression of Coronary Atherosclerosis. JAMA : the journal of the American Medical Association, 297(5), pp.499–508.

Nieminen, M.S., Matilla, K. & Valtonen, V., 1993. Infection and inflammation as risk factors for myocardial infarction. Eur. Heart Journal; 14 (Suppl. K), 12–16.

Nikolaeva, S. *et al.,* 2012. Frog urinary bladder epithelial cells express TLR4 and respond to bacterial LPS by increase of iNOS expression and L-arginine uptake. American journal of physiology. Regulatory, integrative and comparative physiology, 303(10), pp.R1042–52.

Nishida, K. *et al*., 1992. Molecular Cloning and Characterization of the Constitutive Bovine Aortic Endothelial Cell Nitric Oxide Synthase. The Journal of clinical investigation, 90(November), pp.2092–2096.

Noto, D., Cefalù, A.B. & Averna, M.R., 2014. Beyond statins: new lipid lowering strategies to reduce cardiovascular risk. Current atherosclerosis reports, 16(6), p.414.

Nunes, K.P., Rigsby, C.S. & Webb, R.C., 2010. RhoA/Rho-kinase and vascular diseases: what is the link? Cellular and molecular life sciences : CMLS, 67(22), pp.3823–36.

Ohashi, Y. *et al*., 1998. Hypotension and reduced nitric oxide-elicited vasorelaxation in transgenic mice overexpressing endothelial nitric oxide synthase. The Journal of clinical investigation, 102(12), pp.2061–71.

Olsson, A.G. *et al.,* 2003. A 52-week, multicenter, randomized parallel-group, double-blind, double-dummy study to assess the efficacy of Atorvastatin and Simvastatin in Reaching Low-Density Lipoprotein Cholesterol and Triglyceride Targets : The Treat-to-Target (3T) Study. Clinical therapeutics, 265, pp.119–38.

Olukman, M. *et al.,* 2010. Fenofibrate treatment enhances antioxidant status and attenuates endothelial dysfunction in streptozotocin-induced diabetic rats. Experimental diabetes research, 2010, p.828531.

Omae, T. *et al.,* 2012. Fenofibrate, an anti-dyslipidemia drug, elicits the dilation of isolated porcine retinal arterioles: role of nitric oxide and AMP-activated protein kinase. Investigative ophthalmology & visual science, 53(6), pp.2880–6.

Opie, LH. Heart physiology: from cell to circulation. 4th ed. Lippincott Williams & Wilkins, 2004, Philadelphia.

Pan, J. *et al.,* 1996. Tyrosine phosphorylation of inducible nitric oxide synthase: implications for potential post-translational regulation. Biochemistry Journal, 314, pp.889–894.

Panda, K., Ghosh, S. & Stuehr, D.J., 2001. Calmodulin activates intersubunit electron transfer in the neuronal nitric-oxide synthase dimer. The Journal of biological chemistry, 276(26), pp.23349–56.

Panda, K. *et al.,* 2002. Distinct dimer interaction and regulation in nitric-oxide synthase types I, II, and III. The Journal of biological chemistry, 277(34), pp.31020–30.

Pandey, A. V & Flück, C.E., 2013. NADPH P450 oxidoreductase: structure, function, and pathology of diseases. Pharmacology & therapeutics, 138(2), pp.229–54.

Parihar, A. *et al*., 2012. Statins lower calcium-induced oxidative stress in isolated mitochondria. Human & experimental toxicology, 31(4), pp.355–63.

Pearson, T.A., Jamison, D.T. & Trejo-Guitireez, H., 1993. Cardiovascular disease. In: Jamison DT, Mosely WH, Measham AR, Bobadilla JL, eds. Disease control priorities in developing countries. New York: Oxford University Press:577-599.

Perez-Guerrero, C. *et al*., 2003. Effects of Simvastatin on Endothelial Function After Chronic Inhibition of Nitric Oxide Synthase by L -NAME. Journal of Cardiovascular Pharmacology, 42, pp.204–210.

Pheilschifter, J. & Vosbeck, K., 1991. Transforming growth factor B2 inhibits interleukin 1B and tumour necrosis factor alpha induction of nitric oxide synthase in rat renal mesangial cells. Biochemical and biophysical research communications, 175(2), pp.372–379.

Picchi, A. *et al.,* 2006. Tumor necrosis factor-alpha induces endothelial dysfunction in the prediabetic metabolic syndrome. Circulation research, 99(1), pp.69–77.

Pinzón-Daza, M. *et al*., 2012. The association of statins plus LDL receptor-targeted liposome-encapsulated doxorubicin increases in vitro drug delivery across blood-brain barrier cells. British journal of pharmacology, 167(7), pp.1431–47.

Piper H.M. *et al*., 1990. Microvascular endothelial cells from heart. In: Piper HM (editor). Cell culture techniques in heart vessel and research. Springer-Verlag, pp.158-173.

Pober, J.S., 2002. Endothelial activation: intracellular signaling pathways. Arthritis research, 4 Suppl 3, pp.S109–16.

Pollock, J.S. *et al.,* 1992. Endothelial nitric oxide synthase is myristylated. FEBS letters, 309(3), pp.402–4.

Polonsky, T.S. & Davidson, M.H., 2008. Reducing the residual risk of 3-hydroxy-3-methylglutaryl coenzyme a reductase inhibitor therapy with combination therapy. The American journal of cardiology, 101[suppl](8A), p.27B–35B.

Ponnuswamy, P. *et al.,* 2009. Oxidative stress and compartment of gene expression determine proatherosclerotic effects of inducible nitric oxide synthase. The American journal of pathology, 174(6), pp.2400–10.

Pou, S. *et al*., 1992. Generation of superoxide by purified brain nitric oxide synthase. The Journal of biological chemistry, 267(34), pp.24173–76.

Pou, S. *et al*., 1999. Mechanism of Superoxide Generation by Neuronal Nitric-oxide Synthase. Journal of Biological Chemistry, 274(14), pp.9573–9580.

Pries, A.R., Secomb, T.W. & Gaehtgens, P., 2000. The endothelial surface layer. Pflügers Archiv, 440, pp.653–666.

Privett, K., Kunert, M.P. & Lombard, J.H., 2004. Vascular Phenotypes: High throughput characterization of vascular reactivity in rats conditioned on 0.4 % and 4.0 % NaCl diet. Medical College of Wisconsin, (User manual for vascular tension studies).

Qu, C. et al., 2012. Wy14643 improves vascular function in the aorta of the spontaneously hypertensive rat mainly by activating peroxisome proliferator-activated receptors alpha. European Journal of Pharmacology, 696(1-3), pp. 101-10.

Rached, F.H., Chapman, M.J. & Kontush, A., 2014. An overview of the new frontiers in the treatment of atherogenic dyslipidemias. Clinical pharmacology and therapeutics, 96(1), pp.57–63.

Radi, R. *et al*., 1991. Peroxynitrite Oxidation of Sulfhydryls. The Journal of biological chemistry, 266, pp.4244–50.

Radi, R., Cassina, A. & Hodara, R., 2002. Nitric oxide and peroxynitrite interactions with mitochondria. Biol Chem; 383(3-4):401-9.

Radomski, M., Palmer, R.M.J. & Moncada, S., 1987. Endogenous nitric oxide inhibits human platelet adhesion to vascular endothelium. The Lancet, (November), pp.1057–1058.

Raman, C.S. *et al*., 1998. Crystal structure of constitutive endothelial nitric oxide synthase: a paradigm for pterin function involving a novel metal center. Cell, 95(7), pp.939–50.

Rameau, G. A., Chiu, L.-Y. & Ziff, E.B., 2004. Bidirectional regulation of neuronal nitric-oxide synthase phosphorylation at serine 847 by the N-methyl-D-aspartate receptor. The Journal of biological chemistry, 279(14), pp.14307–14.

Rassaf, T. *et al*., 2002. Plasma Nitrosothiols Contribute to the Systemic Vasodilator Effects of Intravenously Applied NO: Experimental and Clinical Study on the Fate of NO in Human Blood. Circulation Research, 91(6), pp.470–477.

Rastaldo, R. *et al.,* 2007. Nitric oxide and cardiac function. Life sciences, 81(10), pp.779–93.

Ratovitski, E.A. *et al.,* 1999a. Kalirin Inhibition of Inducible Nitric-oxide Synthase. Journal of Biological Chemistry, 274(2), pp.993–999.

Ratovitski, E.A. *et al.,* 1999b. An Inducible Nitric-oxide Synthase (NOS)-associated Protein Inhibits NOS Dimerization and Activity. Journal of Biological Chemistry, 274(42), pp.30250–30257.

Ravi, K. *et al.,* 2004. S-nitrosylation of endothelial nitric oxide synthase is associated with monomerization and decreased enzyme activity. Proceedings of the National Academy of Sciences of the United States of America, 101(8), pp.2619–24.

Raza, J.A., Babb, J.D. & Movahed, A., 2004. Optimal management of hyperlipidemia in primary prevention of cardiovascular disease. International journal of cardiology, 97(3), pp.355–66.

Razavi, H.M., Hamilton, J. A. & Feng, Q., 2005. Modulation of apoptosis by nitric oxide: implications in myocardial ischemia and heart failure. Pharmacology & therapeutics, 106(2), pp.147–62.

Rikitake, Y. & Liao, J.K., 2005. Rho GTPases, statins, and nitric oxide. Circulation research, 97(12), pp.1232–5.

Rikitake, Y. *et al*., 2002. Involvement of Endothelial Nitric Oxide in sphingosine-1-phosphate induced angiogenesis. Arteriosclerosis, thrombosis, and vascular biology, 22, pp.108–114.

Robinson, L.J. & Michel, T., 1995. Mutagenesis of palmitoylation sites in endothelial nitric oxide synthase identifies a novel motif for dual acylation and subcellular targeting. Proceedings of the National Academy of Sciences of the United States of America, 92(25), pp.11776–80.

Rodeberg, D.A. *et al*., 1995. Nitric oxide: an overview. Am J Surg. Sep;170(3):292-303.

Rodriguez, J. *et al.,* 2003. Chemical nature of nitric oxide storage forms in rat vascular tissue. Proceedings of the National Academy of Sciences of the United States of America, 100(1), pp.336–41.

Rogers, S.L. *et al.,* 2007. A dose-specific meta-analysis of lipid changes in randomized controlled trials of atorvastatin and simvastatin. Clinical therapeutics, 29(2), pp.242–52.

Roman, L.J. & Masters, B.S.S., 2006. Electron transfer by neuronal nitric-oxide synthase is regulated by concerted interaction of calmodulin and two intrinsic regulatory elements. The Journal of biological chemistry, 281(32), pp.23111–8.

Roos, P.H. & Jakubowski, N., 2008. Cytochrome p450. Analytical and bioanalytical chemistry, 392(6), pp.1015–7.

Ross, R., 1999. Atherosclerosis: an inflammatory disease. The New England journal of medicine, 340, pp.115–126.

Rossig, L. *et al.,* 1999. Nitric Oxide Inhibits Caspase-3 by S-Nitrosationin Vivo. Journal of Biological Chemistry, 274(11), pp.6823–6826.

Rossoni, L.V. *et al*., 2011. Acute simvastatin increases endothelial nitric oxide synthase phosphorylation via AMP-activated protein kinase and reduces contractility of isolated rat mesenteric resistance arteries. Clinical science (London, England : 1979), 121(10), pp. 449-58.

Rothe, F., Langnaese, K. & Wolf, G., 2005. New aspects of the location of neuronal nitric oxide synthase in the skeletal muscle: a light and electron microscopic study. Nitric oxide : biology and chemistry / official journal of the Nitric Oxide Society, 13(1), pp.21–35.

Rozman, D. & Monostory, K., 2010. Perspectives of the non-statin hypolipidemic agents. Pharmacology & therapeutics, 127(1), pp.19–40.

Sacks, F.M., 2008. After the Fenofibrate Intervention and Event Lowering in Diabetes (FIELD) study: implications for fenofibrate. The American journal of cardiology, 102(12A), p.34L–40L.

Saku, K. *et al.,* 1985. Mechanism of Action of Gemfibrozil on Lipoprotein Metabolism. Journal of clinical investigation, 75, pp.1702–12.

Sase, K. & Michel, T., 1997. Expression and regulation of endothelial nitric oxide synthase. Trends in cardiovascular medicine, 7(1), pp.28–37.

Sato, S., Fujita, N. & Tsuruo, T., 2000. Modulation of Akt kinase activity by binding to Hsp90. Proceedings of the National Academy of Sciences of the United States of America, 97(20), pp.10832–7.

Schmidt, A. *et al.,* 2002. Lovastatin-stimulated superinduction of E-selectin , ICAM-1 and VCAM-1 in TNF- a activated human v ascular endothelial cells. Atherosclerosis, 164, pp.57–64.

Schnittler, H.J., 1998. Structural and functional aspects of intercellular junctions in vascular endothelium. Basic research in cardiology, 93 Suppl 3, pp.30–9.

Schulz, E., Schuhmacher, S. & Münzel, T., 2009. When metabolism rules perfusion: AMPK-mediated endothelial nitric oxide synthase activation. Circulation research, 104(4), pp.422–4.

Schulz, R., 2005. Pleiotropic effects of statins: acutely good, but chronically bad? Journal of the American College of Cardiology, 45(8), pp.1292–4.

Schwarz, P.M., Kleinert, H. & Forstermann, U., 1999. Potential Functional Significance of Brain-Type and Muscle-Type Nitric Oxide Synthase I Expressed in Adventitia and Media of Rat Aorta. Arteriosclerosis, Thrombosis, and Vascular Biology, 19(11), pp.2584–2590.

Serrander, L.*et al.,* 2007a. NOX4 activity is determined by mRNA levels and reveals a unique pattern of ROS generation. The Biochemical journal, 406(1), pp.105–14.

Serrander, L.*et al*., 2007b. NOX5 is expressed at the plasma membrane and generates superoxide in response to protein kinase C activation. Biochimie, 89(9), pp.1159–67.

Sessa, W.C. *et al.,* 1992. Molecular cloning and expression of a cDNA encoding endothelial cell nitric oxide synthase. The Journal of biological chemistry, 267(22), pp.15274–6.

Setoguchi, S. *et al.,* 2001. Tetrahydro- biopterin improves endothelial dysfunction in coronary microcirculation in patients without epicardial coronary artery disease. J Am Coll Cardiol; 38: 493-8.

Shah, N.S. & Billiar, T.R., 1998. Role of Nitric Oxide in Inflammation and Tissue Injury during Endotoxemia and Hemorrhagic Shock. Environmental Health Perspectives, 106(October), pp.1139–43.

Sharrett, A.R. *et al.,* 2001. Coronary Heart Disease Prediction From Lipoprotein Cholesterol Levels, Triglycerides, Lipoprotein(a), Apolipoproteins A-I and B, and HDL Density Subfractions: The Atherosclerosis Risk in Communities (ARIC) Study. Circulation, 104(10), pp.1108–1113.

Shaul, P. *et al*., 1996. Acylation Targets Endothelial Nitric-oxide Synthase to Plasmalemmal Caveolae. Journal of Biological Chemistry, 271(11), pp.6518–6522.

Shaw, C. A. *et al.,* 2011. Differential susceptibility to nitric oxide-evoked apoptosis in human inflammatory cells. Free radical biology & medicine, 50, pp.93–101.

Shindo, T. *et al.,* 1994. Nitric oxide synthesis in rat cardiac myocytes and fibroblasts. Life sciences, 55(14), pp.1101–1108.

Shiva, S. *et al*., 2001. Nitric oxide partitioning into mitochondrial membranes and the control of respiration at cytochrome c oxidase. Proceedings of the National Academy of Sciences of the United States of America, 98(13), pp.7212–7.

Siddhanta, U. *et al*., 1998. Domain Swapping in Inducible Nitric-oxide Synthase: electron transfer occurs between flavin and heme groups located on adjacent subunits in the dimer. Journal of Biological Chemistry, 273(30), pp.18950–18958.

Singh, K. *et al*., 1996. Cell Biology and Metabolism : Regulation of Cytokine-inducible Nitric Oxide Synthase in Cardiac Myocytes and Microvascular Endothelial Cells : Role of extracellular signal-regulated kinases 1 and 2 (ERK1/ERK2) and STAT1 alpha. Journal of Biological Chemistry, 271(2), pp.1111–1117.

Singh, S. & Evans, T.W., 1997. Nitric oxide , the biological mediator of the decade : fact or fiction ? European Respiratory Journal, 10, pp.699–707.

Skaletz-Rorowski, A. *et al.,* 2003. HMG-CoA reductase inhibitors promote cholesterol-dependent Akt/PKB translocation to membrane domains in endothelial cells. Cardiovascular research, 57(1), pp.253–64.

Smyth, R. *et al*., 2008. Identification of superoxide dismutase as a potential urinary marker of carbon tetrachloride-induced hepatic toxicity. Food and chemical toxicology : an international journal published for the British Industrial Biological Research Association, 46(9), pp.2972–83.

Soldani, C. & Scovassi, A.I., 2002. Poly (ADP-ribose) polymerase-1 cleavage during apoptosis : An update Cell death mechanisms : Necrosis and apoptosis., 7(4), pp.321–328.

Son, B.-K. *et al*., 2007. Gas6/Axl-PI3K/Akt pathway plays a central role in the effect of statins on inorganic phosphate-induced calcification of vascular smooth muscle cells. European journal of pharmacology, 556(1-3), pp.1–8.

Song, Y., Zweier, J.L. & Xia, Y., 2001. Heat-shock protein 90 augments neuronal nitric oxide synthase activity by enhancing Ca 2 + / calmodulin binding. Biochemistry Journal, 360, pp.357–360.

Springer, T.A., 1994. Traffic signals for lymphocyte recirculation and leukocyte emigration: The multistep paradigm. Cell; 76(2):301-14.

Srinivasan, S. & Avadhani, N.G., 2012. Cytochrome c oxidase dysfunction in oxidative stress. Free radical biology & medicine, 53(6), pp.1252–63.

Staffa, J.A., Chang, J. & Green, L., 2002. Cerivastatin and Reports of Fatal Rhabdomyolysis. The New England journal of medicine, 346(7), pp.533–5.

Stamler, J.S. & Meissner, G., 2001. Physiology of nitric oxide in skeletal muscle. Physiological reviews, 81(1), pp.209–237.

Stary, H.C. *et al.,* 1995. A definition of advanced types of atherosclerotic lesions and a histological classification of atherosclerosis. A report from the Committee on Vascular Lesions of the Council on Arteriosclerosis, American Heart Association. Circulation; 92:1355-74.

Steiner, G., 2008. Fenofibrate for cardiovascular disease prevention in metabolic syndrome and type 2 diabetes mellitus. The American journal of cardiology, 102(12A), p.28L–33L.

Streefkerk, O. *et al.,* 2002. Influence of the nature of pre-contraction on the responses to commonly employed vasodilator agents in rat-isolated aortic rings. Fundamental & Clinical Pharmacology, 16, pp. 485-494.

Strijdom, H. *et al*., 2006. Nitric oxide production is higher in rat cardiac microvessel endothelial cells than ventricular cardiomyocytes in baseline and hypoxic conditions: a comparative study. FASEB journal : official publication of the Federation of American Societies for Experimental Biology, 20(2), pp.314–6.

Strijdom, H., Chamane, N. & Lochner, A., 2009a. Nitric oxide in the cardiovascular system : a simple molecule with complex actions. Cardiovascular journal of Africa, 20(5), pp.303–310.

Strijdom, H. *et al*., 2009b. Hypoxia-induced regulation of nitric oxide synthase in cardiac endothelial cells and myocytes and the role of the PI3-K/PKB pathway. Molecular and cellular biochemistry, 321(1-2), pp.23–35.

Strijdom, H. & Lochner, A., 2009. Cardiac endothelium : More than just a barrier. SAHeart, 6, pp.174–185.

Stroes, E. *et al.,* 1998. Origin of superoxide production by endothelial nitric oxide synthase. FEBS letters, 438(3), pp.161–4.

Stuehr, D.J., 1997. Structure-function aspects in the nitric oxide synthases. Annual review of Pharmacology and Toxicology, 37, pp.339–59.

Stuehr, D.J., 1999. Mammalian nitric oxide synthases. Biochimica et biophysica acta, 1411(2-3), pp.217–30.

Sud N. & Black S., 2009. Endothelin-1 Impairs Nitric Oxide Signaling in Endothelial Cells Through a Protein Kinase Cδ-Dependent Activation of STAT3 and Decreased Endothelial Nitric Oxide Synthase Expression. DNA & Cell Biology [serial online], 28(11), pp.543-553.

Suh, Y.-A. *et al.,* 1999. Cell transformation by the superoxide- generating oxidase Mox1. Nature, 401, pp.79–82.

Sullivan, G.W., Sarembock, I.J. & Linden, J., 2000. The role of inflammation in vascular diseases. Journal of Leukocyte Biology, 67(May), pp.591–602.

Sun, W. *et al*., 2006. Statins activate AMP-activated protein kinase in vitro and in vivo. Circulation, 114(24), pp.2655–62.

Taipale, M., Jarosz, D.F. & Lindquist, S., 2010. HSP90 at the hub of protein homeostasis: emerging mechanistic insights. Nature reviews. Molecular cell biology, 11(7), pp.515–28.

Takahashi, S. & Mendelsohn, M.E., 2003. Synergistic activation of endothelial nitric-oxide synthase (eNOS) by HSP90 and Akt: calcium-independent eNOS activation involves formation of an HSP90-Akt-CaM-bound eNOS complex. The Journal of biological chemistry, 278(33), pp.30821–7.

Takakura, K. *et al*., 1999. Rapid and Irreversible Inactivation of Protein Tyrosine. Archives of biochemistry and biophysics, 369(2), pp.197–207.

Takemoto, M. *et al*., 2001. Statins as antioxidant therapy for preventing cardiac myocyte hypertrophy. Journal of clinical investigation, 108, pp.1429–1437.

Tarbell, J.M. & Pahakis, M.Y., 2006. Mechanotransduction and the glycocalyx. Journal of internal medicine, 259, pp.339–50.

Tatoyan, A. & Giulivi, C., 1998. Purification and Characterization of a Nitric-oxide Synthase from Rat Liver Mitochondria. Journal of Biological Chemistry, 273(18), pp.11044–11048.

Taylor, B.S., Alarcon, L.H. & Billiar, T.R., 1998. Inducible nitric oxide synthase in the liver: regulation and function. Biochemistry;63(7):766-81.

Tejedo, J.R. *et al.,* 2010. Low concentrations of nitric oxide delay the differentiation of embryonic stem cells and promote their survival. Cell death & disease, 1(10), p.e80.

Thomas, D.D. *et al.,* 2010. Determinants of Nitric Oxide Chemistry : Impact of Cell Signaling Processes. In Nitric Oxide: Biology and Pathobiology. Elsevier Inc., pp. 3–25.

Tiede, L.M. *et al.,* 2011. Oxygen matters: tissue culture oxygen levels affect mitochondrial function and structure as well as responses to HIV viroproteins. Cell death & disease, 2(12), p.e246.

Tomizawa, A. *et al.,* 2011. Fenofibrate suppresses microvascular inflammation and apoptosis through adenosine monophosphate-activated protein kinase activation. Metabolism: clinical and experimental, 60(4), pp.513–22.

Török, J. *et al*., 2007. Comparison of the effect of simvastatin, spironolactone and L-arginine on endothelial function of aorta in hereditary hypertriglyceridemic rats. Physiological Research, 56(Supplement 2), pp. S33-40.

Toyama, T. *et al.,* 2004. PPARalpha ligands activate antioxidant enzymes and suppress hepatic fibrosis in rats. Biochemical and biophysical research communications, 324(2), pp.697–704.

Tsimihodimos, V. *et al*., 2005. Fenofibrate: metabolic and pleiotropic effects. Current vascular pharmacology, 3(1), pp.87–98.

Upmacis, R.K. *et al.*, 2011. Inducible nitric oxide synthase provides protection against injury-induced thrombosis in female mice. American journal of physiology, Heart and circulatory physiology, 301(2), pp.H617-24.

Vallabhapurapu, S. & Karin, M., 2009. Regulation and function of NF-kappaB transcription factors in the immune system. Annual review of immunology, 27, pp.693–733.

Van Haperen, R. *et al.*, 2002. Reduction of blood pressure, plasma cholesterol, and atherosclerosis by elevated endothelial nitric oxide. The Journal of biological chemistry, 277(50), pp.48803–7.

Vandesompele, J. *et al.,* 2002. Accurate normalization of real-time quantitative RT-PCR data by geometric averaging of multiple internal control genes. Genome biology, 3(7), p.RESEARCH0034.

Vanhoutte, P.M. *et al.,* 2009. Endothelial dysfunction and vascular disease. Acta physiologica (Oxford, England), 196(2), pp.193–222.

Vasquez-Vivar, J. *et al.*, 2002. Altered tetrahydrobiopterin metabolism in atherosclerosis: implications for use of oxidized tetrahydrobiopterin analogues and thiol antioxidants. Arterioscler Thromb Vasc Biol; 22: 1655-61.

Vásquez-Vivar, J. *et al.,* 1998. Superoxide generation by endothelial nitric oxide synthase: the influence of cofactors. Proceedings of the National Academy of Sciences of the United States of America, 95(16), pp.9220–5.

Vasquez-Vivar, J. *et al.,* 1999. Tetrahydrobiopterin-dependent Inhibition of Superoxide Generation from Neuronal Nitric Oxide Synthase. Journal of Biological Chemistry, 274(38), pp.26736–26742.

Venema, R.C., 2002. Post-translational mechanisms of endothelial nitric oxide synthase regulation by bradykinin. International immunopharmacology, 2(13-14), pp.1755–62.

Viñals, F. & Pouysségur, J., 1999. Confluence of vascular endothelial cells induces cell cycle exit by inhibiting p42/p44 mitogen-activated protein kinase activity. Molecular and cellular biology, 19(4), pp.2763–72.

Virág, L. *et al.,* 2003. Peroxynitrite-induced cytotoxicity: mechanism and opportunities for intervention. Toxicology Letters, 140-141, pp.113–124.

Walker, A.E. *et al.,* 2012. Fenofibrate improves vascular endothelial function by reducing oxidative stress while increasing endothelial nitric oxide synthase in healthy normolipidemic older adults. Hypertension, 60(6), pp.1517–23.

Walter, D.H., 2002. Statin Therapy Accelerates Reendothelialization: A Novel Effect Involving Mobilization and Incorporation of Bone Marrow-Derived Endothelial Progenitor Cells. Circulation, 105(25), pp.3017–3024.

Wang, Y. *et al.,* 2004. Cardioprotection During the Final Stage of the Late Phase of Ischemic Preconditioning Is Mediated by Neuronal NO Synthase in Concert With Cyclooxygenase-2. Circulation Research, 95(1), pp.84–91.

Wang, G. *et al*., 2010a. Chronic treatment with fibrates elevates superoxide dismutase in adult mouse brain microvessels. Brain research, 1359, pp.247–55.

Wang, L. *et al.,* 2010b. Translocation of protein kinase C isoforms is involved in propofol-induced endothelial nitric oxide synthase activation. British journal of anaesthesia, 104(5), pp.606–12.

Wang, L. *et al.,* 2013. The effect of simvastatin on glucose homeostasis in streptozotocin induced type 2 diabetic rats. Journal of Diabetes Research, 2013, pp. 274986 (5 pages).

Webb, A. *et al*., 2004. Reduction of nitrite to nitric oxide during ischemia protects against myocardial ischemia-reperfusion damage. Proceedings of the National Academy of Sciences of the United States of America, 101(37), pp.13683–8.

Wei, Q. & Xia, Y., 2005. Roles of 3-phosphoinositide-dependent kinase 1 in the regulation of endothelial nitric-oxide synthase phosphorylation and function by heat shock protein 90. The Journal of biological chemistry, 280(18), pp.18081–6.

Weitz-Schmidt *et al.,* 2001. Statins selectively inhibit leukocyte function antigen-1 by binding to a novel regulatory integrin site. Nature medicine, 7(6), pp.687–693.

Wever, R.M. *et al.,* 1997. Tetrahydrobiopterin regulates superoxide and nitric oxide generation by recombinant endothelial nitric oxide synthase. Biochemical and biophysical research communications, 237(2), pp.340–4.

Widmaier, E.P., Raff, H. & Strang, K.T., 2004. Vander, Sherman and Luciano's Human Physiology: the mechanisms of body function. 9th ed. McGraw-Hill, USA, New York.

Wiel, E. *et al*., 2005. Pretreatment with peroxysome proliferator-activated receptor alpha agonist fenofibrate protects endothelium in rabbit Escherichia coli endotoxin-induced shock. Intensive care medicine, 31(9), pp.1269–79.

Wilensky, R.L. *et al.,* 1995. Vascular Injury, Repair, and Restenosis After Percutaneous Transluminal Angioplasty in the Atherosclerotic Rabbit. Circulation;92:2995-3005.

Wilkins, R.C. *et al.,* 2002. Analysis of radiation-induced apoptosis in human lymphocytes: flow cytometry using Annexin V and propidium iodide versus the neutral comet assay. Cytometry, 48(1), pp.14–9.

Wilson, P.W. *et al.,* 1980. Prevalence of coronary heart disease in the Framing- ham Offspring Study: role of lipoprotein cholesterols. Am J Cardiol;46:649–54.

Wolfrum, S. *et al.,* 2007. The protective effect of A20 on atherosclerosis in apolipoprotein E-deficient mice is associated with reduced expression of NF-kappaB target genes. Proceedings of the National Academy of Sciences of the United States of America, 104(47), pp.18601–6.

Wolin, M.S., 2000. Interactions of Oxidants with Vascular Signaling Systems. Arteriosclerosis, Thrombosis, and Vascular Biology, 20(6), pp.1430–1442.

Woodman, C.R. *et al.,* 1999. Flow regulation of ecNOS and Cu/Zn SOD mRNA expression in porcine coronary arterioles. The American journal of physiology, 276(3 Pt 2), pp.H1058–63.

Wu, F. & Wilson, J.X., 2009. Peroxynitrite-dependent activation of protein phosphatase type 2A mediates microvascular endothelial barrier dysfunction. Cardiovascular research, 81(1), pp.38–45.

Wu, X. *et al.,* 2010. Statin post-treatment provides protection against simulated ischemia in bovine pulmonary arterial endothelial cells. European journal of pharmacology, 636(1-3), pp.114–20.

Xenos, E.S.*et al.,* 2005. Nitric oxide mediates the effect of fluvastatin on intercellular adhesion molecule-1 and platelet endothelial cell adhesion molecule-1 expression on human endothelial cells. Ann Vasc Surg, 19(3), pp.386-92.

Xia, Y. *et al.,* 1998. Inducible Nitric-oxide Synthase Generates Superoxide from the Reductase Domain. Journal of Biological Chemistry, 273(35), pp.22635–22639.

Xia, Y.F. *et al.,* 2001. NF-kappaB activation for constitutive expression of VCAM-1 and ICAM-1 on B lymphocytes and plasma cells. Biochemical and biophysical research communications, 289(4), pp.851–6.

Xie, Q.W. *et al.,* 1992. Cloning and characterization of inducible nitric oxide synthase from mouse macrophages. Science (New York, N.Y.), 256(5054), pp.225–8.

Xu, K.Y. *et al.,* 1999. Nitric oxide synthase in cardiac sarcoplasmic reticulum. Proceedings of the National Academy of Sciences of the United States of America, 96(2), pp.657–62.

Yang, K.S. *et al.,* 2014. Vascular endothelial growth factor-receptor 1 inhibition aggravates diabetic nephropathy through eNOS signaling pathway in db/db mice. PloS one, 9(4), p.e94540.

Yang, T.-L. *et al.*, 2005. Fenofibrate decreases asymmetric dimethylarginine level in cultured endothelial cells by inhibiting NF-kappaB activity. Naunyn-Schmiedeberg's archives of pharmacology, 371(5), pp.401–7.

Yao, L. *et al.,* 2010. The role of RhoA/Rho kinase pathway in endothelial dysfunction. Journal of cardiovascular disease research, 1(4), pp.165–70.

Ye, Y. *et al.,* 2010. Dipyridamole with low-dose aspirin augments the infarct size-limiting effects of simvastatin. Cardiovascular drugs and therapy / sponsored by the International Society of Cardiovascular Pharmacotherapy, 24(5-6), pp.391–9.

Yoshioka, S., Acosta, T.J. & Okuda, K., 2012. Roles of cytokines and progesterone in the regulation of the nitric oxide generating system in bovine luteal endothelial cells. Molecular reproduction and development, 79(10), pp.689–96.

Yoshizumi, M. *et al.,* 1993. Tumor necrosis factor downregulates an endothelial nitric oxide synthase mRNA by shortening its half-life. Circ. Res; 73: 205–209

Yusuf, S. *et al*., 2001. Global Burden of Cardiovascular Diseases: Part I: General Considerations, the Epidemiologic Transition, Risk Factors, and Impact of Urbanization. Circulation, 104(22), pp.2746–2753.

Zanetti, M. *et al.,* 2008. Inhibitory effects of fenofibrate on apoptosis and cell proliferation in human endothelial cells in high glucose. Journal of molecular medicine (Berlin, Germany), 86(2), pp.185–95.

Zecchin, H.G. *et al.,* 2007. Defective Insulin and Acetylcholine Induction of Endothelial. Diabetes, 56(4), pp.1014–24.

Zhang, G-R., Bourreau, J-P. & Xiao-Hui, L., 2007. The effect of adrenomedullin on the L-type calcium current in myocytes from septic shock rats: signaling pathway. American Journal of Physiology - Heart and Circulatory Physiology, 293(5), pp.H2888–H2893.

Zhang, H. *et al.,* 2009. Role of TNF-alpha in vascular dysfunction. Clinical science (London, England : 1979), 116(3), pp.219–30.

Zhang, Y. *et al.,* 2007. Dynamic receptor-dependent activation of inducible nitric-oxide synthase by ERK-mediated phosphorylation of Ser745. The Journal of biological chemistry, 282(44), pp.32453–61.

Zhang, Y. *et al.,* 2008. Central administration of angiotensin-(1-7) stimulates nitric oxide release and upregulates the endothelial nitric oxide synthase expression following focal cerebral ischemia/reperfusion in rats. Neuropeptides, 42(5-6), pp.593–600.

Zhao, X. *et al.,* 2006. PPAR-alpha activator fenofibrate increases renal CYP-derived eicosanoid synthesis and improves endothelial dilator function in obese Zucker rats. American journal of physiology. Heart and circulatory physiology, 290(6), pp.H2187–95.

Zhao, Y., Vanhoutte, P.M. & Leung, S.W.S., 2013. Endothelial nitric oxide synthase-independent release of nitric oxide in the aorta of the spontaneously hypertensive rat. The Journal of pharmacology and experimental therapeutics, 344(1), pp.15–22.

Zhou, L. & Zhu, D.-Y., 2009. Neuronal nitric oxide synthase: structure, subcellular localization, regulation, and clinical implications. Nitric oxide : biology and chemistry / official journal of the Nitric Oxide Society, 20(4), pp.223–30.

Zhou, Q. & Liao, J.K., 2010. Pleiotropic Effects of Statins. Circulation Journal, 74(5), pp.818–826.

Zhu, M.-X. *et al.,* 2014. Simvastatin Pretreatment Protects Cerebrum from Neuronal Injury by Decreasing the Expressions of Phosphor-CaMK II and AQP4 in Ischemic Stroke Rats. Journal of molecular neuroscience : MN, 286.

Zhu, X.-Y. *et al.,* 2008. Disparate effects of simvastatin on angiogenesis during hypoxia and inflammation. Life sciences, 83(23-24), pp.801–809.

Zhu, Y. *et al*., 2005. Mechanism of inactivation of inducible nitric oxide synthase by amidines. Irreversible enzyme inactivation without inactivator modification. Journal of the American Chemical Society, 127(3), pp.858–68.

Ziolo, M.T. & Bers, D.M., 2003. The real estate of NOS signaling: location, location, location. Circulation research, 92(12), pp.1279–81.

Zou, C. *et al.,* 2013. Simvastatin Activates the PPAR gamma-dependent pathway to prevent left ventricular hypertrophy associated with inhibition of RhoA signalling. Texas Heart Institute Journal, 40(2), pp.140–147.

http://my.clevelandclinic.org/heart/heart-blood-vessels/coronary-arteries.aspx

Addendum

Addendum

The following information is relevant to qPCR analysis:

Table A: Information pertaining to target and reference genes

Gene ID	TaqMan Assay ID	RefSeq ID	Chromosomal Position
iNOS	Rn00561646_m1	NM_012611	Chr.10: 65036884 – 65072453
HPRT1	Rn01527840_m1	NM_012583	Chr.X:139929647 – 139961616
GAPDH	Rn01775763_g1	NM_017008	Chr.4:161282215 - 161286090
Hsp90ab1	Rn01511686_g1	NM_001004082	Chr.9: 11033496 - 11038868

Table B: RNA concentrations and integrity. Samples highlighted in yellow showed lower than acceptable A260/A230 ratios.

Sample ID	Date	ng/ul	260/280	260/230
UC1	2013/12/10	210.24	2.02	1.31
UC2	2013/12/10	212.04	2.03	1.42
UC3	2013/12/10	200.57	2.02	1.33
NSC1	2013/12/10	148.16	2.01	2.07
NSC2	2013/12/10	158.16	2.03	1.96
NSC3	2013/12/10	141.82	2.06	2.2
IL1B 1	2013/12/10	142.02	2.04	1.25
IL1B 2	2013/12/10	150.8	1.96	1.71
IL1B 3	2013/12/10	136.9	2	1.65
FENO1	2013/12/10	174.36	2.06	1
FENO2	2013/12/10	161.66	2.01	2.11
FENO3	2013/12/10	153.14	2.01	1.37
KD5 1	2013/12/10	157.86	1.97	1.74
KD5 2	2013/12/10	189.18	2	1.8
KD5 3	2013/12/10	159.25	2	1.76
KD7 1	2013/12/10	159.05	1.98	1.93
KD7 2	2013/12/10	145.1	2.03	1.88
KD7 3	2013/12/10	163.84	2.03	2.1
NSC+IL1B 1	2013/12/10	128.79	2.06	0.67
NSC+IL1B 2	2013/12/10	117.36	2.01	2.02
NSC+IL1B 3	2013/12/10	147.66	1.97	2.01
KD5+IL1B 1	2013/12/10	140.67	1.69	1.16
KD5+IL1B 2	2013/12/10	139.56	2.02	1.86
KD5+IL1B 3	2013/12/10	127.02	2.03	0.59
KD7+IL1B 1	2013/12/10	126.9	2.01	1.02
KD7+IL1B 2	2013/12/10	150.75	2.04	2.14

KD7+IL1B 3	2013/12/10	128.22	1.94	1.97

Table C: qPCR amplification efficiency for target genes.

Gene name	Slope	R^2 value
iNOS	-4.0	0.99
HPRT	-3.5	0.98
GAPDH	-3.9	0.99
HSP90	-3.7	0.99

The following graph shows the average expression stability of reference genes.

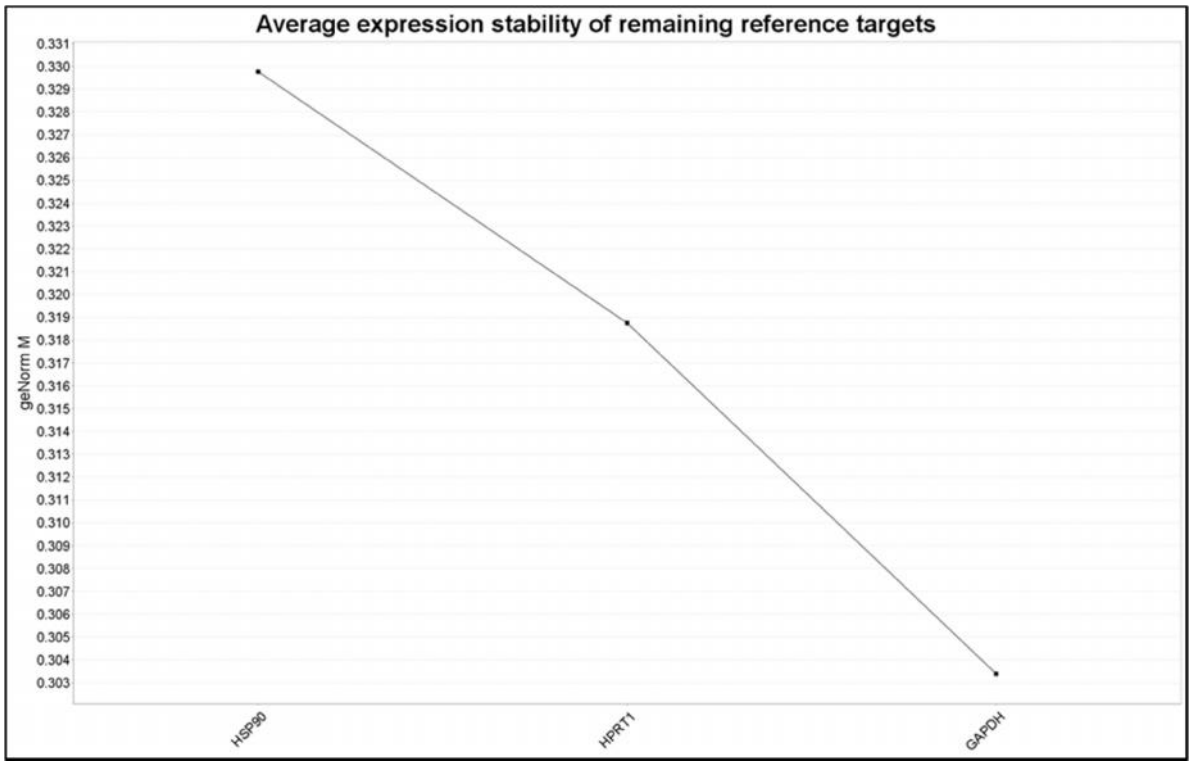

Figure A: *GeNorm analysis of reference gene stability*